FUNDAMENTALS AND RECENT ADVANCES IN NANOCOMPOSITES BASED ON POLYMERS AND NANOCELLULOSE

EDITED BY
MD REZAUR RAHMAN

ELSEVIER

Fundamentals and Recent Advances in Nanocomposites Based on Polymers and Nanocellulose

Fundamentals and Recent Advances in Nanocomposites Based on Polymers and Nanocellulose

Edited by

Md Rezaur Rahman
Department of Chemical Engineering and Energy Sustainability,
Faculty of Engineering, Universiti Malaysia Sarawak (UNIMAS),
Kota Samarahan, Sarawak, Malaysia

ELSEVIER

Elsevier
Radarweg 29, PO Box 211, 1000 AE Amsterdam, Netherlands
The Boulevard, Langford Lane, Kidlington, Oxford OX5 1GB, United Kingdom
50 Hampshire Street, 5th Floor, Cambridge, MA 02139, United States

Notices
Knowledge and best practice in this field are constantly changing. As new research and experience broaden our understanding, changes in research methods, professional practices, or medical treatment may become necessary.

Practitioners and researchers must always rely on their own experience and knowledge in evaluating and using any information, methods, compounds, or experiments described herein. In using such information or methods they should be mindful of their own safety and the safety of others, including parties for whom they have a professional responsibility.

To the fullest extent of the law, neither the Publisher nor the authors, contributors, or editors, assume any liability for any injury and/or damage to persons or property as a matter of products liability, negligence or otherwise, or from any use or operation of any methods, products, instructions, or ideas contained in the material herein.

Library of Congress Cataloging-in-Publication Data
A catalog record for this book is available from the Library of Congress

British Library Cataloguing-in-Publication Data
A catalogue record for this book is available from the British Library

ISBN: 978-0-323-85771-0

Publisher: Matthew Deans
Acquisitions Editor: Edward Payne
Editorial Project Manager: Chiara Giglio
Production Project Manager: Prasanna Kalyanaraman
Cover Designer: Matthew Limbert

Typeset by STRAIVE, India

To

Fahriah Rahman, Faizah Rahman, and Shirin Akther
My amazing daughters and wife, who are very special to me
and made it possible for me to complete this work.

Contents

Contributors

Muhammad Khusairy Bin Bakri
Department of Chemical Engineering and Energy Sustainability, Faculty of Engineering, Universiti Malaysia Sarawak (UNIMAS), Kota Samarahan, Sarawak, Malaysia

Faisal Islam Chowdhury
Nanotechnology and Renewable Energy Research Laboratory (NRERL), Department of Chemistry, University of Chittagong, Chittagong, Bangladesh

Sinin Hamdan
Department of Chemical Engineering and Energy Sustainability, Faculty of Engineering, Universiti Malaysia Sarawak (UNIMAS), Kota Samarahan, Sarawak, Malaysia

Jahidul Islam
Nanotechnology and Renewable Energy Research Laboratory (NRERL), Department of Chemistry, University of Chittagong, Chittagong, Bangladesh

Elammaran Jayamani
Faculty of Engineering, Computing and Science, Swinburne University of Technology Sarawak Campus, Kuching, Sarawak, Malaysia

Perry Law Nyuk Khui
Department of Chemical Engineering and Energy Sustainability, Faculty of Engineering, Universiti Malaysia Sarawak (UNIMAS), Kota Samarahan, Sarawak, Malaysia

Mohammed Mahbubul Matin
Department of Chemistry, Faculty of Science, University of Chittagong, Chattogram, Bangladesh

Md Rezaur Rahman
Department of Chemical Engineering and Energy Sustainability, Faculty of Engineering, Universiti Malaysia Sarawak (UNIMAS), Kota Samarahan, Sarawak, Malaysia

Khairuddin Sanaullah
Department of Chemical Engineering and Energy Sustainability, Faculty of Engineering, Universiti Malaysia Sarawak (UNIMAS), Kota Samarahan, Sarawak, Malaysia

Nur-Azzah Afifah Binti Taib
Department of Chemical Engineering and Energy Sustainability, Faculty of Engineering, Universiti Malaysia Sarawak (UNIMAS), Kota Samarahan, Sarawak, Malaysia

Preface

Fundamentals and Recent Advances in Nanocomposites Based on Polymers and Nanocellulose brings together the latest research in cellulose-based nanocomposites, covering fundamentals, processing, properties, performance, applications, and the state of the art.

The book begins by explaining the fundamentals of cellulose and cellulose-based nanocomposites, including sources, extraction, types, classification, linkages, model structure, model compounds, and characterization techniques. The second part of the book covers the incorporation of cellulose fillers to improve the properties or characteristics of nanocomposites, organized by composite category, including in aerogels, thermoplastic composites, thermoset composites, bioplastic composites, carbon nanofibers, rubber composites, carbon fibers, and foaming materials. Throughout these chapters, there is an emphasis on the latest innovations and application potential. Finally, applications are explored in more detail, notably focusing on the utilization of nanocellulose in biodegradable composites for biomedical applications, along with other important industrial application areas.

Md Rezaur Rahman
Department of Chemical Engineering and Energy Sustainability, Faculty of Engineering, Universiti Malaysia Sarawak (UNIMAS), Kota Samarahan, Sarawak, Malaysia

Acknowledgments

The editor thanks and acknowledges Universiti Malaysia Sarawak (UNIMAS) for their support and allowing use of their facilities. The editor also thanks Elsevier for helping to make this project successful.

CHAPTER

Sources of cellulose

1

Muhammad Khusairy Bin Bakri[a], **Md Rezaur Rahman**[a], **and Faisal Islam Chowdhury**[b]

[a]*Department of Chemical Engineering and Energy Sustainability, Faculty of Engineering, Universiti Malaysia Sarawak (UNIMAS), Kota Samarahan, Sarawak, Malaysia,* [b]*Nanotechnology and Renewable Energy Research Laboratory (NRERL), Department of Chemistry, University of Chittagong, Chittagong, Bangladesh*

Chapter outline

1.1 Introduction of cellulose

The most abundant constitutes and renewable polymer resource available today and worldwide being used is cellulose (Klemm, Heublein, Fink, & Bohn, 2005; Klemm, Schmauder, & Heinze, 2005). Taking the example of the cotton plant seed-hair, through photosynthesis, around $10^{11} \pm 10^{12}$ tons' of cellulose is estimated to be synthesized annually, which generally combined with lignin and other polysaccharides, i.e., hemicelluloses, etc., especially in the cell wall of the woody plants (Krassig, 1993). In centuries, many of these cellulose, such as cotton or flax has been used in both construction and textile materials, mainly for intact wood (adhesion and repairing of wood) and fabricate paper and board, respectively. For chemical conversion, cellulose is a useful as other starting material for cellulose-based threads and

Fundamentals and Recent Advances in Nanocomposites Based on Polymers and Nanocellulose.
https://doi.org/10.1016/B978-0-323-85771-0.00012-9

films as well as a variety of stable cellulose derivatives used in many areas of industry and domestic life, which usually aims as an artificial production (Klemm, Philipp, Heinze, Heinze, & Wagenknecht, 1998). Most of the empirical knowledge on cellulose was acquired a thousand years ago, especially on the dying cellulose fibers, burning wood, preparing charcoal, and biodegradation of cellulose by rotting.

In the annals of polymers, cellulose occupies a unique place. In 1838, Payen (Payen, 1838) recognized and coined "cellulose" as a definitive substance. For chemical modifications, cellulose has been used as a precursor for many applications, even before its polymeric nature was recognized. This pathway milestone contributed to the discovery of cellulose nitrate, which commonly misnamed as nitrocellulose by Schnbein in 1846. The preparation of Schweizer's reagent, i.e., cuprammonium hydroxide solution, representing the first cellulose solvent in 1857, and the synthesis of an organo-soluble cellulose acetate by Schtzenberger in 1865 (Klemm et al., 1998; Klemm, Heublein, et al., 2005; Klemm, Schmauder, & Heinze, 2005). The first officially polymeric materials used as a plastic and a softener was partially functionalized as cellulose nitrate mixed with camphor, which is well known under the trade name of "celluloid". The higher nitrogen content of the cellulose nitrates is used extensively for biomedical and military purposes in those days.

Regenerated cellulose filaments were obtained in a dissolved aqueous bath by spinning cellulose in cuprammonium hydroxide (Woodings, 2016). Invented in 1892 by Cross and his teams, the largest part of cellulose-based artificial fibers called viscose process have also been manufactured (Klemm et al., 1998; Klemm, Heublein, et al., 2005; Klemm, Schmauder, & Heinze, 2005). Today, this process is practiced worldwide with an output annually of about 3 million tons. It makes use of the formation of cellulose xanthogenate/cellulose xanthate. In industrial applications, cellulose xanthate is water-soluble, less-stable anionic ester, which usually prepared by the reaction of cellulose with aqueous sodium hydroxide, NaOH and carbon disulfide, CS_2, while in an acid bath, its decomposition by spinning. Certain xanthate salts and bisxanthates, i.e., dixanthogen are used in many mineral processing as flotation agents. They are intermediates in the *Chugaev* elimination process, which are used to control radical polymerization under the reversible addition-fragmentation chain transfer (RAFT) process. It was also known as macromolecular design via interchange of xanthates (MADIX). In the 1920s to 1930s, the cellulose chemistry origin was as a branch of polymer, and its research can be traced back to Staudinger fundamental experiments of on the acetylation and deacetylation of cellulose, whereas these experiments resulted in the concept of polymer-analogous reactions (Klemm et al., 1998; Klemm, Heublein, et al., 2005; Klemm, Schmauder, & Heinze, 2005). The macromolecules functional groups in cellulose are predominantly hydroxyl groups, which undergo the same kind of reactions as the corresponding low-molecular compounds. It also observed that the supramolecular structure of the polymer would determine the rate and final degree of its conversion, as well as the distribution of the functional groups, which has been well recognized for cellulose.

1.2 Functions of cellulose

Cellulose is a structure based form on protein, which usually found in algae and plant that was crucial in supporting the main structure of the plant (Saxena & Brown Jr, 2001). Alongside with lignin and hemicellulose, it also connected the cells to form tissues (Harris, Bulone, Ding, & DeBolt, 2010; Pauly & Keegstra, 2008; Sarkar, Bosneaga, & Auer, 2009). In stems, plants, and wood, cellulose fibers are distributed as a support structure in a lignin matrix, whereas the cellulose acts as a reinforced bar, while lignin acts similarly to concrete structure (Pereira Oliveira Moreira, Simão, Gouveia, & Strauss, 2020; Sorieul, Dickson, Hill, & Pearson, 2016). It is also functioning to transfer information by signaling cells to grow and can move in divide branches, while controlling the shape of plant cells and allowing cells to withstand the turgor pressure of fluids inside them (Sorieul et al., 2016). However, most of the time, cellulose functioning to support plant cell walls, whereas the cellulose fibers are enmeshed in a polysaccharide matrix (Bousfield, Morin, Jacquet, & Richel, 2018; Holland, Ryden, Edwards, & Grundy, 2020; Xing et al., 2018). Cotton is the purest natural form of cellulose that consisted over 90% cellulose (Björquist, Aronsson, Henriksson, & Persson, 2018; Haigler, Betancur, Stiff, & Tuttle, 2012; Rajasundaram et al., 2014; Runavot et al., 2014; Wan & Cameron, 1942) While, cellulose in wood consisted up to 40%–50% (Freudenberg, 1932; Harding, 1921; Qiyuan, Shengling, Shi, & Liping, 2018; Shilin et al., 2014; Vishtal & Kraslawski, 2011; Wang, Zhang, Xu, Xu, & Wu, 2014; Yao, Wu, Xing, Zhou, & Pu, 2010). On the other hand, there are many species of bacteria that stashed cellulose to produce biofilms (Ashley, 2018; Augimeri, Varley, & Strap, 2015; Gorgieva & Trček, 2019; Rühs, Storz, López Gómez, Haug, & Fischer, 2018; Serra, Richter, & Hengge, 2013). The biofilms allow the bacteria to organize into colonies by providing an attachment on the surface for the microorganisms (Bogino, Oliva, Sorroche, & Giordano, 2013; Mercedes & Ricardo, 2016; Petrova & Sauer, 2012). Animals cannot produce cellulose, even though cellulose is important to their survival (Russell, Muck, & Weimer, 2009). However, some worms and insects, i.e., silkworm, grasshopper, spider, etc. use cellulose as a building material, hunting, and food (Martin, 1983; Martin, 1991; Watanabe & Tokuda, 2010) [(Hirasaka, 1976; Ito, 1960)]. In some cases, most ruminants use symbiotic microorganisms to digest the cellulose (Martin, 1983; Msimango & Fon, 2016). Humans on the other hand, cannot digest cellulose, but it is the main source of insoluble dietary fiber, which affects nutrient absorption and helps in defecation (Russell et al., 2009). Cellulose fiber were used also used as cleaning products, such as the luffa sponges.

1.3 Sources of cellulose

Most of the cellulose sources are extracted and isolated from the plant and algae, while very few were taken from insects and worms. However, there is still a lot of misconception mentioned that cellulose can be extracted and isolated from live

animal and mineral sources directly. Whereas, the cell wall of animals does not contain cellulose, but there are devoid of cell wall (Kost & Chua, 2002; Paulraj et al., 2020). Natural fibers are classified according to their parts of origins, which are generally composed mainly of cellulose, i.e., seed, leaf, bast, etc. Most of these cellulose are isolated and extracted to serve in the manufacture of paper and cloth. This fiber can be further categorized into the following as shown in Table 1.1. The most used cellulose obtained and used are collected from cotton, flax, hemp, sisal, jute, kenaf, and bamboo (Rahman & Bakri, 2021; Rahman, Hamdan, & Ngaini, 2019).

Table 1.1 summaries the sources of cellulose for plants and algae.

1.4 Potentiality of cellulose

1.4.1 Feedstock, foods, medicine, and reinforcement

To produce ethanol and other chemicals, biomass shows promising potential due to its renewable resources. One of the biomasses that show promising potential is cellulose, which is low in cost and abundantly and easily available (Chovau, Degrauwe, & Van Der Bruggen, 2013; Huang, Ramaswamy, Al-Dajani, Tschirner, & Cairncross, 2009). Taking example of sugarcane and corn, which are priced at $60.9/ton and $185.9/ton, while respectively, sugarcane bagasse and corn stover priced at $36.38/ton and $58.50/ton (Bonomi, Otavio, Cunha, & Lima, 2016; da Silva & Marques, 2017), which considered to be cheaper. There are many examples of sources of cellulose can be extracted, from agricultural wastes (corn stover, wheat or rice straw), sugarcane bagasse, wood (hardwood or softwood), grass, municipal waste, and dedicated energy crops (miscanthus and switchgrass) (Kumar, Tabatabaei, Karimi, & Horváth, 2016). Cellulose is one of the main components of lignocellulosic or fiber that consists of glucose chains, which linked by β-1,4 linkages. These crystalline microfibrils chains are highly recalcitrant to degradation (Hamad & Hu, 2010; Pandey, 2008). The proportion of these cellulose substantially varied depending on the type of biomass, locations, soils, weather, and harvest time (Bridgeman, Jones, Shield, & Williams, 2008; Howard, Abotsi, van Rensburg, & Howard, 2003; Li, Kim, Jiang, Kang, & Chang, 2009; Merino & Cherry, 2007; Rosales-Calderon, Trajano, Posarac, & Duff, 2016; Van Dyk & Pletschke, 2012; Wang et al., 2016; Cheng et al., 2014)

In contrast to the production of bioethanol from starch, cellulosic biomass is not fully utilized as a main food source. In the past years, ethanol prices have fluctuated in correlation with gasoline or corn grain prices, which shows the primary drivers of ethanol prices (Rosales-Calderon & Arantes, 2019). Ethanol was traded based on gasoline prices, whereas petroleum prices were increasing and corn grain was relatively inexpensive. As ethanol began to devour a larger percentage of corn grain production, its price increasingly stimulated in synchronization with the corn grain prices. The correlation between corn grain and ethanol prices is anticipated to decline, once substantial volumes are produced from cellulosic feedstock

Table 1.1 Summary contains sources of cellulose in plants and algae.

Category		Description	Examples	Estimated percentage of cellulose (%)
Plant and/ or tree	Seed/fruit	Cellulose extracted and collected from seeds, seed cases and/or fruits	Cotton	85–94
			Gourd (*Citrullus colocynthis*)	65–75
			Kapok	40–65
			Balsa	40–50
			White lead tree (*Leucaena leucocephala*)	20–30
			Sunflower	40–60
			Pumpkin	35–60
			Peanut	
			Acorn	
			Coconut	
			Hazelnut	
			Chestnut	25–60
			Palm/date	20–30
	Leaf/stem	Cellulose extracted and collected from leaves	Pineapple	50–70
			Sisal	60–70
			Abaca	50–75
			Agave	70–80
			Milkweed	70–80
			Aloe Vera	50–60
			Mengkuang (*Pandanus tectorius*)	30–40
			Pandan (Pandanusamaryllifolius Roxb.)	46–94
			Banana	25–30
			Sorghum	40–65
			Tea	15–20

Table 1.1 Summary contains sources of cellulose in plants and algae. *Cont'd*

Category		Description	Examples	Estimated percentage of cellulose (%)	Ref
	Bast/skin/husk/bagasse	Cellulose is extracted and collected from the skin, husk, baggase, and bast of their respective plants	Jute	30–75	Dua et a (20
			Kenaf	60–80	Nish Sula
			Hemp	20–50	Ste Gar
			Ramie	65–80	Li e
			Rattan	35–60	Zur
			Sugarcane	40–50	Sur
	Stalk/straw	Cellulose extracted and collected from the stalks and/or straw of the plants	Rice straw	30–50	Sha
			Barley straw	55–65	For
			Wheat straw	40–50	Per Mul Kap
			Rye straw	35–50	Fan Mas
			Oat straw		Mas
			Triticale straw		Mas
			Corn stalk		Dau
	Trunk/wood/root	Cellulose extracted and collected from trunk, root and/or wood	Hardwood	70–75	Row
			Softwood	65–70	

Algae/seaweeds	Cellulose extracted and collected from algae and/or seaweeds	*Cladophora glomerata* *Chaetomorpha antennina* *Chamaedoris auriculata* *Dictyota dichotoma* *Dictyota bartayresiana* *Sargassum tenerrimum* *Gracilaria debilis* *Gracilaria textorii* *Gracilaria edulis* *Gelidiella acerosa* *Champia indica* *Kappaphycus alvarezii* *Sarconema scinaioides*	40–50 0–15

(Rosales-Calderon & Arantes, 2019). Therefore, cellulose can be further study in order to be used in feedstock applications, as it shows many potentials.

In food sector, microcrystalline cellulose (MCC) is among the most commonly used cellulose derivatives in the food industry after carboxyl methyl cellulose (CMC) (John et al., 2017). Cellulose can be used in emulsion, suspension, and foam stabilization, fat substitutes or replacers and bulking agent, wall materials for encapsulation and reinforcement of edible films (John et al., 2017). The crystals of cellulose within micro or nano scale dimension (MCC/NCC) amphipathically able to stabilize emulsions, as the presence free hydroxyl groups on surface material, which made it acts as hydrophilic, while the crystalline portion would function as the hydrophobic edge, giving overall amphiphilic character (Kalashnikova, Bizot, Cathala, & Capron, 2011). These stabilized particle emulsions are also called 'Pickering' emulsions (Kalashnikova et al., 2011). The stabilization mechanism is based on particle size, shape, and crystallinity of partial dual wettability (Capron & Cathala, 2013; Hu, Ballinger, Pelton, & Cranston, 2015). Meanwhile, for the stabilization of particle-stabilized emulsions, two major mechanisms are identified: (i) As the solid particles can be irreversible (Tavernier, Wijaya, Van der Meeren, Dewettinck, & Patel, 2016), especially to adsorbed at the interface, by creating a layer around the emulsion droplets, while preventing their coalescence (Dickinson, 2013), and (ii) as particle stabilization emulsion by the formation of two or three dimensional networks (Winuprasith & Suphantharika, 2015; Xu, Zhang, Cao, Wang, & Xiao, 2016).

Cellulose are good potential candidates for interfacial stabilization, which was mostly for food used due to their biodegradability, sustainability, nontoxicity, edible, renewability, and excellent native physiochemical properties, which including the high aspect ratio and its elastic modulus (Boluk, Lahiji, Zhao, & McDermott, 2011; Kalashnikova et al., 2011; Winuprasith & Suphantharika, 2015). Kalashnikova et al. (2011) demonstrated that in the absence of a dispersing agent, cellulose microcrystals could effectively stabilize the food by stacking the emulsions by the "Pickering" mechanism of stabilization, only if the particles are dispersed properly. Likewise, nano scale dimension of cellulose obtained from asparagus through hydrolysis of sulfuric acid was used to form stable "Pickering" emulsions in a palm oil/water (30/70, *v*/v) model solution for several weeks (Harding, 1921; Freudenberg, 1932; Qiyuan et al., 2018; Shilin et al., 2014; Vishtal & Kraslawski, 2011; L. Wang et al., 2014; Yao et al., 2010). Colloidal MCC, created by 11% MCC combined with 1% sodium carboxyl methyl cellulose (SCMC) has also been used to stabilize oil in water emulsion, water in oil, and in water multiple emulsions via a formation of a network around the emulsified oils (Jia et al., 2014; Oza & Frank, 1989). Cellulose such as MCC incorporated in the systems, functions to orientate at the oil-water interface, by offering a mechanical barrier to oil droplet coalescence (Dickinson, 2013), while other material in the system, acts mainly as a dispersing and protective colloid for the MCC (Jia et al., 2014). Cellulose, like colloidal MCC help thickens the continuous phase between the droplets and builds a weak three-dimensional network, which anticipated to stabilize the emulsions (Winuprasith & Suphantharika, 2015; Xu et al., 2016). However, the network's

strength formed by the cellulose would rest on its aspect ratio, which is invariably defined by the particles shape and size that was formed. The high aspect ratio microfibrillated cellulose reportedly formed strong entangled disordered networks in contrast to a low aspect ratio MCC, which created feebly by the bonded networks (Pääkkö et al., 2007; Saxena and Brown Jr, 2001).

Cellulose has also been used as replacer or substitute for fat in the food systems. Cellulose is often dispersed into an aqueous medium and used to simulate fat in the food system. To reduce the amount of fats in ground meat, frozen desserts, yogurt, dairy, and baked products, a significant amount of work has been conducted and ongoing research is needed to improve the existing methods. Cellulose insoluble nature in water and as a fat replacement or substitution in food systems reportedly produced excellent results, which shows it potentially to be used in food system (Gibis, Schuh, & Weiss, 2015).

Viktor, Ana, Verica, Steva, and Branko (2011) have reported that the cellulose and carbohydrate polymers can be used as wall materials for encapsulation, due to its edibility, biodegradable, soft and form a barrier between the core and surroundings. While, De Barros, Lechner, Charalampopoulos, Khutoryanskiy, and Edwards (2015) reported that the cellulose can also help for the survival of probiotic cells during extrusion/spheroidization as well as excellent protection from gastric acid, whereas its improved over time, as the fabricated MCC calcium crosslinked alginate as the wall material. Furthermore, sphere disintegration efficiency and rapid release of the probiotics in intestinal conditions could be also be achieved with the combination of MCC and sodium alginate.

The application of an edible film, particularly taken and process directly from the fresh farm production is fundamentally constrained by the need to address diverse properties, i.e., cost, availability, functionality, mechanical properties, attributes, optical behavior, barrier effects against moisture and gases, and its resistance to microbes (Falguera, Quintero, Jiménez, Muñoz, & Ibarz, 2011). Cellulose such as MCC can be isolated from a variety of cellulosic sources and have been used to form composite films with clear improvements in its optical, mechanical properties, and thermal stability (Galus & Kadzińska, 2015; Mihranyan, 2011; Pereda, Amica, Rácz, & Marcovich, 2011; Suppakul, Jutakorn, & Bangchokedee, 2010).

1.4.2 Textile

To meet the rapidly growing demand for textile products and applications, cotton is not the only answer towards sustainability. Therefore, cellulose from wood-based fibers is another attractive alternative towards this sustainability issues, similarly, goes to algae and weeds (Mihranyan, 2011). Even though wood is a highly potential candidate to replace fossil materials, other sources need to be investigated, especially in current high demand of circular economy. Taking examples of high quality textiles made from lyocell fibers, it can be obtained from (i) pure cotton waste pulp, and (ii) blending with conventional dissolving pulp (Mihranyan, 2011). The staple fibers were repeatedly tested, and the results show the two of the studied

fibers had high tenacity and *E*-modulus that exceeded the staple fiber. In addition, the study of yarns was at least as good as the its spun, especially to its reference yarn and the commercial off-the-shelf yarn in terms of wet tenacity. Single jerseys made from the yarns shrunk less upon laundering, even though it could absorb at least as much water at a comparable rate. Dyeability, durability, staining, color fastness, and pilling tendency also showed that the two of the studied fiber tricots performed well and shows a promising results, especially for the special grade pulp to suit niche regenerated fiber products, or to spice up conventional wood-based dissolving pulp (Mihranyan, 2011).

1.5 Summary

In conclusion, cellulose had a high potential to be used to produce edible films, particularly taken from the fresh farm production, whereas it is fundamentally controlled by the need to address its diverse properties, i.e., cost, availability, functionality, mechanical properties, attributes, optical behavior, barrier effects against moisture and gases and resistance to microbes. Cellulose such as MCC can also be isolated from a variety of cellulosic sources and have been used to form composite films with clear improvements in the optical and mechanical properties and thermal stability. Therefore, many applications of cellulose can be explored and extensive research needed to be done in order to fill in the gaps and to create a sustainable environment.

Acknowledgment

The authors would like to thank and acknowledge Universiti Malaysia Sarawak (UNIMAS) for the support.

References

Ahmed, Z., Haque, S., Akhter, F., & Begum, M. (2003). Study of the chemical composition of different pipeline varieties of jute Fibres. *Pakistan Journal of Biological Sciences*, 1463–1467. https://doi.org/10.3923/pjbs.2003.1463.1467.

Ashley, Y. (2018). Naturally modified cellulose in bacterial biofilms. *Nature Reviews Microbiology*, 123. https://doi.org/10.1038/nrmicro.2018.22.

Augimeri, R. V., Varley, A. J., & Strap, J. L. (2015). Establishing a role for bacterial cellulose in environmental interactions: Lessons learned from diverse biofilm-producing Proteobacteria. *Frontiers in Microbiology*, 6. https://doi.org/10.3389/fmicb.2015.01282.

Björquist, S., Aronsson, J., Henriksson, G., & Persson, A. (2018). Textile qualities of regenerated cellulose fibers from cotton waste pulp. *Textile Research Journal*, *88*(21), 2485–2492. https://doi.org/10.1177/0040517517723021.

Bogino, P. C., Oliva, M.d.l. M., Sorroche, F. G., & Giordano, W. (2013). The role of bacterial biofilms and surface components in plant-bacterial associations. *International Journal of Molecular Sciences*, *14*(8), 15838–15859. https://doi.org/10.3390/ijms140815838.

Boluk, Y., Lahiji, R., Zhao, L., & McDermott, M. T. (2011). Suspension viscosities and shape parameter of cellulose nanocrystals (CNC). *Colloids and Surfaces A: Physicochemical and Engineering Aspects*, *377*(1–3), 297–303. https://doi.org/10.1016/j.colsurfa.2011.01.003.

Bonomi, A., Otavio, C., Cunha, M. P., & Lima, M. A. P. (2016). *Virtual biorefinery* (pp. 1–285). https://doi.org/10.1007/978-3-319-26045-7.

Bousfield, G., Morin, S., Jacquet, N., & Richel, A. (2018). Extraction and refinement of agricultural plant fibers for composites manufacturing. *Comptes Rendus Chimie*, *21*(9), 897–906. https://doi.org/10.1016/j.crci.2018.07.001.

Bridgeman, T. G., Jones, J. M., Shield, I., & Williams, P. T. (2008). Torrefaction of reed canary grass, wheat straw and willow to enhance solid fuel qualities and combustion properties. *Fuel*, *87*(6), 844–856.

Capron, I., & Cathala, B. (2013). Surfactant-free high internal phase emulsions stabilized by cellulose nanocrystals. *Biomacromolecules*, *14*(2), 291–296. https://doi.org/10.1021/bm301871k.

Cheng, S., Panthapulakkal, S., Sain, M., & Asiri, A. (2014). Aloe vera rind cellulose nanofibers-reinforced films. *Journal of Applied Polymer Science*, *131*(15). https://doi.org/10.1002/app.40592.

Chovau, S., Degrauwe, D., & Van Der Bruggen, B. (2013). Critical analysis of techno-economic estimates for the production cost of lignocellulosic bio-ethanol. *Renewable and Sustainable Energy Reviews*, *26*, 307–321. https://doi.org/10.1016/j.rser.2013.05.064.

da Silva, H. J. T., & Marques, P. V. (2017). Evolution of Production Costs in Brazilian Sugar-Energy Sector. *China-USA Business Review*. https://doi.org/10.17265/1537-1514/2017.03.001.

Daud, Z., Hatta, M. Z., Mohd, K., Awang, H., & Aripin, A. M. (2013). Analysis the chemical composition and Fiber morphology structure of corn stalk. *Australian Journal of Basic and Applied Sciences*, *7*(9), 401–405.

De Barros, J. M. S., Lechner, T., Charalampopoulos, D., Khutoryanskiy, V. V., & Edwards, A. D. (2015). Enteric coated spheres produced by extrusion/spheronization provide effective gastric protection and efficient release of live therapeutic bacteria. *International Journal of Pharmaceutics*, *493*(1–2), 483–494. https://doi.org/10.1016/j.ijpharm.2015.06.051.

Dickinson, E. (2013). Stabilising emulsion-based colloidal structures with mixed food ingredients. *Journal of the Science of Food and Agriculture*, *93*(4), 710–721. https://doi.org/10.1002/jsfa.6013.

Draman, S. F. S., Daik, R., & Mohd, N. (2016). Eco-friendly extraction and characterization of cellulose from Lignocellulosoic fiber. *ARPN Journal of Engineering and Applied Sciences*, *11*(16), 9591–9595. http://www.arpnjournals.org/jeas/research_papers/rp_2016/jeas_0816_4808.pdf.

Duan, L., Yu, W., & Li, Z. (2017). Analysis of structural changes in jute fibers after peracetic acid treatment. *Journal of Engineered Fibers and Fabrics*, *12*(1), 33–42. https://doi.org/10.1177/155892501701200104.

Falguera, V., Quintero, J. P., Jiménez, A., Muñoz, J. A., & Ibarz, A. (2011). Edible films and coatings: Structures, active functions and trends in their use. *Trends in Food Science and Technology*, *22*(6), 292–303. https://doi.org/10.1016/j.tifs.2011.02.004.

Fang, J. M., Sun, R. C., & Tomkinson, J. (2000). Isolation and characterization of hemicelluloses and cellulose from rye straw by alkaline peroxide extraction. *Cellulose*, *7*(1), 87–107. https://doi.org/10.1023/A:1009245100275.

Faruk, O., & Ain, M. S. (2013). Biofiber reinforced polymer composites for structural applications. In *Developments in Fiber-Reinforced Polymer (FRP) Composites for Civil Engineering* (pp. 18–53). Elsevier Inc. https://doi.org/10.1533/9780857098955.1.18.

Fortunati, E., Benincasa, P., Balestra, G. M., Luzi, F., Mazzaglia, A., Del Buono, D., et al. (2016). Revalorization of barley straw and husk as precursors for cellulose nanocrystals extraction and their effect on PVA_CH nanocomposites. *Industrial Crops and Products*, *92*, 201–217. https://doi.org/10.1016/j.indcrop.2016.07.047.

Freudenberg, K. (1932). The relation of cellulose to lignin in wood. *Journal of Chemical Education*, 1171. https://doi.org/10.1021/ed009p1171.

Galus, S., & Kadzińska, J. (2015). Food applications of emulsion-based edible films and coatings. *Trends in Food Science and Technology*, *45*(2), 273–283. https://doi.org/10.1016/j.tifs.2015.07.011.

Gandolfi, S., Ottolina, G., Riva, S., Fantoni, G. P., & Patel, I. (2013). Complete chemical analysis of carmagnola hemp hurds and structural features of its components. *BioResources*, *8*(2), 2641–2656. https://doi.org/10.15376/biores.8.2.2641-2656.

Gibis, M., Schuh, V., & Weiss, J. (2015). Effects of carboxymethyl cellulose (CMC) and microcrystalline cellulose (MCC) as fat replacers on the microstructure and sensory characteristics of fried beef patties. *Food Hydrocolloids*, *45*, 236–246. https://doi.org/10.1016/j.foodhyd.2014.11.021.

Gorgieva, S., & Trček, J. (2019). Bacterial cellulose: Production, modification and perspectives in biomedical applications. *Nanomaterials*, *9*(10). https://doi.org/10.3390/nano9101352.

Haigler, C. H., Betancur, L., Stiff, M. R., & Tuttle, J. R. (2012). Cotton fiber: A powerful single-cell model for cell wall and cellulose research. *Frontiers in Plant Science*, *3*(May). https://doi.org/10.3389/fpls.2012.00104.

Hamad, W. Y., & Hu, T. Q. (2010). Structure-process-yield interrelations in nanocrystalline cellulose extraction. *Canadian Journal of Chemical Engineering*, *88*(3), 392–402. https://doi.org/10.1002/cjce.20298.

Harding, W. G. (1921). Experiments on wood cellulose. *Journal of Physical Chemistry*, *25*(3), 201–203. https://doi.org/10.1021/j150210a003.

Harris, D., Bulone, V., Ding, S. Y., & DeBolt, S. (2010). Tools for cellulose analysis in plant cell walls. *Plant Physiology*, *153*(2), 420–426. https://doi.org/10.1104/pp.110.154203.

Hirasaka, T. (1976). Study on cellulose, a component of the artificial diet for silkworm larvae. *The Journal of Sericultural Science of Japan*, *45*(5), 426–430. https://doi.org/10.11416/kontyushigen1930.45.426.

Holland, C., Ryden, P., Edwards, C. H., & Grundy, M. M. L. (2020). Plant cell walls: Impact on nutrient bioaccessibility and digestibility. *Food*, *9*(2). https://doi.org/10.3390/foods9020201.

Howard, R. L., Abotsi, E., van Rensburg, E. L. J., & Howard, S. (2003). Lignocellulose biotechnology: Issues of bioconversion and enzyme production. *African Journal of Biotechnology*, 602–619. https://doi.org/10.5897/AJB2003.000-1115.

Hu, Z., Ballinger, S., Pelton, R., & Cranston, E. D. (2015). Surfactant-enhanced cellulose nanocrystal Pickering emulsions. *Journal of Colloid and Interface Science*, *439*, 139–148. https://doi.org/10.1016/j.jcis.2014.10.034.

Huang, H. J., Ramaswamy, S., Al-Dajani, W., Tschirner, U., & Cairncross, R. A. (2009). Effect of biomass species and plant size on cellulosic ethanol: A comparative process and economic analysis. *Biomass and Bioenergy*, *33*(2), 234–246. https://doi.org/10.1016/j.biombioe.2008.05.007.

Islam, J. M. M., Hossan, M. A., Alom, F. R., Khan, M. I. H., & Khan, M. A. (2017). Extraction and characterization of crystalline cellulose from jute fiber and application as reinforcement in biocomposite: Effect of gamma radiation. *Journal of Composite Materials*, *51*(1), 31–38. https://doi.org/10.1177/0021998316636455.

Ito, T. (1960). Effect of sugars on feeding of larvae of the silkworm, *Bombyx mori*. *Journal of Insect Physiology*, *5*(2), 95–107. https://doi.org/10.1016/0022-1910(60)90035-4.

Jia, X., Chen, Y., Shi, C., Ye, Y., Abid, M., Jabbar, S., et al. (2014). Rheological properties of an amorphous cellulose suspension. *Food Hydrocolloids*, *39*, 27–33. https://doi.org/10.1016/j.foodhyd.2013.12.026.

John, N.-A., Maoshen, C., Douglas, G. H., Fang, Z., Rizwan, S. H., & Yue, L. (2017). Functionality and nutritional aspects of microcrystalline cellulose in food. *Carbohydrate Polymers*, 159–174. https://doi.org/10.1016/j.carbpol.2017.04.021.

Kalashnikova, I., Bizot, H., Cathala, B., & Capron, I. (2011). New pickering emulsions stabilized by bacterial cellulose nanocrystals. *Langmuir*, *27*(12), 7471–7479. https://doi.org/10.1021/la200971f.

Kapoor, M., Panwar, D., & Kaira, G. S. (2016). Bioprocesses for enzyme production using agro-industrial wastes: Technical challenges and commercialization potential. In *Agro-industrial wastes as feedstock for enzyme production: apply and exploit the emerging and valuable use options of waste biomass* (pp. 61–93). Elsevier Inc. https://doi.org/10.1016/B978-0-12-802392-1.00003-4.

Klemm, D., Heublein, B., Fink, H. P., & Bohn, A. (2005). Cellulose: Fascinating biopolymer and sustainable raw material. *Angewandte Chemie, International Edition*, *44*(22), 3358–3393. https://doi.org/10.1002/anie.200460587.

Klemm, D., Philipp, B., Heinze, T., Heinze, U., & Wagenknecht, W. (1998). Fundamentals and analytical methods. In *Vol. 1. Comprehensive Cellulose Chemistry* Wiley. https://doi.org/10.1002/3527601929.

Klemm, D., Schmauder, H.-P., & Heinze, T. (2005). Cellulose. *Chemistry, Biotechnology, Applications*, *1*, 275–287. https://doi.org/10.1002/3527600035.bpol6010.

Kost, B., & Chua, N.-H. (2002). The plant cytoskeleton: Vacuoles and cell walls make the difference. *Cell*, *108*(1), 9–12. https://doi.org/10.1016/s0092-8674(01)00634-1.

Kouadri, I., & Satha, H. (2018). Extraction and characterization of cellulose and cellulose nanofibers from Citrullus colocynthis seeds. *Industrial Crops and Products*, *124*, 787–796. https://doi.org/10.1016/j.indcrop.2018.08.051.

Krassig, H. A. (1993). *Cellulose, structure, accessibility and reactivity*. https://doi.org/10.1002/pola.1994.080321221.

Kumar, R., Tabatabaei, M., Karimi, K., & Horváth, I. S. (2016). Recent updates on lignocellulosic biomass derived ethanol—A review. *Biofuel Research Journal*, *3*(1), 347–356. https://doi.org/10.18331/BRJ2016.3.1.4.

Li, H., Kim, N. J., Jiang, M., Kang, J. W., & Chang, H. N. (2009). Simultaneous saccharification and fermentation of lignocellulosic residues pretreated with phosphoric acid-acetone for bioethanol production. *Bioresource Technology*, *100*(13), 3245–3251. https://doi.org/10.1016/j.biortech.2009.01.021.

Li, Z., Li, Z., Ding, R., & Yu, C. (2016). Composition of ramie hemicelluloses and effect of polysaccharides on fiber properties. *Textile Research Journal*, *86*(5), 451–460. https://doi.org/10.1177/0040517515592811.

Macmillan, C. P., Birke, H., Bedon, F., & Pettolino, F. A. (2013). Lignin deposition in cotton cells—Where is the lignin? *Journal of Plant Biochemistry*, *1*(2), 1–4. https://doi.org/10.4172/jpbp.1000e106.

Martin, M. M. (1983). Cellulose digestion in insects. *Comparative Biochemistry and Physiology—Part A: Physiology*, *75*(3), 313–324. https://doi.org/10.1016/0300-9629(83)90088-9.

Martin, M. M. (1991). The evolution of cellulose digestion in insects. *Philosophical Transactions of the Royal Society of London, Series B: Biological Sciences*, 281–288. https://doi.org/10.1098/rstb.1991.0078.

Masłowski, M., Miedzianowska, J., Strąkowska, A., Strzelec, K., & Szynkowska, M. I. (2018). The use of rye, oat and triticale straw as fillers of natural rubber composites. *Polymer Bulletin*, *75*(10), 4607–4626. https://doi.org/10.1007/s00289-018-2289-y.

Mercedes, B., & Ricardo, G. (2016). Living together in biofilms: The microbial cell factory and its biotechnological implications. *Microbial Cell Factories*. https://doi.org/10.1186/s12934-016-0569-5.

Merino, S. T., & Cherry, J. (2007). Progress and challenges in enzyme development for biomass utilization. *Advances in Biochemical Engineering/Biotechnology*, *108*, 95–120. https://doi.org/10.1007/10_2007_066.

Mihranyan, A. (2011). Cellulose from cladophorales green algae: From environmental problem to high-tech composite materials. *Journal of Applied Polymer Science*, *119*(4), 2449–2460. https://doi.org/10.1002/app.32959.

Msimango, N. N. P., & Fon, F. N. (2016). Monitoring the fibrolytic potential of microbial ecosystems from domestic and wild ruminants browsing tanniferous forages. *Animal Nutrition*, *2*(1), 40–44. https://doi.org/10.1016/j.aninu.2015.11.011.

Mullen, A. M., Álvarez, C., Pojić, M., Hadnadev, T. D., & Papageorgiou, M. (2015). Classification and target compounds. In *Food waste recovery: Processing technologies and industrial techniques* (pp. 25–57). Elsevier Inc. https://doi.org/10.1016/B978-0-12-800351-0.00002-X.

Nabili, A., Fattoum, A., Passas, R., & Elaloui, E. (2016). Extraction and characterization of cellulose from date palm seeds (*Phoenix dactylifera* L.). *Cellulose Chemistry and Technology*, *50*, 1015–1023.

Nishimura, N., Izumi, A., & Kuroda, K. I. (2002). Structural characterization of kenaf lignin: Differences among kenaf varieties. *Industrial Crops and Products*, *15*(2), 115–122. https://doi.org/10.1016/S0926-6690(01)00101-7.

Oza, K. P., & Frank, S. G. (1989). Multiple emulsions stabilized by colloidal microcrystalline cellulose. *Journal of Dispersion Science and Technology*, *10*(2), 163–185. https://doi.org/10.1080/01932698908943168.

Pääkkö, M., Ankerfors, M., Kosonen, H., Nykänen, A., Ahola, S., Österberg, M., et al. (2007). Enzymatic hydrolysis combined with mechanical shearing and high-pressure homogenization for nanoscale cellulose fibrils and strong gels. *Biomacromolecules*, 1934–1941. https://doi.org/10.1021/bm061215p.

Pandey, A. (2008). Handbook of plant-based biofuels. In *Handbook of plant-based biofuels* (pp. 1–299). CRC Press. https://doi.org/10.1201/9780789038746.

Paulraj, T., Wennmalm, S., Wieland, D. C. F., Riazanova, A. V., Dėdinaitė, A., Pomorski, T. G., et al. (2020). Primary cell wall inspired micro containers as a step towards a synthetic plant cell. *Nature Communications*. https://doi.org/10.1038/s41467-020-14718-x.

Pauly, M., & Keegstra, K. (2008). Cell-wall carbohydrates and their modification as a resource for biofuels. *Plant Journal*, *54*(4), 559–568. https://doi.org/10.1111/j.1365-313X.2008.03463.x.

Payen, A. (1838). Mémoire sur la composition du tissu propre des plantes et du ligneux. *Comptes Rendus*, *7*(1), 1052–1056.

Peng, F., & Sun, R. C. (2010). Modification of cereal straws as natural sorbents for removing metal ions from industrial waste water. In *Cereal straw as a resource for sustainable biomaterials and biofuels* (pp. 219–237). Elsevier. https://doi.org/10.1016/B978-0-444-53234-3.00008-0.

Pereda, M., Amica, G., Rácz, I., & Marcovich, N. E. (2011). Structure and properties of nanocomposite films based on sodium caseinate and nanocellulose fibers. *Journal of Food Engineering*, *103*(1), 76–83. https://doi.org/10.1016/j.jfoodeng.2010.10.001.

Pereira Oliveira Moreira, R. L., Simão, J. A., Gouveia, R. F., & Strauss, M. (2020). Exploring the hierarchical structure and alignment of wood cellulose fibers for bioinspired anisotropic polymeric composites. *ACS Applied Bio Materials*, *3*(4), 2193–2200. https://doi.org/10.1021/acsabm.0c00038.

Petrova, O. E., & Sauer, K. (2012). Sticky situations: Key components that control bacterial surface attachment. *Journal of Bacteriology*, *194*(10), 2413–2425. https://doi.org/10.1128/JB.00003-12.

Purnawati, R., Febrianto, F., Wistara, I. N. J., Nikmatin, S., Hidayat, W., Lee, S. H., et al. (2018). Physical and chemical properties of kapok (*Ceiba pentandra*) and balsa (*Ochroma pyramidale*) fibers. *Journal of the Korean Wood Science and Technology*, *46*(4), 393–401. https://doi.org/10.5658/WOOD.2018.46.4.393.

Qiyuan, C., Shengling, X., Shi, S., & Liping, C. (2018). Isolation of cellulose from poplar wood by nitric acid-ethanol treatment and its effect on the quality of films cast from ionic liquid. *BioResources*. https://doi.org/10.15376/biores.13.4.8943-8955.

Rahman, M. R., & Bakri, M. K. B. (2021). Bamboo Cellulose Gel/MMT Polymer Nanocomposites for High Strength Materials. In M. R. Rahman (Ed.), *Bamboo Polymer Nanocomposites*. *Engineering Materials*. Cham: Springer. https://doi.org/10.1007/978-3-030-68090-9_7.

Rahman, M. R., Hamdan, S., Ngaini, Z. B., et al. (2019). Cellulose fiber-reinforced thermosetting composites: impact of cyanoethyl modification on mechanical, thermal and morphological properties. *Polym. Bull.*, *76*, 4295–4311. https://doi.org/10.1007/s00289-018-2598-1.

Rahman, N. H. A., Chieng, B. W., Ibrahim, N. A., & Rahman, N. A. (2017). Extraction and characterization of cellulose nanocrystals from tea leaf waste fibers. *Polymers*, *9*(11). https://doi.org/10.3390/polym9110588.

Rajasundaram, D., Runavot, J. L., Guo, X., Willats, W. G. T., Meulewaeter, F., & Selbig, J. (2014). Understanding the relationship between cotton fiber properties and noncellulosic cell wall polysaccharides. *PLoS One*, *9*(11). https://doi.org/10.1371/journal.pone.0112168.

Rashid, N. A. N. A., Husin, M., Yury, N., Othman, M., Shariff, Z. M., Kassim, H., et al. (2019). Cellulose isolation from leucaena leucocephala seed: Effect on concentration sodium hydroxide. *Journal of Academia UiTM Negeri Sembilan*, *7*(2), 36–45. https://doi.org/10.24191/jfast.v7i2.7184.

Reddy, N., & Yang, Y. (2007). Structure and properties of natural cellulose fibers obtained from sorghum leaves and stems. *Journal of Agricultural and Food Chemistry*, *55*(14), 5569–5574. https://doi.org/10.1021/jf0707379.

Reddy, N., & Yang, Y. (2009). Extraction and characterization of natural cellulose fibers from common milkweed stems. *Polymer Engineering and Science*, *49*(11), 2212–2217. https://doi.org/10.1002/pen.21469.

Reddy, N., Yang, Y., Reddy, N., & Yang, Y. (2015). *Fibers from banana pseudo-stems* (pp. 25–27). Berlin Heidelberg: Springer. https://doi.org/10.1007/978-3-662-45136-6_7.

Rosales-Calderon, O., & Arantes, V. (2019). A review on commercial-scale high-value products that can be produced alongside cellulosic ethanol. *Biotechnology for Biofuels*, *12* (1). https://doi.org/10.1186/s13068-019-1529-1.

Rosales-Calderon, O., Trajano, H. L., Posarac, D., & Duff, S. J. B. (2016). Modeling of oxygen delignified wheat straw enzymatic hydrolysis as a function of hydrolysis time, enzyme concentration, and lignin content. *Industrial Biotechnology*, *12*(3), 176–186. https://doi.org/10.1089/ind.2015.0037.

Rowell, R. M., Pettersen, R., & Tshabalala, M. A. (2012). Cell wall chemistry. In *Handbook of Wood Chemistry and Wood Composites* (2nd ed., pp. 33–72). CRC Press. https://doi.org/10.1201/b12487.

Rühs, P. A., Storz, F., López Gómez, Y. A., Haug, M., & Fischer, P. (2018). 3D bacterial cellulose biofilms formed by foam templating. *Npj Biofilms and Microbiomes*, *4*(1). https://doi.org/10.1038/s41522-018-0064-3.

Runavot, J. L., Guo, X., Willats, W. G. T., Knox, J. P., Goubet, F., & Meulewaeter, F. (2014). Non-cellulosic polysaccharides from cotton fibre are differently impacted by textile processing. *PLoS One*, *9*(12). https://doi.org/10.1371/journal.pone.0115150.

Russell, J. B., Muck, R. E., & Weimer, P. J. (2009). Quantitative analysis of cellulose degradation and growth of cellulolytic bacteria in the rumen. *FEMS Microbiology Ecology*, *67* (2), 183–197. https://doi.org/10.1111/j.1574-6941.2008.00633.x.

Sarkar, P., Bosneaga, E., & Auer, M. (2009). Plant cell walls throughout evolution: Towards a molecular understanding of their design principles. *Journal of Experimental Botany*, *60* (13), 3615–3635. https://doi.org/10.1093/jxb/erp245.

Saura-Calixto, F., Cañellas, J., & Garcia-Raso, J. (1983). Determination of hemicellulose, cellulose and lignin contents of dietary fibre and crude fibre of several seed hulls. Data comparison. *Zeitschrift für Lebensmittel-Untersuchung und -Forschung*, *177*(3), 200–202. https://doi.org/10.1007/BF01146796.

M. Saxena, R.M. Brown Jr (2001). (pp. 69–76). Elsevier BV. doi:https://doi.org/10.1016/s0921-0423(01)80057-5.

Serra, D. O., Richter, A. M., & Hengge, R. (2013). Cellulose as an architectural element in spatially structured *Escherichia coli* biofilms. *Journal of Bacteriology*, *195*(24), 5540–5554. https://doi.org/10.1128/JB.00946-13.

Shawky, B. T., Mahmoud, M. G., Ghazy, E. A., Asker, M. M. S., & Ibrahim, G. S. (2011). Enzymatic hydrolysis of rice straw and corn stalks for monosugars production. *Journal, Genetic Engineering & Biotechnology*, *9*(1), 59–63. https://doi.org/10.1016/j.jgeb.2011.05.001.

Sheltami, R. M., Abdullah, I., Ahmad, I., Dufresne, A., & Kargarzadeh, H. (2012). Extraction of cellulose nanocrystals from mengkuang leaves (Pandanus tectorius). *Carbohydrate Polymers*, *88*(2), 772–779. https://doi.org/10.1016/j.carbpol.2012.01.062.

Shilin, C., Xiaojuan, M., Ling, L., Fang, H., Liulian, H., & Lihui, C. (2014). Morphological and chemical characterization of green bamboo (Dendrocalamopsis oldhami (Munro) Keng f.) for dissolving pulp production. *BioResources*. https://doi.org/10.15376/biores.9.3.4528-4539.

Siddhanta, A. K., Prasad, K., Meena, R., Prasad, G., Mehta, G. K., Chhatbar, M. U., et al. (2009). Profiling of cellulose content in Indian seaweed species. *Bioresource Technology*, *100*(24), 6669–6673. https://doi.org/10.1016/j.biortech.2009.07.047.

Sorieul, M., Dickson, A., Hill, S. J., & Pearson, H. (2016). Plant fibre: Molecular structure and biomechanical properties, of a complex living material, influencing its deconstruction towards a biobased composite. *Materials*, *9*(8), 1–36. https://doi.org/10.3390/ma9080618.

Stevulova, N., Cigasova, J., Estokova, A., Terpakova, E., Geffert, A., Kacik, F., et al. (2014). Properties characterization of chemically modified hemp hurds. *Materials*, *7*(12), 8131–8150. https://doi.org/10.3390/ma7128131.

Sulaiman, S., Mokhtar, M. N., Naim, M. N., Baharuddin, A. S., Salleh, M. A. M., & Sulaiman, A. (2016). Penghasilan nano-gentian selulosa (CNF) diperolehi daripada gentian kulit kenaf dan potensinya sebagai penyokong pemegunan enzim. *Malaysian Journal of Analytical Sciences*, *20*(2), 309–317. https://doi.org/10.17576/mjas-2016-2002-12.

Sun, J. X., Sun, X. F., Zhao, H., & Sun, R. C. (2004). Isolation and characterization of cellulose from sugarcane bagasse. *Polymer Degradation and Stability*, *84*(2), 331–339. https://doi.org/10.1016/j.polymdegradstab. 2004.02.008.

Suppakul, P., Jutakorn, K., & Bangchokedee, Y. (2010). Efficacy of cellulose-based coating on enhancing the shelf life of fresh eggs. *Journal of Food Engineering*, *98*(2), 207–213. https://doi.org/10.1016/j.jfoodeng.2009.12.027.

Tavernier, I., Wijaya, W., Van der Meeren, P., Dewettinck, K., & Patel, A. R. (2016). Food-grade particles for emulsion stabilization. *Trends in Food Science and Technology*, *50*, 159–174. https://doi.org/10.1016/j.tifs.2016.01.023.

Van Dyk, J. S., & Pletschke, B. I. (2012). A review of lignocellulose bioconversion using enzymatic hydrolysis and synergistic cooperation between enzymes-factors affecting enzymes, conversion and synergy. *Biotechnology Advances*, *30*(6), 1458–1480. https://doi.org/10.1016/j.biotechadv.2012.03.002.

Viktor, N., Ana, K., Verica, M., Steva, L., & Branko, B. (2011). An overview of encapsulation technologies for food applications. *Procedia Food Science*, 1806–1815. https://doi.org/10.1016/j.profoo.2011.09.265.

Vishtal, A., & Kraslawski, A. (2011). Challenges in industrial applications of technical lignins. *BioResources*, *6*(3), 3547–3568. http:/www.ncsu.edu/bioresources/BioRes_06/BioRes_06_3_3547_Vishtal_K_Challeng_Indust_Appl_Techn_Lignins_1744.pdf.

Wan, C. W.-H., & Cameron, F. K. (1942). Cellulose content of cotton and southern woods. *Industrial and Engineering Chemistry*, 224–225. https://doi.org/10.1021/ie50386a018.

Wang, L., Zhang, X., Xu, G., Xu, H., & Wu, J. (2014). Using lignin content, cellulose content, and cellulose crystallinity as indicators of wood decay in *Juglans mandshurica* Maxim. and *Pinus koraiensis*. *BioResources*, *9*(4), 6205–6213. https://doi.org/10.15376/biores.9.4.6205-6213.

Wang, W., Du, G., Li, C., Zhang, H., Long, Y., & Ni, Y. (2016). Preparation of cellulose nanocrystals from asparagus (*Asparagus officinalis* L.) and their applications to palm oil/water Pickering emulsion. *Carbohydrate Polymers*, *151*, 1–8. https://doi.org/10.1016/j.carbpol.2016.05.052.

Watanabe, H., & Tokuda, G. (2010). Cellulolytic systems in insects. *Annual Review of Entomology*, *55*, 609–632. https://doi.org/10.1146/annurev-ento-112408-085319.

Winuprasith, T., & Suphantharika, M. (2015). Properties and stability of oil-in-water emulsions stabilized by microfibrillated cellulose from mangosteen rind. *Food Hydrocolloids*, *43*, 690–699. https://doi.org/10.1016/j.foodhyd.2014.07.027.

Woodings, C. (2016). *Cellulose fibers, regenerated* (pp. 1–48). Wiley. https://doi.org/10.1002/0471440264.pst046.pub2.

Xing, Y., Jones, P., Bosch, M., Donnison, I., Spear, M., & Ormondroyd, G. (2018). Exploring design principles of biological and living building envelopes: What can we learn from

plant cell walls? *Intelligent Buildings International*, *10*(2), 78–102. https://doi.org/10.1080/17508975.2017.1394808.

Xu, D., Zhang, J., Cao, Y., Wang, J., & Xiao, J. (2016). Influence of microcrystalline cellulose on the microrheological property and freeze-thaw stability of soybean protein hydrolysate stabilized curcumin emulsion. *LWT*, *66*, 590–597. https://doi.org/10.1016/j.lwt.2015.11.002.

Yahya, N. Y., Ngadi, N., & Muhamad, I. I. (2014). Extraction and characterization of cellulose from pandan leaves (Pandanusamaryllifolius Roxb.). *Research Journal of Chemistry and Environment*, *18*(1), 82–88.

Yan, Y. (2016). Developments in fibers for technical nonwovens. In *Advances in Technical Nonwovens* (pp. 19–96). Elsevier Inc. https://doi.org/10.1016/B978-0-08-100575-0.00002-4.

Yao, S., Wu, G., Xing, M., Zhou, S., & Pu, J. (2010). Determination of lignin content in Acacia spp. using near-infrared reflectance spectroscopy. *BioResources*, *5*(2), 556–562. http://www.ncsu.edu/bioresources/BioRes_05/BioRes_05_2_0556_Yao_WXZP_Deter_Lignin_Acacia_NIR_Reflec_Spectrosc_620.pdf.

Zuraida, A., Maisarah, T., & Wan-Shazlin-Maisarah, W. M. Y. (2017). Mechanical, physical and thermal properties of rattan fibre-based binderless board. *Journal of Tropical Forest Science*, *29*(4), 485–492. https://doi.org/10.26525/jtfs2017.29.4.485492.

CHAPTER

Extraction, types, and classification of cellulose

2

Muhammad Khusairy Bin Bakri and Md Rezaur Rahman

Department of Chemical Engineering and Energy Sustainability, Faculty of Engineering, Universiti Malaysia Sarawak (UNIMAS), Kota Samarahan, Sarawak, Malaysia

Chapter outline

2.1 Introduction

Carbohydrate such as cellulose consist of several sugar molecules that are bonded together. Cellulose is also considered as a polysaccharide. Cellulose is composed of a linear chain of β-1,4 linked D-glucose units with a degree of polymerization

Fundamentals and Recent Advances in Nanocomposites Based on Polymers and Nanocellulose.
https://doi.org/10.1016/B978-0-323-85771-0.00003-8

ranged from several hundreds to over ten thousand, which is the most abundant organic polymer on the earth (Sun, Sun, Cao, & Sun, 2016). Human cannot digest cellulose, but it is important as fiber as a dietary. Cellulose also can be synthesized by many living organisms ranging from bacterium, such as *Acetobacter xylinum* to forest trees (Saxena & Brown, 2001). *Acetobacter xylinum* produces abundant amounts of cellulose and this bacterium has been used as a model system for studies on cellulose biosynthesis and structure of the cellulose product. Other than that, cellulose extraction from algae also showed high potential as a model system for studies. Cellulose is a tough due to its fibrous structure and water-insoluble polysaccharide, which plays an integral role in keeping the structure of plant cell walls stable (Brigham, 2017; Bringmann et al., 2012). The plant cell wall is made up from cellulose chains that are arranged in microfibrils or bundles of polysaccharide that are arranged in fibrils (bundles of microfibrils) (Rahman et al., 2019). This showed that the arrangement stabilizes and supports the plant structures, which created cellulosic biomaterial with high strength and other superior mechanical properties (Brigham, 2017).

Cellulose is generally synthesized by an enzyme cellulose synthase, which is a membrane protein. It is a direct polymerization catalyzes of glucose into a cellulose product from the substrate UDP-glucose (Saxena & Brown, 2000). Cellulose synthase is a complex of enzymes that spans the cell membrane in plants and span the entire cell wall in the case of bacteria. The key intermediate in cellulose synthesis in both plants and bacteria is UDP-glucose (UDP-GLC). The cellulose synthase complex uses the glucose moiety from UDP-GLC, which adds the monomer to the nascent extracellular cellulose chain and transports the glucose across the cell wall cell or membrane (Brown, Willison, & Richardson, 1976; Endler, Sánchez-Rodríguez, & Persson, 2010).

At the international level, many researchers have gained their attention on producing more sustainable and environmentally friendly materials, which includes for the search for alternatives to petroleum-based materials (Rahman, Adamu, & Hamdan, 2021; Rahman et al., 2019; Adamu, Rahman, Bakri, Md Yusof, & Khan, 2021). The development of biomaterials related to cellulose may hold a great promise, especially to mitigate many of the sustainability problems, which offered the potential of renewability, biodegradation, and creation of harmful additives. This contributed many researches focuses on the use of cellulosic waste as filler, which over the past few decades have grown rapidly. Agricultural cellulosic wastes such as banana (Harini, Ramya, & Sukumar, 2018; Zuluaga et al., 2009), cassava bagasse (Neftalí et al., 2018; Rosa et al., 2010), coconut (Pasquini, Teixeira, Curvelo, Belgacem, & Dufresne, 2010; Widiarto, Yuwono, Rochliadi, & Arcana, 2017), mulberry (Li, Fei, et al., 2009; Li, Zhou, & Zhang, 2009; Liu, Jiang, & Yao, 2011), soybean (Alemdar & Sain, 2008; Merci, Urbano, Grossmann, Tischer, & Mali, 2015; Reddy & Yang, 2009; Wang & Sain, 2007), wheat (Sun & Tomkinson, 2005; Sun, Sun, Cao, & Sun, 2016), and corns (Costa et al., 2015; Maepa et al., 2015; Reddy & Yang, 2005) have been studied as the production of cellulose resources. In many literatures, numerous terms have been used to describe these celluloses

in their forms, such as in nanoparticles, which includes cellulose nanocrystals, nanowhiskers, mono-crystals, microcrystals, or microcrystallites, and nanocrystalline cellulose (NCC) (Siqueira, Tapin-Lingua, Bras, da Silva Perez, & Dufresne, 2011). Even though a many variety of cellulose materials were investigated extensively, widely, the natural source to produce commercialize cellulose has not been explored yet. Therefore, in this chapter, the extraction/isolation method of the cellulose, types and classification of cellulose and the possibility and the used of commercialize cellulose will be discussed.

2.2 Extraction/isolation method of cellulose

On Earth, the most abundant naturally occurring polymer is called cellulose, which is considered a potential candidate for reinforcing agent or fillers such in the form of nanoparticles (Frone, Panaitescu, & Donescu, 2011; Haymes, Ibrahim, Mischke, Scott, & Saunders, 2004; Khine & Stenzel, 2020). The characteristic of cellulose such as high degree of crystallinity and its stiffness preferably well-matched for reinforcing and load bearing in composites applications. Compared with most fillers use today, cellulose is inexpensive, lightweight, sustainable as resources, naturally biodegradable, and has a much lower density. Cellulose is also known material for bioethanol production (Pulidindi, Kimchi, & Gedanken, 2014; Rosales-Calderon & Arantes, 2019; Zheng, Pan, & Zhang, 2009). Depends on the needed dimensions of the fibers, the cellulose extraction/isolation method may come from plant waste such as agricultural or wood (Bhattacharya, Germinario, & Winter, 2008; Nuruddin et al., 2011; Reddy & Yang, 2006).

2.2.1 Cellulose extraction/isolation by using alkaline

Cellulose is extracted/isolated by removing the greater part of lignin and hemicellulose structures, whereas most of this dried plant tissue is digested at the temperature of 80°C in a 4 wt% sodium hydroxide solution for about 4 h. By bleaching the plants with a mixture of sodium chloride and glacial acetic acid persistent discoloration of the product happened due to removal of any residual lignin and hemicellulose that may have been present. Another method is by bleaching the cellulose fibers, by repeatedly washed it with a 5 wt% of aqueous sodium hydroxide (NaOH), and subsequently deionized water in order to attain a neutral pH (Bhattacharya et al., 2008). Fang et al. (Fang, Sun, & Tomkinson, 2000) used a mixture of wt% alkaline solution ($NaOH/H_2O$; 1 g/100 mL) into 20 wt% hydrogen peroxide solution (H_2O_2/H_2O; 33.36 g/166.7 mL) to create alkaline hydrogen peroxide (AHP) solution. In a stainless-steel digester, for 35 min, 2.5 g of dewaxed wheat straw (DWS) was isolated in 30 mL of AHP solution at 121°C. The residue of the DWS_{AHP}, which is in white color was washed thoroughly after some time with distilled water until it neutralizes and free from excessive chemicals. The residues were filtered and dry in an oven at 75°C. From their results, it shows that less time needed for the alkaline hydrogen

peroxide treatment, however, comparatively it produced less yield of 79% (Fang et al., 2000). This AHP treatment is eco-friendly and chlorine free. Fang et al. (2000)) run an experiment by extracting the water-treated rye straw with 2 wt% of H_2O_2 at pH 11.5 at 20°C, 30°C, 40°C, 50°C, 60°C, and 70°C for 12 h. It shows that it released 44.2–71.9 wt% and 52.7%–87.8% of hemicelluloses and lignin, respectively. Compared with the treatment of the rye straw with a dilute alkaline solution at pH 11.5 at 50°C for 12 h, yielded around 7.3% and 7.4% of hemicelluloses and lignin, respectively with consideration in the absence of H_2O_2. As compared to the hemicelluloses isolated with alkali from delignified rye straw, it shows that under the conditions used for the alkaline peroxide treatment of the straw did not affect the overall structure of the hemicelluloses during the isolation.

2.2.2 Cellulose extraction/isolation by using dilute acid

In order to more remove lignin and hemicelluloses efficiently from biomass during the cellulose isolation, the dilute acid pretreatment is performed (Esteghlalian, Hashimoto, Fenske, & Penner, 1997; Pingali et al., 2010; Shell, Jody, Millie, & McMillan, 2003). Wiley milled is used by air-dried the plant to pass through the 20-mesh screen or 0.05 mm pore size. The Wiley milled material was then presoaked at a room temperature of 25°C, while continuous stirring for 4 h is done with around 1% dilute sulfuric acid solution. The solid material is washed from the presoaked slurry, which has been filtered with an excess of deionized water to neutralize the pH materials (Radotić & Mićić, 2016). The presoaked was then transferred and sealed with around 1% dilute sulfuric acid solution into a 4560 mini-Parr 300 mL pressure reactor. The pressure vessel is heated up to 160°C for around 30 min (at around 6°C/min). As it stable, the reactor is held at 160°C at the pressure of 6.4–6.8 atm for the specified residence time of 2, 5, and 10 min. After sometimes, the pretreatment process was then halted by quenched the reactor in an ice bath to cool to 70°C (Himmel et al., 2007; Radotić & Mićić, 2016). The pretreated slurry is then filtered and washed with an excess of deionized water to remove the solid residue, before dried overnight at room temperature. After pretreatment, all yields for biomass recovered range between 75% and 85% by mass of the initial material (Himmel et al., 2007; Radotić & Mićić, 2016). Pretreatment of biomass using hot dilute sulfuric acid increases digestibility of hemicellulose and lignin by its dissolution and redistribution (Himmel et al., 2007; Radotić & Mićić, 2016). This pretreatment method annealed the cellulose due the removal of hemicellulose and hydrothermal conditions, which increase crystallinity and limit its efficiency. The pretreatment also showed that cellulose network structural does not show any signs of breakdown, but there are changes in the lignin structure (Himmel et al., 2007; Radotić & Mićić, 2016).

Huntley, Crews, Abdalla, Russell, and Curry (2015) carried out cellulose extractions from wheat straw via hydrochloric, nitric, and sulfuric acid hydrolysis methods. Depending on the acid conditions used, a mixture of polymorphs appeared in the structure of the cellulose, which was revealed based on x-ray diffraction (XRD)

spectral analyses. In addition, as determined by XRD and scanning electron microscopy (SEM), the percent crystallinity, length, and diameter of the cellulose fibers varied tremendously. SEM also revealed that during the drying process, the aggregation of cellulose fibers is strongly dependent upon acids concentration and the drying process. As referred to acid concentrations and conditions, the thermal gravimetric analysis (TGA) revealed that the thermal stability of the extracted cellulose may vary (Huntley et al., 2015). Michael (2012) studied the effect of temperature and sulfuric acid concentration on the structure and other properties of cellulose. In the range of the sulfuric acid concentration from 50 to 60 wt%, the initial solubility of the sample at the room temperature gradually increased. As sulfuric acid concentration reached 65 wt%, microcrystalline cellulose sample dissolved completely. Cellulose regenerated by the concentration 65 wt% sulfuric acid had an amorphized structure and high enzymatic digestibility. At increased temperature of 45°C, the yield and degree of polymerization decreased, while the microcrystalline cellulose solubility in sulfuric acid was higher (Michael, 2012). Microcrystalline cellulose after treatment with hot 50–60 wt% sulfuric acid, the crystallinity degree of the cellulose samples slightly changed, and crystalline polymorph is retained. However, as the sulfuric acid concentration reached 65 wt%, the regenerated cellulose had crystalline polymorph, low degree of polymerization and reduced crystallinity degree. With optimum conditions, the acidic treatment in combination with the high-power disintegration may obtained nanocrystalline cellulose particles having sizes of 150–200 × 10–20 nm with the heightened yield of 65%–70%. Therefore, for various composites, nanocrystalline cellulose particles have high potential for used as a reinforced nanofillers (Michael, 2012).

2.2.3 Cellulose extraction/isolation by using ultrasound

Sequential treatment is needed for isolation of cellulose using alkaline peroxide with ultrasonic treatment, which both comprise of the plant to be soaked in the alkaline solution at 55°C for 2 h, follow up with irradiation by ultrasonic for 40 min (Radotić & Mićić, 2016). Subsequently, the material then is treated with 0.5 M NaOH, 0.5%, 1.0%, 1.5%, 2.0%, and 3.0% H_2O_2 in 0.5 M NaOH, and 2 M NaOH at 55°C for 2 h (Radotić & Mićić, 2016). By filtration, the insoluble residue is collected and washed with distilled water until the pH is neutral, before dried at 60°C (Sun, Sun, Zhao, & Sun, 2004). Further isolated cellulose fiber processing, such as nanofibers can be obtained by many methods, using biological, chemical, physical, and mechanical approaches. Therefore, the optimal method mostly rested on the final aimed dimensions of the nanofibers (Frone et al., 2011). Ngo, Hang, Dinh, Cuong, and Hung (2017) conducted a research on the extraction process of cellulose and lignin from rice straw without paraffin pretreatment. With ultrasonic irradiation treatment for 30 min, the rice straw increased yields of lignin separation from 72.8% to 84.7%. When combined for the same yields of extraction with ultrasonic irradiation, the extraction time was reduced from 2.5 to 1.5 h (Ngo et al., 2017). From the modern analytical methods, the results indicated that lignin obtained by ultrasound-assisted

alkaline treatment had a high purity and higher molecular weight than lignin extracted from rice straw without ultrasonic irradiation. The cellulose and lignin extracted from rice straw showed higher thermal stability at a temperature of over 230°C with 5% degradation. Therefore, extraction method using ultrasonic-assisted alkaline was recommended for cellulose and lignin from rice straw (Ngo et al., 2017).

2.2.4 Cellulose extraction/isolation by using enzyme

The used of enzymes for extraction of cellulose from plant has been based on the selected idea of hydrolysis of several components such as fiber, which contain hemicelluloses and lignin, while retaining the cellulosic portion (Janardhnan & Sain, 2006). For biotreatment, as a starting material, oven-dry, bleached kraft pulp may be used. With appropriate amount extract of yeast and sucrose to support growth of the fungi, the fungal culture is further added to the fiber suspension after soaking the plants in water and autoclaving. At room temperature, with slow agitation, the fungus is left to act on the fibers for different duration of time. The fibers are made into sheets of 10% fiber consistency subsequently with autoclaved and washed. In a refiner, the fibers are sheared for 125,000 revolutions (Janardhnan & Sain, 2006). Other than that, cryocryshing are another method used. Using liquid nitrogen, the fibers are frozen and subjected to cryocrushing, where a mortar and pestle is used with a high shear is applied. This step critically liberated the cell wall microfibrils. The cryocrushed fibers are dispersed using a disintegrator into water suspension and filtered through a 60-mesh filter. For further investigation or applications, the filtrate dilutes water suspension of microfibrils is used (Janardhnan & Sain, 2006).

Martelli-Tosi, Torricillas, Martins, Assis, and Tapia-Blácido (2016) studied the use of commercial enzymes to isolate cellulose nanofibrils and produce sugars from chemically pretreated soybean straw by using alkaline and bleaching pretreatments. The yield of cellulose nanofibrils varied from 6.3 to 7.5 g of cellulose nanofibrils/100 g of soybean straw regardless of the alkaline solution concentration of 5% or 17.5%. The cellulose nanofibrils had over 300 nm in length, 15 nm in diameter, and high electrical stability with zeta potentials ranged from −20.8 to −24.5 (Martelli-Tosi et al., 2016). XRD patterns show that the crystallinity index of cellulose nanofibrils ranged from 45% to 68%, dependent on the chemical pretreatment of the material used. Cellulose nanofibrils treated with NaOH 17.5% and $H_2O_2$with (crystallinity index of 45% obtained from soybean straw displayed better thermal stability probably as the lignin-cellulose complex emerged. The first step production of cellulose nanofibrils soluble fraction contained a large amount of reduced sugars, which is about 11.2–30.4 g/100 g of soybean straw. Therefore, it shows that via enzymatic-mechanical treatment, soybean straw potentially can be use as industrial source to produce cellulose nanofibril, while for use in bioenergy production, it may lead to the large reduction amounts of sugars (Martelli-Tosi et al., 2016). Kumari, Pathak, Gupta, Sharma, and Meena (2019) have isolated and characterized cellulose nanofibers using enzymatic hydrolysis. The cellulose nanofiber cytotoxicity was assessed by 3-(4,5-dimethylthiazol-2-yl)-2,5-diphenyl tetrazolium bromide assay

against three different cancer cell lines NCIH460, PA1, and L132 cells. The FTIR results showed the sample of cellulose species and cellulose nanofiber was found free from the noncellulosic components, such as hemicellulose and lignin. The micrographs of cellulose nanofibers showed diverse long fiber structure with 105.7 nm particle size and a bundle like structure. While, the thermal stability was slightly lower compared to cellulose. However, cellulose nanofibers cytotoxic effect did not show when the tested concentrations around ~10–1000 μg/mL in any of the cell lines.

2.3 Types and classification of cellulose

Cellulose is classified into natural and modified. The intra- and intermolecular noncovalent hydrogen bonds of crystalline cellulose make it insoluble in water. The process covered the development and preparation of celluloses and its modified cellulose, which are usually used as food additives and ingredients, such as microcrystalline cellulose, powdered cellulose, and hydroxypropyl methylcellulose (HPMC) (Mudgil, 2017). Both natural and modified celluloses amounts of crystallization and hydrogen bonding may sometimes differ with each other. Water solubility of cellulose derivative cause the lost in the crystallinity of cellulose and hydrogen bonds are rattled (Mudgil, 2017). Several studies have been reported in various models on the influence of cellulose on insulin levels and blood glucose (Brockman, Chen, & Gallaher, 2012; Korotkova, Perelygina, Lobanova, & Stoilov, 1983). Some of this may be dependent on the subject and extremely contradictory, covered from cellulose type, and other unexplored factors. As compared with natural cellulose, modified cellulose reported more consistent with data obtained. Most of the modified cellulose influence lipid metabolism. For a duration of 4 weeks, in hypercholesterolemic case, a 5 g of HPMC per day showed a valuable reduction in total of LDL-C (Maki et al., 2009). This shows that modified celluloses more beneficial and perform better than native cellulose. Fig. 2.1 shows the cellulose classifications.

2.3.1 Hypromellose or HPMC

Hypromellose or HPMC is an inert semisynthetic viscoelastic polymer. It is used as eye drops, excipient, and controlled-delivery component, which easily found in a variety of commercial products (Alemdar & Sain, 2008; Williams, Sykora, & Mahaguna, 2001; Merci et al., 2015; Reddy & Yang, 2009; Wang & Sain, 2007). Hypromellose is usually come in aqueous solution, almost acts like methylcellulose, where it exhibits a thermal gelation property. Sometimes, from a solid hypromellose, it is formed into granules, which is slightly off-white to beige powder in form. In water, the compound forms colloids as it dissolved. This ingredient is nontoxic, combustible and react with oxidizing agents vigorously. The solution congeals into a nonflowable but semiflexible mass when the solution heats up to a critical temperature. This congealing or critical temperature inversely related to both the solution

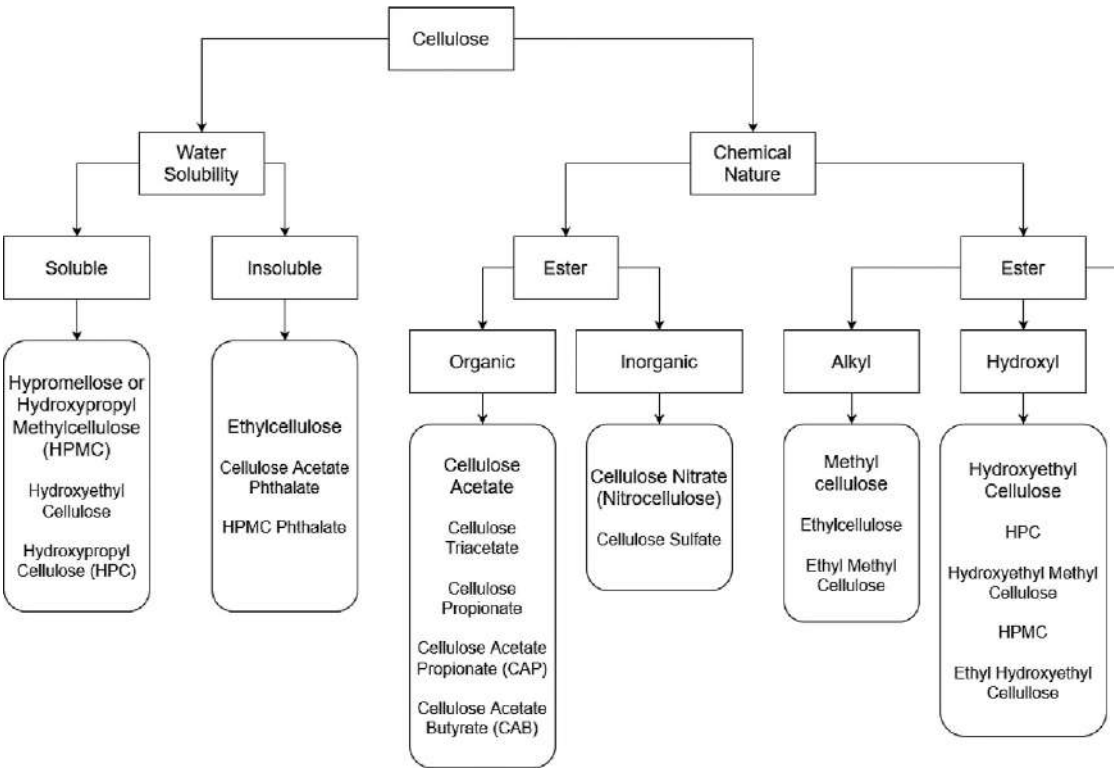

FIG. 2.1

The classification of cellulose based on its water solubility and chemical nature.

concentration of hypromellose and concentration of the methoxy group within the hypromellose molecule, which depends on both molar substitution and the degree of substitution of the methoxy group. Wang et al. (2017), investigated the hypromellose-based hydrophilic composites used for rapid dissolution of ferulic acid.

Electrospun and casting of the hydrophilic composites were prepared from ferulic acid, hypromellose, and polyethylene glycol solution. The effects of its flow rates on the Taylor cone and straight fluid jet were investigated during coaxial processes as ethanol was used as sheath fluid. The drug dissolution rate, hydrophilicity, component state, and morphology of the hydrophilic composites were characterized, and the results showed that all hydrophilic composites were amorphous materials and compatible with its components. Nevertheless, compared with casting hydrophilic composites, the electrospun hydrophilic composite dissolution rate was 10 times faster. The performances are better when smaller diameters of electrospun hydrophilic composites were used. As an alternative approach, the hypromellose-based hydrophilic composites provide effective delivery for poorly water-soluble drugs by utilizing its combinations of drug carriers and modified coaxial electrospinning (Wang et al., 2017). Do Prado et al. (2017) studied the effect of cellulose nanocrystals addition on mechanical properties of biofilms made from hypromellose and cassava starch blends. By acid hydrolysis, the cellulose nanocrystals were produced and characterized. Films were made by casting the pure cassava starch, pure hypromellose, and blends of cassava starch and hypromellose. The cellulose nanocrystals were added the 1%, 3%, and 10% (m/m) concentrations of the blends. The mechanical properties of the films were observed to be improved with the reinforcement of nanocrystals, while the surface fracture showed cellulose nanocrystals improved and promoted the cohesion in the blend of the hypromellose and starch molecules that directly created homogeneous surface (Do Prado et al., 2017).

2.3.2 Hydroxyethyl cellulose

Hydroxyethyl cellulose derived from cellulose as a thickening agent, which acts like a gel. Hydroxyethyl cellulose is widely used in cleaning solutions, cosmetics, and other products for household. In medical applications, also known as hydrophilization, the drugs' dissolution is used to improve the gastrointestinal fluids, whereas hydroxyethyl cellulose is used in capsule formulations hydrophobic drugs. In oil and gas sector, hydroxyethyl cellulose is also used as additive in mud drilling. While in industrial sector, the applications covered from pencils, joint filler paint, coatings, emulsion polymerization, inks, construction, ceramics, adhesives, welding, and rods, Kozlowska, Stachowiak, and Sionkowska (2018) studied the three-dimensional collagen/gelatin/hydroxyethyl cellulose composites development in combination with collagen-gelatin loaded microspheres or gelatin. By using the emulsification/crosslinking method, microspheres were prepared. As a crosslinking agent, a mixture of 1-ethyl-3-(3-dimethyl-aminopropyl)-carbodiimide and *N*-hydroxysuccinimide were used for the obtained materials. A spherical shape of the microspheres is exhibited,

even though in the polymer matrix it is irregularly dispersed. Nevertheless, the addition of microparticles did not significantly change their overall microstructure. It is also observed in the swelling properties, there is a slight decrease of matrices, while in Young's modulus, there is an increase in values (Kozlowska et al., 2018). A promising collagen/gelatin/hydroxyethyl cellulose composites containing microspheres show its suitability for dermatology, cosmetic, or biomedical applications.

2.3.3 Hydroxypropyl cellulose

Hydroxypropyl cellulose (HPC) are both organic and water solubility. It is mostly used lubricant, excipient, and topical ophthalmic protectant. It is categorized as ether in which using propylene oxide, as the hydroxyl groups have been hydroxy propylated to form $–OCH_2CH(OH)CH_3$ groups in the repeating glucose units. The degree of substitution is usually referring to the average number of substituted hydroxyl groups per glucose unit. Most of the degree of substitution would be complete substitution. However, etherification was done during the preparation of HPC. Alharbi and Guirguis (2019) studied the iron (III) oxide nanoparticles (HPC: Fe_2O_3 NPs) and composites of HPC, which were prepared in different ratios (20:0.5, 20:1, 20:1.5 and 20:2wt:wt). The FTIR spectra showed that increasing concentration in the mixture of Fe_2O_3 NPs, variations in the intensity, bandwidth, area, and transmittance values of some bands indicated change in the molecular configuration and vibrational bonds of HPC. The different location of the α-Fe_2O_3 NPs concentration on the chromaticity diagram of the investigated composites confirmed the change in the colors (Alharbi & Guirguis, 2019). In the system of HPC, the induced structural change was due to the increasing presence of α-Fe_2O_3 NP, which is the obtained due to optical parameter variations. Conclusively, the performance properties of HPC improvement are due to the increased existence of α-Fe_2O_3 NPs in the HPC network.

2.3.4 Cellulose acetate phthalate

Cellulose acetate phthalate (CAP) is a polymer commonly in the formulation of pharmaceuticals, for controlled release formulations, capsules, and/or enteric coating of tablets. A quarter of these cellulose polymers are esterified with one or two carboxyl's of a phthalic acid, half of the hydroxyls are esterified with acetyls, while the rest remainder is unchanged. It may in the form of granules, flakes, or hygroscopic white to off-white free-flowing powder. Even though it has a weak odor of acetic acid, mostly it still tasteless and odorless. In pharmaceutical applications, its main use is with enteric formulations, while for coating agents as ethyl cellulose. According to Indumathi, Saral Sarojini, and Rajarajeswari (2019), film-forming biopolymers possessing antimicrobial activity and biodegradability shown a great potential and interest in food packaging applications, by the fabrication and characterization of chitosan (CS)—CAP films combined with ZnO nanoparticles (nano ZnO). By solvent casting method, varying ratios of nano ZnO reinforcement with CS-CAP films were prepared. The increasing amount of nano ZnO in the range

of 2%–7.5% (w/w) cause the fabricated films to increase in the barrier and thermal stability properties. The most optimal stiffness and tensile strength are shown by CS-CAP film loaded with 5% (w/w) nano ZnO. While, the measurements of water contact angle showed low surface wettability and high contact angle up to 90 degrees value for the prepared nano composite films. Within 28 days, the nano composite films biodegradability has ranged between 30% and 50% (Indumathi et al., 2019). The shelf life of black grapefruits had extended up to 9 days when the CS-CAP film loaded with 5% (w/w) nano ZnO. Therefore, in terms of food barrier and protection characteristics, the CS-CAP-ZnO films attested its suitability by increase the shelf life of black grapefruits.

2.3.5 Cellulose acetate

Cellulose acetate is the acetate ester of cellulose, which is created since 1865. It is used as a film base, coatings components, and eyeglasses frame. As a synthetic fiber, it is also used to manufacture filters for cigarette and card games. Nasouri (2019) studied the novel lightweight and flexible of cellulose acetate (CA)/zinc oxide (ZnO)/multiwalled carbon nanotubes (MWCNTs) composite, whereas the nanofibers were fabricated via electrospinning technique. It is aimed to study the potential of such CA/ZnO/MWCNTs composite nanofibers as effective ultraviolet (UV) protecting textile materials. Highest to lowest effects of selected parameters on UV protection values are as follows; thickness $\geq$ ZnO content $>$ MWCNTs content. The optimized quadratic model predicted the highest UV protection value (UPF = 180.8) at conditions of 79.5 μm of the sample thickness, 4.9 wt% ZnO content, and 1.1 wt% MWCNTs loading (Nasouri, 2019).

2.3.6 Cellulose triacetate

A chemical compound produced from cellulose is called cellulose triacetate (CTA), which is also a source of acetate esters, typically acetic anhydride. Triacetate is used to create fibers and film base and at least 92% of the hydroxyl groups are acetylated. The cellulose is completely acetylated during the manufacture of triacetate, whereas it is only partially acetylated, in normal cellulose acetate or cellulose diacetate. Significantly, triacetate is heat resistant more than cellulose acetate. Saeed, Dawood, and Ali (2019) studied the polystyrene (PS) reinforced with CTA with the induction of fusabond (FB) by melt blending it in a twin-screw extruder. Demonstrated by the improvement in storage modulus, the addition of FB enhanced the interfacial adhesion, while reducing the in-damping peak value, and increase the composite thermal stability. Under dynamic loading, FB increases the elongation percentage and improves the impact strength of the CTA-reinforced PS composite. Therefore, the addition of FB is suitable for used in cellulose fiber-reinforced PS composite, especially for applications, such as packaging, biomedical, and automotive (Saeed et al., 2019).

2.3.7 Cellulose nitrate (nitrocellulose)

Nitrocellulose also known as cellulose nitrate, which is used as a guncotton, flash paper, flash string, and flash cotton. The compound formed by nitrating cellulose through exposure to nitric acid is highly flammable. It can also be in a mixture of nitric acid and other acid or powerful nitrating agent, either hydrochloric acid or sulfuric acid. It is also used to replace gun powder, low-order explosive, and other applications. Moreover, partially nitrated cellulose has found use as a wood coating, plastic, film base, and inks. Generally, nitrocellulose products are a mixture of trinitrocellulose, dinitrocellulose, mononitrocellulose, whereas each of the glucose units in the cellulose chain has one, two, or three nitro groups, respectively. Depending on which of the three slots have nitro groups, several of it may be in mono- and di-forms. While being subjected to sonication, Owens (2005) prepared single walled carbon nanotubes (SWNTs) and composites of nitrocellulose (NC), as well as fluorinated SWNTs produced by evaporation of solutions of NC and suspended SWNTs. The Raman analysis of the NC/SWNT composites showed a sizable upward shift of the tangential mode frequency and shift of the radial breathing on the SWNT results, which indicate the interaction between the NC and the SWNT. By weight, composites containing 12.5% SWNTs showed an increase of 21% in hardness, with a resistance of 0.51 Ohm-cm. A similar containing number of fluorinated carbon nanotubes for composites of NC showed a tangential mode frequency down shift, with an increase of 23% in hardness, which is not conducting. As catalysts in the synthesis of the carbon nanotubes and due to the presence of iron nanoparticles used, the composites were ferromagnetic as indicated by ferromagnetic resonance and magnetization analysis.

2.3.8 Carboxymethyl cellulose

Bound to the hydroxyl groups of the glucopyranose monomers, carboxymethyl cellulose (CMC) or cellulose gum is a derivative with carboxymethyl groups ($–CH_2–COOH$) that make up the cellulose backbone. Zhao, Clifford, Poon, Mathews, and Zhitomirsky (2018) been developed electrophoretic deposition (EPD) method for the controlled deposition of CMC films. For the EPD of composite organic-inorganic films, CMC has been utilized as a charging and film forming agent, while the problems related to AH agglomeration were avoided using different liquid-liquid particle extraction strategies by containing aluminum hydroxide (AH) as a flame-retardant additive. Due to polydentate bonding mechanisms, hexadecylphosphonic acid (HDPA) and lauryl gallate (LG) exhibit remarkable adsorption on AH particles, which were used as efficient extracting agents (Zhao et al., 2018). For agglomerate-free processing of AH using HDPA is applied with similar strategies as a capping agent for synthesis and an extractor molecule for liquid-liquid extraction. The test demonstrated the uniformly distributed in the CMC matrix of EPD as composite CMC-AH films, which contained nonagglomerated AH particles.

2.3.9 Ethyl cellulose

Ethyl cellulose is a derivative, whereas the hydroxyl groups of the repeating glucose units are converted into ethyl ether groups. Ethyl cellulose is used as a coating for thin-film, paper, medical pills, and vitamin, and as thickeners. Graded ethyl cellulose in food is nontoxic and nonsoluble thickeners, which allows it to be used to safeguard ingredients from water. Ethyl cellulose also acts emulsifier as in food additive (E462). By solvent casting and electrospinning, Liu et al. (Li et al., 2009; Liu et al., 2018; Li, Zhou, et al., 2009; Liu et al., 2011) managed to fabricate ethyl cellulose (EC)-gelatin (G) composite films. The blending of EC with G improved the spinnability of the composite films with higher thermal stability. Compared with the solvent casting, more hydrogen-forming is provided sites for EC to form a compatible network and electrospinning induced a helix-to-coil transition of G. The cast composite film showed a hydrophilic surface at 67.5 degrees, while the electrospun composite film had a hydrophobic surface with a water contact angle of 113.8 degrees. The confocal laser scanning microscopy observations suggested that after water immersion, the cast composite film collapsed into aggregates, whereas the electrospun composite film maintained the nanofibrous structures well, which indicated water resistance improvement.

2.3.10 Methyl cellulose

Methyl cellulose is used as a thickener and emulsifier in various foods and cosmetic products, while in pharmaceutical, sometimes as a bulk-forming laxative. It is nontoxic, nondigestible, and nonallergenic. Fedorov et al. (2017) studied a series of polymer-inorganic composite films, containing methylcellulose with incorporated cellulose nanocrystals, or thermally treated particle $Ca_{1-x}Ho_xF_{2+x}$ and synthesized fluorite-type $Ca_{1-x}Ho_xF_{2+x}$ nanoparticles. The aqueous dispersions ingredients were mixed and followed by film formation on polystyrene support, which is dried under air at room temperature, before heated up to 85°C. For the first time for the visible spectrum range, the upconversion luminescence of the Ho^{3+}-containing composite films ($^5I_7$ energy level excitation) has been described (Fedorov et al., 2017).

2.4 Commercial-grade cellulose

In industry, cellulose is obtained from wood pulp and cotton (Klemm, Heublein, Fink, & Bohn, 2005). While to extract and isolated cellulose from lignin and other major component from the plant, kraft process is used. In terms of fiber, cellulose is extracted and isolated from cotton, linen, and other plant fibers, which become the main ingredient of textiles. In the 20th century, due to revolutionize and extensive research for textile applications, most of the cellulose fiber extracted and isolated from the plant can be turned into rayon, which is used to make clothes and mattress. In chemical structure, both cellophane and rayon are known for their identities to

cellulose, which usually made from dissolving pulp via viscose, while its cellulose fibers regenerated. The most recent method such as lyocell process are known to be environmentally friendly to produce a form of rayon. For production of paperboard, card stock paper, and paper, cellulose has become one of the major constituents (Julkapli & Bagheri, 2016; Lavoine, Desloges, Manship, & Bras, 2015; Nazari & Bousfield, 2016).

In electrical and electronic applications, cellulose can be modified as an electrical insulation in cables, transformers, and other electrical and electronics material (Jayamani, Tay, Bakri, & Kakar, 2018; Kakar, Jayamani, Soon, & Bakri, 2018; Kohman, 1939). For consumption in drug tablets, powdered cellulose (E460ii) and microcrystalline cellulose (E460i) and other types of cellulose are used as inactive fillers (Abeer, Mohd Amin, & Martin, 2014; Almeida et al., 2014; Badshah et al., 2018; Sun et al., 2019). While, a wide range of soluble cellulose derivatives, such as E461 to E469 are used as thickeners, stabilizers, and emulsifiers in processed foods (Arancibia, Navarro-Lisboa, Zúñiga, & Matiacevich, 2016; Costa, Gomes, Tibolla, Menegalli, & Cunha, 2018; Costa et al., 2019; Gong, Wang, & Chen, 2017; Costa et al., 2015; Maepa et al., 2015; Reddy & Yang, 2005). Cellulose powder is also used in processed cheese, dough, and cake (Lauková et al., 2017; Pérez-Carrillo et al., 2017; Salehi, 2019). In some foods, cellulose may naturally occur, especially as an additive in manufacturing foods, which contributed to an indigestible texture and bulk component used that potentially aiding in defecation (Dhingra, Michael, Rajput, & Patil, 2012). Scientifically, in the lab, most of the cellulose is used as a stationary phase for the chromatography thin layer. To create a filter bed of inert material, with a combination of diatomaceous earth or other filtration media, cellulose fibers is also used in liquid filtration (Bethke et al., 2018; Carpenter, De Lannoy, & Wiesner, 2015; Dong, 2019; Ottenhall, Henschen, Illergård, & Ek, 2018).

The nonfood energy crops, the major combustible component is cellulose, followed by lignin. Its produce more usable energy than edible energy crops, which its large starch component. Typical nonfood energy, industrial crops may include switchgrass, hemp, willow, miscanthus, and or poplar species. Meanwhile, cellulose also can be used to create biofuels. A bacterium and enzyme converted nearly any form of cellulose into butanol fuel (Hood, 2016; Lynd, 2017; Park et al., 2012; Rubin, 2008; Venkatesh, 2014). Pharmaceuticals derivatives of cellulose have water retaining advantages, not only as a stabilizer and thickening agent, but as reinforcement of drug tablets, such as microcrystalline cellulose (MCC) (Thoorens, Krier, Leclercq, Carlin, & Evrard, 2014). In construction and building material, as an alternative to the use of plastics and resins, hydroxyl cellulose bonding in water is easily sprayable and moldable (Ardanuy, Claramunt, & Toledo Filho, 2015; Hospodarova, Stevulova, & Sicakova, 2015; Jiao et al., 2016; Shan et al., 2019). Most of the recyclable material from cellulose can be made from fire- and water-resistant materials, whereas it also provides enough strength to be used in building material (Ardanuy et al., 2015; Hospodarova et al., 2015; Jiao et al., 2016; Shan et al., 2019). The cellulose is treated with boric acid, especially to create fire retardant materials. As an environmentally materials are preferable than nonsustainable materials, insulation, recycled paper

made from recycled cellulose is becoming popular for insulation in buildings. Miscellaneously, cellulose can be converted into a thin transparent film and cellophane. In wallpaper paste, to make water-soluble binder and adhesives, CMC and methyl cellulose are used. Cellulose fabricated as absorbent sponges are known to be highly hydrophilic make it comparable than other synthetic sponges (Jiang, Mei, Jiang, Zhou, & Huang, 2019; Kim, Ha, & Kim, 2017; Satirapipathkul & Dungsri, 2016; Saxena & Brown, 2001; Silliker & Gabis, 1975). In the manufacture of nitrocellulose, the raw cellulose material is used in smokeless gunpowder.

2.5 Summary

Cellulose was extracted by several methods. There are four common methods to apply for cellulose isolation. Among the methods, they have their own advantage and disadvantage due to the different chemical reagent, which depends on the properties needed for the application area. Cellulose was classified in two ways such natural and modified cellulose. Both natural and modified celluloses have amounts of crystallization and hydrogen bond. It may differ with each other depend on the sources. Water solubility of cellulose derivative cause the lost in the crystallinity of cellulose. Several studies have been reported in various models on the influence of cellulose on insulin levels and blood glucose.

Acknowledgment

The authors would like to thank and acknowledge Universiti Malaysia Sarawak (UNIMAS) for the support.

References

Abeer, M. M., Mohd Amin, M. C. I., & Martin, C. (2014). A review of bacterial cellulose-based drug delivery systems: Their biochemistry, current approaches and future prospects. *Journal of Pharmacy and Pharmacology*, *66*(8), 1047–1061. https://doi.org/10.1111/jphp.12234.

Adamu, M, Rahman, MR, Bakri, MKB, Md Yusof, FAB, & Khan, A. (2021). Characterization and optimization of mechanical properties of bamboo/nanoclay/polyvinyl alcohol/styrene nanocomposites using response surface methodology. *J Vinyl Addit Technol*, *27*, 147–160. https://doi.org/10.1002/vnl.21792.

Alemdar, A., & Sain, M. (2008). Isolation and characterization of nanofibers from agricultural residues – Wheat straw and soy hulls. *Bioresource Technology*, *99*(6), 1664–1671. https://doi.org/10.1016/j.biortech.2007.04.029.

Alharbi, N. D., & Guirguis, O. W. (2019). Macrostructure and optical studies of hydroxypropyl cellulose in pure and nano-composites forms. *Results in Physics*, *15*. https://doi.org/10.1016/j.rinp.2019.102637.

Almeida, I. F., Pereira, T., Silva, N. H. C. S., Gomes, F. P., Silvestre, A. J. D., Freire, C. S. R., et al. (2014). Bacterial cellulose membranes as drug delivery systems: An in vivo skin compatibility study. *European Journal of Pharmaceutics and Biopharmaceutics*, *86*(3), 332–336. https://doi.org/10.1016/j.ejpb.2013.08.008.

Arancibia, C., Navarro-Lisboa, R., Zúñiga, R. N., & Matiacevich, S. (2016). Application of CMC as thickener on nanoemulsions based on olive oil: Physical properties and stability. *International Journal of Polymer Science*, 1–10. https://doi.org/10.1155/2016/6280581.

Ardanuy, M., Claramunt, J., & Toledo Filho, R. D. (2015). Cellulosic fiber reinforced cement-based composites: A review of recent research. *Construction and Building Materials*, *79*, 115–128. https://doi.org/10.1016/j.conbuildmat.2015.01.035.

Badshah, M., Ullah, H., Khan, A. R., Khan, S., Park, J. K., & Khan, T. (2018). Surface modification and evaluation of bacterial cellulose for drug delivery. *International Journal of Biological Macromolecules*, *113*, 526–533. https://doi.org/10.1016/j.ijbiomac.2018.02.135.

Bethke, K., Palantöken, S., Andrei, V., Roß, M., Raghuwanshi, V. S., Kettemann, F., et al. (2018). Functionalized cellulose for water purification, antimicrobial applications, and sensors. *Advanced Functional Materials*, *28*(23). https://doi.org/10.1002/adfm.201800409.

Bhattacharya, D., Germinario, L. T., & Winter, W. T. (2008). Isolation, preparation and characterization of cellulose microfibers obtained from bagasse. *Carbohydrate Polymers*, *73*(3), 371–377. https://doi.org/10.1016/j.carbpol.2007.12.005.

Brigham, C. (2017). Biopolymers: Biodegradable alternatives to traditional plastics. In *Green chemistry: An inclusive approach* (pp. 753–770). Elsevier Inc. https://doi.org/10.1016/B978-0-12-809270-5.00027-3.

Bringmann, M., Landrein, B., Schudoma, C., Hamant, O., Hauser, M. T., & Persson, S. (2012). Cracking the elusive alignment hypothesis: The microtubule-cellulose synthase nexus unraveled. *Trends in Plant Science*, *17*(11), 666–674. https://doi.org/10.1016/j.tplants.2012.06.003.

Brockman, D. A., Chen, X., & Gallaher, D. D. (2012). Hydroxypropyl methylcellulose, a viscous soluble fiber, reduces insulin resistance and decreases fatty liver in Zucker Diabetic Fatty rats. *Nutrition and Metabolism*, *9*(1). https://doi.org/10.1186/1743-7075-9-100.

Brown, R. M., Willison, J. H. M., & Richardson, C. L. (1976). Cellulose biosynthesis in Acetobacter xylinum: Visualization of the site of synthesis and direct measurement of the in vivo process. *Proceedings of the National Academy of Sciences of the United States of America*, *73*(12), 4565–4569. https://doi.org/10.1073/pnas.73.12.4565.

Carpenter, A. W., De Lannoy, C. F., & Wiesner, M. R. (2015). Cellulose nanomaterials in water treatment technologies. *Environmental Science and Technology*, *49*(9), 5277–5287. https://doi.org/10.1021/es506351r.

Costa, A. L. R., Gomes, A., Tibolla, H., Menegalli, F. C., & Cunha, R. L. (2018). Cellulose nanofibers from banana peels as a Pickering emulsifier: High-energy emulsification processes. *Carbohydrate Polymers*, *194*, 122–131. https://doi.org/10.1016/j.carbpol.2018.04.001.

Costa, L. A. S., Assis, D.d. J., Gomes, G. V. P., Da Silva, J. B. A., Fonsêca, A. F., & Druzian, J. I. (2015). Extraction and characterization of nanocellulose from corn stover. *Materials Today: Proceedings*, *2*(1), 287–294. Elsevier Ltd https://doi.org/10.1016/j.matpr.2015.04.045.

Costa, C., Medronho, B., Filipe, A., Mira, I., Lindman, B., Edlund, H., et al. (2019). Emulsion formation and stabilization by biomolecules: The leading role of cellulose. *Polymers*, *11*(10). https://doi.org/10.3390/polym11101570.

Dhingra, D., Michael, M., Rajput, H., & Patil, R. T. (2012). Dietary fibre in foods: A review. *Journal of Food Science and Technology*, *49*(3), 255–266. https://doi.org/10.1007/s13197-011-0365-5.

Do Prado, N. R. T., Raabe, J., Mirmehdi, S., Hugen, L. N., Lima, L. C., Ramos, A.d. L. S., et al. (2017). Melhorando a resistência de filmes de hidroxipropil metilcelulose/amido com nanocristais de celulose. *Cerne*, *23*(4), 423–434. https://doi.org/10.1590/01047760201723042303.

Dong, W. (2019). A critical review of cellulose-based nanomaterials for water purification in industrial processes. *Cellulose*, 687–701. https://doi.org/10.1007/s10570-018-2143-2.

Endler, A., Sánchez-Rodríguez, C., & Persson, S. (2010). Glycobiology: Cellulose squeezes through. *Nature Chemical Biology*, *6*(12), 883–884. https://doi.org/10.1038/nchembio.480.

Esteghlalian, A., Hashimoto, A. G., Fenske, J. J., & Penner, M. H. (1997). Modeling and optimization of the dilute-sulfuric-acid pretreatment of corn stover, poplar and switchgrass. *Bioresource Technology*, *59*(2–3), 129–136. https://doi.org/10.1016/S0960-8524(97)81606-9.

Fang, J. M., Sun, R. C., & Tomkinson, J. (2000). Isolation and characterization of hemicelluloses and cellulose from rye straw by alkaline peroxide extraction. *Cellulose*, *7*(1), 87–107. https://doi.org/10.1023/A:1009245100275.

Fedorov, P. P., Luginina, A. A., Kuznetsov, S. V., Voronov, V. V., Lyapin, A. A., Ryabochkina, P. A., et al. (2017). Preparation and properties of methylcellulose/nanocellulose/CaF2:Ho polymer-inorganic composite films for two-micron radiation visualizers. *Journal of Fluorine Chemistry*, *202*, 9–18. https://doi.org/10.1016/j.jfluchem.2017.08.012.

Frone, A. N., Panaitescu, D. M., & Donescu, D. (2011). Some aspects concerning the isolation of cellulose micro- and nano-fibers. *UPB Scientific Bulletin, Series B: Chemistry and Materials Science*, *73*(2), 133–152.

Gong, X., Wang, Y., & Chen, L. (2017). Enhanced emulsifying properties of wood-based cellulose nanocrystals as Pickering emulsion stabilizer. *Carbohydrate Polymers*, *169*, 295–303. https://doi.org/10.1016/j.carbpol.2017.04.024.

Harini, K., Ramya, K., & Sukumar, M. (2018). Extraction of nano cellulose fibers from the banana peel and bract for production of acetyl and lauroyl cellulose. *Carbohydrate Polymers*, *201*, 329–339. https://doi.org/10.1016/j.carbpol.2018.08.081.

Haymes, K. M., Ibrahim, I. A., Mischke, S., Scott, D. L., & Saunders, J. A. (2004). Rapid isolation of DNA from chocolate and date palm tree crops. *Journal of Agricultural and Food Chemistry*, *52*(17), 5456–5462. https://doi.org/10.1021/jf0497962.

Himmel, M. E., Ding, S. Y., Johnson, D. K., Adney, W. S., Nimlos, M. R., Brady, J. W., et al. (2007). Biomass recalcitrance: Engineering plants and enzymes for biofuels production. *Science*, *315*(5812), 804–807. https://doi.org/10.1126/science.1137016.

Hood, E. E. (2016). Plant-based biofuels. *F1000 Research*, *5*, 185. https://doi.org/10.12688/f1000research.7418.1.

Hospodarova, V., Stevulova, N., & Sicakova, A. (2015). Possibilities of using cellulose fibres in building materials. *IOP Conference Series: Materials Science and Engineering*, 012025. https://doi.org/10.1088/1757-899X/96/1/012025.

Huntley, C. J., Crews, K. D., Abdalla, M. A., Russell, A. E., & Curry, M. L. (2015). Influence of strong acid hydrolysis processing on the thermal stability and crystallinity of cellulose isolated from wheat straw. *International Journal of Chemical Engineering*, *2015*. https://doi.org/10.1155/2015/658163.

Indumathi, M. P., Saral Sarojini, K., & Rajarajeswari, G. R. (2019). Antimicrobial and biodegradable chitosan/cellulose acetate phthalate/ZnO nano composite films with optimal oxygen permeability and hydrophobicity for extending the shelf life of black grape fruits. *International Journal of Biological Macromolecules*, *132*, 1112–1120. https://doi.org/10.1016/j.ijbiomac.2019.03.171.

Janardhnan, S., & Sain, M. (2006). Isolation of cellulose microfibrils – An enzymatic approach. *BioResources*, 176–188. https://doi.org/10.15376/biores.1.2.176-188.

Jayamani, E., Tay, C. P., Bakri, M. K. B., & Kakar, A. (2018). Comparative analysis on dielectric properties of polymer composites reinforced with synthetic and natural fibers. *Journal of Vinyl and Additive Technology*, *24*, E201–E216. https://doi.org/10.1002/vnl.21639.

Jiang, M. M., Mei, C. T., Jiang, L. Y., Zhou, X. L., & Huang, H. (2019). Preparation of cellulose sponge from waste newspaper. *IOP Conference Series: Earth and Environmental Science*, 032006. https://doi.org/10.1088/1755-1315/295/3/032006.

Jiao, L., Su, M., Chen, L., Wang, Y., Zhu, H., & Dai, H. (2016). Natural cellulose nanofibers as sustainable enhancers in construction cement. *PLoS One*, *11*(12). https://doi.org/10.1371/journal.pone.0168422.

Julkapli, N. M., & Bagheri, S. (2016). Developments in nano-additives for paper industry. *Journal of Wood Science*, *62*(2), 117–130. https://doi.org/10.1007/s10086-015-1532-5.

Kakar, A., Jayamani, E., Soon, K. H., & Bakri, M. K. B. (2018). Study of dielectric properties of luffa–polylactide quadratic splint composites: The effect of cyclic absorption and desorption of water. *Journal of Vinyl and Additive Technology*, *24*(4), 388–394. https://doi.org/10.1002/vnl.21610.

Khine, Y. Y., & Stenzel, M. H. (2020). Surface modified cellulose nanomaterials: A source of non-spherical nanoparticles for drug delivery. *Materials Horizons*, *7*(7), 1727–1758. https://doi.org/10.1039/c9mh01727e.

Kim, J., Ha, J., & Kim, H. Y. (2017). Capillary rise of non-aqueous liquids in cellulose sponges. *Journal of Fluid Mechanics*, 818. https://doi.org/10.1017/jfm.2017.165.

Klemm, D., Heublein, B., Fink, H. P., & Bohn, A. (2005). Cellulose: Fascinating biopolymer and sustainable raw material. *Angewandte Chemie International Edition*, *44*(22), 3358–3393. https://doi.org/10.1002/anie.200460587.

Kohman, G. T. (1939). Cellulose as an insulating material. *Industrial and Engineering Chemistry*, *31*(7), 807–817. https://doi.org/10.1021/ie50355a005.

Korotkova, V. D., Perelygina, A. A., Lobanova, A. M., & Stoilov, L. D. (1983). Vliianie pishchevykh nagruzok s razlichnym soderzhaniem kletchatki na uroven' gliukozy i insulina v krovi u bol'nykh sakharnym diabetom II tipa. *Problemy Endokrinologii*, *29*(6), 16–19.

Kozlowska, J., Stachowiak, N., & Sionkowska, A. (2018). Collagen/gelatin/hydroxyethyl cellulose composites containing microspheres based on collagen and gelatin: Design and evaluation. *Polymers*, *10*(4). https://doi.org/10.3390/polym10040456.

Kumari, P., Pathak, G., Gupta, R., Sharma, D., & Meena, A. (2019). Cellulose nanofibers from lignocellulosic biomass of lemongrass using enzymatic hydrolysis: Characterization and cytotoxicity assessment. *DARU, Journal of Pharmaceutical Sciences*, *27*(2), 683–693. https://doi.org/10.1007/s40199-019-00303-1.

Lauková, M., Kohajdová, Z., Karovičová, J., Kuchtová, V., Minarovičová, L., & Tomášiková, L. (2017). Effects of cellulose fiber with different fiber length on rheological properties of wheat dough and quality of baked rolls. *Food Science and Technology International*, *23*(6), 490–499. https://doi.org/10.1177/1082013217704122.

Lavoine, N., Desloges, I., Manship, B., & Bras, J. (2015). Antibacterial paperboard packaging using microfibrillated cellulose. *Journal of Food Science and Technology*, *52*(9), 5590–5600. https://doi.org/10.1007/s13197-014-1675-1.

Li, R., Fei, J., Cai, Y., Li, Y., Feng, J., & Yao, J. (2009). Cellulose whiskers extracted from mulberry: A novel biomass production. *Carbohydrate Polymers*, *76*(1), 94–99. https://doi.org/10.1016/j.carbpol.2008.09.034.

Li, Q., Zhou, J., & Zhang, L. (2009). Structure and properties of the nanocomposite films of chitosan reinforced with cellulose whiskers. *Journal of Polymer Science, Part B: Polymer Physics*, *47*(11), 1069–1077. https://doi.org/10.1002/polb.21711.

Liu, L., Jiang, T., & Yao, J. (2011). A two-step chemical process for the extraction of cellulose fiber and pectin from mulberry branch bark efficiently. *Journal of Polymers and the Environment*, *19*(3), 568–573. https://doi.org/10.1007/s10924-011-0300-x.

Liu, Y., Deng, L., Zhang, C., Chen, K., Feng, F., & Zhang, H. (2018). Comparison of ethyl cellulose–gelatin composite films fabricated by electrospinning versus solvent casting. *Journal of Applied Polymer Science*, *135*(46). https://doi.org/10.1002/app.46824.

Lynd, L. R. (2017). The grand challenge of cellulosic biofuels. *Nature Biotechnology*, *35*(10), 912–915. https://doi.org/10.1038/nbt.3976.

Maepa, C. E., Jayaramudu, J., Okonkwo, J. O., Ray, S. S., Sadiku, E. R., & Ramontja, J. (2015). Extraction and characterization of natural cellulose fibers from maize tassel. *International Journal of Polymer Analysis and Characterization*, *20*(2), 99–109. https://doi.org/10.1080/1023666X.2014.961118.

Maki, K. C., Carson, M. L., Kerr Anderson, W. H., Geohas, J., Reeves, M. S., Farmer, M. V., et al. (2009). Lipid-altering effects of different formulations of hydroxypropylmethylcellulose. *Journal of Clinical Lipidology*, *3*(3), 159–166. https://doi.org/10.1016/j.jacl.2009.04.053.

Martelli-Tosi, M., Torricillas, M. D. S., Martins, M. A., Assis, O. B. G. D., & Tapia-Blácido, D. R. (2016). Using commercial enzymes to produce cellulose nanofibers from soybean straw. *Journal of Nanomaterials*, *2016*. https://doi.org/10.1155/2016/8106814.

Merci, A., Urbano, A., Grossmann, M. V. E., Tischer, C. A., & Mali, S. (2015). Properties of microcrystalline cellulose extracted from soybean hulls by reactive extrusion. *Food Research International*, *73*, 38–43. https://doi.org/10.1016/j.foodres.2015.03.020.

Michael, I. (2012). Study of cellulose interaction with concentrated solutions of sulfuric acid. *ISRN Chemical Engineering*, 1–7. https://doi.org/10.5402/2012/428974.

Mudgil, D. (2017). The interaction between insoluble and soluble fiber. In *Dietary fiber for the prevention of cardiovascular disease: Fiber's interaction between gut micoflora, sugar metabolism, weight control and cardiovascular health* (pp. 35–59). Elsevier Inc. https://doi.org/10.1016/B978-0-12-805130-6.00003-3.

Nasouri, K. (2019). Fabrication of lightweight and flexible cellulose acetate composite nanofibers for high-performance ultra violet protective materials. *Polymer Composites*, *40*(8), 3325–3332. https://doi.org/10.1002/pc.25191.

Nazari, B., & Bousfield, D. W. (2016). Cellulose nanofibers influence on properties and processing of paperboard coatings. *Nordic Pulp and Paper Research Journal*, *31*(3), 511–520. https://doi.org/10.3183/npprj-2016-31-03-p511-520.

Neftalí, R.-V. M., Elsa, G.-O., Denise, Y. F.-R., Christian, M.-B., Alejandro, N.-A. H., & Mabel, V.-M. (2018). Isolation of cellulose nanofibrils from coconut waste for the production of sewing thread. *Advanced Material Science*. https://doi.org/10.15761/AMS.1000135.

Ngo, D. V., Hang, T. T., Dinh, B. N., Cuong, D. V., & Hung, V. N. (2017). Lignin and cellulose extraction from Vietnam's rice straw using ultrasound-assisted alkaline treatment method. *International Journal of Polymer Science*, 1–8. https://doi.org/10.1155/2017/1063695.

Nuruddin, M., Chowdhury, A., Haque, S. A., Rahman, M., Farhad, S. F., Jahan, M. S., et al. (2011). Extraction and characterization of cellulose microfibrils from agricultural wastes in an integrated biorefinery initiative. *Cellulose Chemistry and Technology*, *45*(5–6), 347–354.

Ottenhall, A., Henschen, J., Illergård, J., & Ek, M. (2018). Cellulose-based water purification using paper filters modified with polyelectrolyte multilayers to remove bacteria from water through electrostatic interactions. *Environmental Science: Water Research and Technology*, *4*(12), 2070–2079. https://doi.org/10.1039/c8ew00514a.

Owens, F. J. (2005). Characterization of single walled carbon nanotube – Nitrocellulose composites. *Journal of Macromolecular Science – Pure and Applied Chemistry*, *42*(10), 1355–1360. https://doi.org/10.1080/10601320500205335.

Park, J. I., Steen, E. J., Burd, H., Evans, S. S., Redding-Johnson, A. M., Batth, T., et al. (2012). A thermophilic ionic liquid-tolerant cellulase cocktail for the production of cellulosic biofuels. *PLoS One*, *7*(5). https://doi.org/10.1371/journal.pone.0037010.

Pasquini, D., Teixeira, E.d. M., Curvelo, A. A.d. S., Belgacem, M. N., & Dufresne, A. (2010). Extraction of cellulose whiskers from cassava bagasse and their applications as reinforcing agent in natural rubber. *Industrial Crops and Products*, *32*(3), 486–490. https://doi.org/10.1016/j.indcrop.2010.06.022.

Pérez-Carrillo, E., González-Fernández, A. G., Morales-Garza, S. M. A., Treviño-Garza, E. E., Guajardo-Flores, S., Serna-Saldívar, S. O., et al. (2017). Efecto del estearoil-2-lactilato de sodio y las gomas carboximetilcelulosa celulosa, guar-xantana en muffins enriquecidos con leche de soya en polvo y harina de amaranto. *CYTA – Journal of Food*, *15*(4), 538–543. https://doi.org/10.1080/19476337.2017.1309684.

Pingali, S. V., Urban, V. S., Heller, W. T., McGaughey, J., ONeill, H., Foston, M., et al. (2010). Breakdown of cell wall nanostructure in dilute acid pretreated biomass. *Biomacromolecules*, *11*(9), 2329–2335. https://doi.org/10.1021/bm100455h.

Pulidindi, I. N., Kimchi, B. B., & Gedanken, A. (2014). Can cellulose be a sustainable feedstock for bioethanol production? *Renewable Energy*, *71*, 77–80. https://doi.org/10.1016/j.renene.2014.05.032.

Radotić, K., & Mićić, M. (2016). Methods for extraction and purification of lignin and cellulose from plant tissues. In M. Micic (Ed.), *Sample Preparation Techniques for Soil, Plant, and Animal Samples. Springer Protocols Handbooks*. New York, NY: Humana Press. https://doi.org/10.1007/978-1-4939-3185-9_26.

Rahman, M., Adamu, M., Hamdan, S., et al. (2021). Optimization and characterization of acrylonitrile/MAPE/nano-clay bamboo nanocomposites by response surface methodology. *Polymer Bulletin*. https://doi.org/10.1007/s00289-021-03628-7.

Rahman, M. R., Kakar, A., Hamdan, S., Bakri, M. K. B., Julai, N., & Nyuk Khui, P. L. (2019). Introduction of various types of acacia wood. In M. Rahman (Ed.), *Acacia Wood Biocomposites. Engineering Materials*. Cham: Springer. https://doi.org/10.1007/978-3-030-29627-8_1.

Reddy, N., & Yang, Y. (2005). Structure and properties of high quality natural cellulose fibers from cornstalks. *Polymer*, *46*(15), 5494–5500. https://doi.org/10.1016/j.polymer.2005.04.073.

Reddy, N., & Yang, Y. (2006). Properties of high-quality long natural cellulose fibers from rice straw. *Journal of Agricultural and Food Chemistry*, *54*(21), 8077–8081. https://doi.org/10.1021/jf0617723.

Reddy, N., & Yang, Y. (2009). Natural cellulose fibers from soybean straw. *Bioresource Technology*, *100*(14), 3593–3598. https://doi.org/10.1016/j.biortech.2008.09.063.

Rosa, M. F., Medeiros, E. S., Malmonge, J. A., Gregorski, K. S., Wood, D. F., Mattoso, L. H. C., et al. (2010). Cellulose nanowhiskers from coconut husk fibers: Effect of preparation conditions on their thermal and morphological behavior. *Carbohydrate Polymers*, *81*(1), 83–92. https://doi.org/10.1016/j.carbpol.2010.01.059.

Rosales-Calderon, O., & Arantes, V. (2019). A review on commercial-scale high-value products that can be produced alongside cellulosic ethanol. *Biotechnology for Biofuels*, *12*(1). https://doi.org/10.1186/s13068-019-1529-1.

Rubin, E. M. (2008). Genomics of cellulosic biofuels. *Nature*, *454*(7206), 841–845. https://doi.org/10.1038/nature07190.

Saeed, U., Dawood, U., & Ali, A. M. (2019). Cellulose triacetate fiber-reinforced polystyrene composite. *Journal of Thermoplastic Composite Materials*. https://doi.org/10.1177/0892705719847249.

Salehi, F. (2019). Improvement of gluten-free bread and cake properties using natural hydrocolloids: A review. *Food Science and Nutrition*, *7*(11), 3391–3402. https://doi.org/10.1002/fsn3.1245.

Satirapipathkul, C., & Dungsri, P. (2016). Micro-cellulose sponge from waste cotton as controlled-release polyphenol carriers. *MRS Advances*, *1*(36), 2545–2550. https://doi.org/10.1557/adv.2016.479.

Saxena, I. M., & Brown, R. M., Jr. (2001). Biosynthesis of cellulose. *Progress in Biotechnology*, *18*, 69–76. Elsevier BV https://doi.org/10.1016/s0921-0423(01)80057-5.

Saxena, I. M., & Brown, R. M. (2000). Cellulose synthases and related enzymes. *Current Opinion in Plant Biology*, *3*(6), 523–531. https://doi.org/10.1016/S1369-5266(00)00125-4.

Shan, M., Liu, C., Shi, L., Zhang, L., Lin, Y., Zhang, S., et al. (2019). In situ synthesis of Au nanoparticles on viscose cellulose sponges for antibacterial activities. *Polymers*, *11*(8). https://doi.org/10.3390/polym11081281.

Shell, D. J., Jody, F., Millie, N., & McMillan, J. D. (2003). Dilute-sulfuric acid pretreatment of Corn Stover in pilot-scale reactor: investigation of yields, kinetics, and enzymatic digestibilities of solids. *Applied Biochemistry and Biotechnology*, 69–86. https://doi.org/10.1385/ABAB:105:1-3:69.

Silliker, J. H., & Gabis, D. A. (1975). A cellulose sponge sampling technique for surfaces. *Journal of Milk and Food Technology*, *504*. https://doi.org/10.4315/0022-2747-38.9.504.

Siqueira, G., Tapin-Lingua, S., Bras, J., da Silva Perez, D., & Dufresne, A. (2011). Mechanical properties of natural rubber nanocomposites reinforced with cellulosic nanoparticles obtained from combined mechanical shearing, and enzymatic and acid hydrolysis of sisal fibers. *Cellulose*, *18*(1), 57–65. https://doi.org/10.1007/s10570-010-9463-1.

Sun, R. C., & Tomkinson, J. (2005). Separation and characterization of cellulose from wheat straw. *Separation Science and Technology*, *39*(2), 391–411. https://doi.org/10.1081/ss-120027565.

Sun, J. X., Sun, X. F., Zhao, H., & Sun, R. C. (2004). Isolation and characterization of cellulose from sugarcane bagasse. *Polymer Degradation and Stability*, *84*(2), 331–339. https://doi.org/10.1016/j.polymdegradstab. 2004.02.008.

Sun, S., Sun, S., Cao, X., & Sun, R. (2016). The role of pretreatment in improving the enzymatic hydrolysis of lignocellulosic materials. *Bioresource Technology*, *199*, 49–58. https://doi.org/10.1016/j.biortech.2015.08.061.

Sun, B., Zhang, M., Shen, J., He, Z., Fatehi, P., & Ni, Y. (2019). Applications of cellulose-based materials in sustained drug delivery systems. *Current Medicinal Chemistry*, *26*(14), 2485–2501. https://doi.org/10.2174/0929867324666170705143308.

Thoorens, G., Krier, F., Leclercq, B., Carlin, B., & Evrard, B. (2014). Microcrystalline cellulose, a direct compression binder in a quality by design environment – A review. *International Journal of Pharmaceutics*, *473*(1–2), 64–72. https://doi.org/10.1016/j.ijpharm.2014.06.055.

Venkatesh, B. (2014). Current challenges in commercially producing biofuels from lignocellulosic biomass. *ISRN Biotechnology*, 1–31. https://doi.org/10.1155/2014/463074.

Wang, B., & Sain, M. (2007). Isolation of nanofibers from soybean source and their reinforcing capability on synthetic polymers. *Composites Science and Technology*, *67*(11 – 12), 2521–2527. https://doi.org/10.1016/j.compscitech.2006.12.015.

Wang, Q., Yu, D. G., Zhang, L. L., Liu, X. K., Deng, Y. C., & Zhao, M. (2017). Electrospun hypromellose-based hydrophilic composites for rapid dissolution of poorly water-soluble drug. *Carbohydrate Polymers*, *174*, 617–625. https://doi.org/10.1016/j.carbpol.2017.06.075.

Widiarto, S., Yuwono, S. D., Rochliadi, A., & Arcana, I. M. (2017). Preparation and characterization of cellulose and nanocellulose from agro-industrial waste – cassava peel. *IOP Conference Series: Materials Science and Engineering*, 012052. https://doi.org/10.1088/1757-899X/176/1/012052.

Williams, R. O., Sykora, M. A., & Mahaguna, V. (2001). Method to recover a lipophilic drug from hydroxypropyl methylcellulose matrix tablets. *AAPS PharmSciTech*, *2*(2). https://doi.org/10.1208/pt020208.

Zhao, X., Clifford, A., Poon, R., Mathews, R., & Zhitomirsky, I. (2018). Carboxymethyl cellulose and composite films prepared by electrophoretic deposition and liquid-liquid particle extraction. *Colloid and Polymer Science*, *296*(5), 927–934. https://doi.org/10.1007/s00396-018-4314-y.

Zheng, Y., Pan, Z., & Zhang, R. (2009). Overview of biomass pretreatment for cellulosic ethanol production. *International Journal of Agricultural and Biological Engineering*, *2*(3), 51–68. https://doi.org/10.3965/j.issn.1934-6344.2009.03.051-068.

Zuluaga, R., Putaux, J. L., Cruz, J., Vélez, J., Mondragon, I., & Gañán, P. (2009). Cellulose microfibrils from banana rachis: Effect of alkaline treatments on structural and morphological features. *Carbohydrate Polymers*, *76*(1), 51–59. https://doi.org/10.1016/j.carbpol.2008.09.024.

CHAPTER

Cellulose interunit linkages and model compounds

3

Muhammad Khusairy Bin Bakri and Md Rezaur Rahman

Department of Chemical Engineering and Energy Sustainability, Faculty of Engineering, Universiti Malaysia Sarawak (UNIMAS), Kota Samarahan, Sarawak, Malaysia

Chapter outline

3.1 Introduction

3.1.1 Cellulose and hemicellulose

In a biorefinery, which is equivalent to a petroleum refinery, all the components of lignocellulosic biomass, such as cellulose, hemicellulose, and lignin are integrated (Fui Kiew Liew et al., 2015; Liew, Hamdan, Rahman, Rusop, & Khan, 2020; Rahman, Hamdan, & Ngaini, 2019). Through conversion, it has become a value-added products, which have been anticipated by the International Energy Agency (IEA) that make them economically viable and sustainable (Clark et al., 2006). Cellulose is known to have semicrystalline homopolysaccharide structure (Guadix-Montero & Sankar, 2018). Homopolysaccharides are polysaccharides composed of a single monomer type of sugar. Cellulose comprised of unbranched D-glucose or anhydroglucose units, which linked through β-glycosidic bonds or β-1,4 glycosidic bonds at the first and fourth carbon atoms structure (Guadix-Montero & Sankar, 2018; Zakzeski, Bruijnincx, Jongerius, & Weckhuysen, 2010). While, hemicellulose

Fundamentals and Recent Advances in Nanocomposites Based on Polymers and Nanocellulose.
https://doi.org/10.1016/B978-0-323-85771-0.00004-X

is an amorphous polysaccharide branched with short lateral chains consisting of various sugars (Zakzeski et al., 2010).

3.1.2 Lignin

The third component of lignocellulosic biomass and the most abundant carbon source on earth after cellulose is lignin, which is found in all vascular plants (Kubicek, 2012). This natural amorphous polymer provides the plants structural strength and shape. Lignin comprises highly functionalized aromatic units, which shows potential to produce aromatics sustainable feedstock. The final lignocellulose structure includes lignin, which fills the space between the hemicellulose and cellulose, offering strength through carbohydrate polymers cross-linkages (Zakzeski et al., 2010). Up till now, valorization of polysaccharides for both cellulose and hemicellulose have been extensively studied and successfully practiced in the industrial production of bio-based chemicals and material (i.e., biopolymers) and biofuel (i.e., biohydrogen, bioethanol, and biogas) (Berezina & Martelli, 2014; Cherubini & Strømman, 2011; Isikgor & Becer, 2015; Kaparaju, Serrano, Thomsen, Kongjan, & Angelidaki, 2009; Plackett, 2011).

3.2 Common linkages of cellulose

Cellulose is a linear homopolymer. It is made up of β (1–4)-linked glucose residues. While, for cellulose biosynthesis, the UDP-glucose molecule acts a substrate. All alternative glucose residues in the same cellulose chain are rotated at 180 degrees and are β (1–4)-linked by cellulose synthase (CeSa) isoforms. An anhydroglucose is a monomer of cellulose with one glucose residue. The two glucose residues β (1–4)-linked is a dimer, which structural repetitive unit of the cellulose chain called cellobiose. The polymerization degree is determined by the number of monomers of each cellulose compose chain (Delmer, 1999; Malcolm Brown, Sazena, & Kudlicka, 1996). A nonreducing group is present at one end of each of the chains, whereas a closed ring structure is found.

Both aliphatic structure and carbonyl group is found to be shrinking or reduced at the other end of the chains. Therefore, the cellulose chain is also a polarized molecule. According to Koyama, Helbert, Imai, Sugiyama, and Henrissat (1997), the new glucose residues at the nonreducing end of CeSA's allowing chain elongation are added. As occurs in starch, in contrast with α(1–4) linkage, the β(1–4) linkage between glucose residues confers the unique structural features of cellulose. Cellulose is a rigid linear water-insoluble structured. Controlled cellulose biosynthesis create great mechanical strength of fibers, which allows the arrangement of extensive linear chains that were aligned side-by-side. Furthermore, the cellulose tension resistance is comparable to steel (Eckardt, 2003).

In nature, the main structural component of cellulose is the cell wall, which responsible for its numerous distinctive traits. There are six known crystalline cellulose polymorphs, which is cellulose I, II, III_I, III_{II}, IV_I, and IV_{II}. Cellulose I and

II are usually found in nature. Other polymorphs cellulose is obtained using artificially means, which is through chemical or heat means treatments. Found in nature, cellulose I is considered the main form, as it occurs as two allomorphs denominated with I_α and I_β. Both allomorphs, cellulose I_β- and I_α-chains are synthesized by higher quality plants. Like crystalline algal cellulose I_α, the cellulose I_α-chain is accommodated in a different hydrogen-bonding environment (Šturcova, His, Apperley, Sugiyama, & Jarvis, 2004).

Cellulose II is thermodynamically stable in the form of crystalline structure. Cellulose I can be obtained using two processes, which called regeneration and mercerization. Amorphous form usually associated with cellulose I (O'Sullivan, 1997). The two forms have different interchain hydrogen bonding pattern. In cellulose I, the O6-H—O3 interchain hydrogen bonding is dominant. While in cellulose II, O6-H—O2 is the main interchain hydrogen bonding. As shown in Fig. 3.1, the O3-H—O5 intrachain hydrogen bonding is responsible for the linear and rigid shape of cellulose chain, which exists in both polymorphs of cellulose I and II (Langan, Nishiyama, & Chanzy, 2001; Nishiyama et al., 2002, 2003). The cellulose structure reveals the two distinct I_β-chains in a monocyclic unit cell, even though all glucosyl residues are identical except for those in opposite directions (Festucci-Buselli et al., 2007). In contrast, in I_α, there is one chain in a triclinic unit cell, whereas alternative glucosyl residues slightly differ in hydrogen bonding and conformation.

Both allomorphs of I_α and I_β is present in O2-H—O6 intrachain bonding, but it is shorter in I_α (Nishiyama et al., 2002). The anhydroglucose residues conformation and the molecular characteristics of β(1–4) linkages distinguished cellulose I_α and I_β (Kono et al., 2002). Multiple possibilities of hydrogen bonding can occur, especially on O2 and O6 atoms, as shown in Fig. 3.2, which also the reason both O2 and O6 hydroxyl groups are reactive on the cellulose crystalline surface. Contrariwise, due to the strength of the intrachain O3-H—O5 bonding, the O3 atoms are not reactive (Rowland & Howley, 1988). Through heating, cellulose I_α can be converted into I_β, but it is less stable than I_β (Hardy & Sarko, 1996; Kaplan & Seireg, 2002).

3.3 Model structure of cellulose

The model structure of cellulose is formed by the hydrogen bonds between the network of hydroxy groups (Gardner & Blackwell, 1974). Most of the model structure known today is due to the intensive progress and development for more than 100 years, especially in structural analysis methods, such as x-ray diffraction, electron microscopy, and high-resolution solid-state NMR spectroscopy. With consideration of extensive applications, it is required to conduct complete detailed analysis for the procedures of synthetic reactions and cellulose based manmade products (Praveen et al., 2019). The cellulose structure as shown in Fig. 3.2 comprises of β-1,4-glucan hydroxyl groups of cellulose at C2, C3, and C6. Along with O5–C5 bonds shear relativity, the CH_2OH group is located to the C4 and C5 bonds relatively. The solid state of cellulose structure may be present in the crystalline and amorphous, from high to low order. The x-ray diffraction determined the two cellulose chains in a

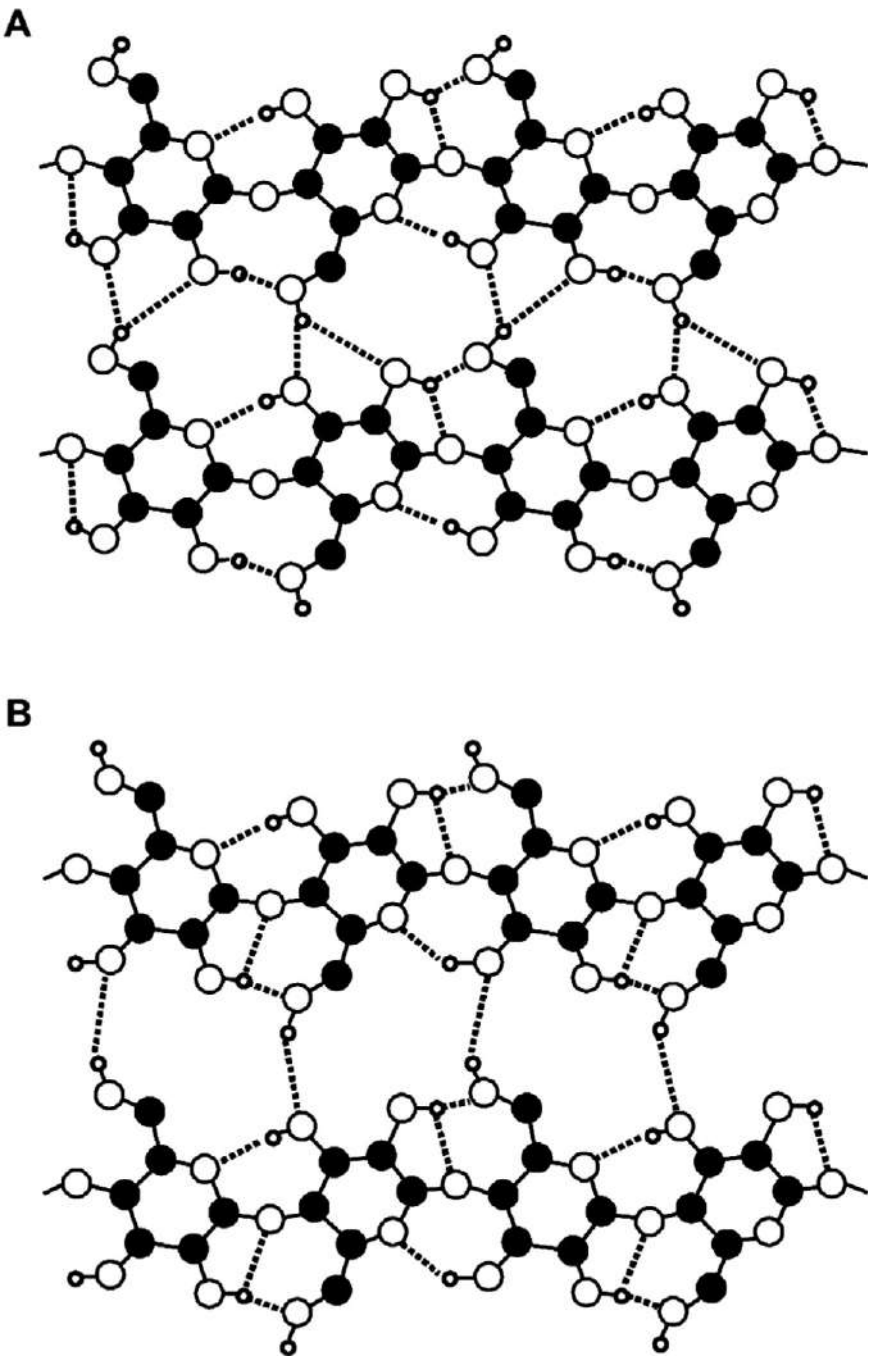

FIG. 3.1

Hydrogen-bonding patterns in (A) cellulose I_{α}, and (B) cellulose I_{β}, which is based on the crystal structures (Nishiyama, Langan, & Chanzy, 2002; Nishiyama, Sugiyama, Chanzy, & Langan, 2003). Hydrogen bonds are the *dotted lines*. It is noted that that both cellulose I_{α} and I_{β} show a different hydrogen-bonding pattern, whereas, arbon *(black sphere)*, oxygen *(white sphere)*, and euterium atoms *(small white sphere)* (Šturcova et al., 2004).

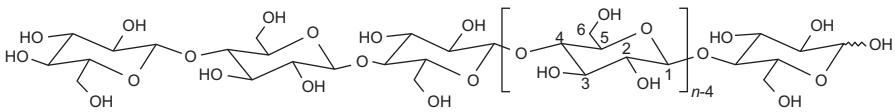

FIG. 3.2

Molecular structure of cellulose (n = DP, degree of polymerization) (Praveen Kumar Gupta et al., 2019; Nobles, Romanovicz, & Brown, 2001).

parallel orientation and twofold screw axis crystal structure by using a monoclinic unit cell (Klemm, Heublein, Fink, & Bohn, 2005). The combined x-ray and neutron diffraction, and electron microbeam diffraction indicated that the triclinic and monoclinic unit cell are usually found in cellulose crystalline structures. Fig. 3.3 shows the schematic diagram for I_β crystal structure. From the figure, it shows that there are two intramolecular chains-stiffening hydrogen bonds. Different H-bonds were shown in the I_β crystal structure with different neighboring chain conformations. Cellulose II is thermodynamically stable, which occur in the form of crystal structures. While, cellulose I can be treated with aqueous sodium hydroxide to form cellulose II.

3.4 Model compounds of cellullose

Most of cellulose model compounds are based on their building blocks i.e., glucose, cellobiose, and other oligomers, while most of it were done by using compounding process during the pyrolysis (Gao, Li, Chen, & Yi, 2019). However, there is a limitation on studying the cellulose pyrolysis process for glucose and cellobiose, especially on the cellulose model compounds. Through pyrolysis, to understand cellulose pyrolysis mechanism, cellulose main product such as levoglucosan (LG) was extensively investigated (Hosoya, Kawamoto, & Saka, 2008; Shafizadeh & Lai, 1972; Shen & Gu, 2009; Zhang, Yang, & Blasiak, 2012). Unfortunately, according to few researchers (Bai, Johnston, Sadula, & Brown, 2013; Patwardhan, Satrio, Brown, & Shanks, 2009), during fast pyrolysis, it is easily found that LG evaporates from the pyrolysis zone, which hinders its cellulose application. In cellulose pyrolysis, as intermediate compounds, studies showed that it mainly contains a degree of polymerization from 2 to 7 anhydro-oligosaccharides (Hosoya et al., 2008; Shafizadeh & Lai, 1972; Shen & Gu, 2009; Zhang et al., 2012; Piskorz, Majerski, Radlein, Vladars-Usas, & Scott, 2000; Zhang et al., 2017), even though, the fast pyrolysis product distribution is almost similar than its cellobiose (Zhang, Yang, & Dong, 2013). Zhang, Yang, and Dong (2013) showed that to produce LG, the LG-end anhydro-oligosaccharides must have the lowest energy barrier. While, accordance with the cellulose pyrolysis experiments, Leng et al. (2018) found that LG-end produce more pyrans oligomers. Therefore, the anhydro-oligosaccharides may have the potential to be model compound to explore the cellulose pyrolysis.

In addition, as according to Guo, Guan, Xu, and Tan (2019), from cellulose pyrolysis, many studies have been done using density functional theory (DFT) to explore

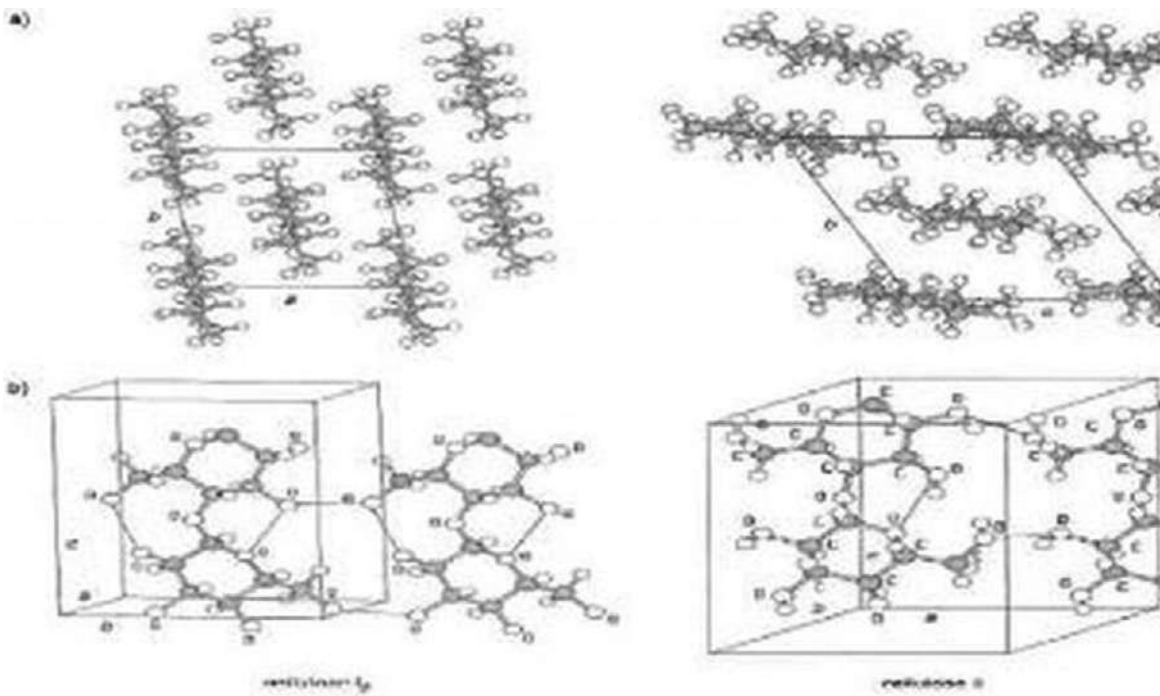

FIG. 3.3

The crystal structures of cellulose I and II: (A) projection of the unit cell along the *a*–*b* plane and (B) projection of UC paralle cellulose I and (010) lattice plane, cellulose II (Praveen Kumar Gupta et al., 2019; Nobles et al., 2001).

the production mechanism of levoglucosan (LG), levoglucosenone (LGO), 5-hydroxymethylfurfural (5-HMF), and levulinic acid (LA), by using glucose, cellobiose, and cellotriose as model compounds (Zhang, Das, Assary, Curtiss, & Weitz, 2016; Zhang, Liao, Lu, Zhang, & Dong, 2013; Zhang, Hu, Qiang, Changqing, & Yang, 2014; Zhang, Yang, & Dong, 2013). Zhang, Liu, and Chen (2015) using DFT study the cellulose pyrolysis mechanism, while cellobiose used as a model compound. Through the depolymerization of cellulose chain, it is found that several primary products i.e., hydroxy acetic aldehyde, 5-HMF, and levoglucononе were achieved, while among the formation of these primary products a competitive reaction is existed. The mechanism of LGO formation by cellobiose and LG was studied by Zhang, Yang, and Dong (2013). It showed in the process of LGO formation, LG is not expected to be in the transitional compound. For the two other reactions, A 1,2-dehydration, keto-enol tautomerization, keto-enol isomerization and hexacyclic hydrogen transfer reaction was the rate-limiting step where the formation of the LGO by either cellobiose or dextran was achieved.

Few researchers (Wang, Guo, Liang, Zhou, & Luo, 2012; Yang, Tsilomelekis, Caratzoulas, & Vlachos, 2015) studied cellulose pyrolysis using gas chromatography/mass spectrometry. The experiments classified three categories of products: (i) pyran derivatives, (ii) furan derivatives, and (iii) small linear molecule compounds. Researchers also found that through DFT, 5-hydroxymethyl furfural production from glucan unit was easier than furfural from levoglucose units. Caratzoulas and Vlachos (2011) stated that more than 100 reaction pathways calculated for production of 5-HMF and LA from glucose catalyzed by protonic acid using the DFT, as shown in Fig. 3.4.

Respectively, LA formation is favored when protonation first occurred on O2 and O3 (Zhao, Sun, Cui, & Liu, 2019). However, when protonated ring-opening first occurs on O5, 5-HMF would be also be generated (Zhao et al., 2019). On the other hand, as O1 and O4 were firstly protonated, through side reactions, glucose had a stronger tendency to produce humus. In acidic aqueous solution, by the regioselectivity of the initial protonation step, the difference in reactivity between glucose and fructose was mainly determined (Zhao et al., 2019). Furthermore, when the initial protonation sites differ, a large difference of products reaction were also shown. It can be summarized that the two parts of the cellulose liquefaction mechanism can be used in real applications.

3.5 Summary

The lignocellulose structure of lignin along with cellulose, which fills the space between the hemicellulose and cellulose, offering strength through carbohydrate polymers cross-linkages. The valorization of polysaccharides for both cellulose and hemicellulose have been extensively studied and successfully practiced in the industrial production of bio-based chemicals and material such as biopolymers and biofuel.

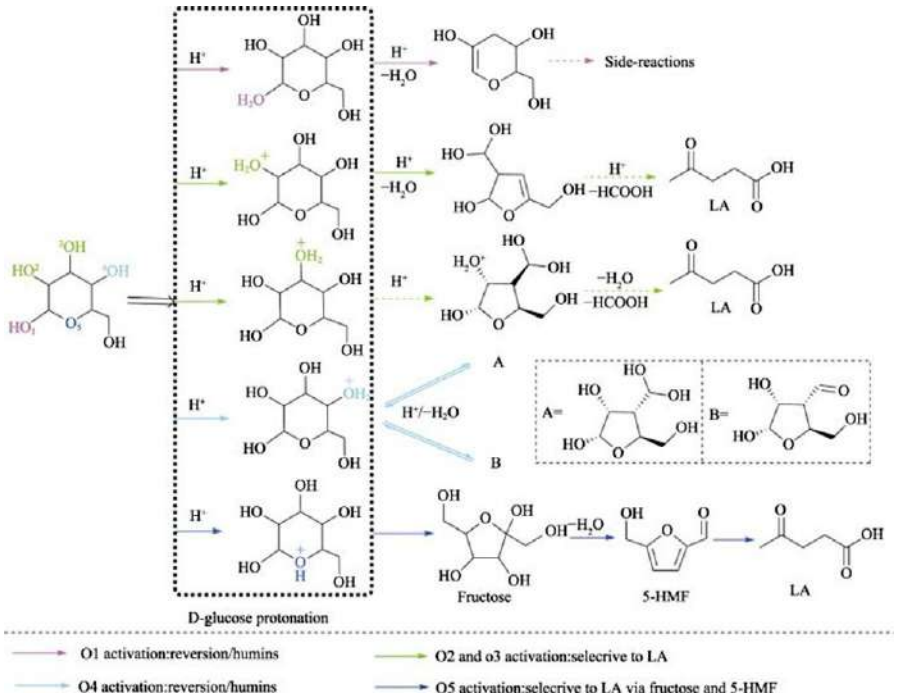

FIG. 3.4

An overview of possible conversion routes of glucose through protonation of different sites (Caratzoulas & Vlachos, 2011; Guo, Guan, Xu, & Tan, 2019).

Acknowledgment

The authors would like to acknowledge Universiti Malaysia Sarawak (UNIMAS) for the support.

References

Bai, X., Johnston, P., Sadula, S., & Brown, R. C. (2013). Role of levoglucosan physiochemistry in cellulose pyrolysis. *Journal of Analytical and Applied Pyrolysis*, *99*, 58–65. https://doi.org/10.1016/j.jaap.2012.10.028.

Berezina, N., & Martelli, S. M. (2014). Bio-based polymers and materials. In *Renewable Resources for Biorefineries* (pp. 1–28). Royal Society of Chemistry. 2014-(27) http://www.rsc.org/shop/books/series/81.asp?seriesid=81.

Caratzoulas, S., & Vlachos, D. G. (2011). Converting fructose to 5-hydroxymethylfurfural: A quantum mechanics/molecular mechanics study of the mechanism and energetics. *Carbohydrate Research*, *346*(5), 664–672. https://doi.org/10.1016/j.carres.2011.01.029.

Cherubini, F., & Strømman, A. H. (2011). Chemicals from lignocellulosic biomass: Opportunities, perspectives, and potential of biorefinery systems. *Biofuels, Bioproducts and Biorefining*, *5*(5), 548–561. https://doi.org/10.1002/bbb.297.

Clark, J. H., Budarin, V., Deswarte, F. E. I., Hardy, J. J. E., Kerton, F. M., Hunt, A. J., et al. (2006). Green chemistry and the biorefinery: A partnership for a sustainable future. *Green Chemistry*, *8*(10), 853–860. https://doi.org/10.1039/b604483m.

Delmer, D. P. (1999). CELLULOSE BIOSYNTHESIS: Exciting times for a difficult field of study. *Annual Review of Plant Physiology and Plant Molecular Biology*, 245–276. https://doi.org/10.1146/annurev.arplant.50.1.245.

Eckardt, N. A. (2003). Cellulose synthesis takes the CesA train. *Plant Cell*, *15*(8), 1685–1687. https://doi.org/10.1105/tpc.150810.

Festucci-Buselli, R. A., Otoni, W. C., & Joshi, C. P. (2007). Structure, organization, and functions of cellulose synthase complexes in higher plants. *Brazilian Journal of Plant Physiology*, *19*(1), 1–13. https://doi.org/10.1590/s1677-04202007000100001.

Gao, Z., Li, N., Chen, M., & Yi, W. (2019). Comparative study on the pyrolysis of cellulose and its model compounds. *Fuel Processing Technology*, *193*, 131–140. https://doi.org/10.1016/j.fuproc.2019.04.038.

Gardner, K. H., & Blackwell, J. (1974). The structure of native cellulose. *Biopolymers*, *13*(10), 1975–2001. https://doi.org/10.1002/bip.1974.360131005.

Guadix-Montero, S., & Sankar, M. (2018). Review on catalytic cleavage of C–C inter-unit linkages in lignin model compounds: Towards lignin depolymerisation. *Topics in Catalysis*, *61*(3–4), 183–198. https://doi.org/10.1007/s11244-018-0909-2.

Guo, K., Guan, Q., Xu, J., & Tan, W. (2019). Mechanism of preparation of platform compounds from lignocellulosic biomass liquefaction catalyzed by Bronsted acid: A review. *Journal of Bioresources and Bioproducts*, *4*, 202–213. https://doi.org/10.12162/jbb.v4i4.009.

Hardy, B. J., & Sarko, A. (1996). Molecular dynamics simulations and diffraction-based analysis of the native cellulose fibre: Structural modelling of the I-α and I-β phases and their interconversion. *Polymer*, *37*(10), 1833–1839. https://doi.org/10.1016/0032-3861(96)87299-5.

Hosoya, T., Kawamoto, H., & Saka, S. (2008). Different pyrolytic pathways of levoglucosan in vapor- and liquid/solid-phases. *Journal of Analytical and Applied Pyrolysis*, *83*(1), 64–70. https://doi.org/10.1016/j.jaap.2008.06.008.

Isikgor, F. H., & Becer, C. R. (2015). Lignocellulosic biomass: A sustainable platform for the production of bio-based chemicals and polymers. *Polymer Chemistry*, *6*(25), 4497–4559. https://doi.org/10.1039/c5py00263j.

Kaparaju, P., Serrano, M., Thomsen, A. B., Kongjan, P., & Angelidaki, I. (2009). Bioethanol, biohydrogen and biogas production from wheat straw in a biorefinery concept. *Bioresource Technology*, *100*(9), 2562–2568. https://doi.org/10.1016/j.biortech.2008.11.011.

Kaplan, H., & Seireg, A. (2002). Lateral thermal expansion of cellulose Iβ and IIII polymorphs. *Journal of Polymer Science, Part B: Polymer Physics*, *40*(11), 1095–1102. https://doi.org/10.1002/polb.10166.

Klemm, D., Heublein, B., Fink, H. P., & Bohn, A. (2005). Cellulose: Fascinating biopolymer and sustainable raw material. *Angewandte Chemie International Edition*, *44*(22), 3358–3393. https://doi.org/10.1002/anie.200460587.

Kono, H., Yunoki, S., Shikano, T., Fujiwara, M., Erata, T., & Takai, M. (2002). CP/MAS 13C NMR study of cellulose and cellulose derivatives. 1. Complete assignment of the CP/MAS 13C NMR spectrum of the native cellulose. *Journal of the American Chemical Society*, *124*(25), 7506–7511. https://doi.org/10.1021/ja010704o.

Koyama, M., Helbert, W., Imai, T., Sugiyama, J., & Henrissat, B. (1997). Parallel-up structure evidences the molecular directionality during biosynthesis of bacterial cellulose. *Proceedings of the National Academy of Sciences of the United States of America*, *94*(17), 9091–9095. https://doi.org/10.1073/pnas.94.17.9091.

Kubicek, C. P. (2012). Fungi and lignocellulosic biomass. In *Fungi and lignocellulosic biomass* Wiley-Blackwell. https://doi.org/10.1002/9781118414514.

Langan, P., Nishiyama, Y., & Chanzy, H. (2001). X-ray structure of mercerized cellulose II at 1 Å resolution. *Biomacromolecules*, *2*(2), 410–416. https://doi.org/10.1021/bm005612q.

Leng, E., Costa, M., Peng, Y., Zhang, Y., Gong, X., Zheng, A., et al. (2018). Role of different chain end types in pyrolysis of glucose-based anhydro-sugars and oligosaccharides. *Fuel*, *234*, 738–745. https://doi.org/10.1016/j.fuel.2018.07.075.

Malcolm Brown, R., Jr., Sazena, I. M., & Kudlicka, K. (1996). Cellulose biosynthesis in higher plants. *Trends in Plant Science*, *1*(5), 80050–80051. https://doi.org/10.1016/S1360-1385(96)80050-1.

Nishiyama, Y., Langan, P., & Chanzy, H. (2002). Crystal structure and hydrogen-bonding system in cellulose Iβ from synchrotron X-ray and neutron fiber diffraction. *Journal of the American Chemical Society*, *124*(31), 9074–9082. https://doi.org/10.1021/ja0257319.

Nishiyama, Y., Sugiyama, J., Chanzy, H., & Langan, P. (2003). Crystal structure and hydrogen bonding system in cellulose Iα from synchrotron X-ray and neutron fiber diffraction. *Journal of the American Chemical Society*, *125*(47), 14300–14306. https://doi.org/10.1021/ja037055w.

Nobles, D. R., Romanovicz, D. K., & Brown, J. (2001). Cellulose in cyanobacteria. Origin of vascular plant cellulose synthase? *Plant Physiology*, *127*(2), 529–542. https://doi.org/10.1104/pp.010557.

O'Sullivan, A. C. (1997). Cellulose: The structure slowly unravels. *Cellulose*, *4*(3), 173–207. https://doi.org/10.1023/A:1018431705579.

Patwardhan, P. R., Satrio, J. A., Brown, R. C., & Shanks, B. H. (2009). Product distribution from fast pyrolysis of glucose-based carbohydrates. *Journal of Analytical and Applied Pyrolysis*, *86*(2), 323–330. https://doi.org/10.1016/j.jaap.2009.08.007.

Plackett, D. (2011). In *Biopolymers – New materials for sustainable films and coatings* (pp. xiii–xiv). Wiley.

Praveen, K. G., Shreeya, S. R., Deepali, V. P., Priyadharsini, V., Vidhya, S., Chandrananthi, C., et al. (2019). An update on overview of cellulose. In *Its structure and applications* IntechOpen. https://doi.org/10.5772/intechopen.84727.

Rowland, S. P., & Howley, P. S. (1988). Hydrogen bonding on accessible surfaces of cellulose from various sources and relationship to order within crystalline regions. *Journal of Polymer Science Part A: Polymer Chemistry*, *26*(7), 1769–1778. https://doi.org/10.1002/pola.1988.080260708.

Shafizadeh, F., & Lai, Y. Z. (1972). Thermal degradation of l,6-anhydro-β-D-glucopyranose. *Journal of Organic Chemistry*, *37*(2), 278–284. https://doi.org/10.1021/jo00967a020.

Shen, D. K., & Gu, S. (2009). The mechanism for thermal decomposition of cellulose and its main products. *Bioresource Technology*, *100*(24), 6496–6504. https://doi.org/10.1016/j.biortech.2009.06.095.

Šturcova, A., His, I., Apperley, D. C., Sugiyama, J., & Jarvis, M. C. (2004). Structural details of crystalline cellulose from higher plants. *Biomacromolecules*, *5*(4), 1333–1339. https://doi.org/10.1021/bm034517p.

Wang, S., Guo, X., Liang, T., Zhou, Y., & Luo, Z. (2012). Mechanism research on cellulose pyrolysis by Py-GC/MS and subsequent density functional theory studies. *Bioresource Technology*, *104*, 722–728. https://doi.org/10.1016/j.biortech.2011.10.078.

Yang, L., Tsilomelekis, G., Caratzoulas, S., & Vlachos, D. G. (2015). Mechanism of Brønsted acid-catalyzed glucose dehydration. *ChemSusChem*, *8*(8), 1334–1341. https://doi.org/10.1002/cssc.201403264.

Zakzeski, J., Bruijnincx, P. C. A., Jongerius, A. L., & Weckhuysen, B. M. (2010). The catalytic valorization of lignin for the production of renewable chemicals. *Chemical Reviews*, *110* (6), 3552–3599. https://doi.org/10.1021/cr900354u.

Zhang, Y., Liu, C., & Chen, X. (2015). Unveiling the initial pyrolytic mechanisms of cellulose by DFT study. *Journal of Analytical and Applied Pyrolysis*, *113*, 621–629. https://doi.org/10.1016/j.jaap.2015.04.010.

Zhang, X., Yang, W., & Blasiak, W. (2012). Thermal decomposition mechanism of levoglucosan during cellulose pyrolysis. *Journal of Analytical and Applied Pyrolysis*, *96*, 110–119. https://doi.org/10.1016/j.jaap.2012.03.012.

Zhang, X., Yang, W., & Dong, C. (2013). Levoglucosan formation mechanisms during cellulose pyrolysis. *Journal of Analytical and Applied Pyrolysis*, *104*, 19–27. https://doi.org/10.1016/j.jaap.2013.09.015.

Zhao, X., Sun, X., Cui, X., & Liu, D. (2019). Production of biojet fuels from biomass. In *Sustainable bioenergy: Advances and impacts* (pp. 127–165). Elsevier. https://doi.org/10.1016/B978-0-12-817654-2.00005-8.

Praveen Kumar Gupta, Shreeya Sai Raghunath, Deepali Venkatesh Prasanna, Priyadharsini Venkat, Vidhya Shree, Chandrananthi Chithananthan, Shreya Choudhary, Krithika Surender and Keerthana Geetha (2019). An Update on Overview of Cellulose, Its Structure and Applications, Cellulose, Alejandro Rodríguez Pascual and María E. Eugenio Martín, IntechOpen, DOI: 10.5772/intechopen.84727. Available from: https://www.intechopen.com/books/cellulose/an-update-on-overview-of-cellulose-its-structure-and-applications.

Fui Kiew Liew, Sinin Hamdan, Md. Rezaur Rahman, Mohamad Rusop, Josephine Chang Hui Lai, Md. Faruk Hossen, Md. Mizanur Rahman, "Synthesis and Characterization of Cellulose from Green Bamboo by Chemical Treatment with Mechanical Process", *Journal of Chemistry*, vol. 2015, Article ID 212158, 6 pages, 2015. https://doi.org/10.1155/2015/212158.

Further reading

Liew, FK, Hamdan, S, Rahman, MR, Rusop, M, & Khan, A. (2020). Thermo-mechanical properties of jute/bamboo/polyethylene hybrid composites: The combined effects of silane coupling agent and copolymer. *Polymer Composites*, *41*, 4830–4841. https://doi.org/10.1002/pc.25755.

Piskorz, J., Majerski, P., Radlein, D., Vladars-Usas, A., & Scott, D. S. (2000). Flash pyrolysis of cellulose for production of anhydro-oligomers. *Journal of Analytical and Applied Pyrolysis*, *56*(2), 145–166. https://doi.org/10.1016/S0165-2370(00)00089-9.

Zhang, J., Das, A., Assary, R. S., Curtiss, L. A., & Weitz, E. (2016). A combined experimental and computational study of the mechanism of fructose dehydration to 5-hydroxymethylfurfural in dimethylsulfoxide using Amberlyst 70, PO_4^{3-}/niobic acid, or sulfuric acid catalysts. *Applied Catalysis B: Environmental*, *181*, 874–887. https://doi.org/10.1016/j.apcatb.2014.10.056.

Zhang, Y., Hu, B., Qiang, L., Changqing, D., & Yang, Y.-p. (2014). *A review on the formation mechanism of levoglucosan during fast pyrolysis of cellulose*. https://doi.org/10.3969/j.issn.1673-5854.2014.03.011.

Rahman, M. R., Hamdan, S., Ngaini, Z. B., et al. (2019). Cellulose fiber-reinforced thermosetting composites: impact of cyanoethyl modification on mechanical, thermal and morphological properties. *Polym. Bull.*, *76*, 4295–4311. https://doi.org/10.1007/s00289-018-2598-1.

Zhang, B., Leng, E., Wang, Y., Gong, X., Zhang, Y., & Xu, M. (2017). Characterization of water-soluble intermediates and solid residues from fast pyrolysis of cellulose in a wire-mesh reactor. *BioResources*, *12*(2), 2731–2747. https://doi.org/10.15376/biores.12.2.2731-2747.

Zhang, J. J., Liao, H. T., Lu, Q., Zhang, Y., & Dong, C. Q. (2013). Mechanistic study on low-temperature fast pyrolysis of fructose to produce furfural. *Ranliao Huaxue Xuebao/Journal of Fuel Chemistry and Technology*, *41*(11), 1303–1309. https://doi.org/10.1016/s1872-5813(14)60001-3.

CHAPTER

Advanced techniques for characterizing cellulose

4

Nur-Azzah Afifah Binti Taib[a], Md Rezaur Rahman[a], Muhammad Khusairy Bin Bakri[a], and Mohammed Mahbubul Matin[b]

[a]*Department of Chemical Engineering and Energy Sustainability, Faculty of Engineering, Universiti Malaysia Sarawak (UNIMAS), Kota Samarahan, Sarawak, Malaysia,* [b]*Department of Chemistry, Faculty of Science, University of Chittagong, Chattogram, Bangladesh*

Chapter outline

4.1 Introduction

Mainly, cellulose is originated from the cell wall of the trees and plants, thus making it the most abundant naturally polymer (Yang, 2017). In 1838, Anselm Payen was the first to recognize the existence of cellulose as the common material of plant cell walls, whereas their mechanical strength properties directly influenced by cellulose

Fundamentals and Recent Advances in Nanocomposites Based on Polymers and Nanocellulose.
https://doi.org/10.1016/B978-0-323-85771-0.00001-4

content (Kalia et al., 2011; Praveen et al., 2019). Besides that, it is the most biodegradable, reusable, sustainable, and compostable organic material on earth (Pan, Farmahini-Farahani, O'Hearn, Xiao, & Ocampo, 2017). Although plants are the main sources of cellulose, but other materials such as algae, bacteria and some sea animals can also produce cellulose (George & Sabapathi, 2015).

Aforesaid, there are several other main sources of cellulose available besides plants, i.e., algae, bacteria, and tunicates. For plants, their abundant availability and relatively cheap price is the main sources of cellulose attractions. About 50% of the cell wall material of plants are represented by cellulose and it is the most widely distributed skeletal polysaccharide (Nair, Sivasubramanian, Balakrishnan, Kumar, & Sreekala, 2013). Apart from that, cellulose acts a structural element in plant fiber, hence providing wood and other plants with strength. In seed hairs of cotton, its cellulose content can reach above 90 wt%, indicating that cellulose can occur in rather pure form. However, most of the cases, lignin, other polysaccharides (e.g., hemicelluloses and pectin), and also small amounts of organic compounds such as extracts occurs together with cellulose (Jedvert & Heinze, 2017). Wood pulp and cotton fibers are among the main sources of cellulose, and their harvesting, processing, and extraction are currently available with the large-scale industrial infrastructures. Other than that, plants such as jute, ramie, flax, hemp, etc., which are also used to produce cellulose (Eichhorn et al., 2001; George & Sabapathi, 2015). Besides that, agricultural wastes (sugarcane bagasse, sawdust, etc.) and municipal residues also contained a major component of cellulose (George & Sabapathi, 2015; Nair et al., 2013). Besides plants, the cell wall of algae is also mainly made up from cellulose. The green algae are the most preferred type of cellulose used in the cellulose extraction, although there are also red and yellow algae that can be used. Cellulose with an exceptionally high degree of crystallinity (up to 95%) can be found from the algae of the *Valoniaor cladophora* group (George & Sabapathi, 2015).

Apart from the plant and algae groups, as an alternative source, various types of bacteria can also be used to produce cellulose. In 1886, bacterial cellulose (BC) was first reported as a white pellicle on a liquid medium during the acetic fermentations. *Bacterium xylimun* (later renamed to *Acetobacter xylimun (A. xylinum)*) generated those cellulose membrane, and it is known as *Komagataeibacter medellinensis*. Similar to silk natural fiber produced from the silkworm, the shape of cellulose produced from BC is in the form of fiber with nano-sized width (Choi & Shin, 2020). BC had a molecular formula of $(C_6H_{10}O_5)_n$ and consists of β-14 glycan chain that used inter- and intrahydrogen bonding to hold it together (Faezah, Masrinda, & Abd, 2014). Through oxidative fermentation in both synthetic and nonsynthetic medium, BC would be produced by the acetic acid bacteria. Although both plant cellulose and BC had similar molecular weight and polymeric structure, but within the unit cells of the crystallites, the arrangement of glycosyl units is different, which made BC had higher crystallinity. Other properties of BC are that its high degree of polymerization, water holding capacity and mechanical strength (Faezah et al., 2014; George & Sabapathi, 2015).

The next cellulose source is a marine invertebrate sea animal named tunicates. Presently, it is the only animal source to produce cellulose in large amount. The entire epidermis of tunicates covered with tunic tissues which the cellulose will act as the

Table 4.1 Main sources of cellulose (Mishra et al., 2018).

Type of sources	Remarks
Plants	The significant sources for cellulose production is still remaining from plants, due to its abundance and cheaper nature. Plant-based resources include wood pulp, cotton fibers, bagasse, straw, ramie, sisal, flax, and hemp. Currently, industrial facilities are available to harvest, process, and extract cellulose from plant resources.
Algae	The most fundamental component present in cell wall of several algal species is cellulose. Green algae serves as the most suitable source for the extraction of cellulose. Also, red and yellow algal species are known to produce cellulose. It is reported that the cellulose extracted from the *valonia* and *Cladophora species*, which belongs to *Cladophorales* and *Siphonocladales* family, presents enormously high crystallinity of ~95%. The characteristics of cellulose microfibrils are dependent on the biosynthesis process that occurs in different algal species.
Bacteria	The bacterial species, namely *Komagataeibacter xylinus* is well known to produce cellulose. This species utilized carbon as well as nitrogen sources such that thick and clear cellulose microfibrils are formed on the growth medium. The cellulose pellicles are further subjected to an alkali treatment to remove water, followed by drying and processing into membranes. The cellulose derived from microbes presents superior characteristics as compared to cellulose derived from plant-based resources. These significances include (i) uniqueness in the nanostructure, (ii) a greater degree of purity and (iii) higher mechanical properties.
Tunicates	Tunicates belong to the family of marine invertebrates. They are capable of the production of cellulose in huge quantity. Enzymes complexes predominant in the epidermal layer of tunicates is responsible for the production of cellulose. The characteristics of the produced cellulose are different with respect to species. The variation in the production process of different species may affect the end characteristics of cellulose microfibrils.

skeletal structure of the tissue. Approximately, 60% cellulose and 27% nitrogen-containing components by dry weight had been historically reported to be contained in the tunic (Zhao & Li, 2014). By using enzyme complexes presents in the membrane of the epidermis, tunicates would be able to produce the cellulose (George & Sabapathi, 2015). Cellulose obtained from tunicates is highly crystalline and had a high aspect ratio besides great degree of polymerization (range between 700 and 3500) (Zhao & Li, 2014). Table 4.1 lists the main sources of cellulose.

4.2 Structure of cellulose

As a polymer of glucose, the cellulose had a molecular formula of ($C_6H_{12}O_6$) and consists of a linear homo-polysaccharide composed of D-glucopyranose units (Chirayil, Mathew, & Thomas, 2013; Maleki, Mohammadi, & Ji, 2016). The β-1,4-glycosodic bonds that linked up the units will be formed residues from the

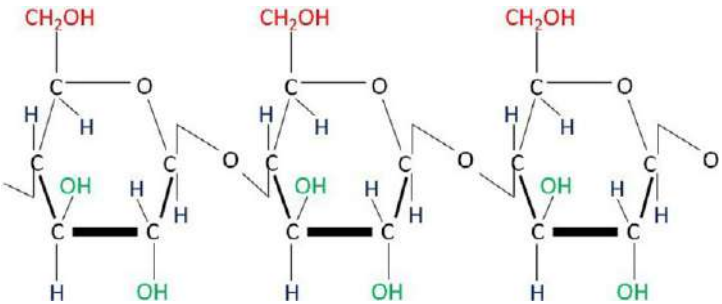

FIG. 4.1

Schematic representation of cellulose (Mishra, Sabu, & Tiwari, 2018).

Modified from Mishra, R., Sabu, A., & Tiwari, S. (2018). Materials chemistry and the futurist eco-friendly applications of nanocellulose: Status and prospect. Journal of Saudi Chemical Society, 22*(8), 949–978. https://doi.org/10.1016/j.jscs.2018.02.005.*

180 degrees rotation of the units with the neighboring unit namely cellobiose unit (Maleki et al., 2016, 2017). A repeating unit of cellobiose would make up the cellulose chain. Fig. 4.1 shows the schematic diagram of cellulose. Cellulose structural properties had made it possible for cellulose to retain a semicrystalline state of aggregation even in an aqueous environment, which is unusual for a polysaccharide (Mishra et al., 2018; Praveen et al., 2019).

The degree of polymerization of native cellulose is difficult to be determined, but it is reported to be around 10,000 and had a molecular weight of 3.2×10^6 g/mol (Mariano, El Kissi, & Dufresne, 2014). The crystalline structure and physical properties of the cellulose are determined by the hydroxyl groups, which different bonds of intermolecular or intramolecular hydrogen could be formed (Yang, 2017). Typically, cellulose is made up from two types of region, the crystalline regions and the amorphous regions as shown in Fig. 4.2 (Mariano et al., 2014). There are different structural levels of cellulose as cellulose chains show a very high tendency to self-order. Those chains would arrange themselves into fibrils with varying degree of order in each of the formed regions, hence resulting in varying texture and density of the layers. The properties and reactivity of different cellulose materials are affected by this unique and complex structure (Jedvert & Heinze, 2017). In the fibril structure, the crystalline domains are interspersed with the amorphous regions (Fernandes, Pires, Mano, & Reis, 2013).

Next, depending on the sources of cellulose, the degree of crystallization varies from 60% to 80% (Yang, 2017). This is due to the distributions of crystalline regions in those sources varies; in plant source, the region can represent up to 50%, while for bacterial cellulose and algae-based cellulose, the region can dominate up to 100% of the fibril which shown in Fig. 4.2 (Mariano et al., 2014). Meanwhile, between the microfibrils would be locating the amorphous or disordered region. The cellulose would have higher accessibility to accept the attack by other molecules when the amorphous region or fraction are higher compared to the crystalline region

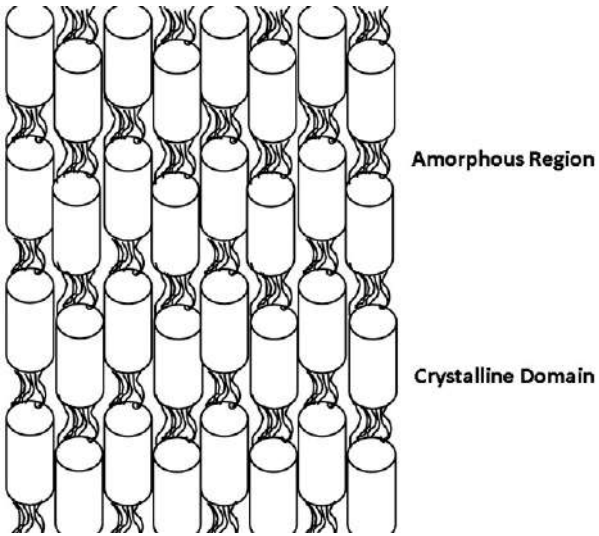

FIG. 4.2

The regions dispersion in the cellulose (Mariano et al., 2014).

Modified from Mariano, M., El Kissi, N., & Dufresne, A. (2014). Cellulose nanocrystals and related nanocomposites: Review of some properties and challenges. Journal of Polymer Science, Part B: Polymer Physics, 52*(12), 791–806. https://doi.org/10.1002/polb.23490.*

(Yang, 2017). The biodegradability can be increased by the presence of the amorphous regions (Fernandes et al., 2013). Cellulose are not only chemically stable and insoluble, but also has very good strength. Like ways staggered bricks add strength and stability to a brick wall, the hydrogen bonding between chains does the same to the cellulose structure. Flat sheets would then be formed, and it lies on top of one another in staggered fashion, adding stability to the cellulose (Flaris & Singh, 2009).

I, II, III_I, III_{II}, IV_I, and IV_{II} are the six crystalline polymorphs of cellulose. However, the most common forms of cellulose are cellulose I and II. As for the others, it is not yet known to exist freely in nature (Maleki et al., 2016). This is because, native cellulose (cellulose that are produced by plants) is found in two crystalline forms, cellulose I and II. Typically occurs in marine algae, cellulose II is a crystalline form that is form when aqueous sodium hydroxide is used to treat cellulose I which shown in Fig. 4.3 (Lavanya et al., 2011). Next, there are two allomorph for cellulose I, which are I_α and I_β. While I_β are more dominant in higher plant cellulose, I_α are mainly stored in lower plants. In terms of crystallinity, a research showed that I_α had higher crystallinity compared to I_β (Yang, 2017). Apart from that, cellulose I are thermodynamically less stable while cellulose II is the most stable structure among the polymorph's cellulose I, II, III, and IV. Crystalline cellulose III is formed when cellulose I and II are treated with liquid ammonia, while cellulose IV crystalline form will be generated when cellulose III is heated. Fig. 4.3 showed the transformation of those cellulose into its various polymorphs.

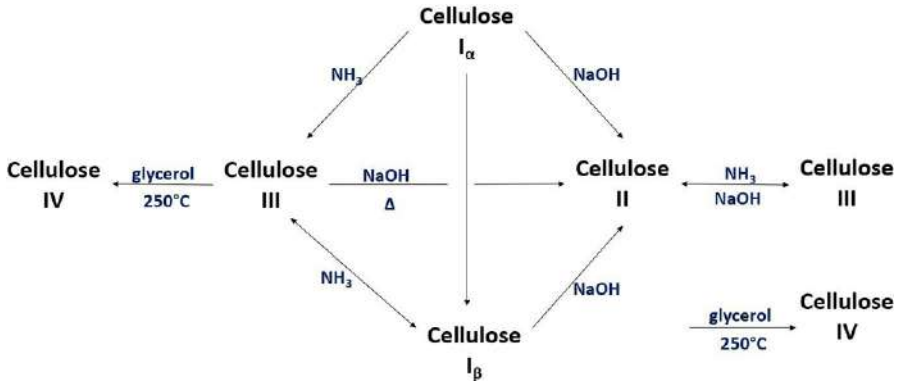

FIG. 4.3

Transformation of the cellulose into its various polymorphs (Lavanya, Kulkarni, Dixit, Raavi, & Krishna, 2011).

Modified from Lavanya, D., Kulkarni, P. K., Dixit, M., Raavi, P. K., & Krishna, L. N. V. (2011). Sources of cellulose and their applications—A review. International Journal of Drug Formulation and Research, *2(6), 19–38.*

4.3 Molecular weight of cellulose

According to Gralén & Svedberg (Gralén & Svedberg, 1943), it had been a great interest in the cellulose chemistry to study regarding the molecular weight of cellulose. Hence, there had been attempts have been made to determine the cellulose's molecular weight. One of the highly relevant parameters for the molecular weight analysis is the degree of polymerization (DP). Generally, the DP is the number of monomeric units that are in either a polymer, macromolecule, or oligomeric molecules. However, there are some authors that describe DP as the number of repeat units, and it might not be identical to the monomeric unit for copolymers (Patkar & Panzade, 2016). Depending on the source, production process and treatment, the cellulose materials will have varying DPs (Oberlerchner, Rosenau, & Potthast, 2015). According to Kunusa et al. (Kunusa, Iyabu, Taufik, & Botutihe, 2018), cellulose not only had high a molecular weight (MW), but its DP levels can reach up to 20,000.

Staudinger had obtained DP of 2000–3000 for native cotton and ramie when he extrapolated his "viscosity rule" from measurements of relatively low molecular weight materials. Meanwhile, Kraemer had obtained values up to 1300 for purifying cotton linters, and estimated that for native cellulose, the molecular weight is to be at least 570,000 (D.P. 3500), when he performed sedimentation equilibrium measurements (Gralén & Svedberg, 1943). Next, according to Oberlerchner et al. (Oberlerchner et al., 2015), for commercial celluloses, the DP values range from 100 to 3000, while form cotton fiber secondary walls, the DP can reach 20,000. As for *Valonia* (a species of algae), the DP value is 44,000. Typically, native cellulose will have higher DP values as compared to cellulose that are regenerated or had

been processed by pulping (Oberlerchner et al., 2015). Hence, it is matched with recent report, which mentioned, as compared to cellulose obtained from other natural sources such as wood, cotton cellulose not only had larger MW but also a higher level of crystallinity. This is because cotton fiber, particularly is greatly dependent on the weight average MW apart from the orientation of cellulose microfibrils in the secondary cell wall (Liyanage & Abidi, 2019). This is due to fact that one of the important variables to determine the polymer's chemical properties are described by the molecular mass value, which is the polymeric molecular size distribution. A polymer will have a stronger property when it has high MW (Kunusa et al., 2018).

Great push regarding the investigation of methods for the determination of weight-average molecular weights of high polymeric compounds exists due to the publication of the Staudinger empirical viscosity—molecular weight relationship (Battista, 1944). There are several methods that had been used in the measurement of the molecular weight, i.e., end group, osmotic pressure, ultracentrifugation, the viscosity of cellulose solutions, light scattering methods, etc. However, the contemporary method of choice to determine the molecular weight in cellulose research is by coupling the size exclusion chromatography (SEC) with a light scattering detector and a refractive index (RI) detector (Oberlerchner et al., 2015).

4.4 Chemical structure characterization techniques

Among the important structural parameters which influence the mechanical properties of the cell wall are the shape, size, and crystallinity of the cellulose microfibrils. The study regarding those parameters are essential, as they are likely to be determinants of cell wall digestibility if lignocellulosic were to be used for the production of biofuels or for biofuel conversion (Martínez-Sanz, Gidley, & Gilbert, 2015; Rongpipi, Ye, Gomez, & Gomez, 2019). Hence, there had been several techniques (individually or in combination) used to extract valuable structural details about the cell wall components, especially cellulose (Rongpipi et al., 2019). Among the essential cellulose structure characterizations and interactions in the plant cell walls are as follows.

4.4.1 Cellulose crystallinity

Crystallinity is a measure of structural order, and it is the ratio of crystalline to crystalline plus amorphous content by volume. Mechanical properties of both cellulose and cellulose-derived materials such as the strength and stiffness are affected by the crystalline. Additionally, the accessibility and reactivity of a given cellulose substrate to enzymes for biomass conversion are also influenced by the relative level of crystalline versus amorphous material within cellulose (Rongpipi et al., 2019). Thus, there had been some techniques which are used to estimate the crystallinity of the cellulose.

4.4.1.1 Updegraff method

This physicochemical method is commonly used to check the amount of crystalline cellulose in a sample. For this method, using an acetic acid/nitric acid reagent, the lignin, hemicellulose and xylosans would be extracted, leaving behind the crystalline cellulose. Next, in 67% H_2SO_4 solution, the cellulose would be dissolved, and after treating with an anthrone reagent to enable colorimetric analysis, the amount of crystalline cellulose can be determined. This physiochemical method generally reports a higher value of crystallinity in comparison to the crystallinity found from the XRD measurements. It is possible that the compositional and structural heterogeneity of the cell walls (particularly primary cell walls) was the reason for this discrepancy, as access to the noncrystalline components were to be complicated (Rongpipi et al., 2019).

4.4.1.2 X-ray diffraction (XRD)

Due to its established reliability and accuracy, besides minimal sample preparation requirements, XRD is the most widely used technique to determine the crystallinity of cellulose. Within the entire sample, XRD gives a measure of crystallinity as the mass fraction of crystalline cellulose (Rongpipi et al., 2019). Additionally, this analysis is not only as a mean to measure the crystallinity but are also significant to examine the factors that are influencing the distribution and transition of highly ordered to least-ordered regions, systematically. The analysis required a powder X-ray diffractometer (PXRD) that are equipped X-ray tube, CuX_{α}, diffracted beam graphite monochromator and a NaI scintillation detector in the experimental protocol. It was then would be used together with the generator that are set to 40 kV and 40 mA (Foster et al., 2018).

For the estimation of crystallinity from XRD, there are several methods that are widely used such as the Segal method (the peak height), peak deconvolution of crystalline and amorphous peaks, Ruland-Vonk method (the amorphous subtraction) and Ruland-Rietveld approach. The most widely used analysis approach to characterize the cellulosic samples crystallinity is the Segal method. However, as the exact amount of the crystalline fraction is proportional to the peak area rather than to the peak height, this method is not very accurate. Hence, depending on the crystallite size and cellulose allomorph, the crystallinity obtained via this method would be affected. Meanwhile, the second method accuracy are depending on the correct peak selections that correspond to the actual diffraction contributed by each fraction (Foster et al., 2018; Rongpipi et al., 2019).

As for the third method, the ratio of an area above an amorphous profile of the total area is what defines crystallinity. Next, in the Ruland-Rietveld approach, the degree of crystallinity, X_c can be determined using Eq. (4.1), assuming that the total diffracted X-ray intensity is made up from the diffracted X-ray intensity from both regions (crystalline and amorphous):

$$X_c\,(\%) = \frac{A_c}{A_c + A_a} \times 100 \tag{4.1}$$

Where A_c is the total crystalline area, and A_a is the total amorphous area of the deconvoluted XRD pattern after the background spectra had been subtracted. Since this approach had accurately permits the quantification of the solid-state properties, it had been used to study the super molecular structure of various polymeric materials (Foster et al., 2018; Rongpipi et al., 2019).

4.4.1.3 Solid-state nuclear magnetic resonance (SSNMR)

By using this technique, the atomic structure of the material can be analyzed, and the most used NMR technique is the ^{13}C CP-MAS NMR as the subject of NMR is vast. The combination of usage of cross-polarization (CP), magic angle spinning (MAS) and high dipolar decoupling devices are required for this ^{13}C CP-MAS NMR spectroscopy as it is a high-resolution technique (HR-ssNMR). It allowed one to record spectra with a resolution comparable to classical liquid-state NMR spectra in comparison to the low resolution ssNMR spectroscopy (LR-ssNMR). Generally, before using 2D-NMR technique for sophisticated analysis to study, for example, the crystalline phase structure, this measurement is a prerequisite.

In order to remain fully quantitative, ^{13}C CP-MAS NMR are typically performed on dry samples, although it has been proven that the resolution of the spectra is improved when using wet samples. Routine experiments would generally require 50 mg of the materials, but variations might occur depending on the specifications and requirements of the equipment. Table 4.2 listed the assignments of ssNMR chemical shifts corresponding to neat cellulose nanomaterials (CNMs), while Table 4.3 compared the crystallinities of cellulose from different sources determined by XRD and NMR analysis methods. Based on those tables, it can be concluded that the obtained value from NMR are lower than those calculated from XRD experiments, but it is still comparable (Foster et al., 2018).

4.4.1.4 Fourier transform infrared spectroscopy (FTIR)

Using this spectroscopy, when infrared light irradiates and interacted with the sample, the amount of light absorbed, transmitted, and/or reflected would be measured by the device. The absorbance would be then reported as a function of wavenumber as listed in Table 4.4. Those molecular vibrations information can be used for the identification of both chemical and physical properties of functional groups within the sample. Generally, the typical wavenumber range in which the measurement is performed in the transmission is between 4000 and 400 cm^{-1} with a 4 cm^{-1} resolution and 16 to 64 sample scans are used (Foster et al., 2018).

4.4.1.5 Raman spectroscopy

Although this technique had been used to analyze the cellulose materials since the 1970s, but only in 2005 that the development of a method to estimate the cellulose crystallinity are developed. Mostly suited to analyze pure cellulose samples, this method (sometimes referred as 1481-Raman) was using CH_2 bending vibrations in cellulose molecules as its basis. However, due to their CH_2 spectral contributions, the presence of hemicellulose and lignin is problematic as the spectral overlap with

Table 4.2 Assignments of ssNMR chemical shifts corresponding to neat cellulose nanomaterials (CNMs) (Foster et al., 2018).

Chemical shifts (ppm)	Carbon	Assignment
105.7; 103.9	C1	Cellulose I_α (native cellulose)
105.0		Cellulose I_β (native cellulose)
107.0; 104.7		Cellulose II (mercerized cellulose)
89.4; 88.7	C4	Cellulose I_α (native crystalline cellulose)
88.7; 87.9		Cellulose I_β (native crystalline cellulose)
84.2; 83.2		Accessible disordered (amorphous) cellulose (thin contribution)
83.4		Inaccessible disordered (amorphous) cellulose (large contribution)
81.7		Hemicelluloses (thin contribution)
78–70	C2, 3, 5	Indistinguishable in 1D experiments
65.3		Cellulose I_α (native cellulose)
65.5; 64.8		Cellulose I_β (native cellulose)
62.9; 62.2		Cellulose II (mercerized cellulose, thin contribution)
61.5		Disordered cellulose (large contribution)

Table 4.3 Crystallinities of cellulose from different sources determined by XRD and NMR (Rongpipi et al., 2019).

	XRD			NMR
Cellulose sample	Peak height	Peak deconvolution	Amorphous subtraction	C4 peak separation
Bacterial microcrystalline cellulose	95.2	73.1	82.4	73.8
Avicel PH-101	91.7	60.6	77.7	56.7
SigmaCell 50	91.2	61.3	79.4	56.1
SigmaCell 20	84.8	64.2	67.0	52.6
JT Baker cellulose	85.5	61.5	69.1	49.1
Fluka cellulose	82.9	52.9	61.6	48.6
SolkaFloc cellulose	78.3	56.8	57.2	43.9
Sigma α-cellulose	78.0	55.9	54.4	41.5

Note: All values are means.

that of cellulose. Hence, 380-Raman method is more suitable to be used to estimate crystallinities as such aforesaid problem does not exist with this method. This is because this 380 cm^{-1} band-based method not only applicable to pure celluloses but can also be used for materials that contained noncellulose components.

Table 4.4 Assignments of IR bands corresponding to neat CNMs (Foster et al., 2018).

Wavenumber (cm^{-1})	Assignment
Between 3000 and 3700	Stretching vibration bands of the O—H bonds of the primary and secondary hydroxy groups
2900	Stretching vibration of the C—H bond
1650 (400 and 700)	Adsorbed water
1315, 1335, 1430 and 1470	In-plane bending vibration bands of the primary and secondary hydroxy groups
1160	Antisymmetric stretching vibration of the C—O—C glycosidic bond
1110, 1060 and 1035	Vibrations of the C—O bond of carbons 2, 3 and 6
665 and 705	Out of plane torsional vibrations of the hydrogen bonded O—H groups (free OH: 240 cm^{-1})

Eq. (4.2) can be used to estimate the cellulose crystallinity using 380-Raman ($X_{380\text{-Raman}}$), where the equation is a regression that correlates the crystallinities and the band intensity ratios at peak height of 380 and 1096 cm^{-1} (I_{380}/I_{1096}) of the calibration set samples:

$$X_{380-\text{Raman}}\,(\text{MultiRam}) = \frac{\left(\frac{I_{380}}{I_{1096}} - 0.0286\right)}{0.0065} \tag{4.2}$$

where the FT-Raman instrument that are used to obtain the spectra are indicated with MultiRam (Foster et al., 2018).

4.4.2 Size and organization of the cellulose microfibrils

The existence of cellulose in a bundled fibrillar structure can be shown with direct visualization of the cell wall trough light microscopy. To fully understand the fibrillar network of cellulose, the characterization of the structural parameters such as the length, size, shape, etc. are crucial. This is because the mechanical and physiochemical properties of cellulose and its derivatives are strongly influenced by those parameters (Rongpipi et al., 2019). Hence, the techniques that can be used to characterize the above-mentioned parameters are as follows:

4.4.2.1 Electron microscopy (EM)

Characterization of cellulose and cellulose-derived materials extensively used EM as exquisite details can be yield using this technique even at the subnanometer scale. However, for the samples to be compatible with EM, the cellulose samples must be prepared through drying, coating, or staining methods (Moran-Mirabal, 2013). In this technique, a focused beam of accelerated electrons is used to produce

magnified images of high resolution of several nanometers or less. When the samples collide with the electrons, an emission of various particles both reflected and transmitted will be generated. Namely, the energy of the electron is transformed with the interaction between samples and an electron, and an image is formed when the differences in electron energy are detected (Foster et al., 2018).

There are two main methods of EM that are commonly used, i.e., scanning electron microscopy (SEM) and transmission electron microscopy (TEM). Taking advantage of the secondary electrons emitted from the sample, SEM is a surface imaging technique, while in TEM, electrons will pass through the sample (Foster et al., 2018). For both methods, by the interaction of electrons with the substance of the specimen, an image is formed; the image will then be magnified and focused onto imaging devices such as a photographic film or a fluorescent screen. Sensor such as CCD camera can also detect the image. A small electronic spot is created when the electron beam generated by an electron gun is focused by condensers (Michael, 2017).

Both SEM and TEM are not only suitable to evaluate the size and shape of nanosized particles but are also feasible to check the particles' degree of dispersion and aggregation. The reason is that SEM and TEM can resolve down to 1 nm and 0.2 nm, respectively, under ideal conditions. Meanwhile, the magnification of TEM and SEM image can reach about 10^6 and 10^5, respectively. But, for characterization of nanoparticles, compared to SEM, TEM are most used method as it has higher spatial resolution (Foster et al., 2018; Michael, 2017).

4.4.2.2 Atomic force microscopy (AFM)

AFM is one of the most widely utilized tools in real-time imaging of biological samples because being a high-resolution Scanning Probe Microscopy (SPM) technique, it was able to record surface topography and properties at the nanoscale (Moran-Mirabal, 2013). The specimen surface is scanned using cantilever which have a sharp tip at its end. Usually, the cantilever is made with silicon or silicon nitride, and the radius of the tip ranges from a few nanometers (for silicon-based tips) to a few angstroms (for carbon nanotube tips). The forces between the tip and the sample will led to a deflection of cantilever when the tip is brought into proximity of a sample surface. By using a laser spot reflected from the top surface of the cantilever in an array of photodiodes, the deflection will be able to be measured (Michael, 2017; Moran-Mirabal, 2013).

Depending on the size of AFM tip used, the resolution of the surface map will be limited, and it can reach up to 0.1 nm, vertically and up to 0.5 nm, laterally, under optimal conditions. Fig. 4.4 showed the general schematic depiction of an AFM setup. By using a feedback mechanism, the tip-to-substrate distance can be controlled, allowing the tip position to be adjusted to maintain a constant force between the tip and the sample. The force applied by the cantilever for imaging of soft biological samples is typically limited to be ranging between 50 and 100 pN. This was done to not only minimize the sample deformation, but also to avoid the Biomolecular interactions disruption (Moran-Mirabal, 2013).

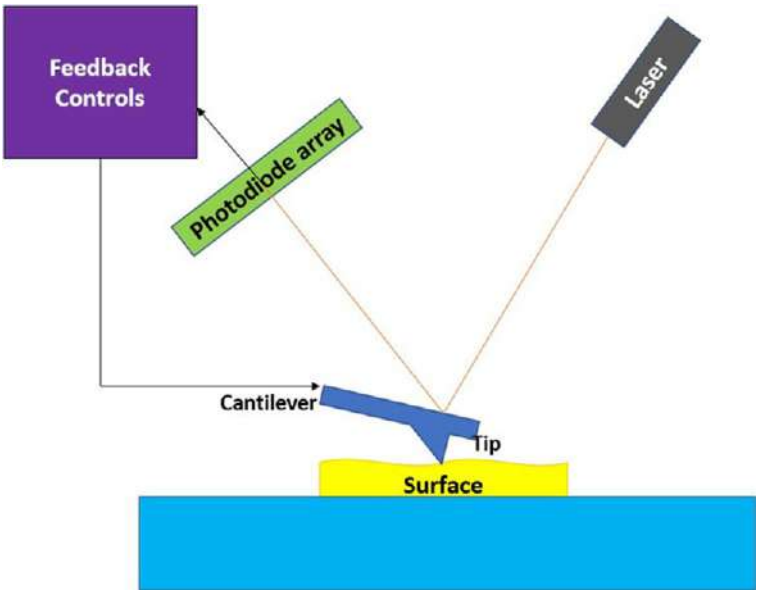

FIG. 4.4

General schematic depiction of an AFM setup (Moran-Mirabal, 2013).

Modified from Moran-Mirabal, J.M. (2013). Advanced-microscopy techniques for the characterization of cellulose structure and cellulose-cellulase interactions. In T. G. M. Van De Ven (Ed.), Cellulose—Fundamental Aspects. *InTechOpen. https:/doi.org/10.5772/56584.*

4.4.2.3 X-ray and neutron small angle scattering technique

The basis of this scattering technique is the analysis of the scattered radiation produced after the interaction of sources (i.e., X-ray and neutrons) with the particles present in the sample. Information such as size, shape and orientation of components in systems can be obtained using these techniques. Typically, a two-dimensional detector was used to measure the radiation scattered by the sample of interest.

Next, depending on the range of scattering angles (and corresponding length scales) covered, the scattering methods are classified into two techniques, namely wide angle and small angle scattering techniques. Small angle scattering techniques, i.e., small angle neutron (SANS) and X-ray (SAXS) scattering can cover a size ranging from 1 nm to several hundreds of nanometers, while the wide-angle scattering techniques are used to probe subnanometer dimensions. In addition, small angle may be coupled with ultra-small angle scattering techniques (USANS and USAXS) to enable it to study larger structures as doing so will extend the size range up to ca. 10 μm. Also, when selecting the proper source of radiation, two matters must be taken into consideration, which are the sample composition and structural features to be probed. Table 4.5 summarized the neutron and X-ray scattering length densities of some plant cell wall components, while Table 4.6 listed some cellulose microfibril cross-section and orientation angle determined from different sources (Martínez-Sanz et al., 2015).

Table 4.5 Neutron and X-ray scattering length densities (SLD) of some plant cell wall components (Martínez-Sanz et al., 2015).

	Neutron SLD (10^{10} cm^{-2})	X-ray SLD (10^{10} cm^{-2})
Cellulose (crystalline)	1.87	14.46
Cellulose (amorphous)	1.73	13.38
Arabinoxylan	1.62	12.64
Xyloglucan	1.62	12.65
Pectin	2.44–2.92	15.51–15.69
Lignin	2.64	12.97
H_2O	−0.56	9.47
D_2O	6.33	9.47

Table 4.6 Cellulose microfibril cross-section and orientation angle determined from different sources (Martínez-Sanz et al., 2015).

Raw material	Microfibril cross-section (nm)	Orientation angle (degrees)	Technique
Celery collenchyma	2.4–3.6		NMR, SAXS, WAXS
	2.9–3.0		SANS, WAXS
	2.6–3.0		SAXS
Spruce wood	2.5	4.6–19.8	TEM, WAXS, SAXS
	2.9	39.0–89.0	WAXS
	3.1–3.2		SANS, WAXS
		5–40	SAXS
	2.9–3.1	−20 to 90	WAXS
Sugi wood *(Cryptomeria japonica)*	2.4–2.6		SAXS
Flax fibers	1.0–5.0	11–15	SAXS
Oak wood	2.9–3.1	4–9	WAXS, SAXS
Onion	2.0		NMR
Mung bean (*Vigna radiata*)	2.5–3.2		WAXS, NMR

4.4.2.4 Surface area analysis

One of the methods that can be used for surface area analysis is by using BJH method, which are developed by Barrer, Joiyner, and Halenda. Mesopore volume and mesopore size distribution are obtained via this method. By using adsorption and desorption techniques, this method can determine the pore area and specific pore volume. The amount of gas absorbed across a wide range of relative pressure at constant temperature (77 K) using liquid nitrogen is measured to obtain the adsorption isotherm. Conversely, by measuring the gas removed, the desorption isotherms are achieved as pressure are reduced.

There are two fundamental assumptions that are implemented by the BJH theory, (i) the pore shape is cylindrical, and (ii) both physical adsorption on the pore walls and capillary condensation in mesopores will make up the adsorbed amount. Thus, the radius of the pore was considered by this BJH method to be the sum of the multilayer thickness (t) and the meniscus radius obtained from the Kelvin equation, as shown in Eq. (4.3).

$$\ln \frac{P}{P_0} = \frac{2\gamma V_m}{rRT} \tag{4.3}$$

Where P/P_0 is the relative pressure in equilibrium with a meniscus; γ is the adsorbent surface tension in liquid form; V_m is the liquid molar volume; R is the universal gas constant; r is the meniscus radius that are formed in the mesopore; and T stands for temperature. The decrement in the relative pressure in the desorption branch was used by BJH to calculate the change in the thickness of adsorbed film. It is considered that the evacuation of the largest pores from the capillary condensate and the reduction in thickness of the physically adsorbed layer are what is causing that decrement to happen (Bardestani, Patience, & Kaliaguine, 2019).

4.5 Thermal properties of cellulose characterization techniques

Some analysis needed to be done regarding the materials and environment that are used in a process as it is crucial, sometimes, for the conditions of the process to be maintained under control. Hence, a variety of important information are provided by thermal analysis (TA) techniques to be used by the researchers. Among the commonly used TA are differential scanning calorimetry (DSC), thermogravimetric analysis (TGA), thermomechanical analysis (TMA), and dynamic mechanical analysis (DMA). However, there are also few relatively new methods which are used to measure the thermal conductivity of planar materials, such as steady-state methods, laser spot periodic heating radiation thermometry method, and flash method (Uetani & Hatori, 2017).

4.5.1 Thermal analysis (TA) technique

Various physical and chemical phenomena accompanied by exothermic or endothermic effects can be provided by all thermo analytical method. Processes such as sorption and desorption, oxidation, and thermal decomposition of the samples can be studied with the introduction of various TA methods. Apart from that, the sample's thermophysical characteristics are also obtainable with the methods (Michael, 2017). The TA techniques are as follows:

4.5.1.1 Differential scanning calorimetry (DSC)

In this thermo-analytical method, the measurement of the difference in the amount of heat energy between the sample and etalon are as a function of temperature. Throughout the experiment, the temperature of both sample and etalon are maintained at nearly the same value. For a DSC analysis, generally, the temperature program is designed such that the sample holder temperature to linearly increase as a function of time (Michael, 2017). Simply, the difference in the amount of heat required to increase the temperature associated with transitions in materials are measured as both time and temperature functions. Via this method, measurements of transition, such as the glass transition, melting and crystallization are measured, besides allowing accurate measurement of temperatures that are related to thermal events (Norhayati, Harfiz, Diana, Mohd, & Idayu, 2019).

The basic principle of this technique is that in order to maintain both sample and reference at the same temperature when the sample undergoes a physical transformation such as phase transition, more or less heat will need to flow to the sample compared to the reference. But, the type of process (exothermic or endothermic) will determine whether heat should flow to the sample. For instance, less heat will be required to raise the sample temperature when it undergoes an exothermic process such as crystallization, and vice versa. Differential scanning calorimeters can measure the amount of heat absorbed or released during such transitions by observing the differences in heat flow between the sample and reference (Norhayati et al., 2019).

4.5.1.2 Modulated DSC (MDSC)

Although DSC offered a wider range of temperature compared to other thermal characterization where the transitions may be observed, but due to the instrumentation of the DSC technique itself, the overlapping of some phase transitions might occur. This is because the average of several hat flow signals is where the heat flow is acquired. Hence, it is suggested that by using larger amounts of samples and decreasing the heating rate, this problem would be overcome, and with MDSC, even at very low heating rates, Cp is able to be directly determined (Norhayati et al., 2019).

As this method superimposes a faster sinusoidal heating rate onto a slower underlying linear heating rate, different thermal events are able to be separated, thus the total heat flow is allowed to be separated into the reversing heat flow (heat capacity related events) and nonreversing heat flow (time and temperature-dependent events). Hidden and weak glass transitions (a transition that can only be detected with very

sensitive method) are likely to be detected due to the fast instantaneous and slower underlying heating rates combination allowed both high sensitivity and resolution (Picker & Hoag, 2002). Next, there are three signals that are acquired during the MDSC, i.e., Total, reversible and nonreversible heat flow. With this technology, the experimental work is simplified, and the measurement is more accurate as direct measurement of heat capacity, even at very low heating rates (quasi-isothermal) conditions. Basically, the disadvantages of conventional DSC are to be overcome by developing this MDSC (Leyva-Porras et al., 2020).

4.5.1.3 Thermogravimetric analysis (TGA)

Changes in the weight of the sample are measured as a function of increasing temperature in this TA method (Michael, 2017). But, when the changes on the materials' physical and chemical properties are in constant temperature and/or constant mass loss, it is measured as a function of time. When a sample is heated, cooled or keep at a constant temperature in a controlled atmosphere, TGA are used to determine the mass loss. It is also possible to study the decomposition of organic materials with TGA, besides observing the progress of individual components. Apart from that, physical information about physical phenomena such as vaporization, sublimation, etc. are also obtainable by using TGA methods. Next, there are three measurements in which TGA relies on a high degree of precision, which are mass change, temperature and temperature change (Leyva-Porras et al., 2020; Norhayati et al., 2019).

Analysis of thermal decomposition, oxidation, dehydration, heat resistance, and kinetic analysis are utilizing TGA to obtain the needed information. Additionally, a variety of data can also be gained from one sample by combining with other measurement technique, and simultaneous TGA-DSC are one of the examples. In a single experiment, simultaneous TGA-DSC had allowed two signals (mass loss and heat flow) to be obtained. In addition, this combination had also made it possible to distinguish the melting from the degradation when both exist in a narrow range of temperatures (Leyva-Porras et al., 2020; Norhayati et al., 2019).

4.5.1.4 Thermomechanical analysis (TMA)

Another useful thermal analysis technique to be used in materials characterization is TMA, where a constant force is applied to a specimen while the temperature is varied (Norhayati et al., 2019). Simply, under controlled conditions of temperature, time, load and atmosphere, TMA are utilized to determine the dimensional changes of solid samples, such as expansion, compression, penetration, deformation, etc. Transitions such as melting temperature (T_m) and glass transition temperature (T_g), thermal expansion coefficient and softening point can also be determined using this analysis. Meanwhile, the analysis samples can be in powder, fibers, coatings, and thin films form (Leyva-Porras et al., 2020).

Among the advantages of this method is the measurement of dimensional changes can be obtained even in thin films and coatings due to the technique sensitive nature in either the penetration or expansion modes. The length detector will measure the sample deformation as the probe displacement, and typically, quartz glass,

alumina and metals are used as the probes' materials. Additionally, depending on the measurement purpose as listed below, the choice of the probes will differ (Norhayati et al., 2019): (a) Expansion/compression probe: To measure the deformation caused by thermal expansion; (b) Penetration probe: To measure the softening temperature, and (c) Tension probe: To measure the thermal expansion and shrinkage of the sample.

4.5.1.5 Dynamic mechanical analysis (DMA)

Also known as dynamic mechanical, thermal analysis (DMTA), by using this method, a more realistic indication of properties is obtained as the material modulus are continuously monitored at different applied frequencies. Fundamentally, as the materials are deformed under periodic stress, their modulus (stiffness) and damping (energy dissipation) are measured. A wide variety of materials in different forms can utilize this analysis method. Apart from that, a quick comparison of material properties between two dissimilar or two similar materials can be processed differently by using DMA. One of the advantages of this technique is that the results generally reflect the actual application since samples can be tested in many forms such as bars, fibers, films, and viscous liquid samples (Norhayati et al., 2019).

According to Leyva-Porras et al. (Leyva-Porras et al., 2020), usually, by using DMA, the results obtained includes three signals which plotted against temperature, time or frequency. Curves of storage modulus (E′), loss modulus (E″) and damping factor (tan δ) are what those signals corresponded to. Additionally, compared to DSC technique, DMA is preferable in the determination of the solid materials' T_g, as in DMA, T_g values are given in ranges rather than in a single value. Also, different deformation modes, i.e., tension, compression, dual cantilever bending, three-point bending, and shear modes, are used to measure various types of materials (Norhayati et al., 2019). Table 4.7 showed TA analysis and properties measurement of different equipment.

4.5.2 Thermal conductivity of planar materials' measurement methods

The specimen morphology and the heat flux direction are significantly being restricted by the measurement system. For anisotropic 2D planar samples such as papers, sheets and films, it is particularly necessary to measure the in-plane and

Table 4.7 TA analysis and properties measured (Norhayati et al., 2019).

Technique	Property
TGA	Mass changes, dehydration, decomposition, oxidation, reduction
DSC	Melting, glass transition, crystallization, specific heat capacity
TMA	Thermal expansion and shrinkage, glass transition, curing reaction
DMA	Relaxation, crystallization, curing reaction

Table 4.8 Thermal conductivity measurement techniques for 2D planar film materials (Uetani & Hatori, 2017).

Method	Thermal conductivity/ diffusivity	Measuring direction	Measuring materials
Steady-state method	κ	In plane	Nanofibrillated cellulose (NFC) and boron nitride composites
Steady-state bridge method	κ	In plane	Cellulose nanocrystal (CNC) films
Laser spot periodic heating radiation thermometry method	α	In plane and through plane	NC sheets NC and resin composites Rubber and carbon fiber composites
Laser flash method	α	Through plane	Rubber and carbon fiber composites
		In plane	CNF and boron nitride nanotube composites
Thermal wave analysis	α	Through plane	CNF and resin composites
Alternating current (AC) calorimetric method	α	In plane	CNF and resin composites
Temperature wave analysis with AC Joule heating method	α	Trough plane	Polymer films Papers

through-plane directions, independently (Uetani & Hatori, 2017). The reported measurement techniques for 2D materials are listed down in Table 4.8, and the measurement methods are elaborated in detail as follows:

4.5.2.1 Steady-state methods

In this method, the thermal conductivity is measured directly from the heat flux density by applying a temperature gradient to the test sample. The steady-state measurements had also been used by some studies where they distinctively applied the measurement to correspond to the sample dimensions or to measure directions. However, there are some downside of this method, i.e., as steady heat flow are applied, there will be heat leakage to the surroundings, and difficulty to measure thin or high-κ samples that give small temperature differences as it needs high accuracy to detect those differences. Apart from that, since sample's temperature gradient needed to be in a steady state condition, long measurement time is expected (Uetani & Hatori, 2017).

4.5.2.2 Laser spot periodic heating radiation thermometry method

Nonequilibrium methods produced a temperature change on the sample surface, contrary to the steady-state methods, and on the sample's back side, the temperature response will be detected. Hence, even in relatively small samples and short time, this type of method allows measurement of the material thermal diffusivity to be determined. Additionally, measurements for samples with high thermal diffusivities can also be obtained. But, to calculate the thermal conductivity, two information's are required, namely the sample's specific heat capacity and density.

Through this contactless method, both in-plane and through-plane thermal diffusivities of the 2D planar samples are independently measured. Also, to absorb the heating laser on the surface, to evade laser penetration or distance errors, and to maintain high emissivity for the radiation thermometer to detect a sufficient signal on the back side, the samples would require thin blackening or metal-sputtering treatment. The boundary conditions can be overlooked, only when the temperature wave does not reach the sample edges, and to do so, the heating frequency needs to be adequately controlled (Uetani & Hatori, 2017).

4.5.2.3 Flash method

As for flash method, thermal diffusivity can be measured by using the half-time method. In flash method, by heating the entire surface of the solid sample with pulsed light, one-dimensional thermal flow is produced. However, compared to the half-time, the pulse width needs to be negligibly small. Also, to avoid heat leakage, the edges of the sample need to be held. The applicability of this method is for solid samples that are in uniform structures, and the measurement of the sample's thermal diffusivity will be in the through-plane direction. Measurement of the sample's thermal diffusivity in the in-plane direction would require a specialized attachment. In addition, like the aforesaid method, blackening treatment of the sample is also needed which shown in Table 4.8 (Uetani & Hatori, 2017).

4.6 Mechanical properties of cellulose characterization techniques

Variety of products and applications such as aerospace, construction, etc. are utilizing composite materials especially lightweight composite structures. Hence, it is important that prior to their applications, wide range of mechanical tests are being done onto the properties of anisotropic and inhomogeneous composite materials prior their applications. A range of test types and plethora of standards (ASTM, ISO, CEN), along with testing conditions, in a variety of different environments are required or involved when conducting the mechanical testing. Determination of mechanical parameters such as strength and stiffness are involved in the testing to investigate its use for in the design of a composite's structure (Saba, Jawaid, & Sultan, 2018). Among the essential mechanical testing are as follows:

4.6.1 Impact (toughness) testing

The ability of a material to withstand sudden impact defines its toughness. Toughness is evaluated using measurement based on energy, unlike strength and stiffness, which are evaluated using force-based measurement. Thus, for impact tests, it does not only involved force, but also units of length and time (Larson, 2015). The toughness, brittleness, notch sensitivity, and impact strength of engineering materials to resist high-rate loading is what impact test is explicitly used. This is because, it is a great advantage in product liability and safety when the impact property can be quantified (Saba et al., 2018).

4.6.1.1 Charpy impact test

Georges Augustin Albert Charpy invented this test in 1900, and since then, it had been viewed as one of the common tests for evaluation of the relative toughness of materials as it is both economical and fast. The energy absorbed by a standard notched specimen while breaking under an impact load is measured using this impact test. Having a notch machined across one of the larger dimensions, the standard Charpy impact test specimen is of dimension 55 mm × 10 mm × 10 mm. The notch on the specimen can be in either V-shaped or U-shaped and faces away from the pendulum. Generally, while the specimen is securely held at each end, a hammer on the pendulum arm would strike the specimen but strike opposite the notch. By measuring the decrease in the pendulum arm motion, the energy absorbed by the specimen is precisely determined. Additionally, the device for the testing can be a bench top size, or a larger, floor size model (Larson, 2015; Saba et al., 2018).

4.6.1.2 Izod test

Named after Edwin Gilbert Izod, an English engineer, this test is used to test materials at low temperature and are almost similar to the Charpy impact test. In this test, a pendulum that has a determined weight at the end of its arm are swinging down to strike the specimen that had been held securely in a vertical position. The pendulum loss of energy is determined by measuring the exact loss of height in the pendulum's swing, and the energy loss are used to quantify the impact strength (Saba et al., 2018).

This bench top test is simple to be conducted, and the test data represent an unusual end-use loading condition, though the resulting data may be useful for material comparison. It is also important to note that for this testing, the specimen has a substantial notch, and the impact measurement are in almost pure shear loading condition (Larson, 2015).

4.6.1.3 Unnotched Izod test

The only difference of this test compared to Izod testing is that the test specimen for this test has no notch. Apart from that minor variation, the testing equipment and procedure had no changes. The fracture of this test specimen is independent of any notch while the load case is still a pure shear loading condition. Via this test too, one can compare the impact data for a given material in a notched versus

unnotched state with ease. Hence, insight regarding the notch sensitivity of the material can be obtained through the comparison (Larson, 2015).

4.6.1.4 Gardner impact testing

Typically known as falling weight testing, this impact testing involved a weight dropped onto a fixed object. For this test, rather than a pendulum, a falling dart is used, and the "dart" is usually a weight with rounded nose. As a floor-based test, dart of a specific weight, a defined drop height, and a few drops before the specimen breaks are the typical test scenarios. Based on the weight and height, the amount of energy is calculated. As for the test result, it only involves Pass (specimen intact) or Fail (specimen breaks). The advantages of this test are its simplicity, real-life conditions representation, and it is also rather inexpensive. But this test is accelerating under gravity since the weight is free falling. Hence, as the height increase, so does the impact velocity of the weight. This will be affecting the test result for material such as plastic since it is rate sensitive. For some applications, this might be an important issue to be addressed (Larson, 2015).

4.6.1.5 Drop testing

Also known as drop weight impact test, it is typically used for the testing of the impact behavior for composite plates and components. ASTM 7136/D7136M-15 ("Standard Test Method for Measuring the Damage Resistance of a Fiber-Reinforced Polymer Matrix Composite to a Drop-Weight Impact Event," 2015) standard is what this test complies to. Via this testing, the impact damage that could occur during in-service periods can be closely resembled. This is because, although generally the test specimen is a fully assembled product, but subassembly or single part can also be the test subject. A variety of heights and surfaces can be used to conduct the drop testing. Depending on the height of the drop and the mass of the object, the impact energy will vary. Apart from that, the impact performance of the object against different surfaces can also be assessed using this test. After a drop weight impact test, there are two categories of damages that can be observed, i.e., macro-damage (visible to naked eyes) and at the microscale (seldom can be observed or seen by naked eyes). For both types of damage, usage of postimpact testing can be utilized to evaluate the damages.

As the testing can be developed to mimic the actual end-use conditions, the materials can be evaluated in that context, making it possible to obtain valuable feedback to confirm the validity of a given design. However, this test cannot or rarely provides useful info in the design early phases and material selection as it often requires fully assembled products. Additionally, the only result that could be obtained through this test is on a pass or fail since the falling weight either stopped on the test specimen or destroyed the specimen and passed through it (Larson, 2015; Navaranjan & Neitzert, 2017).

4.6.1.6 Ballistics test

The ultimate impact strength of composite can be determined via this high-speed testing., as it is done by firing an impactor traveling in the range of 400–2000 m/s. After firing a high-speed projectile at an object, the impact is determined by how localized the damage. In a high velocity impact, the material structural response is less important unlike in a low velocity condition. As for the damage area, the localization of the impact is more important than the geometrical consideration. Next, the Ballistic test is described by the EN 1522/EN 1523 (*Windows, Doors, Shutters and Blinds—Bullet Resistance—Requirements and Classification*, 1998; *Windows, Doors, Shutters and Blinds—Bullet Resistance—Test Method*, 1999) and ASTM E3062/E3062M-20 ("Standard Specification for Indoor Ballistic Test Ranges for Small Arms and Fragmentation Testing of Ballistic-Resistant Items," 2020) standards. Additionally, this test is best suited to test the impact resistance of natural fiber composites (Navaranjan & Neitzert, 2017).

4.6.2 Tensile testing

Information such as tensile strength, yield strength, and ductility of materials can be obtained through this destructive test process. The force required to break a composite or plastic specimen and the extent to which the specimen stretches or elongates to that breaking point are measured via this test. In accordance with standards such as ISO 527-4 ("Plastics—Determination of Tensile Properties—Part 4: Test Conditions for Isotropic and Orthotropic Fibre-Reinforced Plastic Composites. International Organization for Standardization," 1997), ISO 527-5 (*Plastics—Determination of Tensile Properties—Part 5: Test Conditions for Unidirectional Fiber-Reinforced Plastic Composites*. International Organization for Standardization, 2009), ASTM D 638-14 (D638-14, 2014), and ASTM C 297/C297M-16 ("Standard Test Method for Flatwise Tensile Strength of Sandwich Constructions," 2016), the tensile testing of composites is usually in the form of basic tension or flat-sandwich tension testing. The stress-strain diagrams that are used to determine the tensile modulus are produced via those tests (Saba et al., 2018). A few testing machines are commercially available for bulk materials testing such as those from MTS and Instron. Typically, these machines consisted of three parts, (i) servo hydraulic (MTS) or screw driven (Instron) actuator, (ii) a load cell (sensor) and (iii) a pair of grips (Zhu & Chang, 2015). Additionally, based on microelectromechanical system (MEMS) application, there are two tensile testing techniques that can be done as follows:

4.6.2.1 Force controlled tensile testing

A separately fabricated specimen is being applied tensile load onto it by using an electrostatic comb drive actuator that is equipped with a grip and force calibration beam. The actuator can generate a total force of 382 μN at 40 V and has 3150 combs. Meanwhile, at 30 V, the force resolution of the actuator is 1.3 μN. Attached to the moving parts of the actuator is one end of the calibration beam, while the other one is kept fixed. Then, a compressive force will be exerted on the beam upon

actuation, and as the load exceeds a critical value of P_{cr}, the beam will buckle. To prevent any preloading of the specimen, a gap (δ_0) of about 1–2 μm is left between the gripping edge of the specimen and the actuator grip. Next, the calibration beam supports all the force generated by its critical load (P_{cr}) is reached as the voltage is applied. The actuator displacements after that will take place and the generated force will be shared by the actuator springs. The force balance for an axial displacement δ of the actuator is (Eq. 4.4):

$$F = \beta V^2 = k\delta + P_{cr}\left(1 + \frac{\delta}{2L}\right) \text{ for } \delta_0 \geq \delta \tag{4.4}$$

where, V is the applied voltage, k is the constant of the actuator spring, and L is the length of calibration beam. As for β (the actuator force-voltage parameter), it is depending on the number and geometry of moving and fixed interdigitated electrode pairs, besides the medium permittivity constant.

Gripping of the specimen occurs after the actuator has displaced by an amount δ_0, and the tensile force is applied to the specimen. The specimen net force, F_s, is given as (Eq. 4.5)

$$F_s = \beta V^2 - k\delta - P_{cr}\left(1 + \frac{\delta}{2L}\right) \text{for } \delta \geq \delta_0 \tag{4.5}$$

From the applied force and specimen cross-section, the stress on the specimen can be calculated. Calculation of the strain is measured independently from the displacement of the actuator after it has engaged with the specimen (Haque & Saif, 2003).

4.6.2.2 Displacement controlled tensile testing

Since the specimen can be fabricated separately from the actuator using the aforesaid technique's methodology, a wide variety of materials can be tested. However, there are issues involving the specimen alignment and positioning that need to be taken into consideration. Hence, this novel displacement-based experimental setup was developed to help overcome such issue. For this testing, by using microelectronic fabrication procedures, a freestanding specimen, a force sensor, and displacement sensors at both ends of the specimen are integrated on a single silicon chip.

At one end, the freestanding thin-film specimen is held by the force sensor beam, with both ends in clamped configuration. Only in-plane deflections are allowed when using the force sensor beam as it typically has an aspect ratio of 5. The deflection will then be read by the displacement sensor. Meanwhile, a rigid backbone that is connected to a set of supporting springs holding the other end of the specimen, and the second displacement sensor reads the displacement for that one. Next, as an external piezo-actuator pulled the backbone, tensile force is applied onto the specimen. A deflection in the beam will occurs as the motion is transmitted to the force sensor beam through the specimen.

The specimen force, F is given as $F = k\delta$, where k is the force sensor beam spring constant, while δ is the deflection of the beam. Lastly, the elongation/strain of the specimen will be given by the displacements of the two ends of the specimen, which are read by its respective displacement sensors (Broitman, 2016).

4.6.3 Indentation hardness testing

For a solid material, hardness can be defined as the measurement of its resistance to a permanent shape change when there is continuous compressive force is applied onto it. Mechanisms such as indentation, scratching, cutting, etc. can produce deformation onto the materials. In the industry, hardness testing is a simple, fast and economical material quality control method as it has a close relation to other mechanical properties such as strength, ductility and fatigue resistance. In 1856, William Wade was the first person to write a report regarding a machine that are used to measure *indentation* hardness. Using a pyramid-shaped hardened tool, a specified load was applied onto it, and based on the size of the deformed cavity on the surface, the hardness value was evaluated. Next, depending on the scale which the indentation hardness is measured, there are two main categories of the methods, i.e., at macro-, and micro scale (Broitman, 2016).

4.6.3.1 Rockwell test

By measuring the depth of penetration of an indenture under a large load compared to penetration made by smaller preload is how hardness is determined using this test method (Broitman, 2016). Initially, a minor load of 10 kgf is applied and will establish the zero-datum position. Then, the major load (60, 100 or 150 kgf) is applied for a specific period before removed, which leave only the minor load to be applied. The superficial Rockwell test is among the most widely used variants of this testing, where the minor load is 3 kgf and the minor loads are either 15, 30 or 45 kgf, which are relatively low (Sundararajana & Royb, 2001).

By using the equation $\mathrm{HR} = N - 500\,h$, the Rockwell hardness HR can be calculated, where h (in mm) is the difference in the measurements of the two-penetration depth. Meanwhile, the N value varies depending on the type of indenter used: for spheroconical indents, $N = 100$, and for ball indenter, $N = 130$. Next, as established on the standards ISO 6508-1 (*Metallic Materials—Rockwell Hardness Test—Part 1: Test Method*. International Organization for Standardization, 2015) and ASTM E18-20 ("Standard Test Methods for Rockwell Hardness of Metallic Materials," 2020) for metallic materials, and ISO 2039-2 (*Plastics—Determination of Hardness—Part 2: Rockwell Hardness*. International Organization for Standardization, 1987) for plastics, there are several loads types and ball diameters that can be used (Haque & Saif, 2003). Table 4.9 listed down some of the most used Rockwell scales, while in Fig. 4.5, the principle of the macro-indentation Rockwell test is illustrated.

4.6.3.2 Vickers test

Under load of a pyramid-shaped diamond indenter, the hardness is calculated from the size of the impression produced by the indenture. By using the indented load L and the actual surface area of the impression A_c, the Vickers diamond hardness number, HV can be calculated using given equation (Eq. 4.6):

$$HV = \frac{L}{A_c} = \frac{2L}{d^2}\sin\frac{136^\circ}{2} = 1.8544\,\frac{L}{d^2} \tag{4.6}$$

Table 4.9 Main Rockwell scales (Broitman, 2016).

Scale	Name	Indenter	Load (kgf)
A	HRA	120 degrees diamond spheroconical	60
B	HRB	1/16-in.-diameter (1.588 mm) steel sphere	100
C	HRC	120 degrees diamond spheroconical	150
D	HRD	120 degrees diamond spheroconical	100
E	HRE	1/8-in.-diameter (3.175 mm) steel sphere	100
F	HRF	1/16-in.-diameter (1.588 mm) steel sphere	60
G	HRG	1/16-in.-diameter (1.588 mm) steel sphere	150

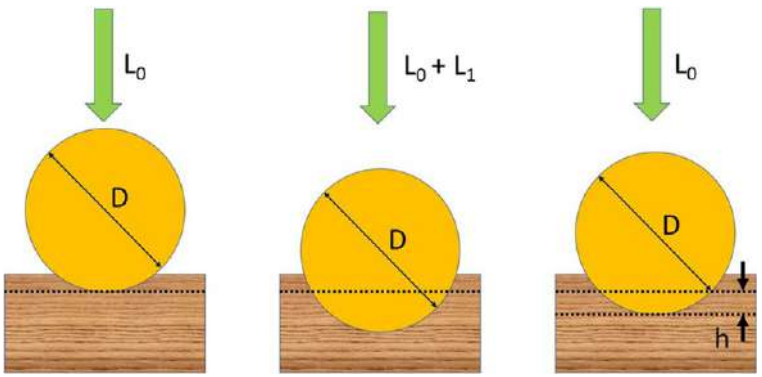

FIG. 4.5

Schematic diagram illustrating the principle of the macro-indentation Rockwell test (Broitman, 2016).

Modified from Broitman, E. (2016). Indentation hardness measurements at macro-, micro-, and nanoscale: A critical overview. Tribology Letters, 65*(1), 23. https:/doi.org/10.1007/s11249-016-0805-5.*

where, d (mm) is the length of the diagonal of the residual impression on the specimen surface, measured from corner to corner, as shown in Fig. 4.6.

The initial application time period of the force is from 2 to 8 s, and during 10–15 s, the test force is maintained. The standard values of applied loads for this test is 5, 10, 20, 30, 50, 100 and 120 kgf, but generally it varies from 1 to 120 kgf (Broitman, 2016).

4.6.3.3 Micro-indentation tests

Indentations loads L for micro-indentation tests are in the range of $L < 2$N with penetration $h > 0.2\,\mu$m. Micro-Vickers and Knoop test are two main tests used at this scale, and similar to aforesaid scale test, under a given load and specific time period, the depth of indented will sink into the material will be the correlation of the hardness. The diamond indenter used are in shape of a pyramid and the indentation caused will determine the material's resistance to the penetration (Broitman, 2016).

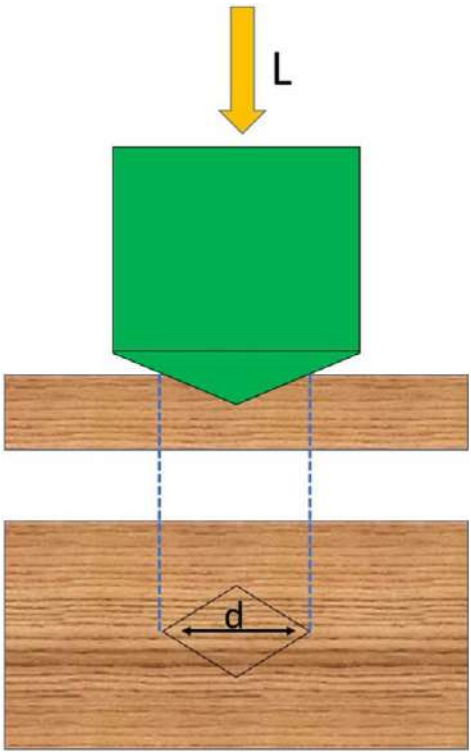

FIG. 4.6

Vickers indentation test (Broitman, 2016).

Modified from Broitman, E. (2016). Indentation hardness measurements at macro-, micro-, and nanoscale: A critical overview. Tribology Letters, 65*(1), 23. https:/doi.org/10.1007/s11249-016-0805-5.*

Micro-Vickers test

Having the same basic principle as the aforesaid Vickers test, the only difference between these two tests are the use of a lower applied load range. In 1936, the first micro-hardness Vickers tester are designed for applied forces $\leq$1 kgf by Lips and Sack. As for the standards, ASTM E384-17 (E384-17, 2017) and ISO 6507-1 (*Metallic Materials—Vickers Hardness Test—Part 1: Test Method*. International Organization for Standardization, 2018) normalized this test (Broitman, 2016).

Knoop test

A rhombic-based pyramidal diamond that produces an elongated diamond shaped indent are the indentured used for the Knoop hardness test. From the opposite faces of the indenture, the angles are 130 and 172.5 degrees, and the indentation produced by the ratio between long and short diagonals for the indenture is approximately 7 to 1. During the measurement test, the indenture is pressed by the load and are

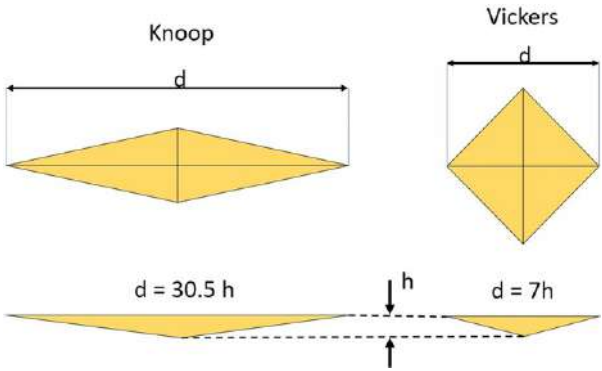

FIG. 4.7

Comparison between the Knoop and Vickers micro-indentations (Broitman, 2016).
Modified from Broitman, E. (2016). Indentation hardness measurements at macro-, micro-, and nanoscale: A critical overview. Tribology Letters, 65*(1), 23. https:/doi.org/10.1007/s11249-016-0805-5.*

maintained by 10–15 s. After completing the dwell time, the indenture is removed from the sample, leaving an elongated diamond shaped indent. A high magnification microscope is necessary for this test to measure the indent size as it is usually done at small test forces, ranging from 10 to 1000 g (~98 mN to 9.8 N) (Broitman, 2016). Fig. 4.7 showed the comparison between the Knoop and Vickers micro-indentations diameter.

4.7 Summary

Throughout the chapter, various techniques for cellulose and cellulose-based material characterization had been elaborated in detail. Apart from explaining the general information about cellulose such as its structure and molecular weight, technique to obtain such information are also discussed. Three of the most important properties, namely chemical structure, thermal, and mechanical properties are elaborated in detail in term of their characterization techniques. In conclusion, cellulose is one of the most abundant materials as its raw materials can be found from various sources. Hence, there had also been several characterization methods that can be used. Even up until now, improvement is kept on being made onto those methods to obtain more useful information regarding this material.

Acknowledgment

The authors would like to acknowledge Universiti Malaysia Sarawak (UNIMAS) for the support.

References

ASTM. (2020). *Standard test methods for Rockwell Hardness of metallic materials* (p. 18). https://doi.org/10.1520/E0018-20.

ASTM C297/C297M-16. (2016). *Standard test method for flatwise Tensile strength of sandwich constructions*. https://doi.org/10.1520/C0297_C0297M-16.

ASTM D7136/D7136M-15. (2015). *Standard test method for measuring the damage resistance of a fiber-reinforced polymer matrix composite to a drop-weight impact event*. https://doi.org/10.1016/10.1520/D7136_D7136M-15.

ASTM E3062/E3062M-20. (2020). *Standard specification for indoor ballistic test ranges for small arms and fragmentation testing of ballistic-resistant items*. https://doi.org/10.1520/E3062_E3062M-20.

Bardestani, R., Patience, G. S., & Kaliaguine, S. (2019). Experimental methods in chemical engineering: Specific surface area and pore size distribution measurements—BET, BJH, and DFT. *Canadian Journal of Chemical Engineering*, *97*(11), 2781–2791. https://doi.org/10.1002/cjce.23632.

Battista, O. A. (1944). Molecular weight of cellulose: Measurement of average degree of polymerization. *Industrial and Engineering Chemistry - Analytical Edition*, *16*(6), 351–354. https://doi.org/10.1021/i560130a001.

Broitman, E. (2016). Indentation hardness measurements at macro-, micro-, and nanoscale: A critical overview. *Tribology Letters*, *65*(1), 23. https://doi.org/10.1007/s11249-016-0805-5.

Chirayil, C. J., Mathew, L., & Thomas, S. (2013). Review of recent research in nano cellulose preparation from different lignocellulosic fibers. *Reviews on Advanced Materials Science*, *37*(2014), 20–28.

Choi, S. M., & Shin, E. J. (2020). The nanofication and functionalization of bacterial cellulose and its applications. *Nanomaterials*, *10*(3). https://doi.org/10.3390/nano10030406.

D638-14. (2014). *Standard test method for tensile properties of plastics*. https://doi.org/10.1520/D0638-14.

E384-17. (2017). *Standard test method for microindentation hardness of materials*. https://doi.org/10.1520/E0384-17.

Eichhorn, S. J., Baillie, C. A., Zafeiropoulos, N., Mwaikambo, L. Y., Ansell, M. P., Dufresne, A., … Wild, P. M. (2001). Current international research into cellulosic fibres and composites. *Journal of Materials Science*, *36*(9), 2107–2131. https://doi.org/10.1023/A:1017512029696.

EN 1522. (1998). *Windows, doors, shutters and blinds—Bullet resistance—Requirements and classification*.

EN 1523. (1999). *Windows, doors, shutters and blinds—Bullet resistance—Test method*.

Faezah, E., Masrinda, T. S., & Abd, R. N. (2014). Overview of bacterial cellulose production and application. *Agriculture and Agricultural Science Procedia*, 113–119. https://doi.org/10.1016/j.aaspro.2014.11.017.

Fernandes, E. M., Pires, R. A., Mano, J. F., & Reis, R. L. (2013). Bionanocomposites from lignocellulosic resources: Properties, applications and future trends for their use in the biomedical field. *Progress in Polymer Science*, *38*(10–11), 1415–1441. https://doi.org/10.1016/j.progpolymsci.2013.05.013.

Flaris, V., & Singh, G. (2009). Recent developments in biopolymers. *Journal of Vinyl and Additive Technology*, *15*(1), 1–11. https://doi.org/10.1002/vnl.20171.

Foster, E. J., Moon, R. J., Agarwal, U. P., Bortner, M. J., Bras, J., Camarero-Espinosa, S., … Youngblood, J. (2018). Current characterization methods for cellulose nanomaterials. *Chemical Society Reviews*, *47*(8), 2609–2679. https://doi.org/10.1039/c6cs00895j.

George, J., & Sabapathi, S. N. (2015). Cellulose nanocrystals: Synthesis, functional properties, and applications. *Nanotechnology, Science and Applications*, *8*, 45–54. https://doi.org/10.2147/NSA.S64386.

Gralén, N., & Svedberg, T. (1943). Molecular weight of native cellulose [1]. *Nature*, *152* (3865), 625. https://doi.org/10.1038/152625a0.

Haque, M. A., & Saif, M. T. A. (2003). A review of MEMS-based miroscale and nanoscale tensile and bending testing. *Experimental Mechanics*, *43*(3), 248–255. https://doi.org/10.1007/BF02410523.

International Organization for Standardization. (1987). *Plastics—Determination of hardness—Part 2: Rockwell hardness. International Organization for Standardization.*

International Organization for Standardization. (1997). *Plastics—Determination of tensile properties—Part 4: Test conditions for isotropic and orthotropic fibre-reinforced plastic composites. International Organization for Standardization.* ISO. 527.

International Organization for Standardization. (2009). *Plastics—Determination of tensile properties—Part 5: Test conditions for unidirectional fibre-reinforced plastic composites. International Organization for Standardization* (527-5).

International Organization for Standardization. (2015). *Metallic materials—Rockwell hardness test—Part 1: Test method. International Organization for Standardization* (6508-1).

International Organization for Standardization. (2018). *Metallic materials—Vickers hardness test—Part 1: Test method. International Organization for Standardization* (6507-1).

Jedvert, K., & Heinze, T. (2017). Cellulose modification and shaping—A review. *Journal of Polymer Engineering*, *37*(9), 845–860. https://doi.org/10.1515/polyeng-2016-0272.

Kalia, S., Dufresne, A., Cherian, B. M., Kaith, B. S., Avérous, L., Njuguna, J., & Nassiopoulos, E. (2011). Cellulose-based bio- and nanocomposites: A review. *International Journal of Polymer Science*, *2011*. https://doi.org/10.1155/2011/837875.

Kunusa, W. R., Iyabu, H., Taufik, M., & Botutihe, D. N. (2018). Characterization and analysis of the molecular weight of corn corbs microcrystalline cellulose (MCC) fiber using mass-spectrometry methods. *Journal of Physics: Conference Series*, *1040*(1). https://doi.org/10.1088/1742-6596/1040/1/012015.

Larson, E. R. (2015). 5—Material selection based on performance. In *Thermoplastic material selection: A practical guide* (pp. 145–205). Elsevier BV. https://doi.org/10.1016/b978-0-323-31299-8.00005-2.

Lavanya, D., Kulkarni, P. K., Dixit, M., Raavi, P. K., & Krishna, L. N. V. (2011). Sources of cellulose and their applications—A review. *International Journal of Drug Formulation and Research*, *2*(6), 19–38.

Leyva-Porras, C., Cruz-Alcantar, P., Espinosa-Solís, V., Martínez-Guerra, E., Piñón-Balderrama, C. I., Martínez, I. C., & Saavedra-Leos, M. Z. (2020). Application of differential scanning calorimetry (DSC) and modulated differential scanning calorimetry (MDSC) in food and drug industries. *Polymers*, *12*(1). https://doi.org/10.3390/polym12010005.

Liyanage, S., & Abidi, N. (2019). Molecular weight and organization of cellulose at different stages of cotton fiber development. *Textile Research Journal*, *89*(5), 726–738. https://doi.org/10.1177/0040517517753642.

Maleki, S. S., Mohammadi, K., & Ji, K. S. (2016). Characterization of cellulose synthesis in plant cells. *Scientific World Journal*, *2016*. https://doi.org/10.1155/2016/8641373.

Mariano, M., El Kissi, N., & Dufresne, A. (2014). Cellulose nanocrystals and related nanocomposites: Review of some properties and challenges. *Journal of Polymer Science, Part B: Polymer Physics*, *52*(12), 791–806. https://doi.org/10.1002/polb.23490.

Martínez-Sanz, M., Gidley, M. J., & Gilbert, E. P. (2015). Application of X-ray and neutron small angle scattering techniques to study the hierarchical structure of plant cell walls: A review. *Carbohydrate Polymers*, *125*, 120–134. https://doi.org/10.1016/j.carbpol.2015.02.010.

Michael, I. (2017). *Characterization of various kinds of nanocellulose* (pp. 51–100). Wiley. https://doi.org/10.1002/9783527689972.ch2.

Mishra, R. K., Sabu, A., & Tiwari, S. K. (2018). Materials chemistry and the futurist eco-friendly applications of nanocellulose: Status and prospect. *Journal of Saudi Chemical Society*, *22*(8), 949–978. https://doi.org/10.1016/j.jscs.2018.02.005.

Moran-Mirabal, J. M. (2013). Advanced-microscopy techniques for the characterization of cellulose structure and cellulose-cellulase interactions. In T. G. M. Van De Ven (Ed.), *Cellulose—Fundamental aspects* InTechOpen. https://doi.org/10.5772/56584.

Nair, A. B., Sivasubramanian, P., Balakrishnan, P., Kumar, K. A. N. A., & Sreekala, M. S. (2013). Environmental effects, biodegradation, and life cycle analysis of fully biodegradable \green\ composites. In *Vol. 3. Polymer composites, biocomposites* (pp. 515–568). Wiley Blackwell. https://doi.org/10.1002/9783527674220.ch15.

Navaranjan, N., & Neitzert, T. (2017). Impact strength of natural fibre composites measured by different test methods: A review. In *Vol. 109. MATEC web of conferences*EDP Sciences. https://doi.org/10.1051/matecconf/201710901003.

Norhayati, P., Harfiz, S. M., Diana, H. N., Mohd, M. A., & Idayu, M. I. (2019). *Thermal behavior of bacterial cellulose-based hydrogels with other composites and related instrumental analysis* (pp. 763–787). Springer Science and Business Media LLC. https://doi.org/10.1007/978-3-319-77830-3_26.

Oberlerchner, J. T., Rosenau, T., & Potthast, A. (2015). Overview of methods for the direct molar mass determination of cellulose. *Molecules*, *20*(6), 10313–10341. https://doi.org/10.3390/molecules200610313.

Pan, Y., Farmahini-Farahani, M., O'Hearn, P., Xiao, H., & Ocampo, H. (2017). An overview of bio-based polymers for packaging materials. *Journal of Bioresources and Bioproducts*, *1*(3), 106–113. https://doi.org/10.21967/JBB.V1I3.49.

Patkar, S. N., & Panzade, P. D. (2016). Fast and efficient method for molecular weight analysis of cellulose pulp, in-process and finished product. *Analytical Methods*, *8*(15), 3210–3215. https://doi.org/10.1039/c5ay03012a.

Picker, K. M., & Hoag, S. W. (2002). Characterization of the thermal properties of microcrystalline cellulose by modulated temperature differential scanning calorimetry. *Journal of Pharmaceutical Sciences*, *91*(2), 342–349. https://doi.org/10.1002/jps.10018.

Praveen, K. G., Shreeya, S. R., Deepali, V. P., Priyadharsini, V., Vidhya, S., Chandrananthi, C., … Keerthana, G. (2019). *An update on overview of cellulose, its structure and applications*. IntechOpen. https://doi.org/10.5772/intechopen.84727.

Rongpipi, S., Ye, D., Gomez, E. D., & Gomez, E. W. (2019). Progress and opportunities in the characterization of cellulose—An important regulator of cell wall growth and mechanics. *Frontiers in Plant Science*, *9*. https://doi.org/10.3389/fpls.2018.01894.

Saba, N., Jawaid, M., & Sultan, M. T. H. (2018). An overview of mechanical and physical testing of composite materials. In *Mechanical and physical testing of biocomposites, fibre-reinforced composites and hybrid composites* (pp. 1–12). Elsevier. https://doi.org/10.1016/B978-0-08-102292-4.00001-1.

Sundararajana, G., & Royb, M. (2001). Hardness testing. In *Encyclopedia of materials: Science and technology* (2nd ed., pp. 3728–3736). Elsevier BV. https://doi.org/10.1016/b0-08-043152-6/00665-3.

Uetani, K., & Hatori, K. (2017). Thermal conductivity analysis and applications of nanocellulose materials. *Science and Technology of Advanced Materials*, *18*(1), 877–892. https://doi.org/10.1080/14686996.2017.1390692.

Yang, J. (2017). *Manufacturing of nanocrystalline cellulose*.

Zhao, Y., & Li, J. (2014). Excellent chemical and material cellulose from tunicates: Diversity in cellulose production yield and chemical and morphological structures from different tunicate species. *Cellulose*, *21*(5), 3427–3441. https://doi.org/10.1007/s10570-014-0348-6.

Zhu, Y., & Chang, T. H. (2015). A review of microelectromechanical systems for nanoscale mechanical characterization. *Journal of Micromechanics and Microengineering*, *25*(9). https://doi.org/10.1088/0960-1317/25/9/093001.

CHAPTER

Cellulose-based aerogels

5

Perry Law Nyuk Khui, Md Rezaur Rahman, and Muhammad Khusairy Bin Bakri
Department of Chemical Engineering and Energy Sustainability, Faculty of Engineering, Universiti Malaysia Sarawak (UNIMAS), Kota Samarahan, Sarawak, Malaysia

Chapter outline

5.1 Introduction

Aerogels are the mostly derived materials from silica, which are currently and extensively investigated by many researchers. Many literatures have characterized their properties, as well as their applications in numerous fields (Bakri, Jayamani, Rahman, & Kakar, 2018; Kakar, Jayamani, Bakri, & Rahman, 2018a, 2018b). Some researchers have also extensively investigated the development and characterization of silica-based aerogel composites. The fascinating properties of silica-based aerogels/composites covered from its low density, high thermal conductivity, good acoustic insulation, high surface area, and functional porosity, which lead researchers and manufacturers to develop more sustainable and improved product application in society (Rahman, Hamdan, & Hossen, 2018; Rahman, Hui, & Hamdan, 2018). In contrast, within the last past 10 years, aerogels derived from a cellulose-based material has gained popularity among researchers, and some literatures have shown

Fundamentals and Recent Advances in Nanocomposites Based on Polymers and Nanocellulose.
https://doi.org/10.1016/B978-0-323-85771-0.00008-7

that it may have some advantages and potential in numerous fields in comparison to silica-based aerogels. This chapter would discuss numerous topics, using a compilation of literatures regarding; silica-based aerogels as a comparative for properties and applications, cellulose-based composite aerogels, characterization, and application of cellulose-based aerogels.

5.2 Silica-based aerogel

Silica-based aerogel products have grown in the marketplace and have projected worldwide sales of around 500 million US$ for the year 2013. Additionally, the study states that the benchmark value for a cubic meter of silica aerogel is 4000 US$, and by the year 2020, the researchers foresee the value could drop below 1500 US$ per cubic meter, due to commercialization (Koebel, Rigacci, & Achard, 2012).

Energy consumption and CO_2 emission are a great concern globally, in Northern and Central Europe, most of the energy consumption is generally towards heating or temperature control in buildings. Olden buildings in Central Europe (Switzerland) particular, do not have the suitable insulating components during construction, when compared to modern buildings in recent times. Due to being poorly insulated, the residents would then need to consume more energy to compensate the energy lost. To assist the conservation of cultural heritage, numerous buildings that date back as far as 1500s to 1800s are being restored. Aerogel technologies were implemented in this restoration project, which supports both the quality of life of the community (Ganobjak, Brunner, & Wernery, 2020). According to the literature, preservation of the main structure and design of the building are key requirements of the project.

Restoring olden buildings with conventional methods and materials may provide good thermal insulation properties, however; the application of thick insulating layers may be impractical involving construction which may alter the main features of both exterior and interior of the building. Furthermore, thick insulating layers (i.e., mineral wool, polyurethane foam, etc.) often do not conform with the key requirements to preserving the architectural design and structures. The advantages of silica-based aerogel are well suited in many cases to improve the thermal properties and the comfort of olden buildings, as only thin layers are required, as aerogel materials are water resistant/hydrophobic with better water vapor diffusion control. In addition, according to Ganobjak et al. (2020), the thick internal foam/fiber insulating layers may be affected by the humid/colder climate in Central Europe (Switzerland), hence condensation due to water vapor diffusion is a high occurrence. Silica-based aerogels as an alternative insulating material may allow for a higher flexibility in these circumstances (Ganobjak et al., 2020). Hence the aerogel technology implemented in the restoration process are; aerogel boards, renders, blankets, granules, and panels. Silica-based aerogels insulating properties and water vapor diffusion control may be attributed to the high surface area and porosity within the material (Gurav, Jung, Park, Kang, & Nadargi, 2010). The low thermal conductivity of silica-based aerogel ranges between 0.014 and 0.019 W/m K, additional information on the physical properties of silica-based aerogels are in Table 5.1.

Table 5.1 General physical properties of silica-based aerogels (Riffat & Qiu, 2013; Ganobjak et al., 2020; Soleimani Dorcheh & Abbasi, 2008).

Properties	Value
Density (kg/m^3)	3–350 (average 100)
Surface area (m^2/g)	600–1000
Pore diameter (nm)	1–100 (average 20)
Porosity (%)	85–99 (average 95)
Thermal conductivity (W/m K)	0.01–0.02
Longitudinal sound speed (m/s)	100–300
Index of refraction	1.0–1.05
Thermal tolerance (°C)	500–1200
Tensile strength (MPa)	0.016
Coefficient of thermal expansion (1/°C)	$2.0–4.0 \times 10^{-6}$

Table 5.1 shows the relative average values of the physical properties of silica-based aerogel according to numerous literatures which correlates application of the material for issues ranging from thermal, humidity/vapor diffusion, and sound insulation, as well as light refraction (Ganobjak et al., 2020; Riffat & Qiu, 2013; Soleimani Dorcheh & Abbasi, 2008). According to numerous literatures, aerogels are composed of a sole-gel, when dried, reveals the highly porous solid network/structure. Considering classical aerogels made from silica, pore sizes may form into groups of mesopores ranging from 2 to 50 nm clusters. There are a large variety of aerogels compositions (i.e., silica, metal oxide, alumina, melamine-formaldehyde, cellulose, alginates, chitosan), though the main methodology of the synthesis of aerogels is mainly through sol-gel processing (Baetens, 2013; Montes & Maleki, 2020).

The aerogels composition and networking could be manipulated by controlling the chemical reaction parameter to form a wet gel and processes to convert into a dry highly porous body in the shape of the mold used or granules. Researchers have recognized aerogels structures to be mainly amorphous in contrast to a crystalline structure. The microstructures of aerogels are formed by a solid continuous network of primary and secondary colloidal particles connected to each other through processes such as, i.e., condensation, cross-linking, formation, and aggregation of fibrils due to the rearrangement of polymer chains/macromolecules (Baetens, 2013; Montes & Maleki, 2020).

In order to convert a wet gel into aerogel, numerous drying techniques (i.e., ambient drying, freeze drying/lyophilization, supercritical drying) were investigated by researchers with the goal of extracting the liquid medium from the wet gel with minimal deformation/shrinkage occurring in the end product solid skeletal structure. The literature describes the process where a sol converts into a gel is through gelatin. In general terms, gelation involves dispersion of nanoparticles in a liquid phase, colliding nanoparticles then forms the solid continuous network (Matter, Luna, & Niederberger, 2020). Parameters such as (i.e., concentration, reagents, solvents,

temperature, pH level) significantly impact the gelation of the wet gel, therefore also affecting the microstructure and properties of the dried aerogel. Van der Waals and double layer forces of colloidal particles could be lowered as the sol destabilized due to the external stimulus, which are the mentioned parameters. Hence, inducing a change under experimental conditions to convert the sol into a gel. In addition, according to the nature and surface chemistry interaction of the colloidal particles, dispersing medium may vary from polar to nonpolar solvent (Matter et al., 2020).

Varied drying processes of wet gel may determine the dried gel outcome and quality, according to various literatures, supercritical drying, ambient drying and freeze drying are popular techniques to extract liquids from the wet gel (Ganesan, Dennstedt, Barowski, & Ratke, 2016). Supercritical drying utilizing CO_2, which as a result yield an aerogel, it was observed by researchers that this method has the least amount of shrinkage occurring in the wet gel body during drying, in comparison to xerogel and cryogel. This is owing to the absences of a liquid-vapor interface at the state of the supercritical fluid CO_2, due to both being high temperature and pressure condition. Ambient drying method utilizes atmospheric temperature and pressure to evaporate the liquid solvent medium from the wet gel body, yielding a xerogel. An evaporating liquid solvent medium (e.g., ethanol, isopropanol) is typically used for the ambient drying method, yielding a xerogel. Researchers observed the yield xerogel resulting in a high percentage of shrinkage owing to the capillary forces collapsing the solid skeletal structure.

Freeze drying/lyophilization method utilizes either slow or flash freezing techniques, with the liquid solvent medium being washed/replace with distilled water, which is then frozen into ice. The removal of ice is through sublimation, hence yielding the cryogel. The shrinkage of cryogel was observed by researchers to be less than xerogel but more than aerogel. Generally, among the three methods, the supercritical drying method is currently the ideal method by researchers to obtain a variation of a dried gel. In this case, an aerogel, with the least amount of shrinkage, preserving the quality of the solid skeletal structure and properties developed during the sol-gel and aging process (Ganesan et al., 2016; Gurav et al., 2010). Fig. 5.1 shows the general preparation of aerogel.

5.3 Cellulose-based aerogel

Silica-based aerogel products are generally promoted as an alternative towards conventional insulating materials (e.g., mineral wool and foam boards). Owing the performance due to the physical properties of the material, which allows it to be lightweight with excellent thermal and sound insulating capabilities, as investigated by researchers.

In contrast, researchers have investigated the use of cellulose as precursors to synthesize aerogels and discovered that to be a material with great potential for numerous applications. Firstly, cellulose is an organic polymer naturally in abundance on earth. Cellulose could be extracted and modified into various derivatives

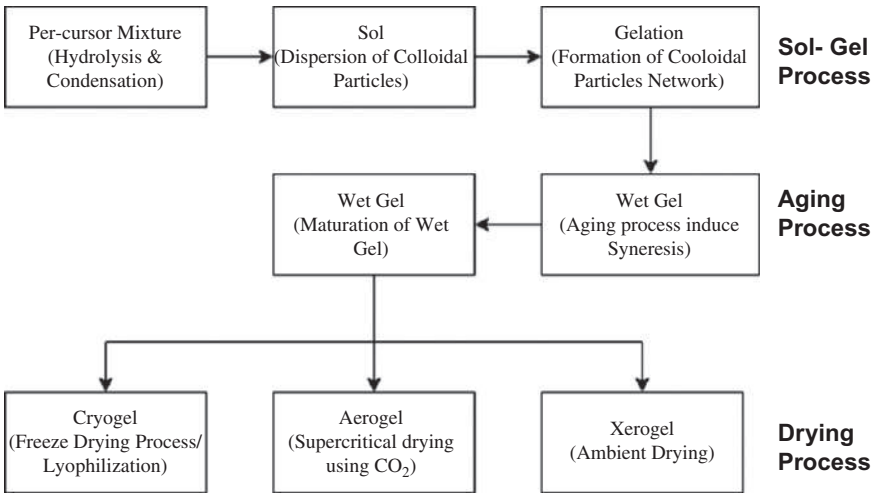

FIG. 5.1

General preparation procedure of aerogel.

from lignocellulosic resources/biomass in agriculture, as well as cultivation through a specific type of microorganism. Cellulose-based aerogels are viewed by researchers to be a variation of an aerogel material in which has characteristics of the precursor cellulose (e.g., biodegradability, biocompatibility, renewability). There many research articles and review papers investigating the progression of cellulose-based aerogels, in terms of preparation procedures, characterizing the physical and chemical properties, as well as discussing the potential applications and performance in numerous fields (Ahsan, Fei, Man, Wei, & Zuowan, 2020; Ciolacu, Rudaz, Vasilescu, & Budtova, 2016; Ferreira et al., 2020; Ganesan et al., 2016; Long, Weng, & Wang, 2018; Zhang et al., 2020). Some articles discuss the differences in characteristics (e.g., physical and chemical properties) and application of cellulose-based and silica-based aerogels. One of the noticeable differences observed by researchers is the mechanical strength of cellulose-based aerogel is higher in comparison to silica-based aerogel. Some studies investigate different iterations of silica-based precursors for aerogels with without reinforcements. The compressive strength was observed to range between (Long et al., 2018) (500 kPa–4.2 MPa) according to Wong, Kaymak, Brunner, and Koebel (2014), which uses Polyethoxydisiloxane (PDMS) as precursors, (47–160 kPa) according to Omranpour, Dourbash, and Motahari (2014), which uses Tetraethyl orthosilicate (TEOS) as precursors. However, cellulose-based aerogels were observed to have a higher compressive strength, range of (5.2 kPa–16.67 MPa) according to a Long et al. (2018). Furthermore, the researchers manage to accumulate a large selection of data on the properties of natural cellulose, regenerated cellulose, and derived cellulose-based aerogels.

The synthesis of cellulose-based aerogels utilizes the similar type of processes as synthesis silica-based aerogels, such as the sol-gel process and drying, i.e., supercritical drying, freeze drying, and ambient drying. However, the types of solvents, reagents, the catalyst may be different, according to the type of cellulose precursors (Long et al., 2018). There are numerous factors that could influence the structural network, developed during synthesis, as well as the physical and chemical properties of the cellulose-based aerogels. This includes the synthesis of the precursor; cellulose. The cellulose extraction processes of plant/lignocellulosic biomass sources during production include pre-treatment, post-treatment, and disintegration processes, which determine the quality of the cellulose.

In addition, further processing with reagents could modify the cellulose into ester or ether derivatives, hence may alter the structure, properties and performance of the aerogels (Lee, Jeong, & Kang, 2015; Nasir, Hashim, Sulaiman, & Asim, 2017). Additionally, cellulose could also be synthesized through culturing of bacteria such as *Gluconacetobacter xylinum, Gluconacetobacter hansenii*, and *Gluconacetobacter pasteurianus* (Torres, Arroyo, & Troncoso, 2019). Comparing the cellulose extracted from plant/lignocellulosic biomass, although the chemical structure of cellulose extracted from culturing bacteria is similar, researchers have observed that bacterial cellulose has a higher degree of crystallinity of about 60%–80%. Furthermore, bacterial cellulose does not contain impurities which are available in plants (i.e., lignin, pectin, wax, and hemicellulose) in which researchers have observed that the physical properties of bacterial cellulose, are better than plant-based cellulose (Ahrem et al., 2014; Lin & Dufresne, 2014; Park, Jung, & Khan, 2009). The preparation of cellulose-based aerogel could be categorized into three stages: dissolving/dispersing cellulose or cellulose derivatives, gelation of cellulose by the sol-gel process, and drying cellulose gel while retaining its skeletal porous structure. Fig. 5.2 shows the general of the preparation process of cellulose-based aerogels as well as xerogel and cryogel according to numerous literatures (El-Naggar, Othman, Allam, & Morsy, 2020; Gupta, Singh, Agrawal, & Maji, 2018; Liebner, Aigner, Schimper, Potthast, & Rosenau, 2012; Long et al., 2018).

Cellulose-based aerogel synthesized from nanofibrillated or nanocellulose could be prepared by first; dispersion of nanocellulose in distilled water through ultrasonication or high-speed homogenizer and other means of mechanical treatments. Followed by solvent exchange and the drying process of choice according to Fig. 5.2. Utilizing the supercritical drying method, shrinkage of the aerogel was observed to be ($<15\%$), and with compressive modulus of about 16 MPa. Structures developed by nanocellulose aerogels comprises of randomly connected network nanofibers. Researchers observed it to be white and opaque, limiting the application for optics, which requires optical transparency. In addition to nonlinear elasticity, and lower surface area in contrast to conventional silica-based aerogels (Ilknur et al., 2015).

Aerogels synthesize with bacterial cellulose could be prepared by obtaining the cultivated bacterial cellulose in vitro after 30 days of cultivation at 30°C. This typically yields 3–4 cm layer sheets, depending on the vessel size and volume of growth medium used. An alkaline treatment of (0.1 M aqueous NaOH at 90°C) was utilized

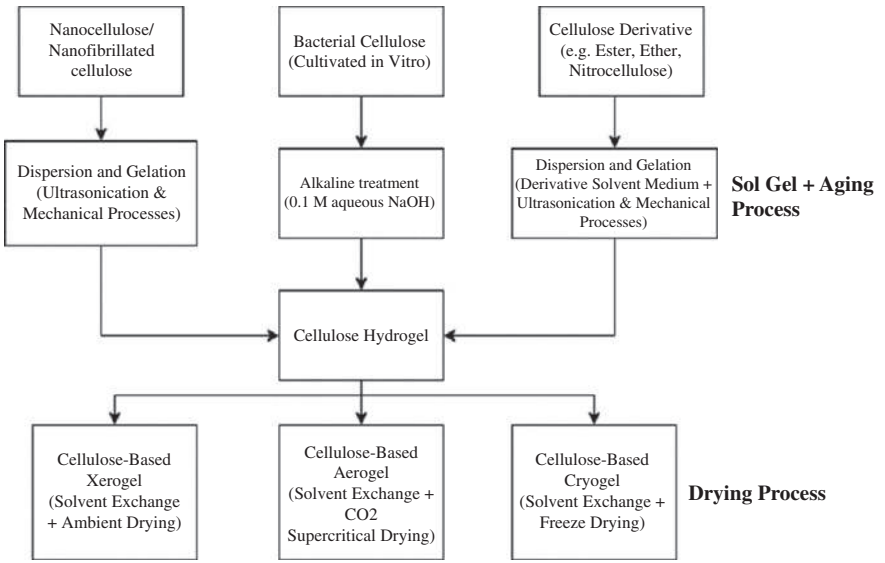

FIG. 5.2

General preparation process of cellulose-based aerogels, xerogels and cryogels.

to get rid of protein residues and by-products, this step is repeated numerous times for proper bleaching. The batch is neutralized by rinsing with deionized water for 24 h. Comparing to nanocellulose aerogels, after supercritical drying, researchers observed it to resist shrinking, with the percentage of shrinkage (1%–5%). The compressive specific modulus of bacterial cellulose aerogel is about 19–25 MPa cm^3 g^{-1} (Pircher et al., 2014). SEM images observed by researchers shows that dense network of nanofibers. Sample appearance are similar to other cellulose-based aerogels, which are white and opaque (Liebner et al., 2012).

Cellulose derivatives and regenerated cellulose have an array of different solvent mediums used during sol-gel process, therefore, resulting aerogels may have different performance and properties. There is more literature on regenerated cellulose aerogels, as the production process of is simple and low-cost. However, the preparation of regenerated cellulose aerogels requires dispersion/dissolution and regeneration, followed by a repetitive solvent exchange for a successful aerogel sample upon drying. This increases production time for the aerogel. According to researchers, the rate of shrinkage of regenerated cellulose aerogels are generally between (15%–30%) for freeze drying method and about (6.5%) for supercritical drying method. This may result in denser aerogels in comparison to natural cellulose aerogels (Shi, Lu, Guo, Liu, & Cao, 2015). Cellulose diacetate, cellulose triacetate, and carboxymethyl cellulose, are common types of cellulose derivatives used in numerous industries. The synthesis of cellulose derivatives involves chemical modifications of cellulose, which alters the performance, physical and chemical properties. This

enables the cellulose to be more functional for different applications as it enables solubility in different solvent mediums such as; distilled water and organic solvents (i.e., dicholoromethane, dioxane, acetone, isopropanol). Furthermore, organic solvents such as acetone is soluble during supercritical CO_2 drying, skipping the need for the solvent exchange process (Fang et al., 2016), enabling better efficiency during aerogel synthesis.

5.4 Cellulose-based aerogel composite

Main reasons of the development of composites aerogels are to improve performance and modify their properties. In cases of silica-base aerogels, it is well known for being very lightweight, sound and thermal insulating with fire-retardant characteristics. In contrast on the cellulose-based aerogels, literatures have shown some characteristics that are different in comparison to silica-based aerogels. Some cellulose-based aerogels may have a slightly higher density with similar sound and thermal insulating characteristics, but researchers have observed that cellulose-based aerogels are highly flammable and considered a fire hazard (Luo & Wang, 2018). Therefore, cellulose-based aerogels may deem inapplicable as insulation products such as silica-based aerogels currently on the market. There are a few ways to develop composite cellulose-based aerogel: (i) By adding reinforcements and other components in the solution/suspension of the cellulose, during sol-gel process, and (ii) Surface modification by coating, grafting and chemical modification of the cellulose, this could be applied after the drying process.

There numerous literatures which manage to improve fire retardant capabilities by developing composite cellulose-based aerogels. Gupta et al. (2018), manages to synthesize a composite cellulose-based aerogel with varied amounts of sepiolite clay dispersed in the cellulose nano-fibers hydrogel (0.2 wt%) solution. The resulting aerogel has a density ranging between 11.5 and 32.5 kg/m^3), with porosity (99.2%–98.3%) with good dimensional stability. The vertical burning test with V-0 performance, horizontal burning test and flame penetration supports the material's thermal conductivity, shielding and fire retardancy (Gupta et al., 2018).

Fan, Chen, Yao, Sun, and Jin (2017) utilize a similar strategy of developing the composite through the soil-gel process, using a hydrothermal method. The researchers have managed to prepare a cellulose nanofiber and aluminum sulfate octadecahydrate (AlOOH) composite aerogel for flame retardant and thermal insulation. The density of the neat cellulose nanofiber aerogel was 2 $mg\,cm^{-3}$ and the porosity was 99.88%, while the cellulose nanofiber (A1OOH) composite aerogel has the density of 2.5 $mg\,cm^{-3}$ and porosity of 99.85%. Both aerogels utilized the freeze-drying method, shrinkage was not a significant feature of the study, however the combustion test shown that the composite cellulose aerogel maintained its integral shape above 60 s and did not combust. In comparison to the neat cellulose-based aerogel, which immediately ignites and combust into flames, burning the cellulose-based aerogel quickly. Fan et al. (2017), cellulose nanofiber (AlOOH) composite

aerogels displayed good flame retardant and thermal insulation properties through the flammability test. This demonstrates that the cellulose composite aerogels may have a place as products for thermal insulation and providing enough fire retarding capabilities (Fan et al., 2017).

Another similar literature by Zhou et al. (2020), utilizes cladophora cellulose extracted from freshwater green macroalgae, aluminum nitrite nonahydrate ($Al(NO_3)_3{\cdot}9H_2O$) as metal-organic framework were used to fabricate composite aerogels. The fabrication process involves coating and cross-linking of the cellulose nanofibers with the continuous nucleation in a solution of nanolayers of the metal-organic framework. The resulting composite cellulose-based aerogels produce properties (e.g., thermal conductivity of $40\,mW\,m^{-1}\,K^{-1}$, 80% maximum recoverable strain, $100\,MPa\,cm^3\,g^{-1}$ specific stress, and $200\,MPa\,cm^3\,g^{-1}$ specific compression modulus). The metal organic-framework nanolayers are observed to be hydrophobic, thermally stable, if the material is coated/wrapped around the cellulose nanofibers, it results in good moisture resistance and fire retardancy. Therefore, Zhou et al. (2020) demonstrates that metal organic-framework could be utilized to develop a composite enhancing the cellulose based aerogels properties. Furthermore, techniques implemented such as ion-exchange, interfacial synthesis, freeze-drying and crosslinking allows a systematic way of reinforcing/developing the composite cellulose-based aerogels properties (Zhou et al., 2020).

On the other hand, some researchers have enhanced mechanical properties of cellulose-based aerogels, developing a composite by adding a reinforcement component. Zheng et al. (2017) manages to enhance the mechanical properties of the cellulose-based aerogel by incorporating two types of cellulose, which cellulose extracted from cotton linter with α-cellulose content of above 95%, and nanocrystalline cellulose (NCC) as the reinforcement component. Aerogels in general are quite brittle and do not have high mechanical strength and integrity, hence there is a need for development in this area to increase functionality for applications. Zheng et al. (2017) was successful in preparing the composite cellulose-based aerogel using cellulose precursor and incorporating NCC during the sol-gel process. It was observed that the SEM and TEM results shown the NCC was embedded/incorporated well into the cellulose-based aerogel. The high compressive modulus of the NCC reinforced composite cellulose aerogel was $489.1 \pm 18.25\,kPa$, which is a good improvement comparable to the high compressive modulus of neat cellulose-based aerogel of $207.1 \pm 8.66\,kPa$. In addition, surface modification was conducted on the NCC reinforced composite cellulose aerogel utilizing trimethylchlorosilane via cold plasma treatment. The surface modification enables the aerogel to behave more hydrophobic. However, it was observed that the aerogel retains its affinity towards oil (oleophilic). The material developed may have potential in applications such as removal of oil-spill pollutants and organic solvents from water. Enhanced mechanical properties of the NCC reinforced composite cellulose aerogel may also influence the reusability upon application, as it has high adsorption capacity while upholding its integral shape (Zheng et al., 2017).

5.5 Applications of cellulose-based aerogels and composites

Cellulose-based aerogels and its composites acquired a range of unique properties which functionalize them for numerous applications. Currently, numerous literatures are investigating the performances during application, it was observed that these aerogels and composites were mainly used in thermal and sound insulation, adsorption and separation, and biomedical applications.

5.5.1 Fire retardant

According to the previous section, examples on cellulose based aerogel composites, some literatures have managed to improve cellulose-based aerogel properties by developing the aerogel into a composite. The improved properties of aerogel enable the material to be more functional for application. Zhou et al. (2020), Gupta et al. (2018), and Fan et al. (2017) investigates the modification of cellulose-based aerogels for thermal insulation and fire-retardant application. These successfully improve the properties and characteristics which support the applications of thermal insulation and fire retardancy. In contrast, silica-based aerogel insulating products are currently on the market and served well upon application as both thermal insulation and fire-retardant material. Initially, cellulose-based aerogels are a fire hazard and flammable due to the cellulose content in the aerogel structure. Surface modifications, coatings and reinforcement material added into the cellulose-based aerogel has positive effects on the material properties to support thermal insulation and fire retardancy. It is notable by the literatures that cellulose-based aerogels and its composite are more biodegradable in comparison to silica-based aerogels, in addition, the mechanical properties of cellulose-based aerogels are observed to be higher than silica-based aerogels (Ilknur et al., 2015; Long et al., 2018; Wong et al., 2014). Therefore, cellulose-based aerogel composites may have potential as an alternative for conventional insulation products as well as silica-based aerogels. One study reviewed the applications of fire retardant bioproducts for green buildings.

Yildirim et al. (2020) investigates the green building trend, fire-retardant bioproducts used in the construction and building industry. The study revealed that even with the increased usage of bioproducts in building and construction industry. There was increasing necessity in fire safety and standards, there was a problem regarding the reliability of bioproducts and how fire safety could be ensured most effectively, and not becoming a fire hazard instead (Yildirim et al., 2020). Future product developers on cellulose-based aerogels and its composites should follow certain standards upon testing, before launching into real world applications (e.g., building and construction, insulation). Examples of ASTM standards for fire retardant material characterization includes: (i) ASTM E906/E906M-17, Standard Test Method for Heat and Visible Smoke Release Rates for Materials and Products Using a Thermopile Method (ASTM E906, 2017), (ii) ASTM E1354, Standard Test Method for Heat

and Visible Smoke Release Rates for Materials and Products Using an Oxygen Consumption Calorimeter (ASTM E1354-17, 2017), (iii) ASTM E119-20, Standard Test Methods for Fire Tests of Building Construction and Materials (ASTM E119-10, 2020), (iv) ASTM E1321-18, Standard Test Method for Determining Material Ignition and Flame Spread Properties (ASTM E1321, 2018), and (v) ASTM E84-20, Standard Test Method for Surface Burning Characteristics of Building Materials (ASTM E84-20, 2019).

5.5.2 Water treatment

In contrast, cellulose-based aerogels and its composites also gather attention on the materials, absorbent, lightweight and high porosity characteristics/properties. Hence, numerous literatures have investigated the performance applied in oil spill treatment, and water pollutant removal (Ahsan et al., 2020; Ciolacu et al., 2016; Ferreira et al., 2020; Ganesan et al., 2016; Long et al., 2018; Zhang et al., 2020). A good adsorbent material for both oil spill and water pollutant treatment process involve the material successfully adsorb the substance, high adsorption capacity, and reusability.

Chhajed, Yadav, Agrawal, and Maji (2019) investigated the application of cellulose-based aerogel composite for oil spill treatment. The combination of nanofibrillated cellulose (NFC) and polyvinyl alcohol (PVA) produces a composite aerogel with a porosity of 98%. It was observed that the NFC/PVA aerogel has good hydrophobic characteristics (contact angle higher than 159°) caused by a modification through coating utilizing stearic acid chloride (SAC) solution. NFC/PVA aerogel were also oleophilic and able to separate a series of oil/water mixtures and various organic solvents, adsorption capacity of the aerogels was considerably high in comparison to their dry weight, in addition the aerogel has good reusability for at least 15 times (Chhajed et al., 2019).

An example of the application adsorption heavy metal ion and dye removal is demonstrated by Tang et al. (2019), which developed a cellulose nanofibril (CNF) aerogel adsorbent. The researchers utilized the CNF aerogel with the goal of removing various contaminants in wastewater. Surface modification was made through coating of polydopamine onto the surface of CNFs, which were cross-linked with polyethylenimine (PEI) to synthesize the aerogels. Adsorption studies were conducted on two representative contaminants, Copper II (Cu^{2+}) and methyl orange (MO). It was noted that a high adsorption capacity could be maintained within a wide range of pH values, the crosslinked networks of the aerogel with high porosity influence the adsorption of methyl orange and copper (II) ions. The results presented by Tang et al. (2019) showed that the CNF aerogel has considerable potential for the removal of heavy metal ion and synthetic dyes (i.e., MO and Cu^{2+}). However, for future development of adsorbent cellulose-based aerogels and its composites, standards should be implemented to ensure reliability (Tang et al., 2019). Examples of applicable ASTM standards for adsorbent material characterization includes: (i) ASTM F716-18 Standard Test Methods for Sorbent Performance of Absorbents for Use on Chemical and Light Hydrocarbon Spills (ASTM F716-18, 2018), and (ii)

ASTM F726-17 Standard Test Method for Sorbent Performance of Adsorbents for use on Crude Oil and Related Spills (ASTM F726-17, 2017).

5.5.3 Biomedical

In terms of biomedical application utilizing cellulose-based aerogels, Zhang et al. (2019) reviewed recent progressing in utilizing biomaterials to develop aerogels (i.e., cellulose, chitosan, collagen, gelatin, silk fibroin, etc.). According to the literature, these biomaterial-aerogels are natural macromolecules which is an ideal choice and good biocompatibility for biomedical/clinical application (e.g., facilitate wound healing, tissue regeneration, bone regeneration, and drug delivery). It was stated that the biomaterial-aerogels mimics a natural extracellular matrix environment for cell attachment, proliferation, and differentiation, due to their 3D network, porosity, permeability, surface area, and biocompatibility.

Wound dressings are expected to absorb exudate and toxic substances, allow gas exchange, and preventing growth of bacteria/microorganism. Cellulose-based aerogels have high hydration characteristics are capable of absorbing large amounts of aqueous fluids, maintaining moisture as well as pH level. In addition, cellulose-based aerogels also have a low endotoxin level (45 EU/g) and high absorption capacity of 4 to 5 times in comparison to alginate-based wound dressings (Nordli, Chinga-Carrasco, Rokstad, & Pukstad, 2016). For clinical applications in humans, biomaterials in general should be endotoxin free. According to the review, numerous studies confirmed that the cellulose-based aerogels are safe and a good alternative option over conventional wound dressing products (Zheng et al., 2017). In terms of drug delivery application, cellulose-based aerogels are utilized for its high surface area, porosity, hygroscopic, and swelling tendency, which allows good drug-loading capacity. Cellulose-based aerogels also has floating tendency, swelling ability, and the mucoadhesive properties which enable a controllable drug release, enabling the possibility of releasing/dispensing drugs by skin penetration and implant coating (Bhandari et al., 2017; Zheng et al., 2020). Overall, cellulose-based aerogels display biocompatibility, biodegradation, high porosity, surface area, permeability, which intrigue researchers in material science.

The cellulose-based aerogels partially mimic the characteristics of a natural extracellular matrix, hence promoting wound healing of the native tissues fabricating a biocompatible scaffold/construction of living tissues. Cellulose-base aerogel could provide a controlled local administration of the growth factors and other medications at the treatment area, due to the drug loading capacity, promoting healing, tissue regeneration and preventing infections. Zheng et al. (Zheng et al., 2020), review that aerogels from biomaterial's, which includes cellulose-based aerogels, could be utilized for a series of functions, influencing the outcome of clinical applications such as duration of healing and inhibiting pathological inflammation/inflammatory response (Bhandari et al., 2017). Future development for biomedical applications, similar to cellulose-based aerogels applications (i.e., adsorption/absorption, thermal insulation and fire-retardant) has certain procedure/standards that should be adhere

upon to ensure the product could be trusted. As of human clinical applications, products must be safe, biocompatible, and consistently reliable upon application. However, literatures have reviewed that it is still within the early stages of development, but cellulose-based aerogels have shown some promising results for clinical/biomedical applications.

5.6 Summary

It may describe silica-based aerogels as a high porosity, specific surface area, lightweight but brittle structure with low mechanical strength. However, cellulose-based aerogel was observed to have a higher mechanical strength and share a similar range of physical properties (e.g., porosity, density, specific surface area) to silica-based aerogel. In terms of fire retardancy and thermal insulation, cellulose-based aerogels required additional modifications in order to become an effective insulation and fire-retardant material with silica-based aerogel, as cellulose-based aerogels are flammable as a neat standalone material. In addition to modifications, by adding reinforcements, a composite cellulose-based aerogel could be developed which improved physical and chemical properties. Adsorbent and absorbent capabilities of cellulose-based aerogels and its composites are recognized and have good reusability. Biomedical applications may take advantage of this trait for drug delivery and wound dressing applications. Future developments of cellulose-based aerogels may include developing simple and effective methods to increase efficiency during synthesis, conducting more standardized testing to ensure reliability of the product These may be an important factor to progress forward with the advancement of aerogel technology.

Acknowledgment

The authors would like to acknowledge Universiti Malaysia Sarawak (UNIMAS) for the support

References

Ahrem, H., Pretzel, D., Endres, M., Conrad, D., Courseau, J., Müller, H., et al. (2014). Laser-structured bacterial nanocellulose hydrogels support ingrowth and differentiation of chondrocytes and show potential as cartilage implants. *Acta Biomaterialia*, *10*(3), 1341–1353. https://doi.org/10.1016/j.actbio.2013.12.004.

Ahsan, Z., Fei, H., Man, J., Wei, W., & Zuowan, Z. (2020). Preparation, properties, and applications of natural cellulosic aerogels: a review. *Energy and Built Environment*, 60–76. https://doi.org/10.1016/j.enbenv.2019.09.002.

ASTM E119-10. (2020). *Test methods for fire tests of building construction and materials*. ASTM International.

ASTM E1321. (2018). *Test method for determining material ignition and flame spread properties*. ASTM International.

ASTM E1354-17. (2017). Test method for heat and visible smoke release rates for materials and products using an oxygen consumption calorimeter. ASTM International.

ASTM E84-20. (2019). *Test method for surface burning characteristics of building materials. 84*. ASTM International.

ASTM E906. (2017). *Test method for heat and visible smoke release rates for materials and products using a thermopile method ASTM international*. ASTM International.

ASTM F716-18. (2018). Standard test methods for sorbent performance of absorbents for use on chemical and light hydrocarbon spills. ASTM International.

ASTM F726-17. (2017). Standard test method for sorbent performance of adsorbents for use on crude oil and related spills. ASTM International.

Baetens, R. (2013). High performance thermal insulation materials for buildings. In *Nanotechnology in eco-efficient construction: materials, processes and applications* (pp. 188–206). Elsevier Ltd. https://doi.org/10.1533/9780857098832.2.188.

Bakri, M. K. B., Jayamani, E., Rahman, M. R., & Kakar, A. (2018). Improvement of epoxy nanocomposites on physical, morphology, and mechanical properties as well as fracture behavior with the addition of mesoporous silica/nano-silica. Rahman M.R., Silica and Clay Dispersed Polymer Nanocomposites. *Woodhead Publishing*, 259–280. https://doi.org/10.1016/B978-0-08-102129-3.00012-9.

Bhandari, J., Mishra, H., Mishra, P. K., Wimmer, R., Ahmad, F. J., & Talegaonkar, S. (2017). Cellulose nanofiber aerogel as a promising biomaterial for customized oral drug delivery. *International Journal of Nanomedicine*, *12*, 2021–2031. https://doi.org/10.2147/IJN.S124318.

Chhajed, M., Yadav, C., Agrawal, A. K., & Maji, P. K. (2019). Esterified superhydrophobic nanofibrillated cellulose based aerogel for oil spill treatment. *Carbohydrate Polymers*, *226*. https://doi.org/10.1016/j.carbpol.2019.115286.

Ciolacu, D., Rudaz, C., Vasilescu, M., & Budtova, T. (2016). Physically and chemically cross-linked cellulose cryogels: Structure, properties and application for controlled release. *Carbohydrate Polymers*, *151*, 392–400. https://doi.org/10.1016/j.carbpol.2016.05.084.

El-Naggar, M. E., Othman, S. I., Allam, A. A., & Morsy, O. M. (2020). Synthesis, drying process and medical application of polysaccharide-based aerogels. *International Journal of Biological Macromolecules*, *145*, 1115–1128. https://doi.org/10.1016/j.ijbiomac.2019.10.037.

Fan, B., Chen, S., Yao, Q., Sun, Q., & Jin, C. (2017). Fabrication of cellulose nanofiber/AlOOH aerogel for flame retardant and thermal insulation. *Materials*, *10*(3). https://doi.org/10.3390/ma10030311.

Fang, Y., Chen, S., Luo, X., Wang, C., Yang, R., Zhang, Q., et al. (2016). Synthesis and characterization of cellulose triacetate aerogels with ultralow densities. *RSC Advances*, *6*(59), 54054–54059. https://doi.org/10.1039/c6ra06067f.

Ferreira, F. V., Otoni, C. G., De France, K. J., Barud, H. S., Lona, L. M. F., Cranston, E. D., et al. (2020). Porous nanocellulose gels and foams: Breakthrough status in the development of scaffolds for tissue engineering. *Materials Today*, *37*, 126–141. https://doi.org/10.1016/j.mattod.2020.03.003.

Ganesan, K., Dennstedt, A., Barowski, A., & Ratke, L. (2016). Design of aerogels, cryogels and xerogels of cellulose with hierarchical porous structures. *Materials and Design*, *92*, 345–355. https://doi.org/10.1016/j.matdes.2015.12.041.

Ganobjak, M., Brunner, S., & Wernery, J. (2020). Aerogel materials for heritage buildings: Materials, properties and case studies. *Journal of Cultural Heritage*, *42*, 81–98. https://doi.org/10.1016/j.culher.2019.09.007.

Gupta, P., Singh, B., Agrawal, A. K., & Maji, P. K. (2018). Low density and high strength nanofibrillated cellulose aerogel for thermal insulation application. *Materials and Design*, *158*, 224–236. https://doi.org/10.1016/j.matdes.2018.08.031.

Gurav, J. L., Jung, I. K., Park, H. H., Kang, E. S., & Nadargi, D. Y. (2010). Silica aerogel: Synthesis and applications. *Journal of Nanomaterials*, *2010*. https://doi.org/10.1155/2010/409310.

Ilknur, K., Björn, S., Maria, S., Barbara, M., Thomas, G., & Lorenz, R. (2015). Production of porous cellulose aerogel fibers by an extrusion process. *The Journal of Supercritical Fluids*, 105–114. https://doi.org/10.1016/j.supflu.2015.06.011.

Kakar, A., Jayamani, E., Bakri, M. K. B., & Rahman, M. R. (2018). Durability and sustainability of the silica and clay and its nanocomposites. In M. R. Rahman (Ed.), *Silica and Clay Dispersed Polymer Nanocomposites* (pp. 137–157). Woodhead Publishing. https://doi.org/10.1016/B978-0-08-102129-3.00009-9.

Kakar, A., Jayamani, E., Bakri, M. K. B., & Rahman, M. R. (2018). Biomedical and packaging application of silica and various clay dispersed nanocomposites. Rahman M.R., Silica and Clay Dispersed. *Polymer Nanocomposites Woodhead Publishing*, 109–136. https://doi.org/10.1016/B978-0-08-102129-3.00008-7.

Koebel, M., Rigacci, A., & Achard, P. (2012). Aerogel-based thermal superinsulation: An overview. *Journal of Sol-Gel Science and Technology*, *63*(3), 315–339. https://doi.org/10.1007/s10971-012-2792-9.

Lee, S., Jeong, M. J., & Kang, K. Y. (2015). Preparation of cellulose aerogels as a nano-biomaterial from lignocellulosic biomass. *Journal of the Korean Physical Society*, *67* (4), 738–741. https://doi.org/10.3938/jkps.67.738.

Liebner, F., Aigner, N., Schimper, C., Potthast, A., & Rosenau, T. (2012). Bacterial cellulose aerogels: From lightweight dietary food to functional materials. *ACS Symposium Series*, *1107*, 57–74. https://doi.org/10.1021/bk-2012-1107.ch004.

Lin, N., & Dufresne, A. (2014). Nanocellulose in biomedicine: Current status and future prospect. *European Polymer Journal*, *59*, 302–325. https://doi.org/10.1016/j.eurpolymj.2014.07.025.

Long, L. Y., Weng, Y. X., & Wang, Y. Z. (2018). Cellulose aerogels: Synthesis, applications, and prospects. *Polymers*, *8*(6). https://doi.org/10.3390/polym10060623.

Luo, J., & Wang, H. (2018). Preparation, thermal insulation and flame retardance of cellulose nanocrystal aerogel modified by TiO2. *International Journal of Heat and Technology*, *36* (2), 614–618. https://doi.org/10.18280/ijht.360226.

Matter, F., Luna, A. L., & Niederberger, M. (2020). From colloidal dispersions to aerogels: How to master nanoparticle gelation. *Nano Today*, *30*. https://doi.org/10.1016/j.nantod.2019.100827.

Montes, S., & Maleki, H. (2020). *Aerogels and their applications* (pp. 337–399). https://doi.org/10.1016/B978-0-12-813357-6.00015-2.

Nasir, M., Hashim, R., Sulaiman, O., & Asim, M. (2017). Nanocellulose: Preparation methods and applications. In *Cellulose-reinforced nanofibre composites: Production, properties and applications* (pp. 261–276). Elsevier Inc. https://doi.org/10.1016/B978-0-08-100957-4.00011-5.

Nordli, H. R., Chinga-Carrasco, G., Rokstad, A. M., & Pukstad, B. (2016). Producing ultrapure wood cellulose nanofibrils and evaluating the cytotoxicity using human skin cells. *Carbohydrate Polymers*, *150*, 65–73. https://doi.org/10.1016/j.carbpol.2016.04.094.

Omranpour, H., Dourbash, A., & Motahari, S. (2014). Mechanical properties improvement of silica aerogel through aging: Role of solvent type, time and temperature. In *Vol. 1593. AIP conference proceedings* (pp. 298–302). American Institute of Physics Inc. https://doi.org/10.1063/1.4873786.

Park, J. K., Jung, J. Y., & Khan, T. (2009). Bacterial cellulose. In *Handbook of hydrocolloids* (2nd ed., pp. 724–739). Elsevier Inc. https://doi.org/10.1533/9781845695873.724.

Pircher, N., Veigel, S., Aigner, N., Nedelec, J. M., Rosenau, T., & Liebner, F. (2014). Reinforcement of bacterial cellulose aerogels with biocompatible polymers. *Carbohydrate Polymers*, *111*, 505–513. https://doi.org/10.1016/j.carbpol.2014.04.029.

Rahman, M. R., Hamdan, S., & Hossen, M. F. (2018). The effect of clay dispersion on polypropylene nanocomposites: Physico-mechanical, thermal, morphological, and optical properties. In M. R. Rahman (Ed.), *Silica and Clay Dispersed Polymer Nanocomposites* (pp. 201–257). Woodhead Publishing. https://doi.org/10.1016/B978-0-08-102129-3.00011-7.

Rahman, M. R., Hui, J. L. C., & Hamdan, S. (2018). Polyvinyl alcohol/silica/clay nanocomposites: effect of clay on surface morphology, electrical and thermo-mechanical properties. In M. R. Rahman (Ed.), *Silica and Clay Dispersed Polymer Nanocomposites* (pp. 45–57). Woodhead Publishing. https://doi.org/10.1016/B978-0-08-102129-3.00004-X.

Riffat, S. B., & Qiu, G. (2013). A review of state-of-the-art aerogel applications in buildings. *International Journal of Low Carbon Technologies*, 1–6. https://doi.org/10.1093/ijlct/cts001.

Shi, J., Lu, L., Guo, W., Liu, M., & Cao, Y. (2015). On preparation, structure and performance of high porosity bulk cellulose aerogel. *Plastics, Rubber and Composites*, *44*(1), 26–32. https://doi.org/10.1179/1743289814Y.0000000107.

Soleimani Dorcheh, A., & Abbasi, M. H. (2008). Silica aerogel: synthesis, properties and characterization. *Journal of Materials Processing Technology*, *199*(1), 10–26. https://doi.org/10.1016/j.jmatprotec.2007.10.060.

Tang, J., Song, Y., Zhao, F., Spinney, S., da Silva Bernardes, J., & Tam, K. C. (2019). Compressible cellulose nanofibril (CNF) based aerogels produced via a bio-inspired strategy for heavy metal ion and dye removal. *Carbohydrate Polymers*, *208*, 404–412. https://doi.org/10.1016/j.carbpol.2018.12.079.

Torres, F. G., Arroyo, J. J., & Troncoso, O. P. (2019). Bacterial cellulose nanocomposites: An all-nano type of material. *Materials Science and Engineering C*, *98*, 1277–1293. https://doi.org/10.1016/j.msec.2019.01.064.

Wong, J. C. H., Kaymak, H., Brunner, S., & Koebel, M. M. (2014). Mechanical properties of monolithic silica aerogels made from polyethoxydisiloxanes. *Microporous and Mesoporous Materials*, *183*, 23–29. https://doi.org/10.1016/j.micromeso.2013.08.029.

Yildirim, N., Erdonmez, F. S., Ozen, E., Avci, E., Yeniocak, M., Acar, M., et al. (2020). Fire-retardant bioproducts for green buildings. In *Series in civil and structural engineering* (pp. 67–79). https://doi.org/10.1016/B978-0-12-819481-2.00004-0.

Zhang, S., Huang, X., Feng, J., Qi, F., Dianyu, E., Jiang, Y., et al. (2020). Structure, compression and thermally insulating properties of cellulose diacetate-based aerogels. *Materials and Design*, *189*. https://doi.org/10.1016/j.matdes.2020.108502.

Zhang, Y., Yin, M., Lin, X., Ren, X., Huang, T. S., & Kim, I. S. (2019). Functional nanocomposite aerogels based on nanocrystalline cellulose for selective oil/water separation and antibacterial applications. *Chemical Engineering Journal*, *371*, 306–313. https://doi.org/10.1016/j.cej.2019.04.075.

Zheng, T., Li, A., Li, Z., Hu, W., Shao, L., Lu, L., et al. (2017). Mechanical reinforcement of a cellulose aerogel with nanocrystalline cellulose as reinforcer. *RSC Advances*, *7*(55), 34461–34465. https://doi.org/10.1039/c7ra04904h.

Zheng, L., Zhang, S., Ying, Z., Liu, J., Zhou, Y., & Chen, F. (2020). Engineering of aerogel-based biomaterials for biomedical applications. *International Journal of Nanomedicine*, *15*, 2363–2378. https://doi.org/10.2147/IJN.S238005.

Zhou, S., Apostolopoulou-Kalkavoura, V., Tavares da Costa, M. V., Bergström, L., Strømme, M., & Xu, C. (2020). Elastic aerogels of cellulose nanofibers@metal–organic frameworks for thermal insulation and fire retardancy. *Nano-Micro Letters*, *12*(1). https://doi.org/10.1007/s40820-019-0343-4.

CHAPTER

Cellulose reinforcement in thermoplastic composites

6

Nur-Azzah Afifah Binti Taib, Md Rezaur Rahman, and Muhammad Khusairy Bin Bakri

Department of Chemical Engineering and Energy Sustainability, Faculty of Engineering, Universiti Malaysia Sarawak (UNIMAS), Kota Samarahan, Sarawak, Malaysia

Chapter outline

6.1 Introduction

Thermoplastics can repeat the heating and cooling process, as they are just a simple resin, which can form liquids at heating and hardened when cooling takes places (Rahman, Adamu, & Hamdan, 2021; Rahman & Bakri, 2021; Rahman, Hamdan, & Bakri, 2021; Rahman, Khui, & Bakri, 2021). When placed at a temperature, the flow in the thermoplastic for different types of thermoplastics such as polypropylene (PP), polystyrene (PS) and polyvinyl chloride (PVC) are found (Rahman, Hamdan, & Bakri, 2021). Until the temperature rises to a certain number, thermoplastics, aforesaid, can maintain their shape. Also, by using a universal tensometer, the tensile data of the polymer resin are collected at $25 \pm 2°C$ (Dhinakaran, Surendar, Riyaz, & Ravichandran, 2020). In general, compared to thermoset polymer materials, thermoplastic is tougher and more ductile (Dixit, Pal, Kapoor, & Stabenau, 2016). Table 6.1 lists the typical

Fundamentals and Recent Advances in Nanocomposites Based on Polymers and Nanocellulose.
https://doi.org/10.1016/B978-0-323-85771-0.00005-1

Table 6.1 Properties of some general unfilled thermoplastic resin (Dixit et al., 2016).

Resin material	Density (g/cm^3)	Tensile modulus (GPa)	Tensile strength (MPa)
Nylon	1.1	1.3–3.5	55–90
PEEK	1.3–1.35	3.5–4.4	100
PPS	1.3–1.4	3.4	80
Polyester	1.3–1.4	2.1–2.8	55–60
Polycarbonate	1.2	2.1–3.5	55–70
Acetal	1.4	3.5	70
Teflon	2.1–2.3	–	10–35

PEEK: polyether ether ketone, PPS: polyphenylene sulfide.

Table 6.2 Application of thermos and thermosetting plastics (Dhinakaran et al., 2020).

Thermoplastic	Thermosetting plastics
Clench-film Grocery bags Blood bags and tubing Foundation garments Raincoats, swimwear Tarpaulins and tents	Pump Sliding bearings Bushes Shaft seals Gelatin materials Gears

unfilled thermoplastic resin properties, while Table 6.2 lists some applications of thermosets and thermoplastics.

Additionally, thermoplastic is either semicrystalline or amorphous depending on their macromolecules order or orientation. For semicrystalline thermoplastic resins, their macromolecules are nearly ordered as they are embedded with crystalline phase. As for amorphous resins, the macromolecules are in disordered statistical orientation. Polycarbonate (PC), PS and PVC are among the typical amorphous resins while PP and polyamide (PA) are categorized as semicrystalline thermoplastic resins (Maddah, 2016).

6.1.1 Polypropylene (PP)

First discovered in 1954, due to having the lowest density among commodity plastics, PP quickly gained strong popularity. There are three major sources of which PP can be derived from. The major source is from the steam-cracking process using naphtha, as PP are the by-product from the cracking process. Depending on the crude oil feedstock, PP can be produced at various ratios. The next source is from the gasoline refining process, and the last one is the dehydrogenation of propane into propylene monomer, which later are used for PP production. The last method is a relatively new method in the production of PP. Additionally, depending on the process conditions, copolymer components, molecular weight and molecular weight distribution, the PP properties will vary. Fig. 6.1 shows the structure of PP where

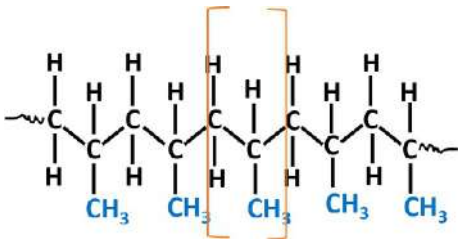

FIG. 6.1

Structure of PP (Maddah, 2016).

every carbon atom is attached to a methyl group since it is a vinyl polymer (Maddah, 2016; Shubhra, Alam, & Quaiyyum, 2013). Meanwhile, Fig. 6.2 illustrates the three possible arrangements form polymerization of nonsymmetrical PP molecule $CH_2=CHCH_3$. Among the three arrangements, the head-to-tail arrangement are highly preferred due to the high chemical regularity of PP chain and steric effect of the methyl group (Zaaba & Ismail, 2019). According to Graziano et al. (Antimo, Shaffiq, & Mohini, 2019), there are three stereo specific configurations of PP available, which are:

Atactic PP (aPP): Methyl groups are randomly placed on the main chain and are completely amorphous. This PP just softens upon heating until it flows like a very viscous liquid since it does not have a melting temperature.
Syndiotactic PP (sPP): The methyl side groups are alternatively oriented and positioned along the main chain and are a semicrystalline polymers. Compared to aPP, sPP are more homogeneous.
Isotactic PP (iPP): Having the highest degree of crystallinity, these semicrystalline polymers' methyl groups are all oriented on one side of the main chain. Hence, this PP are both stable and very homogeneous.

Next, PP can further be classified into three different types depending on the type of monomer exists in the polymer, i.e., *homo-polymer PP* (HPP), *random copolymer* (RCP), and *impact copolymer* (ICP). HPP contained only propylene monomer in

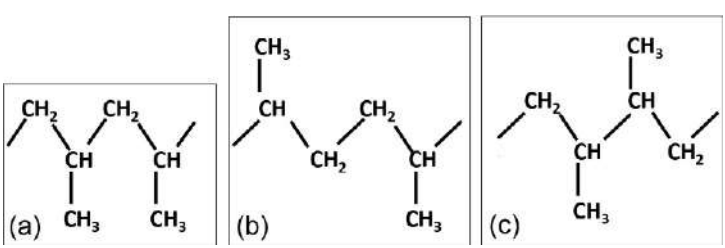

FIG. 6.2

Isomerism for positions in PP for (A) head-to-tail, (B) head-to-head, and (C) tail-to-tail (Zaaba & Ismail, 2019).

a semicrystalline solid form, while for RCP, at levels in the range of 1%–8%, ethylene exists in the PP chains as a co-monomer. As for ICP, it is formed when HPP contained a co-mixed RCP phase that has ethylene content of 45%–65% (Maddah, 2016).

Compared to other plastic materials, the variability of existing PP grades is generally broader. The average molecular weight of PP varies from 2,00,000 g/mol to 6,00,000 g/mol, and while it exhibits highly chemically resistance, PP had lower water absorption and permeability due to its nonpolar structure. Apart from that, PP's crystalline melting point ranging from 160°C to 165°C, while its glass transition temperature is 0°C (Zaaba & Ismail, 2019). Hence, PP is not suitable to be used at temperature below 0°C even though it has density of 0.90 g/cm^3 which indicates it is a lightweight polymer that are suitable to be used in many industrial applications. When used in room temperature applications, PP showed excellent and desirable physical, mechanical and thermal properties (Jayamani, Hamdan, Rahman, & Bakri, 2015). Not only it had high melting point and relatively stiff, but PP also had relatively good resistance to impact. Additionally, PP also had good electrical resistance, dimensional stability, high resistance to flexing stress and nontoxicity property (Khui, Rahman, Jayamani, Bakri, & Khan, 2021; Maddah, 2016). The mechanical and thermal properties of PP and its advantages and disadvantages are listed in Tables 6.3 and 6.4, respectively.

Apart from that, PP is particularly suitable for manufacturing of items such as trays, funnels, pails, bottles, carboys, and instrument jars that have to be frequently sterilized (cleaned) for usage in a clinical environment due to its high temperature resistance. Also, since PP had excellent chemical resistance, many converting methods such as injection molding, extrusion, etc. can be used to process this thermoplastic (Maddah, 2016). In addition, PP is also widely used as a matrix material as it has some excellent characters for composite fabrication. Processes such as filling, reinforcing, and blending are also incorporating PP as one of the materials (Shubhra et al., 2013).

Table 6.3 Mechanical and thermal properties of commercial PP (Maddah, 2016).

Property	Homopolymer			Copolymer	
Melt flow index	3	0.7	0.2	3	0.2
Tensile strength (MPa)	34	30	29	29	25
Elongation at break (%)	350	115	175	40	240
Flexural modulus (MPa)	1310	1170	1100	1290	1030
Brittleness temp. (°C)	+15	0	0	−15	−20
Vicat softening point (°C)	154–150	148	148	148	147
Rockwell hardness (R-scale)	95	90	90	95	88.5
Impact strength (ft lb.)	10	25	34	34	42.5

Table 6.4 Advantages and disadvantages of PP (Maddah, 2016).

Advantages of PP		Disadvantages of PP
Homo-polymer	**Copolymer**	**Degraded by UV (ultraviolet)**
Process ability: Good	Process ability: High	Flammable, but retarded grades available
Impact resistance: Good	Impact resistance: High	Attacked by chlorinated solvents and aromatics
Stiffness: Good	Stiffness: High	Difficult to bond
Food contact: Acceptable	Food contact: Not preferable	Several metals accelerate oxidative degrading
		Low temperature impact strength is poor

6.1.2 Polyethylene (PE)

With ethylene being the single monomer constituent, PE is a semicrystalline thermoplastic polyolefin (POE) that are most widely used commodity plastic in the world (Antimo et al., 2019). There are five main forms of PE exists that are divided based on density and branching, i.e., high-density polyethylene (HDPE), high molecular weight HDPE (HMW HDPE), ultrahigh molecular weight density polyethylene (UHMW-HDPE), linear low-density polyethylene (LLDPE), and very low-density polyethylene (VLDPE). However, HDPE, low-density polyethylene (LDPE) and medium-density are generally the most used PE grades (Khanam & AlMaadeed, 2015; Rahman, Hamdan, & Jayamani, 2019). Table 6.5 shows the PE classification based on density, molecular weight (MW), percent crystallinity (%Xtal) and the

Table 6.5 PE classification based on density, molecular weight (MW), percent crystallinity (%Xtal) and degree of molecule branching (Jordan et al., 2016).

Polymer	Conformation	Density (g/cm^3)	MW (g/mol)	% Xtal
LDPE	Long branches do not pack into crystal well	0.910–0.925		25–50
LLDPE	Shorter branches than LDPE	0.915–0.925		41
MDPE		0.926–0.940		60–80
HDPE	Linear chains increase crystal packing	0.941–0.965		
UHMWPE	Long, linear chains effectively transfer load to the polymer backbone	0.930–0.935	3–6×10^6	39
PEX	Crosslinked chains	0.940		37

Table 6.6 Density and MFI of different PE (Khanam & AlMaadeed, 2015).

Type of PE	Density (g/cm^3)	MFI (g/10 min)
HDPE	0.941–0.965	0.2–3.0
MDPE	0.926–0.940	1–2.0
LDPE	0.915–0.925	0.3–2.6
LLDPE	0.915–0.925	0.1–10.0
VLDPE	0.870–0.914	0.026–0.1

degree of molecular branching, while Table 6.6 lists the density and melt flow index (MFI) of different PE types.

The elaboration of the different types of PE is as follows:

- **HDPE**: The most versatile among all the Pes as it has the highest degree of crystallinity, hence making it to be more rigid than LDPE Additionally, because it has a smaller number of short branches, it is also the most stable PE as the chains pack into the crystal structure very well when the chains become more linear. Apart from that, less than 1 side chain per 200 par carbon atoms exists in the main chain of the HDPE as it mainly consists of long chains without major branching. Products and packaging such as milk jugs, detergent bottles, margarine tubs, garbage containers and water pipes used HDPE in their manufacturing (Antimo et al., 2019; Jordan et al., 2016; Khanam & AlMaadeed, 2015).
- **LDPE**: Having a unique flow property, LDPE is a ductile and flexible material. It has weak intermolecular interaction due to its high degree of chain branching, which prevent the molecules from forming close packing in the polymer. Thus, it does not pack well into crystallites. In comparison to HDPE, this type of PE is flexible and has low tensile and compressive strength because of its irregular packing of polymer chains. Food packaging materials, rigid containers, and plastic film applications such as plastic bags and film wraps generally made using LDPE (Antimo et al., 2019; Jordan et al., 2016; Khanam & AlMaadeed, 2015).
- **MDPE**: Good impact and drop resistance are possessed by MDPE as it has mixed properties of both HDPE and LDPE. Apart from that, compared to HDPE, it has less notch sensitivity and better cracking resistance, but lower hardness and rigidity. MDPE are also never sleek as LDPE and are softer than HDPE. In terms of branching, it has lesser branching than LDPE but more branches than HDPE. Gas pipes and fittings, sacks, shrink film, packaging film, carrier bags, and screw closures typically manufactured using MDPE (Khanam & AlMaadeed, 2015).
- **LLDPE**: Useful for film applications as it has a linear structure and very high number of short branches. Thus, LLDPE are flexible, tough, and transparent (Antimo et al., 2019).
- **Ultra-high molecular weight polyethylene (UHMWPE)**: Load are able to be carried as it has long, linear chains along the polymer backbone (Jordan et al., 2016).

– **Crosslinked PE (PEX)**: Had improved high temperature properties and chemical resistance due to existence of crosslinked bonds in the polymer (Jordan et al., 2016).

6.1.3 Acrylonitrile butadiene styrene (ABS)

Since the 1940s, acrylonitrile-styrene copolymers had been used, but due to the drawbacks of those copolymers, the third monomer, butadiene rubber is added which had imparted higher strength and impact resistance character onto the plastic. Thus, ABS is merely a product of the systematic polymerization of acrylonitrile, butadiene and styrene monomers as shown in Fig. 6.3. The three different monomers provide ABS properties when combined, which means by changing the blend ratios of those three monomers and their interactions, the number and size distribution of PB rubber particles, thermoplastic, and rubbery phase characteristics, grafting degree and morphology, the ABS properties would also differ. Hence, appropriate combination of thermal, electrical, and mechanical properties is exhibited by ABS, such as good durability and resilience, high impact strength, and easy processing properties. ABS has also shown adequate rigidity, high toughness (even in cold conditions), and good thermal stability, besides high resistance to chemical attack and environmental stress cracking. Additionally, ABS are also relatively cheap and had low coefficient of thermal expansion (Olivera, Muralidhara, Venkatesh, Gopalakrishna, & Vivek, 2016; Sadat, Ehsan, Parizad, & Mahmoud, 2018).

In ABS terpolymer, there are two phases exists, namely continuous phase of styrene-acrylonitrile (SAN) and dispersed phase of polybutadiene (PB) (Olivera et al., 2016). PB is a rubbery dispersed phase while SAN is an amorphous continuous phase. Additionally, preparation of ABS copolymer generally is consisted of two methods: (a) SAN copolymer mechanical blending with a butadiene base elastomer butadiene/ acrylonitrile rubber, and (b) styrene and acrylonitrile are grafted onto PB. Content, molecular weight and distribution of SAN in the polymer controlled its processability, heat resistance, surface hardness and chemical resistance. Specifically, rigidity and ease of processability are provided by styrene, and acrylonitrile imparted

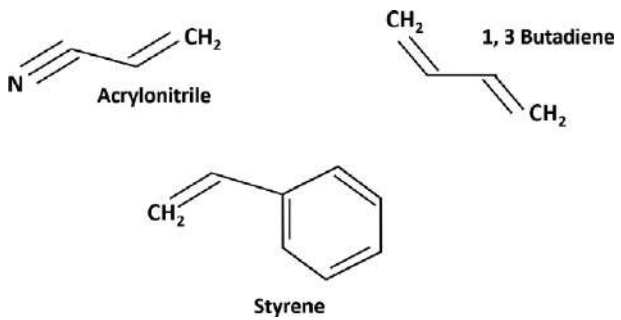

FIG. 6.3

The monomer units of ABS (Olivera et al., 2016).

Table 6.7 General properties of ABS (Sadat et al., 2018).

Specific gravity	1.06	
Density (g/cm^3)	1.02–1.07	
Molecular weight	–	AN: 53.06, PB: 54.092, S: 104.153
Glass transition temperature (T_g) (°C)	108.98–110	AN: 100–104, PB: −85 to 90, S: 100
Self-ignition (°C)	480	
Flash ignition (°C)	390	
Decomposition temperature (°C)	249–399	

chemical resistance, rigidity, and heat stability for the polymer. As for PB, toughness and impact strength are related to it. In addition, the proportion of the monomers in the polymers generally vary with 15%–35% for acrylonitrile, 40%–60% for styrene, and 5%–30% for polybutadiene rubber (Sadat et al., 2018).

Aforesaid, the proportions of the three monomers and preparation conditions greatly influenced the ABS properties. For instance, in term of hydrophilicity/hydrophobicity properties, acrylonitrile is hydrophilic, while styrene and butadiene are both hydrophobic components. Hence, depending on the variation of the blend ratio of those three components, the hydrophilicity of ABS can change. Meanwhile, ABS general properties are listed down in Table 6.7.

6.1.4 Polycarbonate (PC)

One of the important thermoplastic engineering polymers is PC due to its fine processing, thermal, mechanical, and optical properties. Having a carbonate group (-O-(C=O)–O–) in its backbone, PC resins can be divided into two chemical categories, namely, straight chain aliphatic and aromatic. However, the useful thermoplastics are the aliphatic PCs that are prepared from CO_2 and epoxide. Poly (bisphenol A carbonate) is the most common aromatic PC. The first aromatic PC was prepared by reacting hydroquinone or resorcinol with phosgene in pyridine in the late 1890s. Crystalline in nature, this colorless and transparent polymer are low in quality, brittleness and difficult to process. But, having many technical applications to it, poly (bisphenol A carbonate) is an important polymer. Optical data storage devices, bulletproof windows, food packaging, and water bottles are some of the objects that are produced using this type of aromatic PC.

Generally, PCs are used due to their toughness, strength, and optical transparency because balancing properties such as heat and impact resistance, and optical features are important for engineering applications. Those properties had made the polymers easy to process and molded, besides being thermoformable. But, in advance materials, the use of PCs is limited due to limitations such as limited chemical functionality, strong hydrophobicity, notch sensitivity of mechanical properties, high melt viscosity and relative softness. Hence, to overcome those limitations and improve its physical and blend properties, PC can be blended with other thermoplastic

polymers as well as incorporation of reinforcement materials including organic and inorganic fillers into the polymer (Kausar, 2018).

6.2 Cellulose in thermoplastic composites and its blend

6.2.1 Isolation or extraction methods of cellulose nanomaterials

Generally, there are three main processes that are used for the isolation of cellulose nanomaterials and nanofillers, namely acid hydrolysis, enzymatic hydrolysis, and mechanical treatment. To acquire the desired particles or nanomaterials morphology, these extraction or isolation techniques can either be used separately or in combination (dos Santos, Iulianelli, & Tavares, 2016). The processes are as follows:

6.2.1.1 Acid hydrolysis

Among the common process used to isolate the cellulose nanofillers from the cellulosic sources are by using chemical, and to promote hydrolysis at the cellulose's amorphous region, strong acids are used. In most studies, sulfuric acid (SA) in a concentration of 64–65 wt% are used. Meanwhile, hydrochloric acid (HA) although are less common in usage for acid hydrolysis, but there are few studies that used it to isolate the nanoparticles. During hydrolysis, stable crystallites will remain intact, thus are able to be isolated as rod-like nanocrystalline particles. As for the disordered amorphous domains and local interfibrillar contacts of cellulose, they are favorably hydrolyzed. This occurs because those in the amorphous region had lower resistance to acid attack compared to those in the crystalline regions. Material with high degree of crystallinity are able to produce via this method due to the differences in the kinetics of hydrolysis between the amorphous and crystalline regions (dos Santos et al., 2016; Hanieh, Michael, Ishak, Sabu, & Alain, 2017).

By using this method, crystalline particles from various sources of cellulose such as wood, tunicate, algae, bacteria, and from microcrystalline cellulose are able to be extracted. The process will start by mixing the selected cellulosic source into deionized water with a given concentration of acid (typically SA or HA are used). Then, the reaction conditions such as temperature, agitation and time of the mixture are strictly controlled. After that, a series of separation steps will be done onto the generated suspension that contains the cellulose nanocrystals. Steps such as centrifugation or filtration and washing or rinsing are done. The last washing step to remove the remaining acid and neutralized salts is conducted using a dialysis against deionized water. Meanwhile, to facilitate the dispersion of cellulose nanocrystal (CNC) in the suspension, ultrasonic treatments can be used. Additionally, after the dialysis procedure, the suspension can be freeze-dried to obtain powdered CNC (dos Santos et al., 2016). Among the advantages of using this technique are not only it requires only the simplest laboratory equipment, but it can also be performed on very small quantities of cellulose. Apart from that, cellulose nanofibers (CNFs) can be obtained without any induced imperfections which are caused when mechanical processing are used (Pérez-Pacheco et al., 2016).

For CNC production using this method, when the acid concentrations are higher, reaction times are longer and temperature of reaction are higher, the CNC produced are low in yield with decreasing crystallinity and thermal stability. But that CNC had higher surface charge and narrow in size. Apart from that, when the cellulose hydrolysis is done using 60 wt% acid, the CNC produced are in the range of 65–70 wt% yield. However, the cellulose sample was completely dissolved when the acid concentration was above 65 wt%, and the yield are also relatively low (about 20 wt%) (Hanieh et al., 2017). Meanwhile, for CNF production using this method, the exaggerated hydrolysis can generally be noted as the solutions turn dark or black in color (Pérez-Pacheco et al., 2016).

6.2.1.2 Enzymatic hydrolysis

Enzymatic hydrolysis, which is carried out using cellulases can also be used to obtain CNCs. This method is similar to the aforesaid method where the nanofillers are obtained when enzymatic attack occurs at the amorphous regions of the cellulose substrate, while the crystalline regions are maintained. However, generally, this method is used together with other chemical and mechanical or ultrasound treatments. For instance, combination of acid hydrolysis, enzymatic hydrolysis and sonication processes are used by Tang et al. in their study of producing CNC from old corrugated container pulp fiber. From the result, it was shown that the crystallinity and thermal stability of produced CNC are increased when enzymatic treatment are included. Not only that, after phosphoric acid hydrolysis, this method is also effective in enhancing the CNC yield. But, detailed knowledge of the surface chemistry of the available forms of cellulose and specific interactions between enzymes and the substrates are required to develop a cost-effective conversion of cellulose via enzymatic fermentation (dos Santos et al., 2016; Pérez-Pacheco et al., 2016).

6.2.1.3 Mechanical treatment

Extraction of cellulose fibrils from wood, tunicates, algae, microcrystalline cellulose, and bacterial source materials can be done using mechanical processes such as:

High-pressure homogenization (HPH)

Large-scale production of CNF and laboratory-scale preparation of nanofibrils usually uses this method. In this technique, under a high pressure of 50–2000 MPa, the suspension would be forced to go through a very narrow channel or orifice using a piston. Depending on the viscosity of the suspension of the suspension and the applied pressure, the width of the homogenization gap varies, ranging from 5 to 20 μm (Hanieh et al., 2017).

During the process, the size of the fibers would be downsized into nanoscale due to the high velocity and pressure produced in the process, as well as the impact of the shear forces on fluid generate shear rates in the stream. CNF with diameters of about 5–100 nm are produced via this process as the shear forces serve to disintegrate the microfibrils or microfibril bundles in the plant cell wall. Often being combined with other treatment, this method is commonly used by researchers to break up the

cellulosic fibers into nano-sized component structures. Additionally, due to its high efficiency, simplicity, and lack of organic solvents, HPH is considered as a competent method to refine cellulose fibers. However, clogging might occurs due to the small size of the orifice. Hence, to overcome the limitation, it is important to reduce the fiber size before passing samples through the system (dos Santos et al., 2016; Pérez-Pacheco et al., 2016).

High-intensity ultrasonication (HIUS)

Through the hydrodynamic forces of ultrasound, the oscillating power of HIUS is used to isolate cellulose fibrils. Cavitation will lead to a powerful mechanical oscillating power during the process, hence producing high-intensive waves when water molecules absorb ultrasonic energy. The high intensive waves are consisted of formation, expansion and implosion of microscopic gas bubbles. The defibrillation of the cellulose fibers occurs as the results of the action of the hydrodynamic forces of the ultrasound on the pulp. Generally, the nanocellulose particles produced via this method are reported to be shorter and less fibrillar (dos Santos et al., 2016; Hanieh et al., 2017).

In this process, the elimination of lignin from the cellulosic sample are done first to obtain the cellulose fiber. It is done by immersing the samples in a solution of previously acidified sodium chlorite for 1 h at 75°C. Then, the samples are treated with 3% potassium hydroxide at boiling point for 2 h after the bleaching. Next, to further eliminates hemicellulose, residual starch, and pectin from the samples, they are subjected once again to the potassium hydroxide treatment but at different concentration (6%). The samples are then washed with distilled water after the chemical treatment, and the resulting cellulose fibers are immersed in distilled water. After that, inside an ultrasound generator of 20–25 kHz in frequency equipped with cylindrical titanium alloy probe tip of 1.5 cm in diameter, 120 mL of the solution containing purified cellulose fibers are placed. To isolate CNF, the subsequent ultrasonication is conducted for 30 min. Thus, it can be concluded that this technique is the combination of chemical pretreatment with high-intensity ultrasonication (Pérez-Pacheco et al., 2016).

Microfluidization

Microfibrillated cellulose can also be obtained using this process, similar to HPH process. In this process, a microfluidizer are used, where it consist of (i) intensifier pump to increase the pressure, and (ii) interaction chamber for the fiber defibrillation against the colliding streams and channel walls through shear and impact forces (dos Santos et al., 2016). The microfluidizer operates at a constant shear rate unlike homogenizer that operates at constant pressure. Through a z-shaped chamber, the fluid slurry is pumped where it reached a high shear force. In the process, the pressure levels can reach up to until 40,000 psi or approximately 276 MPa. Additionally, in order to improve the degree of fibrillation, it is essential that the process are repeated several times and different sized chambers are used (Hanieh et al., 2017).

Cryocrushing

Another fibrillation process of cellulose that can be used is cryocrushing, where in this process, the water-swollen cellulosic material would be crushed with a mortar and pestle after being immersed in liquid nitrogen. The intense freezing had made it possible to achieve the brittle fracture of nanofibers in combination with intense mechanical forces (dos Santos et al., 2016). The cell walls of the frozen cellulosic fibers would rupture due to the pressure exerted by the ice crystals when high impact forces are applied, causing the nanofibers to be liberated. Then, using a routine disintegrator, the cryocrushed fibers may be uniformly dispersed in water. Fibrils with relatively large diameters are produced via this method, ranging between 0.1 and 1 μm. Various cellulose materials can be used in this procedure, and it can also be used as the fiber pretreatment process before homogenization. However, this method are expensive due to its high energy consumption, besides has low productivity (Hanieh et al., 2017).

The similarity of these processes are that in order to mechanically liberate the CNF from the original plant cell wall structure, they rely on the application of high shear forces on the cellulose fiber suspensions (Pérez-Pacheco et al., 2016). In addition, these methods can cause a dramatic decrease in both the yield and fibril length as they involved high energy consumption. Thus, in this regard, positive results had been obtained by doing pretreatment of cellulose or by combining two or more methods (dos Santos et al., 2016).

6.2.2 Processing technique of thermoplastic reinforced with cellulose

According to Pérez-Pacheco et al. (2016), most of the conventional synthetic thermoplastic processing can be used for the processing of TPS reinforced with cellulose fibers. In those operations, it involved heating and formation of TPS into desired shaped before it was being cooled down. Those processing techniques include hot-melt extrusion (HME), injection molding, compression molding, and blow molding to name a few. The elaboration regarding those methods are as follows:

6.2.2.1 Hot-melt extrusion (HME)

In the HME process, heat is used to convert plastic raw materials into melted form before turning them into a product of uniform shape and density by forcing them through a die, and a rotating screw is generally employed in this method. This continuous process is well-known and widely used in the production of polymer products that had uniform shape and density. Many diverse industrial fields have been using this method especially food processing and plastic manufacturing industry. Early 1930s marked the first industrial usage of single-screw extruders to manufacture thermoplastic materials via extrusion method. Only in the 1940s the first commercially available twin-screw extruders came to the market. Extrusion requires a high viscosity to work properly, unlike casting process. The melt must hold its shape long enough for the heat transfer and solidification to take place as they exit the die.

Hence, for this process, melted thermoplastic polymer are ideally suited as they can retain their shape during the solidification on cooling when they exit the die (Francis, 2016; Mali, Gavali, Choudhari, Anekar, & Gavhane, 2019).

The equipment for HME generally consisted of an extruder, extruder auxiliary equipment, equipment for the downstream processing, and other monitoring tools that are used for evaluation of the performance and product quality. By forcing the polymeric components and active substances including any additives or plasticizers through an orifice or die under controlled temperature, pressure, feeding rate and screw speed, the polymer would be melted and formed into products of different shapes and sizes such as plastic bags, sheets and pipes. Fig. 6.4 shows the schematic diagram of an extrusion molding machine. Inside a stationary cylindrical barrel, the extruder is generally consisted of one or two rotating screws (corotating or counter rotating). Manufacturing of the barrel are often in sections, which are bolted or clamped together. Meanwhile, the shape of the extruded product is determined by the end-plate die which are connected to the end of the barrel (Mali et al., 2019; Mohammed, Boateng, Snowden, & Dennis, 2012).

Additionally, by dividing the process of flow into four sections, the theoretical approach for further understanding the melt extrusion process are as follows (Mali et al., 2019):

1. Extruder are fed through a hopper,
2. Mixing, grinding, particle size reduction, venting and kneading,
3. Flow through the die, and
4. From the die, extrusion is done before being processed further downstream.

Aforesaid, there are two types of extruders available for this process, namely single-screw and twin-screw extruder. The most widely used extrusion system in the world

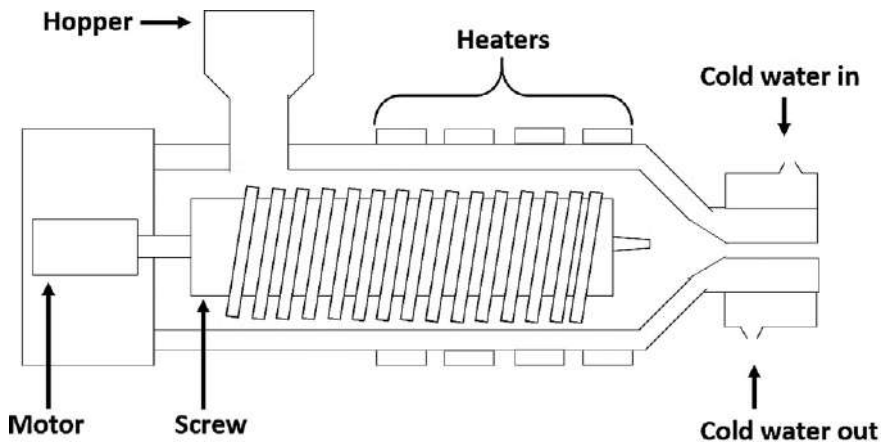

FIG. 6.4

Schematic diagram of extrusion molding machine (Dai & Fan, 2013).

is the single screw extruder as it is simpler and cheaper. Inside the barrel, there will be a single screw that is used for feeding, melting, devolatilizing, and pumping. Additionally, for less demanding applications, mixing can also be accomplished. Next, depending on the intended manufacturing process, the single screw extruders can either be flood or starve fed. This type of extruder can generate thousands of pounds of pressure while melting and mixing the viscous materials as it a continuous, high-pressure pump. As the most extruder screw is driven from the hopper end, the screw will become weak once it is reduced to less than 18 mm. Hence, solids transportation is far less reliable (Mali et al., 2019).

The extrusion process using a single screw extruder started when the unit is being fed with the polymer pellets or granules through the hopper. Then, the turning screw will be encountered by the pellets as it enters the extruder's body, where the flights would push the pellets forward. The pellets are then compacted and heated by both external heaters and internal processes (including friction and viscous dissipation) as they are pushed forward. The polymer pellets become molten and eventually filled up the entire space in the screw channel in the compression zone. The channel depth drops to accommodate the volume change. Next, inside the metering section (the last section), homogenization and pressurization would be occurred to the melt. Due to the constriction at the end of the extruder, pressure would be built and are used to push the molten polymer through the die. Although this system are simple, but it still does not attain a twin-screw machine mixing capability (Francis, 2016; Mohammed et al., 2012).

As for twin-screw extruders, as the name suggested, there are two side-by-side screws are used, and those screw can either be co-rotating or counter-rotating. Inside a barrel, the placement of the screw closely accommodates those two screws with a tight clearance between the flight tips and the barrel. Generally, the flights of one screw penetrate into the channels of the other as the design is based on intermeshing of the screws. As for the operating principles of this type of extruder, it is similar to the single-screw type, but more complex as the flow mechanisms are depending on the type of operation (co-rotating vs. counter-rotating) and specifics of the screw design. The advantages of twin-screw type are that the material feeding, and capacities dispersion is easier, there are less tendency of over heating and the transit times are also shorter. In addition, due to their modular designs, incorporation of a series of different screw elements or sections down the screw's length are possible (Francis, 2016; Mali et al., 2019).

6.2.2.2 Injection molding

One of the most important processes for mass production of objects from thermoplastics are injection molding, and generally this process does not require any additional finishing. In this process, basically, the thermoplastic polymer will be heated above its melting point, producing a molten fluid with reasonably low viscosity. Then, in order to obtain the desired final object, the melt is mechanically forced or injected into the mold in the shape of the desired product. Due to the molten polymer's low viscosity, complete filling of the mold is achievable, where the article resides until it

is cooled below the polymer's freezing point. Although this process principle is simple, but the practice of the injection molding is not. This is because the process consisted of the intricate behavior of plastic melts and process ability to incorporate complicated products. Also, the most important mechanisms in this process are heat transfer and pressure flow (Ebnesajjad, 2015).

Fig. 6.5 shows the schematic diagram of an injection molding apparatus. The process started with the feeding of plastic pellets into the screw from the feed hopper, and the to ensure that the plastic comes out of the screw are completely melted, deaired and dried, it is subjected to several heating zones. The plastic melt that comes out is in a viscous state compressed to 3000 kg/cm^2, and it comes out from the nozzle that are located at the other end of the screw. Then, for the melt to fill up the mold at the required speed, high pressure is applied, and to compensate for shrinkage, it might require extra melt. Two halves that are clamped together made up the mold cavity. One of the two halves of the mold is opened to eject the component when the component had been cooled with chilled water and the shape is set. Release agents are laid in the walls of the mold before the process started to avoid the object to stick to the mold. Typically, if good practice is followed in the manufacturing phase, components made via this method does not require finishing. Hence, large quantities of small components manufacturing are possible at reasonable cost (Ardebili, Zhang, & Pecht, 2018; Stefano, 2016). Fig. 6.6 illustrated the plastic injection molding cycle since this method is a cyclic operation because as the process cycle is repeated, parts are produced periodically (Francis, 2016). Meanwhile, in Table 6.8, the molding cycle process steps are summarized.

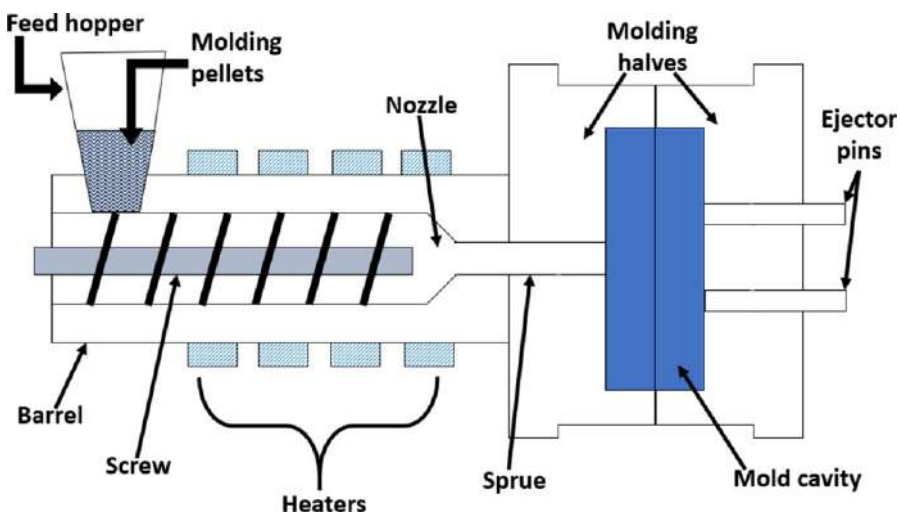

FIG. 6.5

Schematic diagram of an injection molding apparatus (Ardebili et al., 2018).

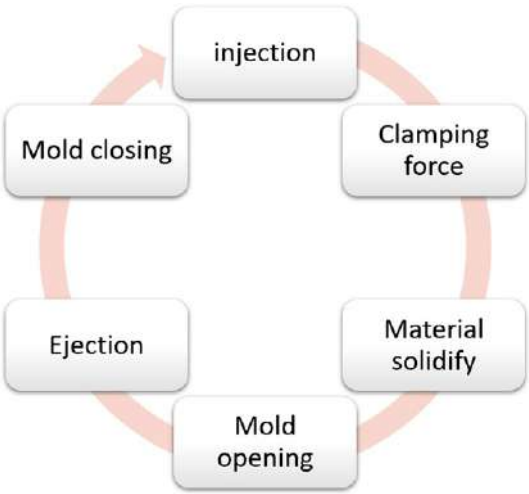

FIG. 6.6

Plastic injection molding cycle (Khan & Acharya, 2016).

Table 6.8 Steps in injection molding process (Francis, 2016).

Step	Injection unit	Mold	Clamp unit
Mold closing	The shot is prepared, screw rotating, check the valve is open	Closed	Closed
Injection	Screw, nonrotating, pushes forward, check valve is closed	Closed, mold is filling	Closed
Hold On	Screw pushes forward, check valve is closed	Closed, packing continues, the polymer is solidifying	Closed
Shot preparation and cooling	Screw retracts and begins rotating, check the valve is open	Closed, the polymer is solidified, cooling	Closed
Ejection	Screw continues rotating, check the valve is open	Opened, part ejected	Opened

6.2.2.3 Compression molding

Among the oldest materials processing techniques is the compression molding technique. The suitability of this method for the production of profiles with any thermoplastic and thermoset composites had been proven. In this method, using a two-part mold system, the molding material would be preheated first before placed in a heated, open mold cavity (female) or form (male). Then, top force is used to close

the mold, and to force the material into contact with all mold areas, pressure is applied. Then, until the molding material are cured, heat and pressure are maintained. Next, there are few matter that influenced the mechanical properties and dimensional stability of the compression molded composites namely the mold cavity's design, charge location and processing parameters such as the temperature of compound, mold cooling or heating rate, closing speeds and the filler loading (Dai & Fan, 2013; Dixit et al., 2016; Tatara, 2017).

The compression molding cycle execution is relatively straightforward, and the process can be divided into four distinct stages as shown in Fig. 6.7. First, the lower mold half would be filled with unreacted resin. During the time period heating up both mold halves, a force would then be applied to compact the charge. Heat is also drawn in by the pressurized charge, and the part begins to harden. Then, the part continues to cure within the third step as the pressure and temperature are maintained. The final step consisted of the part being released from the lower mold half as the mold is opened with the aid of an ejector pin. Generally, all compression molding consisted of the same sequence. But, to avoid from the deformation of the parts when ejected from the mold, those thermoplastic parts must be completely cooled first (Tatara, 2017).

By using this method, parts with great strength and durability are able to be produced, with or without reinforcement. Additionally, high-strength composite

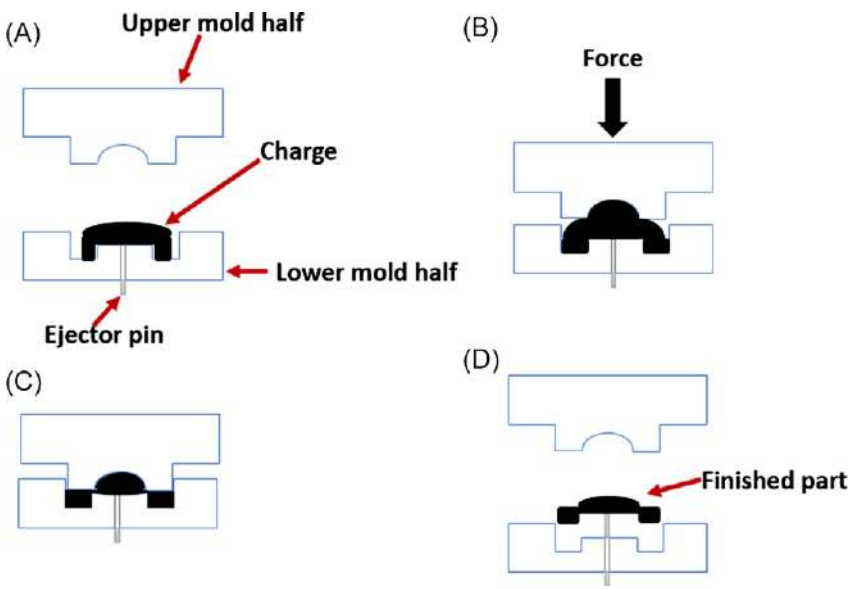

FIG. 6.7

Compression molding process in four-step simplified procedure (A) Loading of charge into mold, (B) Compaction of charge in heated mold, (C) Curing of part inside mold cavity, and (D) Removal of solidified part (Tatara, 2017).

structures and complex parts in a wide variety of sizes are able to be produced via this technique. Apart from that, this process requires only moderate press cost, tooling cost and cycle time, besides the presence of less automation (Dixit et al., 2016; Tatara, 2017).

6.2.2.4 Blow molding

The production of hollow three-dimensional objects, especially bottles for the food packaging sector usually used the blow molding technique. Basically, in this method, by inflating or blowing a thermoplastic molten tube called a "parison" in the shape of the mold cavity, the hollow object is formed. After blowing, the parison will take the shape of the mold, and retains the shape upon leaving the mold. In addition, there are three main thermoplastic processes that are covered under blow molding; extrusion blow molding (PP bottles that have hot-filling capability and good contact clarity are produced by this method), stretch blow molding (used to produce bi-axially oriented jars and bottles that had greater clarity, strength and barrier properties) and injection blow molding (relatively small bottles and wide-mouth jars are produced using this method). Among the three processes, extrusion is the most commonly used process, followed by stretch blow molding and injection blow molding (Belcher, 2017; Maddah, 2016; Stefano, 2016).

Next, blow molding has three key steps regardless of the type of materials used. First, parison or preform is made up using a controlled quantity of melt. Then, to increase the container volume and define the shape, the parison is forced against a mold. At the last step, in order to retain the shape, the molded object is cooled down. Next, in blow molding of polymers, to make the parison, there are two variants, namely extrusion blow molding and injection blow molding. Depending of the requirement of the final product, either extrusion-based process or injection molding-based process will be selected. As the extrusion blow molding process is the cheaper one of those two processes, containers and vessels that do not demand outstanding precision and properties are produced using this method. Meanwhile, more demanding container applications (e.g., carbonated beverage bottles) are produced using an injection blow molding process as it offers much better control over wall thickness and screw caps. Apart from that, that type of blow molding also stretch better mechanical and barrier properties (Francis, 2016). Table 6.9 lists the process comparison for extrusion, injection molding and blow molding techniques.

6.2.3 Performance of thermoplastic with cellulose reinforcement materials

Recently, among the scientific and industrial communities, polymer nanocomposites have received a great deal of interests as they can achieve significant improvements in mechanical properties, dimensional stability, and solvent or gas barrier properties with respect to the matrix polymer at very low concentration of fillers. Additionally, compared to unfilled polymer matrix counterpart, cellulose has a great potential to be used as fillers to increase the properties of composite materials. The improvement of

Table 6.9 Process comparison extrusion, injection molding and blow molding techniques (David, 2017).

	Extrusion	Injection molding	Blow molding
Type of process	Continuous	Cyclic	Cyclic
Type of product	Extruded profile	Complex but not hollow	Hollow
Design complexity	Low	High	Medium
Forming mechanism	Viscous flow	Viscous flow	Inflation
Forming pressure	Medium	High	Low
Cooling mechanism	Two-sided convection or conduction	Two-sided conduction	One-sided conduction
Cooling rate	Medium	High	Low
Dimensional variation	Medium	Low	High
Tooling cost	Low	High	Medium

the overall performance of the polymer nanocomposites can be obtained with incorporating nanosized cellulosic materials as nanofillers for the polymer fabrication. Depending on the source of lignocellulosic biomass, pretreatment and preparation process, the shape, size, surface morphology, yield and properties of the nanocellulose would vary. The important chemical properties of cellulose and the interesting phenomena of nanoscale materials are combined in the nanocelluloses. The properties of the polymer nanocomposites with cellulose nanofillers as reinforcement phase are depending on the polymer matrix, characteristics of the cellulosic nanofillers, and the interaction between them. Apart from that, the properties of a polymeric nanocomposites are very much dependent on the dispersion and distribution of nanomaterials in the continuous matrix phase for a specific nanoreinforcement phase and matrix polymer (Crews, Huntley, Cooley, Phillips, & Curry, 2016; dos Santos et al., 2016; Mondal, 2018). There are three main properties of the polymeric nanocomposites that had been affected by the incorporation of cellulose nanofillers, which are mechanical, thermal and barrier properties.

6.2.3.1 Mechanical properties

Nanomaterials dispersion and distribution in the polymer matrix, and interfacial interaction between the fillers and matrix are important to improve the mechanical properties of nanocellulose polymer nanocomposites. Those are important to enable the matrix to effectively transfer the applied load to the strong nanoreinforcement

phase. Due to the stiffening effect of cellulosic nanomaterials at low concentration due to their large specific surface area, the mechanical properties of the nanocomposites are able to be improved. Large surface area contributes to the better interfacial interaction between the nanocellulose and polymer matric when the nanofillers' dispersion and distribution in the matrices in uniform. Hence, the mechanical properties of the nanocomposites will lie between the properties of nanocellulose and polymer matrix when the aforesaid parameters are in good condition (Mondal, 2018).

In a study by Cao, Dong and Li, by adding CNC into polyurethane (PU) nanocomposite films obtained by casting, both Young's modulus and tensile strength had shown a significant increase. Until the CNC content reach 10 wt%, the Young's modulus is exponentially increasing relative to the amount of nanocrystal added. Apart from that, when the NCC concentration increased from 0 wt% to 30 wt%, the tensile strength increased from 4.3 to 14.9 MPa. From this study, the researchers came to conclusion that due to the strong interactions between the matrix and the CNC, it has restricted the movement of the polymer matrix's chains, hence hindering its deformation, which produced those results. Next, Gong et al. also had conducted a study where the systems are obtained via extrusion of poly (vinyl acetate) reinforced with cellulose nanofibrils that are isolated from the wood of coniferous tree. An increase of 20% in tensile strength and 59% in the Young's modulus of the nanocomposites relative to the values of these properties found in polymer matrix processed without nanofiller, are found when 10 wt% of cellulose nanofibers are added. Based on those studies, the addition of nanocellulose as nanofillers not only improved the material's tensile strength and Young's modulus, but also affecting their elongation (dos Santos et al., 2016). However, the improvement would only be until certain loading of nanofiller in the polymer matrix. This is because, due to the agglomeration of nanocellulose in the polymer matrices with further increase of filler content, the mechanical properties would start to decline. As a result of mechanical failure of the polymer nanocomposites, the aggregation of nanofillers in the nanocomposite domain structure can promote local concentrations of stress (Mondal, 2018).

6.2.3.2 Thermal properties

From the application point of view, thermal property of the nanocellulose polymer nanocomposite is very crucial. The characterization of the thermal properties can be shown by melting temperature (T_m), glass transition temperature (T_g), crystallization temperature and the thermal degradation property's measurement. Apart from that, there are studies that proved that with the addition of cellulose nanofillers, thermal stability of polymer nanocomposites increased. For instance, in a study by Qua et al., compared to that of a pure matrix, the thermal stability of nanocomposites, based on polyvinyl alcohol (PVA) with both MCC and flax nanofibers showed an increment. Initially, due to a loss of moisture, the weight loss at 75°C occurred in all samples, and the rate of weight loss is similar until the temperature reached 217°C. The material decomposition rate above this temperature showed substantial decrease in the presence of cellulose nanofibers, and maximum difference of 70°C is reached, relative to the decomposition temperature of PVA without reinforcement. Addition of

cellulose nanofibers and their homogeneous distribution in the polymer matrix had caused restricted mobility to the polymer chains which contributed to the result (dos Santos et al., 2016; Mondal, 2018).

Also, due to the strong hydrogen bond formation between PVA matrices and nanocellulose, the T_g of nanocellulose reinforced PVA nanocomposites increased. The segmental mobility of the polymer chains is restricted by the strong hydrogen bonding, hence increasing the T_g. Also, as the nanocellulose filler loading increased, the thermal degradation properties of the nanocomposite's films would also increase. This was shown in a study conducted by Lee et al. using a nanocellulose reinforced PVA based nanocomposite. Strong hydrogen bonding between PVA matrix and nanocellulose reinforcing phase had made this possible (Mondal, 2018).

Next, in a study by Yu, Qin and Zhou, when cellulose nanocrystals are added into films of poly(3-hydroxybutyrate-*co*-3-hydroxyvalerate) (PHBV), there are increment on T_m. For the film with 5 wt% of CNC, the increment is from 130°C to 156°C while for the film with 10 wt% of CNC, T_m increased to 168°C. They concluded that the presence of the cellulose nanofiller had enhanced the crystalline perfection of the nanocomposites of PHBV/CNC (dos Santos et al., 2016).

6.2.3.3 Barrier properties

To achieve poor permeability of the nanocellulose polymer nanocomposite, the tortuosity path for the diffusing molecules are to be increased, which can be done by the nanocellulose crystalline nature and its ability to form a percolating network with matrix by hydrogen bonding. The cellulose nanofiller would reduce the chain segmental mobility when the nanocellulose are well dispersed and distributed, besides strong interfacial interaction between nanofiller/polymer. When that occurred, it would further decrease the penetrant diffusivity. In a study by Khan et al., it is shown that there are 26% reduction of water vapor permeability in a methyl cellulose (MC) film with 1% of nanocellulose. This happened as the penetrating molecules are slower in diffusion when the tortuosity in the MC-based films increased as there are less permeable nanofillers present (Mondal, 2018). It can be concluded that slower diffusion of water, hence lower permeability is related to the presence of crystalline fibers. Also, when the nanofiller is less permeable and have both good dispersion in the matrix and high aspect ratio, the barrier properties would be enhanced (dos Santos et al., 2016).

6.3 Summary

Throughout the chapter, thermoplastic and few examples of the thermoplastics had been defined and elaborated in detail. For the thermoplastics, their basic information such as properties are discussed. Additionally, the extraction methods to obtain the cellulose nanomaterials or nanofillers are also explained. Then, the processing techniques for thermoplastic reinforced with cellulose are also discussed. Lastly, the performance of the thermoplastic or polymeric nanocomposites reinforced with

nanocellulose are explained in terms of their mechanical, thermal and barrier properties. From this chapter, it can be concluded that the great property of cellulose helps in improving the polymeric nanocomposites' properties, and more researches should be done in order to further enhance the incorporation of cellulose as nanofiller in every aspect (extraction, processing, etc.).

References

Antimo, G., Shaffiq, J., & Mohini, S. (2019). Review on modification strategies of polyethylene/polypropylene immiscible thermoplastic polymer blends for enhancing their mechanical behavior. *Journal of Elastomers & Plastics*, 291–336. https://doi.org/10.1177/0095244318783806.

Ardebili, H., Zhang, J., & Pecht, M. G. (2018). Injection molding. In *Encapsulation technologies for electronic applications* (pp. 183–194). Elsevier. https://doi.org/10.1016/B978-0-12-811978-5.00004-3.

Belcher, S. L. (2017). Blow molding. In *Applied plastics engineering handbook: processing, materials, and applications* (2nd ed., pp. 265–289). Elsevier Inc. https://doi.org/10.1016/B978-0-323-39040-8.00013-4.

Crews, K., Huntley, C., Cooley, D., Phillips, B., & Curry, M. (2016). Influence of cellulose on the mechanical and thermal stability of ABS plastic composites. *International Journal of Polymer Science*, *2016*. https://doi.org/10.1155/2016/9043086.

Dai, D., & Fan, M. (2013). Wood fibres as reinforcements in natural fibre composites: Structure, properties, processing and applications. In *Natural fibre composites: materials, processes and applications* (pp. 3–65). Elsevier Inc. https://doi.org/10.1533/9780857099228.1.3.

David, K. (2017). Design of plastic parts. *Applied Plastics Engineering Handbook* (2nd ed., pp. 593–615). Elsevier BV.

Dhinakaran, V., Surendar, K. V., Riyaz, M. S. H., & Ravichandran, M. (2020). Review on study of thermosetting and thermoplastic materials in the automated fiber placement process. *Materials Today: Proceedings*, *27*, 812–815. Elsevier Ltd https://doi.org/10.1016/j.matpr.2019.12.355.

Dixit, D., Pal, R., Kapoor, G., & Stabenau, M. (2016). Lightweight composite materials processing. In *Lightweight ballistic composites: military and law-enforcement applications* (*2nd ed.*, pp. 157–216). Elsevier Inc. https://doi.org/10.1016/B978-0-08-100406-7.00006-4.

dos Santos, F. A., Iulianelli, G. C. V., & Tavares, M. I. B. (2016). The use of cellulose nanofillers in obtaining polymer nanocomposites: Properties, processing, and applications. *Materials Sciences and Applications*, 257–294. https://doi.org/10.4236/msa.2016.75026.

Ebnesajjad, S. (2015). Injection molding. In *Vol. 2. Melt processible fluoropolymers—the definitive user's guide and data book* (pp. 236–281). https://doi.org/10.1016/B978-1-4557-3197-8.00010-9.

Francis, L. F. (2016). Melt process. In *Materials processing* (pp. 105–249). Elsevier BV. https://doi.org/10.1016/b978-0-12-385132-1.00003-3.

Hanieh, K., Michael, I., Ishak, A., Sabu, T., & Alain, D. (2017). *Methods for extraction of nanocellulose from various sources* (pp. 1–49). Wiley. https://doi.org/10.1002/9783527689972.ch1.

Jayamani, E., Hamdan, S., Rahman, M., & Bakri, M. (2015). Study of sound absorption coefficients and characterization of rice straw stem fibers reinforced polypropylene composites. BioResources, 10(2), 3378–3392. Retrieved from https://ojs.cnr.ncsu.edu/index.php/BioRes/article/view/6684.

Jordan, J. L., Casem, D. T., Bradley, J. M., Dwivedi, A. K., Brown, E. N., & Jordan, C. W. (2016). Mechanical properties of low density polyethylene. *Journal of Dynamic Behavior of Materials*, *2*(4), 411–420. https://doi.org/10.1007/s40870-016-0076-0.

Kausar, A. (2018). A review of filled and pristine polycarbonate blends and their applications. *Journal of Plastic Film & Sheeting*, *34*(1), 60–97. https://doi.org/10.1177/8756087917691088.

Khan, R. M., & Acharya, G. (2016). Plastic injection molding process and its aspects for quality: A review. *European Journal of Advances in Engineering and Technology*, *3*(4), 66–70. http://www.ejaet.com/PDF/3-4/EJAET-3-4-66-70.pdf.

Khanam, P. N., & AlMaadeed, M. A. A. (2015). Processing and characterization of polyethylene-based composites. *Advanced Manufacturing: Polymer and Composites Science*, *1*(2), 63–79. https://doi.org/10.1179/2055035915Y.0000000002.

Khui, P. L. N., Rahman, M. R., Jayamani, E., Bakri, M. K. B., & Khan, A. (2021). Electrical properties in reinforced polymer composites. In M. R. Rahman (Ed.), *Advances in Sustainable Polymer Composites* (pp. 131–140). Elsevier B.V. https://doi.org/10.1016/B978-0-12-820338-5.00006-0.

Maddah, H. A. (2016). Polypropylene as a promising plastic: A review. *American Journal of Polymer Science*, *6*(1), 1–11. https://doi.org/10.5923/j.ajps.20160601.01.

Mali, A. S., Gavali, K. V., Choudhari, R. G., Anekar, V. P., & Gavhane, Y. N. (2019). Review on hot melt extrusion technology and it's application. *International Journal of Scientific Research in Science and Technology*, 253–260. https://doi.org/10.32628/ijsrst196653.

Mohammed, M., Boateng, J. S., Snowden, M. J., & Dennis, D. (2012). A review of hot-melt extrusion: Process technology to pharmaceutical products. *ISRN Pharmaceutics*, 1–9. https://doi.org/10.5402/2012/436763.

Mondal, S. (2018). Review on nanocellulose polymer nanocomposites. *Polymer - Plastics Technology and Engineering*, *57*(13), 1377–1391. https://doi.org/10.1080/03602559.2017.1381253.

Olivera, S., Muralidhara, H. B., Venkatesh, K., Gopalakrishna, K., & Vivek, C. S. (2016). Plating on acrylonitrile–butadiene–styrene (ABS) plastic: A review. *Journal of Materials Science*, *51*(8), 3657–3674. https://doi.org/10.1007/s10853-015-9668-7.

Pérez-Pacheco, E., Canto-Pinto, J. C., Moo-Huchin, V. M., Estrada-Mota, I. A., Estrada-León, R. J., & Guerrero, L. (2016). Thermoplastic starch (TPS)- cellulosic fibers composites : Mechanical properties and water vapor barrier : A review. In *Composites from renewable and sustainable materials* (pp. 85–105). https://doi.org/10.5772/65397.

Rahman, M. R., & Bakri, M. K. B. (2021). Bamboo nanocellulose reinforced polylactic acid nanocomposites. In M. R. Rahman (Ed.), *Bamboo Polymer Nanocomposites*. *Engineering Materials*. Cham: Springer. https://doi.org/10.1007/978-3-030-68090-9_8.

Rahman, M., Adamu, M., Hamdan, S., et al. (2021). Optimization and characterization of acrylonitrile/MAPE/nano-clay bamboo nanocomposites by response surface methodology. *Polymer Bulletin*. https://doi.org/10.1007/s00289-021-03628-7.

Rahman, M. R., Hamdan, S., & Bakri, M. K. B. (2021). Investigation on the brittle and ductile behavior of bamboo nano fiber reinforced polypropylene nanocomposites. In M. R. Rahman (Ed.), *Bamboo Polymer Nanocomposites*. *Engineering Materials*. Cham: Springer. https://doi.org/10.1007/978-3-030-68090-9_5.

Rahman, M. R., Hamdan, S., Jayamani, E., et al. (2019). Tert-butyl catechol/alkaline-treated kenaf/jute polyethylene hybrid composites: Impact on physico-mechanical, thermal and morphological properties. *Polymer Bulletin*, *76*, 763–784. https://doi.org/10.1007/s00289-018-2404-0.

Rahman, M. R., Khui, P. L. N., & Bakri, M. K. B. (2021). Bamboo nanocomposites future development and applications. In M. R. Rahman (Ed.), *Bamboo Polymer Nanocomposites. Engineering Materials*. Cham: Springer. https://doi.org/10.1007/978-3-030-68090-9_9.

Sadat, K. F., Ehsan, S., Parizad, S. N., & Mahmoud, M. S. (2018). Modifications and research potentials of acrylonitrile/butadiene/styrene (ABS) membranes: A review. *Polymer Composites*, 2835–2846. https://doi.org/10.1002/pc.24276.

Shubhra, Q. T. H., Alam, A. K. M. M., & Quaiyyum, M. A. (2013). Mechanical properties of polypropylene composites: A review. *Journal of Thermoplastic Composite Materials*, *26* (3), 362–391. https://doi.org/10.1177/0892705711428659.

Stefano, F. (2016). Main manufacturing processes for food packaging materials. *Reference Module in Food Science*. Elsevier BV.

Tatara, R. A. (2017). Compression molding. In *Applied plastics engineering handbook: processing, materials, and applications* (2nd ed., pp. 291–320). Elsevier Inc. https://doi.org/10.1016/B978-0-323-39040-8.00014-6.

Zaaba, N. F., & Ismail, H. (2019). Thermoplastic/natural filler composites: A short review. *Journal of Physical Science*, *30*, 81–99. https://doi.org/10.21315/jps2019.30.s1.5.

CHAPTER

Cellulose reinforcement in thermoset composites

7

Muhammad Khusairy Bin Bakri[a], **Md Rezaur Rahman**[a], **and Mohammed Mahbubul Matin**[b]

[a]*Department of Chemical Engineering and Energy Sustainability, Faculty of Engineering, Universiti Malaysia Sarawak (UNIMAS), Kota Samarahan, Sarawak, Malaysia,* [b]*Department of Chemistry, Faculty of Science, University of Chittagong, Chattogram, Bangladesh*

Chapter outline

7.1 Introduction

Either as a filler or reinforcement for polymers, cellulose fibers are known to exhibits a significant contribution on the properties of the composites made. Due to extensive research, in the last decade, synthetic fiber reinforced polymer composites have been developed for applications involve high performance structural or nonstructural materials (Piggott, 1980; Rahman et al., 2019; Zadorecki, Karnerfors, & Lindenfors, 1986; Zadorecki & Michell, 1989). Due to the high cost production and maintenance of existing metallic components for certain application, especially those involve in the aircraft and automobile applications, this create many limitations,

Fundamentals and Recent Advances in Nanocomposites Based on Polymers and Nanocellulose.
https://doi.org/10.1016/B978-0-323-85771-0.00011-7

which pushes the used of composites to its potential (Dami, Kenichiro, Masayuki, & Kiyotaka, 2016; Ishikawa et al., 2018; Lee, Aitomäki, Berglund, Oksman, & Bismarck, 2014; Liu et al., 2019).

In the green composites' framework, low density and biodegradability properties, low cost production and maintenance, and renewable resource of origin is the key important aspects, which made most of the natural fibers such as cellulose are often regarded as ideal candidate reinforcement (Khalil, Bhat, & Yusra, 2012). It is also impossible to create total zero waste in this world, therefore, minimization of pollution toward ecofriendly environment can be done by filtering the generate waste from manufacturing, while attributes to the technical and economical adaptation, by applying the fundamental applications of green composites into real situation. The current uncertainty in world of economical and depletion of natural resources, such as oil and metal have paved the way for cheap and high-quality materials that can be utilized from bio-renewable resource (Banerjee et al., 2013). Natural cellulosic fibers, which is part or bio-renewable polymers, have been subjected for study from a variety of applications starting from biomedical to defense in both native and modified form (Ahmed, Sagir, Tahir, & Ullah, 2018; Banerjee et al., 2013; Rangel-Vázquez & Leal-García, 2010; Thakur, Thakur, & Gupta, 2013).

Generally, most of the polymers obtained from bio-renewable different resources are arbitrated as biobased polymers. Having its place to the distinct class of polymers, natural polymers found in nature such as natural fibers, starch, proteins, etc., which usually hold a well-defined structure (Dhakal, Zhang, Guthrie, MacMullen, & Bennett, 2013). People of earlier civilization for long back in many centuries ago have been using natural polymers-based materials, in which prove that is it not something new but innovated through time (Thakur et al., 2013). Polysaccharides are among these bio-renewable polymers, which are the most abundant natural polymers that are usually extracted from agricultural and biomass resources (Rani, Sen, Mishra, & Jha, 2012). These polymers are biodegradability, biocompatibility and antibacterial activity and bio-renewable resources (Rahman, Hamdan, & Bakri, 2021; Nyuk Khui et al., 2021; Bogoeva-Gaceva et al., 2007; Eichhorn et al., 2010; George, Sreekala, & Thomas, 2001; Rani et al., 2012; Rani, Mishra, & Sen, 2013). For composites applications involving polysaccharides such as natural fibers were usually used as reinforcing materials (Bajpai, Meena, Vatsa, & Singh, 2013). Therefore, on phenol formaldehyde, cellulose-based polyurethanes, cellulose-modified epoxy, etc., were further discussed in detail.

7.2 Phenol formaldehyde resins

The first thermosetting plastic discovered in early 20th century is called Bakelite that is used in electrical equipment, which trademarked phenolic plastics and revolutionized the market for molded and laminated parts (Handique & Baruah, 2002; Sami et al., 2014). It was widely used in molding and in laminated products due to its stability in heating environments and moisture resistant (Burmistr et al., 2014; Dami,

Kenichiro, Masayuki, & Kiyotaka, 2016; Liu, Li, Li, Zhang, & Zhang, 2014; Ullah et al., 2015; Ishikawa et al., 2018; Lee et al., 2014; Liu et al., 2019). Phenol formaldehyde resin is one type of thermosetting polymer, which can be used in various applications. High-performance mechanical and high-stability thermal, and highly chemical resistance properties is the biggest advantage of phenol formaldehyde, which protect it from micro-organism attacks. Phenol formaldehyde resin is synthetically been made form a reaction between both phenols, i.e., hydroxy benzene and formaldehyde by using a specific catalyst (Dabbagh & Shahraki, 2013).

Basically, phenol formaldehyde is used as an antiseptic for materials and as a binder to strengthen paper, which for longer periods, it protects the paper from microorganism attacks (Ahmed et al., 2018; Banerjee et al., 2013; Rangel-Vázquez & Leal-García, 2010; Thakur et al., 2013). Upon drying, Kraft paper becomes waterproof due to the impregnate hydrophobic nature of phenol formaldehyde to make evaporative cooling pads. This property also decreases the cooling efficiency. As it cured, especially incorporated into the fibers of the paper, it can protect it from microorganism activity and water dissociation (Ganeshram & Achudhan, 2013; Lenghaus, Qiao, & Solomon, 2001). Thus, it is vital for phenol formaldehyde resin unaffected by the hydrophilic nature of paper. It happened as the cellulosic fiber is exposed to water, as it was broken like a salt, which provided mechanical strength to the fibers for a longer time as it required. Therefore, decreased in its absorption ability may increase the mechanical strength of cellulosic paper (Alamri & Low, 2012). Wet strength is also defined as the ability of fiber that determines how long without breakage it can sustain water (Azwa, Yousif, Manalo, & Karunasena, 2013). Conclusively, without disturbing its absorbing ability while enhanced the mechanical strength, phenol formaldehyde may be the suitable agent for it.

Atta-Obeng, Via, Fasina, Auad, and Jiang, (2013) conducted a research by characterization and chemometric elucidation on cellulose reinforcement of phenol formaldehyde. For thermal and shear strength test, at loadings of 0, 3, 6, and 10 wt% in phenol formaldehyde (PF), the micro sized crystalline cellulose was uniformly dispersed. The cellulose PF matrix application is considered advantageous because composite strength increase allows petroleum-based PF reduction utilized while lower the overall formaldehyde concentrations (Atta-Obeng et al., 2013; El-Zawawy & Ibrahim, 2003; Graham & Nath, 2006; Wang et al., 2019). Regardless of cellulose loading, even in a very narrow temperature range, this system exhibit cure temperatures, which would assist in process changes during manufacturing as studies on characterization found prove it (Atta-Obeng et al., 2013). Nevertheless, almost all significant and the limiting factor is shown by viscosity, as it increases along cellulose loading (Atta-Obeng et al., 2013; Vineeth & Gadhave, 2019; Wei et al., 2017; Yang et al., 2019; Zhang et al., 2020). An interaction between cellulose and PF polymer optimized at 3% cellulose suggested the heat of reaction and nonlinear behavior in lap shear strength with cellulose loading (Atta-Obeng et al., 2013). By utilizing novel chemometric techniques, in FTIR spectra, the partition out of the variation, attributed to the cure bulk PF and cellulose interaction to PF (Atta-Obeng et al., 2013).

Wei et al. (2017) conducted research with different aspect ratio extracted from sisal fiber on mechanical properties of phenol/formaldehyde resin composites reinforced by cellulose microcrystal. Sisal cellulose fiber (SCF) and sisal fiber cellulose microcrystal (SFCM) were produced with the sulfate pulping method and ball milled. Both of this was in-situ polymerized and dispersed into phenol/formaldehyde (PF) resin to manufacture SCF/PF and SFCM/PF composites via rolling and molding method. The effect of SCF and SFCM on the impact, flexural, and dynamic mechanical properties of the SCF/PF and SFCM/PF composites were investigated (Wei et al., 2017). Results show that under the same content condition, SFCM could enhance these properties resulting better dispersion in a resin matrix than SCF. Particularly, 7% SFCM content provides more impact strength and equilibrium relaxation modulus on the SFCM/PF composite, which increased by 26.5% and 37.7%, while the creep deformation was decreased by 26.5% when compared with SCF (Wei et al., 2017). In addition, 5% SFCM content flexural strength, initial storage modulus and glass transition temperature of SFCM/PF composite were increased by 8.5%, 22.6%, and 13°C, respectively (Wei et al., 2017).

Cong et al. (Cong, Yang, Siqun, Yujie, & Omid, 2014) research on micromechanical properties of the interphase in cellulose nanofiber-reinforced phenol formaldehyde bondlines. In this study, cellulose nanocrystals (CNC), lab-processed commercial cellulose nanofibrils (CNF-C), and cellulose nanofibrils (CNF-L) were used as reinforced materials in phenol formaldehyde (PF) resin (Cong et al., 2014). By nanoindentation, mechanical modification of adhesives and the cell wall layers by the three types of cellulose particles was investigated. Based on the results, it showed that the mechanical properties of both adhesives and the cell wall structure of cellulose nanomaterials are improved. Within the glue line, CNF-C had the most obvious reinforcing effect on the elastic modulus (Er) and hardness. Respectively, with modification, the Er and hardness reached 13.0 and 0.436 GPa, in the second layer far from the glue line. In comparison, the control sample had an Er and hardness of 7.31 and 0.256 GPa, respectively (Cong et al., 2014).

7.3 Cellulose-based polyurethanes

In the wastewater treatment, from wood waste, polyurethane synthesized with cellulose are a potential material to be used. Silva, Takahashi, Chaussy, Belgacem, and Silva (2010) conducted research on composites of rigid polyurethane foam and cellulose fiber residue. Acts as a filler, this rigid polyurethane composite foams were prepared with cellulose fibers. The cellulose fibers used are an industrial residue taken from blanched cellulose pulp production. The cellulose fiber concentration influence of the foams on the mechanical, structural, thermal, and morphological properties was investigated by placing a suspension of known fungus in contact with the surface of the foam and following the morphological evolution as a function of time (for 60 days), the cellulose fibers influence on the foam resistance to fungal attack (Silva et al., 2010). The increased of cellulose filler concentration in the

foams, with respect to the polyol up to 16% w/w causes decrease in cell size, constant thermo oxidative stability and mechanical properties, decrease in the thermal conductivity and fungal growth (Silva et al., 2010). Therefore, as a filler, such as a cellulosic fibrous residue from industry is rationally valorized into classical rigid polyurethane foams, whereas in a wet environment, these materials may yield with mechanical resistance and a susceptibility to fungi (Silva et al., 2010).

Góes et al. (2016) conducted a study on polyurethane foams synthesized from cellulose-based wastes through kinetics studies of dye adsorption. Without cellulose polyurethane foam, unmodified cellulose, and chemically modified cellulose at molar ratios of 1OH:1NCO (cellulose 1:1) and 3OH:1NCO (cellulose 3:1) 4,4′-diphenylmethane diisocyanate (MDI) were fabricated and the adsorption processes efficiency for the Procion Yellow HE-4R, Procion Red HE-7B, and Methylene Blue dyes from the adsorption kinetic data was evaluated (Góes et al., 2016). Maceration process to extract wood waste cellulose and the reaction between cellulose and MDI was effective as nuclear magnetic resonance 13C (NMR 13C) and Fourier transformed infra-red (FTIR) analysis confirmed it. The adsorption kinetic studies showed highest efficiency removal of dyes it at approximately 240 min for Procion Red and Procion Yellow at pH 5 and 420 min for Methylene Blue at pH 7 (Góes et al., 2016). It was possible to achieve approximately 70% of the efficient dye removal. Kinetic studies revealed the adsorption data of Procion Yellow HE-4R, Procion Red HE-7B and Methylene Blue dyes on foams are best fitted by the model of pseudo-second order ($r2 > 0{,}971$). The maximum adsorption capacity (Qe) values obtained by pseudo-second order approved with experimental values. The adsorption process rate is controlled by chemisorption, whereas described as the intraparticle diffusion model, based on the adsorption mechanism.

Ekebafe, Olugbemide, and Akpa (2017) studied biodegradation of cellulose based polyurethane foams. Sugar bagasse cellulose microfibers were isolated, while from polyols, polyurethane foams were made containing 25 mL liquid cellulose. The results shown that the foams under anaerobic conditions biodegraded. After biological exposure, as observed, the foams changed in the tensile strength and weight loss. During the biodegradation, the liquid cellulose and the composition of the foams used to play a significant role in its yield to microbial attack.

In wood construction industry, cellulose nanofibrils (CNF) modified polyurethane foam (PUF) has great potential as a structural insulated material. Leng and Pan (2019) investigated the thermal Insulating and mechanical properties of cellulose nanofibrils modified polyurethane foam composite as structural insulated material. PUF modified with spray-dried CNF was fabricated, while the mechanical and physical performance were studied. Results showed that CNF foam microstructure upon foaming increases the precursor viscosity and imposing resistant strength (Leng & Pan, 2019). During the foaming process, the high mechanical CNF strength provided an extra force resistant against cell expansion and formed smaller cells, which reduced the defective cells. The mechanical foam performance of the composite is improved as CNF introduces into the PUF matrix. Compared with the controlled PUF, the specific bending, tensile strength, and compression strength, the

CNF modified PUF increased up to three-fold (Leng & Pan, 2019). The closed cell size influenced the thermal conductivity of PUF composite, while the introduction of CNF improved thermal insulating performance, with a decreased thermal conductivity from 0.0439 to 0.02724 W/mK.

Kosmela, Hejna, Formela, Haponiuk, and Piszczyk (2018) studied on the application of biopolyols obtained by cellulose biomass liquefaction performed with crude glycerol for the synthesis of rigid polyurethane foams. To obtained rigid polyurethane foams (PUR), in the presence of crude glycerol, 0–70 wt% of petrochemical polyol with bio-polyol obtained were replaced via cellulose liquefaction. The different content of foams of bio-polyol were prepared by single step method of 1.5 equals ratios of NCO/OH. The foams produced with by the biomass-based polyols shown slightly increased apparent density and enhanced compressive strength, due to the differences in chemical structure connected by bio-polyols and petrochemical polyols (Kosmela et al., 2018). The morphological study on the surface of rigid polyurethane foams showed decrease in cell size with the addition of bio-polyol and changed in cell aspect ratio and cell roundness. The petrochemical polyol replacement by bio-polyol resulted in lowering of thermal stability of foams.

Ikhwan, Ilmiati, Adi, and Arumsari (2017) discussed on novel route of synthesizes cellulose fiber-based hybrid polyurethane. Polyurethanes are obtained by the reaction of a diisocyanate compound with bifunctional or multifunctional reagent such as diols or polyols. To build polyurethanes, the wide range modifier such as chemical structures and molecular weight led to the materials designs, which meet the functional product demand that promoting these materials in market (Ikhwan et al., 2017). Cellulose fiber, as a biomass material mostly contained abundant hydroxyl, a promising material which acts as a chain extender for building hybrid polyurethanes. In the past, cellulose fiber was used as filler in the synthesis of polyurethane composites, however newly reported there is a route of hybrid polyurethane synthesis, which a cellulose fiber used potentially as a chain extender. To obtained prepolyurethane, with variation of molecular weight, the reacting 4,4′-Methylenebis (cyclohexyl isocyanate) (HMDI) and polyethylene glycol is continued by adding variation types and composition mixture of microfiber cellulose (MFC) (Ikhwan et al., 2017). Based on the results obtained, STA showed hybrid polyurethane has good thermal stability, NMR and FTIR confirmed the reaction of the hybrid polyurethane, and SEM showed good distribution and dispersion of sorghum-based MFC (Ikhwan et al., 2017).

7.4 Cellulose-modified epoxy resins

Many applications nowadays used cellulose, which are modified for epoxy applications. Leelachai et al. (2017) studied on the effect of cellulose functionalization on thermal and mechanical properties of epoxy resin. Cured cycloaliphatic polyamine, diglyceryl ether of bisphenol A (DGEBA) was modified with functionalized celluloses. Three different types of surface-modified cellulose investigated and used as reinforcing agents in epoxy resins; carboxymethyl cellulose (CMC),

polyacrylamide-g-cellulose (PGC), and aminopropoxysilane-g-cellulose (SGC) (Leelachai et al., 2017). This modified epoxy storage modulus was found to increase with the addition of up to 1 wt% cellulose content of cellulose fillers. An improved fracture toughness (K_{IC}) with increasing cellulose loading content with PGC and SGC was also observed. Among the surface-modified celluloses, at 1.0 wt% cellulose addition, epoxy modified with SGC was found to have the highest fracture toughness followed by PGC and CMC, which is due to the chemical surface compatibility. In respond on the toughening mechanisms of the cellulose/epoxy composites, morphological images revealed that fiber-debonding, fiber-bridging, and fiber-pull out were responsible for increased toughness (Leelachai et al., 2017).

Hsu, Huang, Asoh, and Uyama (2020) prepared anhydride-cured epoxy resin reinforcing with citric acid-modified cellulose. To increase the adhesion between cellulose and epoxy resin, CAC was prepared from carboxyl functionalization with citric acid. The epoxy resin composites were prepared by using cellulose or CAC as filler, 4-methylcyclohexane-1,2-dicarboxylic anhydride (MHHPA) as curing agent and 2,2-bis (4-glycidyloxyphenyl) propane (BADGE) as the component (Hsu et al., 2020). The tensile strength of cellulose/epoxy resin composites obtained decreases, as the content of cellulose increases. However, compared with tensile strength of CAC/epoxy resin composites, it increased with the content of CAC. Moreover, compared with both cellulose/epoxy resin and pure epoxy resins composites, the Young's modulus and the toughness of CAC/epoxy resin composites increased with the present of 10 wt% CAC (Hsu et al., 2020). Morphological images showed in epoxy resin cellulose agglomerated, which in contrast, CAC dispersed uniformly. This determined that the adhesion between epoxy resins and CAC improved and contributed to high performance mechanical properties, as after introducing carboxyl groups to cellulose. To decrease the usage of toxic curing agent, CAC can also be used partially to replace methyl hexahydro phthalic anhydride (MHHPA). In addition, the mechanical properties of CAC/epoxy resin composites increased with lower MHHPA content. Therefore, CAC partially can be used as replacement for conventional curing agent in composite preparation, which may further decrease the production cost and improve the mechanical properties of product (Hsu et al., 2020).

Nair, Dartiailh, Levin, and Yan (2019) fabricated highly toughened and transparent bio-based epoxy composites reinforced with cellulose nanofibril (CNF). The addition of 18–23 wt% CNFs to epoxy increased the strength, strain, and modulus of the composites. For the composites compared to the neat epoxy, the addition of fibrils also led to an increase in strain energy density or modulus of toughness by almost 184 times. It is also observed that the addition of CNFs did not affect the high thermal stability of epoxy. However, the presence of nanofibrils provided strong reinforce effect in both glassy and glass transition region of the composites. The addition of CNFs decreased the intensity of tan δ peak epoxy matrix during the phase transition, which indicate high interaction between fibrils and epoxy (Nair et al., 2019). The water vapor permeability of the neat epoxy resin by more than 50% decreases showed the presence of highly crystalline and high aspect ratio CNFs at 23 wt% content.

7.5 Miscellaneous

7.5.1 Vulcanized rubber

Vulcanization scaled down rubber to a smaller size, without altering or deforming its shape deforming. In addition, its shape is retained, which protects the rubber from future deformation. Visakh, Thomas, Oksman, and Mathew (2012) studied the effect of cellulose nanofibers isolated from bamboo pulp residue on vulcanized natural rubber. Using two bioresources, cellulose nanofibers (CNFs) extracted from bamboo paper-pulp waste as the reinforcing phase and natural rubber (NR) as the matrix phase, nanocomposites were prepared. Up to 50 nm diameters size of CNFs were isolated from bamboo pulp waste, while through two-roll mill mixing of solid natural rubber with a master batch containing 20 wt% CNFs, nanocomposites with 5% and 10% CNFs were obtained (Visakh et al., 2012). By using sulfur vulcanization, the NR phase was cross-linked. The morphology dispersion of CNF in NR matrix was not optimal, and visible aggregates were shown on the fracture surface. With the addition of CNFs, at 50% elongation, the tensile strength and modulus increased for the nanocomposites, while decrease in elongation at break, moderately. Upon nanofiber addition, the natural rubber storage modulus increased above its glass-rubber transition temperature (Visakh et al., 2012). The CNFs addition impacted on the thermal stability of natural rubber. For the nanocomposites, the susceptibility to organic solvents decreased, as compared to crosslinked NR, which indicated in the NR matrix, polymer chain mobility restriction in the nanosized CNFs vicinity (Visakh et al., 2012).

The sulfur-vulcanized natural rubber using cellulose nanofibers (CNFs) reinforcement was investigated by Kato, Nakatsubo, Abe, and Yano (2015). *cis*-1,4-Polyisoprene natural rubber becomes stretchable after vulcanization. Using sulfur and unsaturated fatty acids (oleic acid), via crosslinking, vulcanization was performed with the polyisoprene double bonds, incorporated on the CNF surfaces, which resulted in highly efficient of CNFs reinforcement (Kato et al., 2015). While retaining 300% strain to failure rate, the Young's modulus of rubber reinforced with 5 wt% oleoyl was 27.7 MPa, which is 15 times higher than that of neat rubber. Meanwhile, for natural rubber, after the addition of 5 wt% oleoyl CNFs, the thermal expansion coefficient of 226.1 ppm K^{-1} was reduced to 18.6 ppm K^{-1} (Kato et al., 2015).

Srirachya, Boonkerd, Nakajima, and Kobayashi (2018) successfully fabricated bio-composite hydrogels which consist of cellulose and vulcanized natural rubber (VNR) by phase inversion. At 10, 15 and 20 wt% VNR loading level, the cellulose and VNR hydrogel preparation was performed by mixing a cellulose solution in 6 wt% lithium chloride in *N*, *N*-dimethylacetamide with VNR in toluene (Srirachya et al., 2018), in which later the solution was exposed to ethanol vapor for a day. At 10–20 wt% VNR, the cellulose-VNR composites showed an excellent reinforcement, with its high elasticity and mechanical properties, while the composite hydrogels retained a high amount of water, which is about 870%–2400% (Srirachya et al., 2018). The nanosized morphology of hydrogels composite indicated the rough

aggregate VNR found in the cellulose medium, which is formed through interconnection layer between both cellulose and VNR components. This is also indicated that the VNR was surrounded with fibrous cellulose medium. The hydrophobic VNR and hydrophilic cellulose interconnection between domains at higher VNR-loading levels improved the hydrogel's bio-composite elasticity and mechanical properties (Srirachya et al., 2018).

Nunes and Mano (1995) investigated the influence of cellulose as a filler in vulcanized rubber composites by using copolymers of styrene-butadiene rubber (SBR) and acrylonitrile-butadiene rubber (NBR) as well as natural rubber (NR), which were compounded with regenerated cellulose (Cellulose II). The incorporation of filler technique used for was based on the mixture of coprecipitation rubber latex-cellulose xanthate (Nunes & Mano, 1995). While, the cellulose filler used is in the range of 0 to 30 phr, the results based on the natural rubber-regenerated cellulose systems showed that the reinforcement mechanism for NR compositions, which involves an induced crystallizing rubber (NR) seems to be different from the mechanism for SBR and NBR (Nunes & Mano, 1995).

7.5.2 Polyimides

Polyimide (PI) is an imide monomers polymer, which have been in mass production since 1955. Polyimides have diverse roles of application demands due to its rugged organic materials and high heat-resistance, i.e., high temperature fuel cells, displays, and various military roles. Lee et al. (Dami et al., 2016; Ishikawa et al., 2018; Lee et al., 2014; Liu et al., 2019) studied the modified cellulose nanocrystals (AF-CNCs) with (3-aminopropyl) triethoxysilane (APTES) by preparing poly (amic acid)/AF-CNC nanocomposite films via spin coating. The films were thermally imidized after spin coating to convert poly (amic acid) into polyimide (PI). With an increasing content of 0–3 wt% AF-CNC, PI/AF-CNC nanocomposite films tensile modulus and storage modulus increased without a decrease in their optical transmittance (Lee, Kim, & Ha, 2017). The PI/AF-CNC nanocomposite films water vapor transmission rate and tan δ peak height decrease with increasing of 0–3 wt% AF-CNC content. As compared, 2 wt% PI/AF-CNC nanocomposite films show better mechanical and physical properties than 2 wt% PI/CNC nanocomposite films (Lee et al., 2017).

In battery applications, Wang et al. (Atta-Obeng et al., 2013; El-Zawawy & Ibrahim, 2003; Graham & Nath, 2006; Wang et al., 2019) showed that for lithium-ion batteries, the antimony-based electrodes have potential to be used as fast charging anodes because of its operating potential, which is about 0.8 V vs. Li/Li+, even though it is far away from the plating potential of Li. Yet, due to large volume expansion, the capacity decayed faster, which the issue has often been addressed by the used of nano-sized materials. For high rate applications, an ion-dipole is utilized for the interaction between carboxymethyl cellulose and polyimide, which suppresses and holds particle cracking together, to enable antimony anodes utilized the micron-sized Sb particles (Wang et al., 2018). With excellent cycle performance, 9.4% polyimide coated Sb anode exhibits a high reversible capacity of 580 mAh g^{-1}

at 1 A g^{-1}. During the polyimide coating process, the electrode performance rate was further improved by adding 5% acetylene black, in which at a current rate of 20C (13.2 A g^{-1}), a highly reversible capacity of 380 mAh g^{-1} still can be obtained. Further verification by full-cell tests with LiFePO4 cathodes showed the Sb anodes excellent stability and high-rate capability (Wang et al., 2018).

Nguyen et al. (2016) derived cellulose nanocrystals from tunicates (t-CNC), which is used as reinforcing nanofiller for polyimide aerogels. Two sets of polyimide aerogels, 4,4′-oxydianiline (ODA) or 2,2′-dimethylbenzidine (DMBZ), and 3,3′,4,4′-biphenyltetracarboxylic acid dianhydride (BPDA) cross-linked with 1,3,5-tris(4-aminophenoxy) benzene (TAB), were also studied (Nguyen et al., 2016). With 0–13.33 wt% of the total solids being the carboxylic acid-functionalized t-CNC (t-CNC-COOH) filler, the total solids composition of the aerogels was kept constant at 7.5 t %, For the final materials, either 560 or 920 mmol/kg incorporated with t-CNC-COOH and carboxylic acid content in the polyimide aerogel networks improved the physical and mechanical properties (Nguyen et al., 2016). The t-CNC-COOH aerogel composites isothermal aging was also conducted at 150°C and 200°C for 24 h, where t-CNC-COOH/polyimide aerogels higher content showed reduced shrinkage during aging and less change in their density, which the effect of the t-CNC-COOH reinforcement in retaining the structural integrity of the aerogel further emphasized (Nguyen et al., 2016).

7.5.3 Cyanate esters

Chemical substances such as cyanate esters are usually fall under the phenolic OH group in which the hydrogen atom is substituted by a cyanide group. Therefore, an -OCN group is named a cyanate ester. In the production of resins, cyanate esters based on a bisphenol or novolac derivative are usually used. As matrix materials in composites, cyanate esters (CEs) are recognized for its high-temperature structural applications, excellent thermal and dimensional stability, low moisture absorption, resistance to micro-cracks, and low dielectric loss (Inamdar, Cherukattu, Anand, & Kandasubramanian, 2018). By virtue of the resulting two-phase morphology, thermoplastic toughening has paved the way to circumvent their innate brittle attribute, though the brittle nature of CEs curtails their effective utilization.

Ohashi, Kilbane, Heyl, and Ishida (2015) synthesized and characterized cyanate ester functionalize benzoxazine and its polymer. The differential scanning calorimetry (DSC) exhibits two clearly separated exotherm maxima, corresponding to cyanate ester trimerization and benzoxazine, respectively. Both Kissinger's and Ozawa's methods are used to determine the activation energies for cyanate ester trimerization and benzoxazine ring-opening polymerization (Ohashi et al., 2015). Through observation, both exothermic temperatures showed lower than those of the published values of benzoxazine and dicyanate ester blends (Ohashi et al., 2015).

7.5.4 Furan

Furan is a heterocyclic organic compound. It consisted of five-member of aromatic ring, with four carbon atoms and one oxygen. Chemical compounds containing such rings are also referred to as furans. While highly volatile liquid with a boiling point close to room temperature, Furan is also flammable and colorless. Tao, Song, and Chou (2012) studied the efficient conversion of cellulose into furans catalyzed by metal ions in ionic liquids. From the hydrolysis of microcrystalline cellulose (MCC) with metal ions in ionic liquids as catalyst under mild conditions, while 5-Hydroxymethylfurfural (HMF) and furfural, two of the most important intermediates derived from biomass, were produced. SO3H-functionalized ionic liquids exhibited better activity than nonfunctionalized ILs, while 1-(4-sulfonic acid) butyl-3-methylimidazolium hydrogen sulfate (IL-1) showed the highest catalytic activity than others (Tao et al., 2012). With a catalytic amount of these metal ions, the co-catalysis effect of Cr^{3+}, Mn^{2+}, Fe^{3+}, Fe^{2+}, Co^{2+} are better than other metal ions, while 10%–19% increase in MCC conversion and the selectivity's of products were improved.

Chen et al. (Chen, Chen, et al., 2018; Chen, Yang, et al., 2018) studied on the catalytic fast pyrolysis of cellulose to produce furan compounds with SAPO type catalysts. Furfural (FF) and 5-hydroxymethyl-furfural (HMF) are recognized as target high-value chemicals produced through catalytic fast pyrolysis (CFP) of biomass. SAPO type catalysts were introduced in the CFP of cellulose to promote the generation of furans. Results indicate that under the catalysis of SAPO type catalysts, the content of sugars decreases considerably as the formation of furans is promoted (Chen, Chen, et al., 2018; Chen, Yang, et al., 2018). For furan formation, AlCu-SAPO-34 and ZrCu-SAPO-18 performed best, in which their furans peak area percentage covered was at 56.94% and 63.86%, respectively. Furthermore, these two catalysts had more mild acidity, which is lower in density and strength that favored the formation of furans. The optimum operation temperature is at 500–600°C for SAPO catalysts. Due to the catalyst promotes direct conversion of oligosaccharides to furans, SAPO type catalysts may be favored in this process.

7.5.5 Vinyl ester

Vinyl ester is a resin produced by the esterification of an epoxy resin with methacrylic or acrylic acids. The "vinyl" groups referred to ester substituents that prone to polymerization. Alhuthali and Low (Alhuthali & Low, 2013) studied the effect of prolonged water absorption on the physical and mechanical properties of vinyl-ester composites reinforced with natural fibers. The modeling results revealed that the experimental data matched the data predicted by the Cox-Krenchel model, whereas prolonged exposure to water absorption caused a reduction in elastic modulus and strength of the composite.

Chen, Chen, et al. (2018) studied the transesterification reaction between cellulose and vinyl esters, which is regarded as a clean and facile strategy for the tunable

synthesis of cellulose esters. Under mild conditions, a series of cellulose esters with 0.58–3.0 degrees of substitution have been prepared without adding any external catalysts, while cellulose was dissolved in the 1,8-diazabicyclo[5.4.0]undec-7-ene (DBU)/DMSO/CO2 solvent system, followed by adding equimolar amounts of long chain fatty, branched, aromatic, and steric vinyl esters (Chen, Yang, et al., 2018). The optimization study of different reaction parameters like reaction time, temperature and amounts of substrates demonstrates that the reaction can proceed smoothly even at room temperature, which evidenced by a cellulose benzoate with a DS of 2.6 obtained, as the reaction is performed at 25°C in 4 h (Chen, Yang, et al., 2018). The DBU not only acts as a reagent for the CO_2-derivative dissolution of cellulose in DMSO, but also acts as an in situ organ catalyst for the subsequent transesterification reaction (Chen, Yang, et al., 2018).

7.6 Summary

In this research, thermoset polymer composites were investigated. Its shows that the thermoset composites were prolonged exposure to water absorption caused a reduction in elastic modulus and strength of the composite. Two-phase morphology shows that the thermoplastic toughening has paved the way to circumvent the thermoset composites attributed the brittleness, though the brittle nature of composites curtails their effective utilization.

Acknowledgment

The authors would like to acknowledge Universiti Malaysia Sarawak (UNIMAS) for the support.

References

Ahmed, W., Sagir, M., Tahir, M. S., & Ullah, S. (2018). Phenol formaldehyde resin for hydrophilic cellulose paper. In *Advances in sustainable and environmental hydrology, hydrogeology, hydrochemistry and water resources. CAJG 2018. Advances in science, technology & innovation (IEREK interdisciplinary series for sustainable development)* (pp. 89–92). https://doi.org/10.1007/978-3-030-01572-5_22.

Alamri, H., & Low, I. M. (2012). Mechanical properties and water absorption behaviour of recycled cellulose fibre reinforced epoxy composites. *Polymer Testing*, *31*(5), 620–628. https://doi.org/10.1016/j.polymertesting.2012.04.002.

Alhuthali, A., & Low, I. M. (2013). Mechanical properties of cellulose fibre reinforced vinylester composites in wet conditions. *Journal of Materials Science*, *48*(18), 6331–6340. https://doi.org/10.1007/s10853-013-7432-4.

Atta-Obeng, E., Via, B. K., Fasina, O., Auad, M. L., & Jiang, W. (2013). Cellulose reinforcement of phenol formaldehyde: Characterization and chemometric elucidation. *International Journal of Composite Materials*, *3*, 61–68. https://doi.org/10.5923/j.cmaterials.20130303.04.

Azwa, Z. N., Yousif, B. F., Manalo, A. C., & Karunasena, W. (2013). A review on the degradability of polymeric composites based on natural fibres. *Materials and Design*, *47*, 424–442. https://doi.org/10.1016/j.matdes.2012.11.025.

Bajpai, P. K., Meena, D., Vatsa, S., & Singh, I. (2013). Tensile behavior of nettle fiber composites exposed to various environments. *Journal of Natural Fibers*, *10*(3), 244–256. https://doi.org/10.1080/15440478.2013.791912.

Banerjee, C., Ghosh, S., Sen, G., Mishra, S., Shukla, P., & Bandopadhyay, R. (2013). Study of algal biomass harvesting using cationic guar gum from the natural plant source as flocculant. *Carbohydrate Polymers*, *92*(1), 675–681. https://doi.org/10.1016/j.carbpol.2012.09.022.

Bogoeva-Gaceva, G., Avella, M., Malinconico, M., Buzarovska, A., Grozdanov, A., Gentile, G., et al. (2007). Natural fiber eco-composites. *Polymer Composites*, *28*(1), 98–107. https://doi.org/10.1002/pc.20270.

Chen, X., Chen, Y., Chen, Z., Zhu, D., Yang, H., Liu, P., et al. (2018). Catalytic fast pyrolysis of cellulose to produce furan compounds with SAPO type catalysts. *Journal of Analytical and Applied Pyrolysis*, *129*, 53–60. https://doi.org/10.1016/j.jaap.2017.12.004.

Burmistr, M. V., Boiko, V. S., Lipko, E. O., Gerasimenko, K. O., Gomza, Y. P., Vesnin, R. L., et al. (2014). Antifriction and construction materials based on modified phenol-formaldehyde resins reinforced with mineral and synthetic fibrous fillers. *Mechanics of Composite Materials*, *50*(2), 213–222. https://doi.org/10.1007/s11029-014-9408-0.

Chen, H., Yang, F., Du, J., Xie, H., Zhang, L., Guo, Y., et al. (2018). Efficient transesterification reaction of cellulose with vinyl esters in DBU/DMSO/CO2 solvent system at low temperature. *Cellulose*, *25*(12), 6935–6945. https://doi.org/10.1007/s10570-018-2078-7.

Cong, L., Yang, Z., Siqun, W., Yujie, M., & Omid, H. (2014). Micromechanical properties of the interphase in cellulose nanofiber-reinforced phenol formaldehyde bondlines. *BioResources*. https://doi.org/10.15376/biores.9.3.5529-5541.

Dabbagh, H. A., & Shahraki, M. (2013). Mesoporous nano rod-like γ-alumina synthesis using phenol-formaldehyde resin as a template. *Microporous and Mesoporous Materials*, *175*, 8–15. https://doi.org/10.1016/j.micromeso.2013.03.011.

Dami, M., Kenichiro, T., Masayuki, S., & Kiyotaka, T. (2016). Effect of cellulose nanofibers composites in automotive components on greenhouse gas emissions. *Journal of the Japan Institute of Energy*, 648–652. https://doi.org/10.3775/jie.95.648.

Dhakal, H. N., Zhang, Z. Y., Guthrie, R., MacMullen, J., & Bennett, N. (2013). Development of flax/carbon fibre hybrid composites for enhanced properties. *Carbohydrate Polymers*, *96*(1), 1–8. https://doi.org/10.1016/j.carbpol.2013.03.074.

Eichhorn, S. J., Dufresne, A., Aranguren, M., Marcovich, N. E., Capadona, J. R., Rowan, S. J., et al. (2010). Review: Current international research into cellulose nanofibres and nanocomposites. *Journal of Materials Science*, *45*(1), 1–33. https://doi.org/10.1007/s10853-009-3874-0.

Ekebafe, L. O., Olugbemide, A. D., & Akpa, F. A. (2017). Biodegradation studies of cellulose-based polyurethane foams. *Macromolecules: An Indian Journal*, *12*(2), 1–9.

El-Zawawy, W. K., & Ibrahim, M. M. (2003). Synthesis and characterization of cellulose resins. *Polymers for Advanced Technologies*, *14*(9), 623–631. https://doi.org/10.1002/pat.384.

Ganeshram, V., & Achudhan, M. (2013). Synthesis and characterization of phenol formaldehyde resin as a binder used for coated abrasives. *Indian Journal of Science and Technology*, *6*(6), 4814–4823. http://www.indjst.org/index.php/indjst/article/download/33969/27919.

George, J., Sreekala, M. S., & Thomas, S. (2001). A review on interface modification and characterization of natural fiber reinforced plastic composites. *Polymer Engineering and Science*, *41*(9), 1471–1485. https://doi.org/10.1002/pen.10846.

Góes, M. M., Keller, M., Masiero Oliveira, V., Villalobos, L. D. G., Moraes, J. C. G., & Carvalho, G. M. (2016). Polyurethane foams synthesized from cellulose-based wastes: Kinetics studies of dye adsorption. *Industrial Crops and Products*, *85*, 149–158. https://doi.org/10.1016/j.indcrop.2016.02.051.

Graham, A. G., & Nath, N. A. (2006). The mechanism of adhesion of phenol-formaldehyde resins to cellulosic and lignocellulosic substrates. *The Journal of Adhesion*, 13–18. https://doi.org/10.1080/00218467108075002.

Handique, J. G., & Baruah, J. B. (2002). Polyphenolic compounds: and overview. *Reactive and Functional Polymers*, *52*, 91–93. https://doi.org/10.1016/S1381-5148(02.

Hsu, Y. I., Huang, L., Asoh, T. A., & Uyama, H. (2020). Anhydride-cured epoxy resin reinforcing with citric acid-modified cellulose. *Polymer Degradation and Stability*, *178*. https://doi.org/10.1016/j.polymdegradstab.2020.109213.

Ikhwan, F. H., Ilmiati, S., Adi, H. K., Arumsari, R., & Chalid, M. (2017). Novel route of synthesis for cellulose fiber-based hybrid polyurethane. In *IOP conference series: materials science and engineering* (p. 012019). https://doi.org/10.1088/1757-899X/223/1/012019.

Inamdar, A., Cherukattu, J., Anand, A., & Kandasubramanian, B. (2018). Thermoplastic-toughened high-temperature cyanate esters and their application in advanced composites. *Industrial and Engineering Chemistry Research*, *57*(13), 4479–4504. https://doi.org/10.1021/acs.iecr.7b05202.

Ishikawa, T., Amaoka, K., Masubuchi, Y., Yamamoto, T., Yamanaka, A., Arai, M., et al. (2018). Overview of automotive structural composites technology developments in Japan. *Composites Science and Technology*, *155*, 221–246. https://doi.org/10.1016/j.compscitech.2017.09.015.

Kato, H., Nakatsubo, F., Abe, K., & Yano, H. (2015). Crosslinking via sulfur vulcanization of natural rubber and cellulose nanofibers incorporating unsaturated fatty acids. *RSC Advances*, *5*(38), 29814–29819. https://doi.org/10.1039/c4ra14867c.

Khalil, H. P. S. A., Bhat, A. H., & Yusra, A. F. I. (2012). Green composites from sustainable cellulose nanofibrils: A review. *Carbohydrate Polymers*, 963–979. https://doi.org/10.1016/j.carbpol.2011.08.078.

Kosmela, P., Hejna, A., Formela, K., Haponiuk, J., & Piszczyk, Ł. (2018). The study on application of biopolyols obtained by cellulose biomass liquefaction performed with crude glycerol for the synthesis of rigid polyurethane foams. *Journal of Polymers and the Environment*, *26*(6), 2546–2554. https://doi.org/10.1007/s10924-017-1145-8.

Lee, K. Y., Aitomäki, Y., Berglund, L. A., Oksman, K., & Bismarck, A. (2014). On the use of nanocellulose as reinforcement in polymer matrix composites. *Composites Science and Technology*, *105*, 15–27. https://doi.org/10.1016/j.compscitech.2014.08.032.

Lee, H. G., Kim, G. H., & Ha, C. S. (2017). Polyimide/amine-functionalized cellulose nanocrystal nanocomposite films. *Materials Today Communications*, *13*, 275–281. https://doi.org/10.1016/j.mtcomm.2017.10.010.

Leelachai, K., Ruksanak, S., Hongkeab, T., Kambutong, S., Pearson, R. A., & Dittanet, P. (2017). Effect of cellulose functionalization on thermal and mechanical properties of epoxy resin. In *Vol. 757. Key engineering materials* (pp. 62–67). Trans Tech Publications Ltd. https://doi.org/10.4028/www.scientific.net/KEM.757.62.

Leng, W., & Pan, B. (2019). Thermal insulating and mechanical properties of cellulose nanofibrils modified polyurethane foam composite as structural insulated material. *Forests*, *10*(2). https://doi.org/10.3390/f10020200.

Lenghaus, K., Qiao, G. G., & Solomon, D. H. (2001). *The effect of formaldehyde to phenol ratio on the curing and carbonisation behaviour of resole resins* (pp. 710–712). https://doi.org/10.1016/S0032-3861(00.

Liu, C., Li, K., Li, H., Zhang, S., & Zhang, Y. (2014). The effect of zirconium incorporation on the thermal stability and carbonized product of phenol-formaldehyde resin. *Polymer Degradation and Stability*, *102*(1), 180–185. https://doi.org/10.1016/j.polymdegradstab.2014.01.013.

Liu, Y., Li, G., Hu, Y., Wang, A., Lu, F., Zou, J. J., et al. (2019). Integrated conversion of cellulose to high-density aviation fuel. *Joule*, *3*(4), 1028–1036. https://doi.org/10.1016/j.joule.2019.02.005.

Nair, S. S., Dartiailh, C., Levin, D. B., & Yan, N. (2019). Highly toughened and transparent biobased epoxy composites reinforced with cellulose nanofibrils. *Polymers*, *11*(4). https://doi.org/10.3390/polym11040612.

Nguyen, B. N., Cudjoe, E., Douglas, A., Scheiman, D., McCorkle, L., Meador, M. A. B., et al. (2016). Polyimide cellulose nanocrystal composite aerogels. *Macromolecules*, *49*(5), 1692–1703. https://doi.org/10.1021/acs.macromol.5b01573.

Nunes, R. C. R., & Mano, E. B. (1995). Influence of cellulose as a filler in vulcanized rubber composites. *Polymer Composites*, *16*(5), 421–423. https://doi.org/10.1002/pc.750160511.

Nyuk Khui, P., Rahman, M., Ahmed, A., King Kuok, K., Bakri, M., Tazeddinova, D., et al. (2021). Morphological and thermal properties of composites prepared with poly(lactic acid), poly(ethylene-alt-maleic anhydride), and biochar from microwave-pyrolyzed jatropha seeds. *BioResources*, *16*(2), 3171–3185. Retrieved from https://ojs.cnr.ncsu.edu/index.php/BioRes/article/view/BioRes_16_2_3171_Nyuk_Khui_Morphological_Thermal_Properties_Composites.

Ohashi, S., Kilbane, J., Heyl, T., & Ishida, H. (2015). Synthesis and characterization of cyanate ester functional benzoxazine and its polymer. *Macromolecules*, *48*(23), 8412–8417. https://doi.org/10.1021/acs.macromol.5b02285.

Piggott, M. R. (1980). *Load-bearing fibre composites* (pp. 1–288). https://doi.org/10.1016/B978-0-08-024231-6.50006-4.

Rahman, M. R., Hamdan, S., & Bakri, M. K. B. (2021). Polylactic acid activated bamboo carbon nanocomposites. In M. R. Rahman (Ed.), *Bamboo Polymer Nanocomposites. Engineering Materials*. Cham: Springer. https://doi.org/10.1007/978-3-030-68090-9_4.

Rahman, M. R., Hamdan, S., Ngaini, Z. B., Jayamani, E., Kakar, A., Bakri, M. K. B., et al. (2019). Cellulose fiber-reinforced thermosetting composites: Impact of cyanoethyl modification on mechanical, thermal and morphological properties. *Polymer Bulletin*, *76*(8), 4295–4311. https://doi.org/10.1007/s00289-018-2598-1.

Rangel-Vázquez, N. A., & Leal-García, T. (2010). Spectroscopy analysis of chemical modification of cellulose fibers. *Journal of the Mexican Chemical Society*, *54*(4), 192–197. http://www.jmcs.org.mx/PDFS/V54/4/03.-%20Rangel.pdf.

Rani, P., Mishra, S., & Sen, G. (2013). Microwave based synthesis of polymethyl methacrylate grafted sodium alginate: Its application as flocculant. *Carbohydrate Polymers*, *91*(2), 686–692. https://doi.org/10.1016/j.carbpol.2012.08.023.

Rani, P., Sen, G., Mishra, S., & Jha, U. (2012). Microwave assisted synthesis of polyacrylamide grafted gum ghatti and its application as flocculant. *Carbohydrate Polymers*, *89*(1), 275–281. https://doi.org/10.1016/j.carbpol.2012.03.009.

Sami, U., Bustam, M. A., Nadeem, M., Naz, M. Y., Tan, W. L., & Shariff, A. M. (2014). Synthesis and thermal degradation studies of melamine formaldehyde resins. *The Scientific World Journal*, 1–6. https://doi.org/10.1155/2014/940502.

Silva, M. C., Takahashi, J. A., Chaussy, D., Belgacem, M. N., & Silva, G. G. (2010). Composites of rigid polyurethane foam and cellulose fiber residue. *Journal of Applied Polymer Science*, *117*(6), 3665–3672. https://doi.org/10.1002/app.32281.

Srirachya, N., Boonkerd, K., Nakajima, L., & Kobayashi, T. (2018). Bio-composite hydrogels of cellulose and vulcanized natural rubber with nanointerconnected layers for reinforced water-retaining materials. *Polymer Bulletin*, *75*(12), 5493–5512. https://doi.org/10.1007/s00289-018-2341-y.

Tao, F., Song, H., & Chou, L. (2012). Efficient conversion of cellulose into furans catalyzed by metal ions in ionic liquids. *Journal of Molecular Catalysis A: Chemical*, *357*, 11–18. https://doi.org/10.1016/j.molcata.2012.01.010.

Thakur, V. K., Thakur, M. K., & Gupta, R. K. (2013). Rapid synthesis of graft copolymers from natural cellulose fibers. *Carbohydrate Polymers*, *98*(1), 820–828. https://doi.org/10.1016/j.carbpol.2013.06.072.

Ullah, S., Bustam, M. A., Ahmad, F., Nadeem, M., Naz, M. Y., Sagir, M., et al. (2015). Synthesis and characterization of melamine formaldehyde resins for decorative paper applications. *Journal of the Chinese Chemical Society*, *62*(2), 182–190. https://doi.org/10.1002/jccs.201400226.

Vineeth, S. K., Gadhave, R. V., & Gadekar, P. T. (2019). Nanocellulose applications in wood adhesives—Review. *Open Journal of Polymer Chemistry*, 63–75. https://doi.org/10.4236/ojpchem.2019.94006.

Visakh, P. M., Thomas, S., Oksman, K., & Mathew, A. P. (2012). Effect of cellulose nanofibers isolated from bamboo pulp residue on vulcanized natural rubber. *BioResources*, *7*(2), 2156–2168. https://doi.org/10.15376/biores.7.2.2156-2168.

Wang, X., Chen, X., Xie, X., Yuan, Z., Cai, S., & Li, Y. (2019). Effect of phenol formaldehyde resin penetration on the quasi-static and dynamic mechanics ofwood cellwalls using nanoindentation. *Nanomaterials*, *9*(10). https://doi.org/10.3390/nano9101409.

Wang, S., Lee, P. K., Yang, X., Rogach, A. L., Armstrong, A. R., & Yu, D. Y. W. (2018). Polyimide-cellulose interaction in Sb anode enables fast charging lithium-ion battery application. *Materials Today Energy*, *9*, 295–302. https://doi.org/10.1016/j.mtener.2018.06.007.

Wei, C., Wang, W., Liu, H., Qin, A., Yu, C., & Wang, B. (2017). Mechanical properties of phenol/formaldehyde resin composites reinforced by cellulose microcrystal with different aspect ratio extracted from sisal fiber. *Polymers for Advanced Technologies*, *28*(8), 1013–1019. https://doi.org/10.1002/pat.3831.

Yang, W., Rallini, M., Natali, M., Kenny, J., Ma, P., Dong, W., et al. (2019). Preparation and properties of adhesives based on phenolic resin containing lignin micro and nanoparticles: A comparative study. *Materials and Design*, *161*, 55–63. https://doi.org/10.1016/j.matdes.2018.11.032.

Zadorecki, P., Karnerfors, H., & Lindenfors, S. (1986). Cellulose fibers as reinforcement in composites: Determination of the stiffness of cellulose fibers. *Composites Science and Technology*, *27*(4), 291–303. https://doi.org/10.1016/0266-3538(86)90072-2.

Zadorecki, P., & Michell, A. J. (1989). Future prospects for wood cellulose as reinforcement in organic polymer composites. *Polymer Composites*, *10*(2), 69–77. https://doi.org/10.1002/pc.750100202.

Zhang, B.x., Zhang, Y., Li, J., Sun, Y., Li, H., Qiu, W., et al. (2020). Tough macroporous phenolic resin/bacterial cellulose composite with double-network structure fabricated by ambient pressure drying. *Cellulose*, *27*(9), 5029–5039. https://doi.org/10.1007/s10570-020-03122-9.

CHAPTER

Cellulose reinforcement in bioplastic composites

8

Perry Law Nyuk Khui, Md Rezaur Rahman, and Muhammad Khusairy Bin Bakri
Department of Chemical Engineering and Energy Sustainability, Faculty of Engineering, Universiti Malaysia Sarawak (UNIMAS), Kota Samarahan, Sarawak, Malaysia

Chapter outline

8.1 Introduction

In general, a polymer reinforced composite material could be made of two or more components which comprises of a matrix and reinforcement material. However, the reinforcement material is one of the common variable altered by researchers accordingly to the matrix used (Bakri, Jayamani, & Kakar, 2018). The improvement and modification of environmentally friendly reinforcement material is a popular topic within the material science field, where some may claim to be as strong conventional materials (Rahman, Hamdan, Jayamani, Bakri, & Islam, 2017). Cellulose is an example of an environmentally friendly reinforcement material that could be extracted from plants/lignocellulosic biomass through multiple mechanical and chemical processes (Rahman & Bakri, 2021; Khui, Rahman, & Bakri). It is known by many researchers that cellulose is an organic polymer which is largely abundant on earth, and due to the development of nanocellulose (i.e., fibers, fibrils, crystalline,

Fundamentals and Recent Advances in Nanocomposites Based on Polymers and Nanocellulose.
https://doi.org/10.1016/B978-0-323-85771-0.00016-6

derivatives, etc.) the potential applications of cellulose has been broadened (Khui, Rahman, & Bakri). Bioplastic could be categorized as polymers which are biodegradable or environmentally friendly. It is also a popular topic among researchers to study these biodegradable plastics/polymers and develop composite materials which could be applied to numerous applications. This chapter covered studies that relate the usage of biodegradable polymer matrices and cellulose based reinforcement materials to develop "Green Composites", which are environmentally friendly or biodegradable.

8.2 Bioplastics for "green composites"

Biodegradable plastics are polymers that could be degraded simply by exposure to environmental affects, in combination with enzymes. Some researchers investigate possible solutions of reducing plastic wastes, the utilization of the biodegradability properties of bioplastics influences the implementation of commercializing bioplastics in replacement of conventional plastic materials (Luyt, Malik, & Al-Salem, 2019). Bioplastics from natural polymers are identified as substance that are obtained or synthesized from natural renewable resources from agriculture and/or their biomass. Examples of biodegradable polymers that are commercially used are Poly (lactic acid) (PLA), Polyhydroxyalkanoates (PHA), Poly(hydroxybutyrate-*co*-valerate) (PHBV), Polyhydroxybutyrate (PHB) and Poly(hydroxyvalerate) (PHV).

Common natural renewable resources used for synthesizing these natural polymers include; sugar cane, potatoes, corn (maize), sugar beet and cassava. For researchers studying the production of natural polymers, these resources are attractive due to the starch content available, the fermentation of starch is part of the steps to obtain the monomer, before proceeding with the process of polymerization. PLA is most noticeably used as feedstock filaments for 3D printing (Liu et al., 2019), the manufacturing of food and beverage packaging material (Özge, 2017), as well absorbable suture material for medical applications (Lou et al., 2008; Schneider, Feussner, Schneider, & Feussner, 2017). In terms of developing polymer based "Green Composites", the bioplastic matrix and reinforcements should possess good biocompatibility with each other and the environment once it has reached its lifecycle for application purposes, as it is desired for the composite material to have a shorter degradation rate with less environmental implications, in comparison to both conventional plastic matrix and reinforcements. An example of a conventional and highly commercialized plastic material is Polyethylene (PE), which is most known to be the raw materials to manufacture most plastic household appliances, food and beverage packaging materials, and piping construction material which maybe be known under the classification of its density such as; High-density Polyethylene (HDPE) and Low-density Polyethylene (LDPE) (Ronca, 2017).

The degradation of PE in the natural environment is quite poor, as the material contains a backbone of carbon-carbon covalent bonds which do not undergo hydrolysis as easily, PE resists photo-oxidative degradation as the material has a scarce amount of Ultraviolet (UV)-visible absorption chromophores and with the absence of sunlight (Chamas et al., 2020). The thermal-oxidative degradation of PE also does

not occur at significant rate at temperatures below 100°C, additionally, in an environment found in the landfills, where sunlight and oxygen may not be present as wastes are piling up by the tons, anaerobic thermal degradation is unlikely to occur for PE, due to the high temperatures (≥350°C) required by the material. In general, some research shows that polymers with high crystallinity are less susceptible to anaerobic thermal degradation in comparison with polymers with low crystallinity (Ahmad et al., 2015; Chamas et al., 2020; Gardette et al., 2013; Onwudili, Insura, & Williams, 2009).

In contrast, the degradation of PLA in the natural environment is significantly better in comparison to PE. In an environment found in the landfill, slow hydrolysis may occur for PLA ester linkages when exposed in an aerobic environment with the presence of moisture and temperatures of at least 30°C. Research also shows that PLA also degrade at a significant rate under industrial composting conditions which are (>60°C) under similar environmental conditions (Chamas et al., 2020; Musioł et al., 2016). The degradation of PLA could occur through either hydrolysis, thermal-oxidative degradation, or photo-oxidative degradation. Some research on the biodegradation of PLA simulated under landfill conditions has shown results where the material incubated has a significant weight loss of around 90% for the duration of 90 days, with PLA samples (0.5 mm thick, $2 \times 2 cm^2$ transparent films) were becoming small fragile fragments with the size less than 1 mm (Boonmee, 2016).

On the other hand, PLA could undergo anaerobic thermal degradation, but only at higher temperatures (≥230°C), which is unlikely in the environment of a landfill (Chamas et al., 2020). The characteristics of bioplastics biodegradation and being environmentally friendly under landfill conditions is quite interesting, as it supports the potential for a sustainable future, being an alternative material by replacing single use conventional and nondegradable plastic material. In order to increase the applicability of the bioplastics for different types of applications, the bulk properties (i.e., mechanical, thermal, and electrical) of the bioplastic requires some modifications, therefore, comes the use of reinforcement material and/or additives for the development of composite materials, more details are in the following section on filler selection (cellulose reinforcement).

8.3 Cellulose as filler for "green composites"

The vast application of additives for polymers could produce varied products, for example the conventional natural rubber could be converted into vulcanized shoe outsoles, tires, latex, elastic foam, rubber bands, seals etc. with the varied mixtures of additives. According to Al-Malaika et al. (Al-Malaika, Axtell, Rothon, & Gilbert, 2017), the following are a list of additives commonly utilized for modifying polymers/plastics and composite materials (Al-Malaika et al., 2017):

- Fillers
- Crosslinking additives
- Surface modifiers

- Viscosity modifiers
- Compatibilizers for polymer blends
- Biocides
- Nucleating and clarifying agents
- Plasticizers and softeners
- Colorants
- Antioxidants
- Lubricants and flow promoters
- Impact modifiers
- Flame retardant additives
- Blowing agents.

However, among the vast categories of additives listed, this section would discuss more toward the selection of fillers and specifically regarding cellulose as reinforcement fillers for bioplastic composite material. According to Rothon and DeArmitt, fillers are solid additives which form separate phases in the composite matrix, fillers could be describe as particulates and fibrous reinforcement material (Rothon & DeArmitt, 2017).

The field of cellulose has attracted many researchers from different fields, it is a well-known renewable resource for the natural polymer found to be in abundance in agriculture (plants) and their lignocellulosic biomass. Cellulose come in numerous derivatives, applicable for numerous applications ranging from the development of cellophane films for packaging purposes (Paunonen, 2013), thickening agents to develop gels for medical and food & beverage industry (Ullah, Wahid, Santos, & Khan, 2016), as well as reinforcement fillers for polymer composites (Lee, Aitomäki, Berglund, Oksman, & Bismarck, 2014). The main reason cellulose was utilized as fillers for polymer composites fabrication, was regarding the concern of the biodegradability of fillers, and environmental impact of polymer filler reinforced composites. Most researched conducted on cellulose fillers used for reinforcing polymer composites are micro-crystalline cellulose (MCC), nano-crystalline cellulose (CNC), and fibrillated cellulose, where the terminology of these cellulose sizes (macro, micro & nano) is the result of extraction process. Further processing such as; chemical pretreatments & hydrolysis, ultrasonication and ball milling may influence the size and properties of the cellulose (Abraham et al., 2011; Morelli, Marconcini, Pereira, Bretas, & Branciforti, 2012; Phanthong, Guan, Ma, Hao, & Abudula, 2016; Trache, Hussin, Haafiz, & Thakur, 2017). The research on nanocellulose has gained significant progress over the pass 10+ years (Rahman & Bakri, 2021). An example of a study conducted on the effect of wet spinning and stretching of cellulose nano-fibrils into filaments, have shown that the resulting 20% stretched spun filaments were demonstrating good mechanical properties, with young modulus, tensile strength, yield strength of 37.5 GPa, 543.1 MPa and 340.4 MPa respectively. The researchers attributes the improvement of mechanical properties to the wet spinning and stretching method, aligning the cellulose nano-fibrils within the filament (Kim, Kim, Lee, Zhai, & Kim, 2019). The study

states that natural fiber reinforced composites owe its mechanical and physical properties to the cellulose nano-fibrils contain within the natural fibers. However, in comparison to natural fibers, the length of cellulose nano-fibrils is too short to form filaments, therefore requires special processing techniques (wet spinning) to the increase applicability as fillers (Kim et al., 2019). Some example of factors for a filler to affect the mechanical properties of polymer composites are

- Stiffness
- Specific Gravity (Density)
- Morphology (i.e., shape, size, length, diameter)
- Surface area
- Dispersibility
- Adhesion

Cellulose may also be an influence by the factors, as it is utilized specifically as a filler for polymer composites (Rahman & Bakri, 2021). The factors of adhesion and dispersibility within the polymer matrix are plays a big role enhancing the polymer composite mechanical properties, regardless of the morphology, density, stiffness, and surface area of the filler, if the filler have poor adhesion and do not disperse well, it may have adverse effects on the mechanical properties of the reinforced polymer composite (Cheng, Zhou, Wei, Cheng, & Zhu, 2019; Hao et al., 2020; Lee et al., 2014; Rothon & DeArmitt, 2017). Based on a study by Dufresne, an improvement in mechanical properties should be observed with the incorporation of cellulose nanocrystals or microfibrils if they are homogeneously dispersed within the polymer matrix (Dufresne, 2017a, 2017b).

As an example, a study was conducted on the comparison of micro-fibrillated cellulose (MFC), cellulose nanocrystals (CNC), and cellulose nanofiber (CNF) reinforcement dispersed in a starch matrix, developing a polymer reinforced composite by film casting. It was noted that the adhesion was attributed to the large aspect ratio, increasing hydrogen bonding interactions between the filler and starch matrix. The mixing process utilized by the researcher, was enough to contribute to well-dispersed cellulose fillers, and it was noted that as the filler loading increased (0, 1, 3, 5, 10, and 20 wt%), the mechanical properties of the cellulose/starch composite also increase. Among the reinforcements utilized, MFC has shown to be the best filler to reinforce the starch in comparison to CNC and CNF. MFC manage to increase the (tensile strength and tensile modulus) respectively from (3.1 MPa and 146.7 MPa for pure starch sample), to (10.6 MPa and 757.4 MPa for starch/MFC composite) (Cheng et al., 2019).

Ghasemi et al. reported an improvement of mechanical properties of nanocellulose (CNF) reinforced PLA and compatibilizer maleated PLA (PLA-g-MA). The tensile modulus and strength from neat PLA to (PLA/CNF/PLA-g-MA) increased from 1.1 GPa to 1.54 GPa, and 22.4 MPa to 60.3 MPa respectively. It was stated the optimal weightage is (90%, PLA 5%, CNF 5% PLA-g-MA) which is the highest weightage producing the best mechanical properties; tensile modulus of 1.54 GPa, with tensile strength of 60.3 MPa (Ghasemi, Behrooz, Ghasemi, Yassar, & Long, 2018). Other

case study also shared similar results, affecting tensile and flexural strength with the development of micro/nanocellulose (MNC) fillers reinforced PLA composite wire rods for the 3D printing applications. The researchers utilized fillers weightage up to 30 wt% of MNC, the results showed that the interfacial compatibility of MNC and PLA was improved by adding silane coupling agent (KH-550) up to 1 wt% of the MNC. The optimum ratio for the preparation of MNC/PLA composites for 3D printing was determined to also be at highest weightage of 30 wt% MNC, (1 wt% based on filler wt%) KH-550, 5 wt% Polyethylene glycol (PEG 6000), and 65 wt% PLA. The 3D MNC/PLA composite products printed at optimal conditions, produce mechanical properties at a similar level to neat PLA, with the elongation at break of 12%, flexural strength of 50.7 MPa and tensile strength 59.7 MPa. These results may support the aim to reduce the utilization of PLA matrix material, and more filler material, where the cost in manufacturing the product is a priority (Wang et al., 2017).

8.4 Processing of cellulose reinforced green composites

Bioplastics mentioned in this section are mostly thermoplastics, therefore in this section, covers the processing of bioplastics behaving as thermoplastics and cellulose as fillers. In terms of the types fabrication processes utilized over the pass 10+years, nanocellulose reinforced polymer composites have been commonly prepared by either solvent based processing, melt processing, and electro spinning (Ferreira et al., 2018; Kalia et al., 2011).

8.4.1 Melt processing

Melt processing seem to be popular in the industrial zone-based manufacturing, due to its short processing time in comparison to solvent casting. Studies have shown that nanocellulose still could utilize common melt processing as they act as solid fillers. According to some studies (Clarkson et al., 2019; Marcos & Alain, 2017; Mokhena et al., 2018) some examples of melt processing are

- Melt spinning
- Melt mixing/blending
- Extrusion
- Injection molding
- Compression molding

This processing method utilizes a heat element/source to raise the temperature of the polymer to soften it into a molten state. This method may only be applicable for thermoplastics, as solvents was not utilized, resulting in less chemical waste in the overall manufacturing process (Marcos & Alain, 2017). Nanocellulose filler does not exhibit classical thermal behavior of semicrystalline polymers during high temperature melt mixing. The nanocellulose do no soften at high temperatures, as glass transition and melting temperature were estimated to be above the nanocellulose

degradation temperature (Dufresne, 2017a). Based on a study, melt processing of nanocellulose fillers and thermoplastic polymer feedstocks were demonstrated to be inefficient due to poor dispersion and adhesion between filler and matrix, resulting in particle agglomeration of nanocellulose within odd areas of the composite (Graupner & Müssig, 2017; Mokhena et al., 2018). In order to influence filler-matrix interfacial adhesion and dispersion, surface modification of nanocellulose through chemical processing may be required (Abdulkhani, Hosseinzadeh, Ashori, Dadashi, & Takzare, 2014; Immonen, Lahtinen, & Pere, 2017) (Fig. 8.1).

Chemical modification of the nanocellulose surfaces may influence the nanocellulose filler to resist thermal degradation, especially during melt processing such as injection molding and extrusion. Due to processing conditions (e.g., temperature, time, speed, flowrate, and pressure); especially at high temperatures, it is more likely for the end product composite to be affected by thermal degradation, hence may instead cause adverse effects onto the composite (Gan, Sam, Abdullah, & Omar, 2020). An example of a study conducted on the effects of silane surface treatment of cellulose nanocrystals to developed cellulose reinforced polyvinyl chloride composites, the crystallinity of the CNC was decreased after the surface modification. The study demonstrated that the modification with silane could contribute to the improvement in the interfacial bonding between the filler and matrix. The optimal tensile strength achieved by the silane modified CNC composites was high than unmodified CNC composites of about 39 MPa and 32 MPa respectively (Sheltami, Kargarzadeh, & Abdullah, 2015).

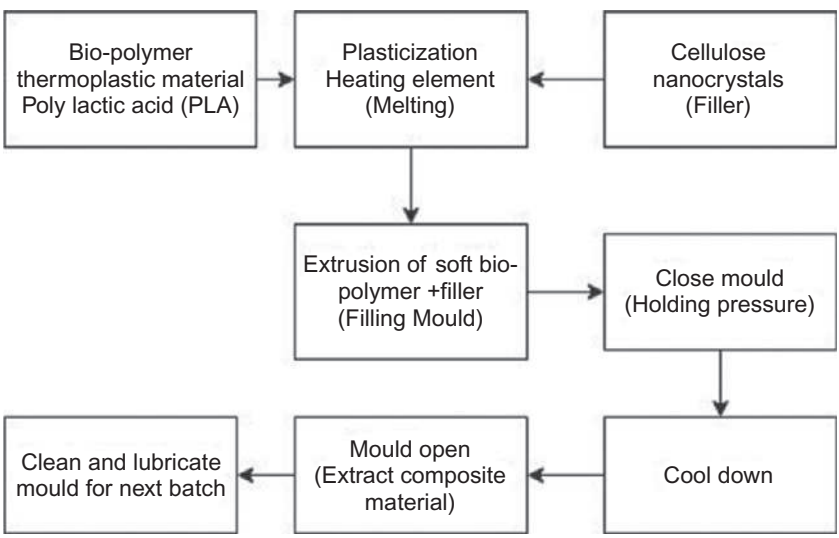

FIG. 8.1

Example flowchart for a common melt processing (injection molding) (Mokhena et al., 2018).

8.4.2 Solvent-based processing

Cellulose could be extracted and processed into numerous derivatives through alteration of chemical and mechanical treatments during the extraction process. The majority of the cellulose extracted may require special types of solvent mediums to undergo solvent based processing for composite fabrication. Some examples of solvent based processing for reinforced polymer composites with nanocellulose fillers by solution casting are demonstrated by numerous literatures (Arjmandi, Hassan, Haafiz, Zakaria, & Inuwa, 2014; Liu et al., 2019; Sanchez-Garcia, Gimenez, & Lagaron, 2008; Trifol, van Drongelen, Clegg, Plackett, & Szabo, 2019).

An example of the methodology solution casting, one study prepared flax nanocellulose fiber/PLA composite films, utilizing chloroform as solvent with concentration of 5.0 wt%. The PLA pellets were mixed into the solvent and the solution was continuously stirred at room temperature until the PLA pellets were fully dissolved within the solvent. The flax nanocellulose fiber of (2.5% and 5 wt%) suspension was incorporated separately in the mixed solution of PLA/chloroform and was continuously stirred for 12 h. The flax nanocellulose fiber/PLA composite film solution was cast into petri dishes and the chloroform solvent was then evaporated at under ambient conditions, as shown in Fig. 8.2.After fully evaporation takes place, the resulting composite films were oven dried for 12 h at 40°C. In terms of resulting mechanical properties, the solution casting composite film with 2.5 wt% flax nanocellulose

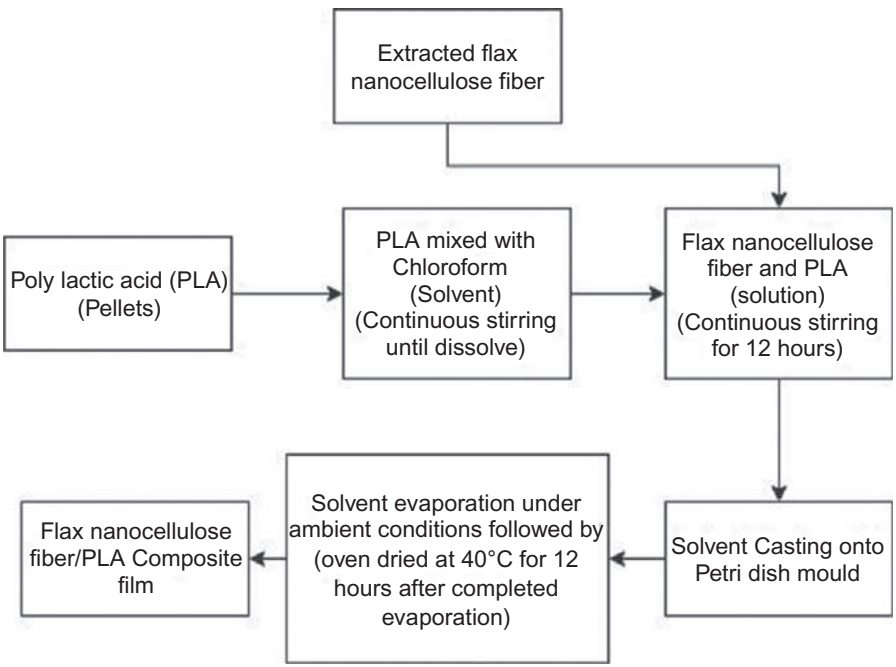

FIG. 8.2

Example flowchart for solvent based processing (solution casting) (Liu et al., 2019).

demonstrates good tensile strength and ductile qualities with tensile strength of 24.3 MPa and 70% elongation at break (Liu et al., 2019).

According to Mathew and Oksman (Mathew & Oksman, 2013), the solution casting is a simple process and requires less complex processing procedures or equipment to develop the composite. Solution casting usually involves fabrication at low processing temperature and is a common method to develop sheet/layer of films with uniform thickness, low haze, optical purity, and isotropy. The slow evaporation process allows the formation of networks of cellulose nanocrystals/fibers in the matrix phase, which may influence the composite film mechanical properties. The disadvantages of solution casting might include slow processing speed, utilization of more chemicals (solvents), the cost for solvent recovery, and the limitation on repeatability in a large scale (Mathew & Oksman, 2013).

Furthermore, solvent based processing by solution casting could involve the aqueous phase or a nonaqueous phase depending on the type of the matrix polymer. If the polymer matrix is a water-soluble (e.g., starch, gelatin, chitosan, carboxymethyl cellulose etc.), solution casting would typically result with homogeneous dispersion. For nonwater-soluble polymer matrix, additional procedure (e.g., solvent exchange, freeze-drying, and surface modification by surfactant) may become a requirement for a successful fabrication. Dispersion of the fillers may be a problem for some nonwater soluble solution casting and result in a heterogenous mixture rather than a homogenous dispersion of the fillers (Mathew & Oksman, 2013).

8.4.3 Electrospinning

Electrospinning is a manufacturing process utilizing electrostatic force to generate threads of micro and nano size fibers from a polymer solution. It was attributed that the electro spun micro-nano size fibers possess high aspect ratio of length and diameter, large specific surface area, small pore size, and good mechanical properties (Jiang et al., 2018). The electrospinning process operates using a high DC voltage to generate an electrical field, where strong repulsive electrical forces are pulling on the weaker surface tension at the tip of the capillary, in which is the electrical charged polymer solution. When the repulsive electrical forces could overcome the weaker forces of the polymer solution surface tension, the polymer solution would flow out from the spinneret in a whipping motion and would land onto the collector. The space between the spinneret and collector allows the polymer solution to evaporate the solvent used and dry/cured, this space is the zone for the polymer solution to transition from liquid to solid. It was also stated that synthetic and natural polymers could quickly undergo electrospinning, as long it is in liquid form, which is after it is fully dissolved in the appropriate solvent and becomes a solution (Asmatulu, Khan, Asmatulu, & Khan, 2019; Bhardwaj & Kundu, 2010). Some literatures demonstrate electrospinning of cellulose and bioplastic to develop a composite material are based on incorporating CNC into a dissolved bioplastic solution, therefore, the outcome of electrospinning is a CNC/Bioplastic composite fiber threads (Jiang et al., 2018; Wenqiang, Yu, Dongyan, Yuxia, & Xiuzhen, 2018).

A study conducted by Wenqiang et al. was able demonstrate the development of PLA/cellulose nanowhiskers (CNWs) composite nanofiber mats by electrospinning processing (Wenqiang et al., 2018). It was stated that the incorporation of CNWs into the PLA matrix may enhance numerous properties of the resulting electro spun nanofiber composite mats. According to a similar study, mechanical properties have been improved, as the tensile strength and young modulus increase about 5 and 22 times more than neat electro spun PLA mats, with the incorporation of 5 wt% CNWs into the PLA matrix. The tensile strength and young modulus are 6.3 MPa and 125.6 MPa respectively (Shi et al., 2012). In addition, the water absorption test was conducted by Liu et al. on the electro spun CNWs/PLA composite nanofiber mats, and results shown good water absorption ratio of about 1600% at 7.5 wt% CNWs. In comparison to neat PLA electro spun mats, water absorption ratio was about 200% (Fig. 8.3). The

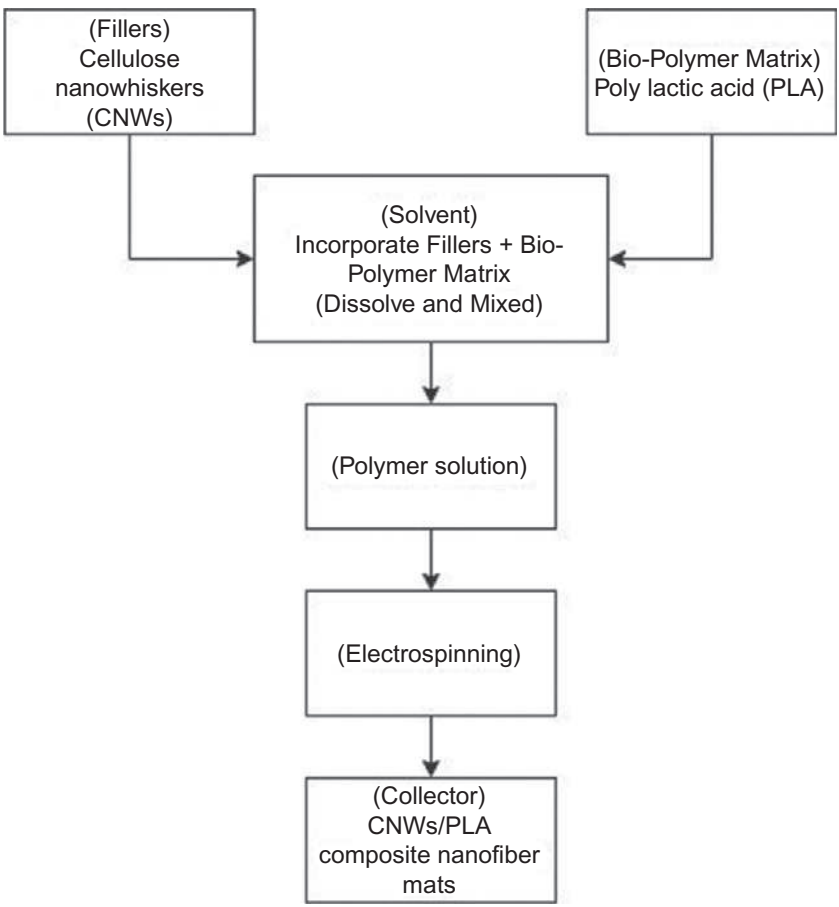

FIG. 8.3

Example of flowchart for electrospinning processing (Wenqiang et al., 2018).

researchers claim that, these electro spun CNWs/PLA composite nanofibers may be applicable for biomedical applications as sutures to promote tissue scaffolding, as the material has good water absorption capabilities (Wenqiang et al., 2018; Liu et al., 2018).

8.5 Performance of cellulose reinforcing green composites

This section discusses the applications and performance of utilizing cellulose for reinforcing biodegradable polymers and developing "Green Composites". The terminology of cellulose "reinforcing" "Green Composites", involves any enhancement of the properties of the biodegradable polymer matrix or composite, hence showcasing the performance of cellulose as a factor toward developing better and sustainable products for future generations. On the previous section on electrospinning processes, Wenqiang et al. stated the applicability of electro spun cellulose/PLA composite nanofibers as sutures for biomedical application and tissue engineering (Wenqiang et al., 2018).

A similar research was conducted by electrospinning processing, by developing a bio-nanocomposite scaffolding for the purpose of bone tissue engineering, cellulose nanocrystals (CNCs) was utilized for reinforcing maleic anhydride grafted poly lactic (acid) (MPLA). According to Chengjun et al. (2013), the electro spinning of MPLA/CNCs composite nanofibers was successful developed by grafting maleic anhydride onto the PLA matrix for improving adhesion or filler-matrix interaction of CNCs and PLA. Based on the morphological test conducted, it was noted that the electro spun MPLA/CNCs composite nanofibers became more uniform and finer as the CNCs weightage increased (e.g., 0, 1, 2, 5 wt%). In addition, the thermal and tensile test results show that the incorporation of CNCs could effectively enhance the mechanical properties of the electro spun MPLA/CNCs nanofiber composites. Optimum tensile strength and modulus was observed to be about 10 MPa and 135 MPa, respectively, with the incorporation of 5 wt% of CNCs. In terms of weight loss during in vitro degradation, the MPLA/CNCs-5 wt% nanofiber composite has demonstrated to resist in vitro degradation in comparison to the pure MPLA, with percentage of weight loss of 19.9% and 26.9%, respectively. Regarding the performance for real life application of these MPLA/CNCs nanofiber composite scaffolds for bone tissue engineering, the researchers have demonstrated that, MPLA/CNCs nanofiber composite scaffolds were nontoxic to human adult adipose derived mesenchymal stem cells (hASCs) as a model used in bone regeneration. It was noted that the incorporation of CNCs as fillers did not have a significant cytotoxic effect, and the resulting MPLA/CNCs nanofiber composites scaffolds are capable of supporting cell proliferation (Chengjun et al., 2013). This case study managed to fulfill numerous requirements for supporting the use of electrospinning processes to fabricate a cellulose reinforced bio-polymer material for the purpose of promoting bone tissue engineering.

According to another case study under the biomedical field for wound dressing applications, Fouad et al. developed an antimicrobial interactive single dose nanofibrous wound dressing mat from cellulose acetate (CA) reinforced PLA composite (Gomaa, Madkour, Moghannem, & El-Sherbiny, 2017). The method of fabrication is similar to previous literature examples; (Chengjun et al., 2013; Wenqiang et al., 2018), where electrospinning processing was utilized to develop the nanofibrous wound dressing mat. The polymer solution utilized for electrospinning contains PLA/CA and solvents dichloromethane (DCM) and dimethyl formamide (DMF). An antimicrobial agent called thymoquinone (TQ) was incorporated into the developed electro spun wound dressing mats, which results in wound dressing mat having a steady release of drugs and mimicking the extracellular matrix (ECM) due to the electro spun composite 3D networking, hence promoting cell proliferation. The performance of the CA being a polysaccharide derivative, has been attributed by the researchers, to be a good material due to CAs ability to assist cellular interaction between the wound dressing mat and fibroblast. According to the study, in order to investigate the effectiveness of TQ-loaded PLA/CA composite nanofibers as a material for wound dressing, an in vivo wound closure assay was performed on mice dorsal wounds. According to healing progression from (3, 7, 10, and 14 days) mark, wound dressing mat code TQ-F1 shown the fastest rate of healing, among the other 2 wound dressing types evaluated, where there is complete closure of the dorsal wound on the mice, in addition there were almost no scarce formation at the end of 14 days. This may be due to the cumulative drug release % of TQ-F1 within the duration of 24 h and 9 days mark, which are 55.9% and 79.7%, respectively. The cumulative drug release of TQ-F1 were higher especially during the 24 h mark, in comparison to TQ-F2 and TQ-F3 wound dressings. Furthermore, part of the reason TQ-F1 may have better cumulative drug release among the other 2 wound dressings, might be due to the measure porosity % and mean pore size (μm) which are 79%, 4.201 μm, respectively. It was noted by the researchers that the decreased in pore size and increase in measure porosity, leads to a high surface area, which is an advantage for absorbing not only drugs/medication (TQ), but also absorbing exudates and fluids secreted by the open wound (Gomaa et al., 2017).

8.6 Summary

This chapter discusses bioplastics, cellulose as fillers/reinforcement material, processing, and performance of cellulose for the development and application of "Green Composites". The terminology of "Green Composite" could be stated as an environmentally friendly and biodegradable composite material develop from a natural and renewable resource. Cellulose and bioplastic may have great potential in the biomedical field in regards to wound healing or tissue engineering, as they have good biocompatibility with live tissues and being nontoxic.

Acknowledgment

The authors would like to acknowledge Universiti Malaysia Sarawak (UNIMAS) for the support.

References

Abdulkhani, A., Hosseinzadeh, J., Ashori, A., Dadashi, S., & Takzare, Z. (2014). Preparation and characterization of modified cellulose nanofibers reinforced polylactic acid nanocomposite. *Polymer Testing*, *35*, 73–79. https://doi.org/10.1016/j.polymertesting.2014.03.002.

Abraham, E., Deepa, B., Pothan, L. A., Jacob, M., Thomas, S., Cvelbar, U., et al. (2011). Extraction of nanocellulose fibrils from lignocellulosic fibres: A novel approach. *Carbohydrate Polymers*, *86*(4), 1468–1475. https://doi.org/10.1016/j.carbpol.2011.06.034.

Ahmad, I., Ismail Khan, M., Khan, H., Ishaq, M., Tariq, R., Gul, K., et al. (2015). Pyrolysis study of polypropylene and polyethylene into premium oil products. *International Journal of Green Energy*, *12*(7), 663–671. https://doi.org/10.1080/15435075.2014.880146.

Al-Malaika, S., Axtell, F., Rothon, R., & Gilbert, M. (2017). Additives for plastics. In *Brydson's plastics materials* (8th ed., pp. 127–168). Elsevier Inc. https://doi.org/10.1016/B978-0-323-35824-8.00007-4.

Arjmandi, R., Hassan, A., Haafiz, M. K. M., Zakaria, Z., & Inuwa, I. M. (2014). Pencirian komposit polilaktik asid/selulosa mikrohablur/hibrid montmorilonit. *Malaysian Journal of Analytical Sciences*, *18*(3), 642–650. http://www.ukm.my/mjas/v18_n3/Reza%20Arjmandi_18_3_18.pdf.

Asmatulu, R., Khan, W. S., Asmatulu, R., & Khan, W. S. (2019). Chapter 1—introduction to electrospun nanofibers. In *Micro and nano technologies* (pp. 1–15). Elsevier. https://doi.org/10.1016/B978-0-12-813914-1.00001-8.

Bakri, M. K. B., Jayamani, E., & Kakar, A. (2018). Potential in the development of Borneo Acacia wood reinforced polyhydroxyalkanoates bio-composites. *Key Engineering Materials*, *779*, 19–24. https://doi.org/10.4028/www.scientific.net/kem.779.19.

Bhardwaj, N., & Kundu, S. C. (2010). Electrospinning: A fascinating fiber fabrication technique. *Biotechnology Advances*, *28*(3), 325–347. https://doi.org/10.1016/j.biotechadv.2010.01.004.

Boonmee, C. (2016). Degradation of poly(lactic acid) under simulated landfill conditions. *Environment and Natural Resources Journal*. https://doi.org/10.14456/ennrj.2016.8.

Chamas, A., Moon, H., Zheng, J., Qiu, Y., Tabassum, T., Jang, J. H., et al. (2020). Degradation rates of plastics in the environment. *ACS Sustainable Chemistry & Engineering*, *8*(9), 3494–3511. https://doi.org/10.1021/acssuschemeng.9b06635.

Cheng, G., Zhou, M., Wei, Y. J., Cheng, F., & Zhu, P. X. (2019). Comparison of mechanical reinforcement effects of cellulose nanocrystal, cellulose nanofiber, and microfibrillated cellulose in starch composites. *Polymer Composites*, *40*, E365–E372. https://doi.org/10.1002/pc.24685.

Chengjun, Z., Qingfeng, S., Weihong, G., Lekeith, T., Qureshi, A. T., Hayes, D. J., et al. (2013). Electrospun bio-nanocomposite scaffolds for bone tissue engineering by cellulose nanocrystals reinforcing maleic anhydride grafted PLA. *ACS Applied Materials & Interfaces*, 3847–3854. https://doi.org/10.1021/am4005072.

Clarkson, C. M., El Awad Azrak, S. M., Chowdhury, R., Shuvo, S. N., Snyder, J., Schueneman, G., et al. (2019). Melt spinning of cellulose nanofibril/polylactic acid (CNF/PLA)

composite fibers for high stiffness. *ACS Applied Polymer Materials*, 160–168. https://doi.org/10.1021/acsapm.8b00030.

Dufresne, A. (2017a). Cellulose nanomaterial reinforced polymer nanocomposites. *Current Opinion in Colloid and Interface Science*, *29*, 1–8. https://doi.org/10.1016/j.cocis.2017.01.004.

Dufresne, A. (2017b). Nanocellulose: From nature to high performance tailored materials. In *Nanocellulose: From nature to high performance tailored materials* (2nd ed., pp. 1–634). Walter de Gruyter GmbH. https://doi.org/10.1515/9783110480412.

Ferreira, F. V., Dufresne, A., Pinheiro, I. F., Souza, D. H. S., Gouveia, R. F., Mei, L. H. I., et al. (2018). How do cellulose nanocrystals affect the overall properties of biodegradable polymer nanocomposites: A comprehensive review. *European Polymer Journal*, *108*, 274–285. https://doi.org/10.1016/j.eurpolymj.2018.08.045.

Gan, P. G., Sam, S. T., Abdullah, M. F., & Omar, M. F. (2020). Thermal properties of nanocellulose-reinforced composites: A review. *Journal of Applied Polymer Science*, *137*(11). https://doi.org/10.1002/app.48544.

Gardette, M., Perthue, A., Gardette, J. L., Janecska, T., Földes, E., Pukánszky, B., et al. (2013). Photo- and thermal-oxidation of polyethylene: Comparison of mechanisms and influence of unsaturation content. *Polymer Degradation and Stability*, *98*(11), 2383–2390. https://doi.org/10.1016/j.polymdegradstab. 2013.07.017.

Ghasemi, S., Behrooz, R., Ghasemi, I., Yassar, R. S., & Long, F. (2018). Development of nanocellulose-reinforced PLA nanocomposite by using maleated PLA (PLA-g-MA). *Journal of Thermoplastic Composite Materials*, *31*(8), 1090–1101. https://doi.org/10.1177/0892705717734600.

Gomaa, S. F., Madkour, T. M., Moghannem, S., & El-Sherbiny, I. M. (2017). New polylactic acid/ cellulose acetate-based antimicrobial interactive single dose nanofibrous wound dressing mats. *International Journal of Biological Macromolecules*, *105*, 1148–1160. https://doi.org/10.1016/j.ijbiomac.2017.07.145.

Graupner, N., & Müssig, J. (2017). Cellulose fiber-reinforced PLA versus PP. *International Journal of Polymer Science*, *2017*. https://doi.org/10.1155/2017/6059183.

Hao, W., Wang, M., Zhou, F., Luo, H., Xie, X., Luo, F., et al. (2020). A review on nanocellulose as a lightweight filler of polyolefin composites. *Carbohydrate Polymers*, *243*. https://doi.org/10.1016/j.carbpol.2020.116466.

Immonen, K., Lahtinen, P., & Pere, J. (2017). Effects of surfactants on the preparation of nanocellulose-PLA composites. *Bioengineering*, *4*(4). https://doi.org/10.3390/bioengineering4040091.

Jiang, S., Chen, Y., Duan, G., Mei, C., Greiner, A., & Agarwal, S. (2018). Electrospun nanofiber reinforced composites: A review. *Polymer Chemistry*, *9*(20), 2685–2720. https://doi.org/10.1039/c8py00378e.

Kalia, S., Dufresne, A., Cherian, B. M., Kaith, B. S., Avérous, L., Njuguna, J., et al. (2011). Cellulose-based bio- and nanocomposites: A review. *International Journal of Polymer Science*, *2011*. https://doi.org/10.1155/2011/837875.

Khui, PLN, Rahman, MR, & Bakri, MKB. (June 2021). A review on the extraction of cellulose and nanocellulose as a filler through solid waste management. *Journal of Thermoplastic Composite Materials*. https://doi.org/10.1177/08927057211020800.

Kim, H. C., Kim, D., Lee, J. Y., Zhai, L., & Kim, J. (2019). Effect of wet spinning and stretching to enhance mechanical properties of cellulose nanofiber filament. *International Journal of Precision Engineering and Manufacturing—Green Technology*, *6*(3), 567–575. https://doi.org/10.1007/s40684-019-00070-z.

Lee, K. Y., Aitomäki, Y., Berglund, L. A., Oksman, K., & Bismarck, A. (2014). On the use of nanocellulose as reinforcement in polymer matrix composites. *Composites Science and Technology*, *105*, 15–27. https://doi.org/10.1016/j.compscitech.2014.08.032.

Liu, J., Sun, L., Xu, W., Wang, Q., Yu, S., & Sun, J. (2019). Current advances and future perspectives of 3D printing natural-derived biopolymers. *Carbohydrate Polymers*, *207*, 297–316. https://doi.org/10.1016/j.carbpol.2018.11.077.

Lou, C. W., Yao, C. H., Chen, Y. S., Hsieh, T. C., Lin, J. H., & Hsing, W. H. (2008). Manufacturing and properties of PLA absorbable surgical suture. *Textile Research Journal*, *78*(11), 958–965. https://doi.org/10.1177/0040517507087856.

Luyt, A. S., Malik, S. S., & Al-Salem, S. M. (2019). 16—Can biodegradable plastics solve plastic solid waste accumulation? In *Plastics design library* (pp. 403–423). William Andrew Publishing. https://doi.org/10.1016/B978-0-12-813140-4.00016-9.

Marcos, M., & Alain, D. (2017). *Nanocellulose: Common strategies for processing of nanocomposites* (pp. 203–225). American Chemical Society (ACS). https://doi.org/10.1021/bk-2017-1251.ch011.

Mathew, A. P., & Oksman, K. (2013). Processing of bionanocomposites: Solution casting. In *Vol. 5. Handbook of green materials* (pp. 35–52). World Scientific. https://doi.org/10.1142/9789814566469_0018.

Mokhena, T. C., Sefadi, J. S., Sadiku, E. R., John, M. J., Mochane, M. J., & Mtibe, A. (2018). Thermoplastic processing of PLA/cellulose nanomaterials composites. *Polymers*, *1363*. https://doi.org/10.3390/polym10121363.

Morelli, C. L., Marconcini, J. M., Pereira, F. V., Bretas, R. E. S., & Branciforti, M. C. (2012). Extraction and characterization of cellulose nanowhiskers from balsa wood. *Macromolecular Symposia*, *319*(1), 191–195. https://doi.org/10.1002/masy.201100158.

Musioł, M., Sikorska, W., Adamus, G., Janeczek, H., Richert, J., Malinowski, R., et al. (2016). Forensic engineering of advanced polymeric materials. Part III—Biodegradation of thermoformed rigid PLA packaging under industrial composting conditions. *Waste Management*, *52*, 69–76. https://doi.org/10.1016/j.wasman.2016.04.016.

Onwudili, J. A., Insura, N., & Williams, P. T. (2009). Composition of products from the pyrolysis of polyethylene and polystyrene in a closed batch reactor: Effects of temperature and residence time. *Journal of Analytical and Applied Pyrolysis*, *86*(2), 293–303. https://doi.org/10.1016/j.jaap.2009.07.008.

Özge, S. (2017). Poly (lactic acid) films in food packaging systems. *Food Science & Nutrition Technology*. https://doi.org/10.23880/fsnt-16000131.

Paunonen, S. (2013). Strength and barrier enhancements of cellophane and cellulose derivative films: A review. *BioResources*, *8*(2), 3098–3121. https://doi.org/10.15376/biores.8.2.3098-3121.

Phanthong, P., Guan, G., Ma, Y., Hao, X., & Abudula, A. (2016). Effect of ball milling on the production of nanocellulose using mild acid hydrolysis method. *Journal of the Taiwan Institute of Chemical Engineers*, *60*, 617–622. https://doi.org/10.1016/j.jtice.2015.11.001.

Rahman, M. R., & Bakri, M. K. B. (2021). Bamboo cellulose gel/MMT polymer nanocomposites for high strength materials. In M. R. Rahman (Ed.), *Bamboo Polymer Nanocomposites. Engineering Materials*. Cham: Springer. https://doi.org/10.1007/978-3-030-68090-9_7.

Rahman, M. R., & Bakri, M. K. B. (2021). Bamboo nanocellulose reinforced polylactic acid nanocomposites. In M. R. Rahman (Ed.), *Bamboo Polymer Nanocomposites. Engineering Materials*. Cham: Springer. https://doi.org/10.1007/978-3-030-68090-9_8.

Rahman, M. R., & Bakri, M. K. B. (2021). Bamboo cellulose gel/MMT polymer nanocomposites for high strength materials. In M. R. Rahman (Ed.), *Bamboo Polymer Nanocomposites. Engineering Materials*. Cham: Springer. https://doi.org/10.1007/978-3-030-68090-9_7.

Rahman, M. R., Hamdan, S., Jayamani, E., Bakri, M. K. B., & Islam, M. S. (2017). Biocomposite materials and its applications in acoustical comfort and noise control. In M. Jawaid, M. Salit, & O. Alothman (Eds.), *Green Biocomposites. Green Energy and Technology*. Cham: Springer. https://doi.org/10.1007/978-3-319-49382-4_11.

Ronca, S. (2017). Polyethylene. In *Brydson's plastics materials* (8th ed., pp. 247–278). Elsevier Inc. https://doi.org/10.1016/B978-0-323-35824-8.00010-4.

Rothon, R., & DeArmitt, C. (2017). Fillers (including fiber reinforcements). In *Brydson's plastics materials* (8th ed., pp. 169–204). Elsevier Inc. https://doi.org/10.1016/B978-0-323-35824-8.00008-6.

Sanchez-Garcia, M. D., Gimenez, E., & Lagaron, J. M. (2008). Morphology and barrier properties of solvent cast composites of thermoplastic biopolymers and purified cellulose fibers. *Carbohydrate Polymers*, *71*(2), 235–244. https://doi.org/10.1016/j.carbpol.2007.05.041.

Schneider, A., Feussner, H., Schneider, A., & Feussner, H. (2017). *Chapter 6—Classical (Open) Surgery* (pp. 221–267). Academic Press. https://doi.org/10.1016/B978-0-12-803230-5.00006-3.

Sheltami, R. M., Kargarzadeh, H., & Abdullah, I. (2015). Effects of silane surface treatment of cellulose nanocrystals on the tensile properties of cellulose-polyvinyl chloride nanocomposite. *Sains Malaysiana*, *44*(6), 801–810. https://doi.org/10.17576/jsm-2015-4406-05.

Shi, Q., Zhou, C., Yue, Y., Guo, W., Wu, Y., & Wu, Q. (2012). Mechanical properties and in vitro degradation of electrospun bio-nanocomposite mats from PLA and cellulose nanocrystals. *Carbohydrate Polymers*, *90*(1), 301–308. https://doi.org/10.1016/j.carbpol.2012.05.042.

Trache, D., Hussin, M. H., Haafiz, M. K. M., & Thakur, V. K. (2017). Recent progress in cellulose nanocrystals: Sources and production. *Nanoscale*, *9*(5), 1763–1786. https://doi.org/10.1039/c6nr09494e.

Trifol, J., van Drongelen, M., Clegg, F., Plackett, D., Szabo, P., & Daugaard, A. E. (2019). Impact of thermal processing or solvent casting upon crystallization of PLA nanocellulose and/or nanoclay composites. *Journal of Applied Polymer Science*, 47486. https://doi.org/10.1002/app.47486.

Ullah, H., Wahid, F., Santos, H. A., & Khan, T. (2016). Advances in biomedical and pharmaceutical applications of functional bacterial cellulose-based nanocomposites. *Carbohydrate Polymers*, *150*, 330–352. https://doi.org/10.1016/j.carbpol.2016.05.029.

Wang, Z., Xu, J., Lu, Y., Hu, L., Fan, Y., Ma, J., et al. (2017). Preparation of 3D printable micro/nanocellulose-polylactic acid (MNC/PLA) composite wire rods with high MNC constitution. *Industrial Crops and Products*, *109*, 889–896. https://doi.org/10.1016/j.indcrop.2017.09.061.

Wenqiang, L., Yu, D., Dongyan, L., Yuxia, B., & Xiuzhen, L. (2018). Polylactic acid (PLA)/cellulose nanowhiskers (CNWs) composite nanofibers: Microstructural and properties analysis. *Journal of Composites Science*, *4*. https://doi.org/10.3390/jcs2010004.

CHAPTER

Cellulose-based composite carbon nanofibers

9

Muhammad Khusairy Bin Bakri and Md Rezaur Rahman
Department of Chemical Engineering and Energy Sustainability, Faculty of Engineering, Universiti Malaysia Sarawak (UNIMAS), Kota Samarahan, Sarawak, Malaysia

Chapter outline

9.1 Introduction to cellulose

9.1.1 An overview of cellulose-based composite carbon nanofibers

Desirable cellulose properties make cellulose important and versatile material, i.e., high thermal stability, tensile strength and modulus, biocompatibility (Eichhorn et al., 2010; Quesada Cabrera, Meersman, McMillan, & Dmitriev, 2011). Cellulose was used widely in many industries, i.e., smart materials, packaging, coatings, upholstery, food and pharmaceutical. In addition, the excellent mechanical properties of cellulose in composites was extensively used as a bio-based reinforcement (Bledzki & Gassan, 1999; Eichhorn et al., 2010; Gray, 1974; Nabi & Jog, 1999; Wambua, Ivens, & Verpoest, 2003). Wood fibers were one of the main source of cellulose fibers (Bakri, Jayamani, & Hamdan, 2018). Several polymers were applied as a matrix material, i.e., low density polyethylene, polypropylene, high density polyethylene, polyvinyl chloride, and ethylene vinyl acetate copolymer (Anirudhan, Sekhar, Shainy, & Thomas, 2019; Augier, Sperone, Vaca-Garcia, & Borredon, 2007; Bledzki & Faruk, 2006; Dikobe & Luyt, 2007; Hristov & Vlachopoulos, 2007; Karmarkar,

Fundamentals and Recent Advances in Nanocomposites Based on Polymers and Nanocellulose.
https://doi.org/10.1016/B978-0-323-85771-0.00009-9

Chauhan, Modak, & Chanda, 2007; Lei, Wu, Yao, & Xu, 2007; Lu, Negulescu, & Wu, 2005; Nourbakhsh & Ashori, 2008; Sretenovic, Müller, & Gindl, 2006). Other natural fibers have been widely studied, i.e., kenaf, hemp, flax, and jute (Anirudhan et al., 2019; Bos, Molenveld, Teunissen, Van Wingerde, & Van Delft, 2004; Chen & Porter, 1994; Doan, Gao, & Mäder, 2006; Kalia, 2005; López Manchado, Arroyo, Biagiotti, & Kenny, 2003; Pan et al., 2008; Sahoo, Mohanty, & Nayak, 2018; Sahoo, Sahu, Rana, & Das, 2005; Sarkhel & Choudhury, 2008; Thygesen, Daniel, Lilholt, & Thomsen, 2006).

9.1.2 Cellulose-based composite carbon nanofibers

Huge amounts of energy are consumed daily by the modern world society, which forces the researcher to find a suitable alternative toward efficient methods of harvesting, storage, and delivery energy (Kuzmenko et al., 2017). Therefore, to satisfy the need of high storage for the most various applications, which constantly evolving, the boundaries of energy storage must be expanded (Kuzmenko et al., 2017). Thus, to dwell in the niche area of high-power energy storage devices, supercapacitors are the one of the best solutions due to its long cycle life, low maintenance cost, safe, pollution-free operation, and the capability to function at high temperatures (Hibino, Kobayashi, Nagao, & Kawasaki, 2015; Liu, Shen, Song, Chen, & Zhang, 2017; Liu, Yang, Wang, Wang, & Ji, 2017; Zhou, Ye, Wan, & Jia, 2015). For instance, typical advantages of supercapacitors may be used for uninterruptible power supplies, wearable electronics, electric hybrid vehicles, wireless sensors, energy harvester for wind turbines, piezoelectric systems, or solar cells (Bao & Li, 2012; Jost et al., 2013; Kühne, 2010; Lahyani, Venet, Guermazi, & Troudi, 2013; Miller & Simon, 2008; Pavković, Hoić, Deur, & Petrić, 2014; Staaf, Lundgren, & Enoksson, 2014; Yuan et al., 2012). These applications most of placed a strict limitation on available space, especially for the energy storage devices, which brought with it a high volumetric capacitance, which up the need of compact supercapacitors (Wang, Tammela, Zhang, Strømme, & Nyholm, 2014).

Carbon materials used as electrodes for supercapacitors, mostly due its capability to be manufactured from various renewable resources in a cost-effective manner, strong fundamental properties such as high mechanical robustness, electrical conductivity, electrochemical and thermal stability (Rahman, Hamdan, & Bakri, 2021; Béguin, Presser, Balducci, & Frackowiak, 2014; Hu & Hsieh, 2017; Kuzmenko, Naboka, Gatenholm, & Enoksson, 2014; Patrice & Yury, 2008; Zhang & Zhao, 2009). Nevertheless, without considerable weakening of the electrochemical performance, carbon materials need enough high bulk density and thickness to satisfy the volumetric requirements imposed on commercial supercapacitors (Patrice & Yury, 2008). Unfortunately, all these valuable characteristics are a big of a task to be fitted into one material itself. The reason behind the carbon composite materials designed is by combining its constituents beneficial properties (Ghidiu, Lukatskaya, Zhao, Gogotsi, & Barsoum, 2015; Kuzmenko, Naboka, Haque, et al., 2015; Kuzmenko, Naboka, Stafaf, et al., 2015; Li, Li, & Shen, 2013; Niu et al., 2015): (i) Volume-limited portable electronics with fast ionic

transportation that have high packing density and high meso-porosity, and (ii) Low charge transfer resistance that convenient handling with high electrical conductivity that is robust and freestanding nature.

A graphene has a big potential as a constituent of the flawless electrode material, which earned its right. In early 2004, the introduction of graphene has attracted many attentions from many sectors in the world, especially electrical and electronic industries, which seem fully utilized the used to it by incorporated in every application including energy storage (Béguin et al., 2014; Hu & Hsieh, 2017; Kuzmenko et al., 2014; Patrice & Yury, 2008; Zhang & Zhao, 2009). Single sheet of graphene with a high specific surface area of approximately $2630\,m^2\,g^{-1}$, could create many active binding sites for double-layer capacitance (Peigney, Laurent, Flahaut, Bacsa, & Rousset, 2001). The open atomic planar structure of graphene's with the addition of its high electrical conductivity offers fast admittance for electrolyte ions contact on its surface and excellent electrons transferred to a collector. After a few charge–discharge cycles, the high mechanical and chemical stability would allow electrochemical durability of graphene in different electrolytes (Huang, Liang, & Chen, 2012; Huang et al., 2015).

Theoretically, for a supercapacitor, a perfect electrode material is a single-layer graphene. However, with appropriate thickness, the bulk graphene or multi-layer capacitance could practically produce on a large scale, which is far from a single-layer graphene (Wang, Wu, et al., 2011; Wang, Tammela, Zhang, Strømme, & Nyholm, 2014). The Van der Waals of graphene sheets attractions created the undesirable deviation, which is due to stacking or agglomeration that resulting in hindered ion diffusion to the surface of individual sheets (Cao, Yin, & Zhang, 2014; Stankovich et al., 2006). In order to prevent aggregation on the sheet, graphene needs a harmonizing part, which retained the ion permeability, material integrity, and good conductivity (Gao et al., 2013). Electro-spun precursors of the carbon nanofibers (CNFs) possess desired advantages, which attributable to their excellent properties i.e., nanosized sieve-like morphology, well-interconnected porosity, and freestanding nature (Chee et al., 2017; Ghidiu, Lukatskaya, Zhao, Gogotsi, & Barsoum, 2015; Kuzmenko, Naboka, Haque, et al., 2015; Li et al., 2013; Niu et al., 2015).

9.2 Fabrication of cellulose-based composite carbon nanofibers

By carbonization, cellulose nanofibers of the carbon nanofibers can be created from urea, bacterial filter paper, plant-derived cellulose, or nanocellulose (Bao & Li, 2012; Jost et al., 2013; Kühne, 2010; Lahyani et al., 2013; Miller & Simon, 2008; Pavković et al., 2014; Staaf et al., 2014; Yuan et al., 2012). Chemical vapor deposition (CVD) is another method of preparing carbon nanofibers (Price, Ellison, Haberstroh, & Webster, 2004). Most of these carbon nanofibers, such as graphene, or with other carbon nanoparticles, can be further combined. For instance, for a supercapacitor, a nitrogen-doped carbon nanofibers composite paper, reduced bacterial cellulose and graphene oxide (rGO) was premeditated as a mechanically tough,

high-performance, and bend-able electrode (Bacakova et al., 2020). For the newly created material, the bacterial nanocellulose is exploited as a supporting substrate and biomass precursor for the creation of carbon nanofibers by pyrolysis (Ma et al., 2016). Meanwhile, for constructing alternating current (AC) filtering supercapacitors and for the growth of vertically oriented graphene sheets, highly conductive freestanding cross-linked carbon nanofibers, which was derived from bacterial cellulose in a rapid plasma pyrolysis process were used as substrates (Li, Islam, Ren, Li, & Fan, 2019). Through microwave treatment, a slight amount of rGO acts as an active initiator for cellulose nanofibers carbonization (Shi et al., 2019). The mixture of cellulose nanofibers, PVA, and GO by freeze-drying as the carbonization of aerogels enhanced the specific surface area, hydrophobic properties, and adsorption capacity. These materials would be used for environmental protection and oil–water separation (Xu et al., 2018). As for graphene, the cellulose-derived carbon nanofibers is combined with other various nanostructures and nanoparticles i.e., for lithium ion batteries, Fe_3O_4 nanoparticles and TiO_2 films (Xu et al., 2018), for methanol oxidation reaction platinum (Pt) nanoparticles (Yuan et al., 2018), for hydrogen evolution reaction $NiCo_2S_4$ nanoparticles or for lithium-sulfur batteries tin oxide (SnO) nanoparticles (Celik et al., 2018; Li, Islam, Ren, Li, & Fan, 2019; Xu et al., 2019; Li, Wang, Luo, & Huang, 2016; Ma et al., 2016; Shi et al., 2019; Xu et al., 2018; Yuan et al., 2018). Meanwhile, for biomedical applications, carbon nanofibers show promising results, particularly to those bone tissue engineering. In addition, nanoscale diameter produced could be beneficial, especially its compacts nanoscale surface roughness or their composite with poly-lactic-*co*-glycolic acid (PLGA). Particularly fibroblasts, compared with other cell types, the nano roughness promoted preferential adhesion of osteoblasts, which prevent bone implants fibrous encapsulation (Price et al., 2004).

Kuzmenko et al. (2017) studied the sustainable and efficient CNFs and reduced graphene oxide (rGO) composite. They have fabricated the composites via carbonization of the electro-spun fibrous cellulose functionalized with graphene oxide (GO). The abundant functionalities from both sides of polar surface of the water-soluble GO has a strong affinity for hydrophilic cellulose, which contributed to the homogeneous cellulosic fibers' coverage with GO flakes (Béguin, Presser, Balducci, & Frackowiak, 2014; Zhang, Cao, Feng, & Wu, 2012; Zheng, Cai, Ma, & Gong, 2015; Hu & Hsieh, 2017; Kuzmenko et al., 2014; Patrice & Yury, 2008; Zhang & Zhao, 2009). At 800 °C, after simultaneous one-step carbonization/reduction into CNF/rGO of cellulose/GO, this structure remains freestanding and integral. It is noted that the stacking problem of graphene sheet is diminished due to the following factors: (i) The CNFs nano-spacer effect, which stick between graphene layers, and (ii) Solid-state high temperature reduction, which prevents graphene layers agglomeration (Presser et al., 2011).

Cao et al. (Cao et al., 2014; Stankovich et al., 2006) to modify lignin and cellulose-acetate (CA) to be used during the simple phosphating process, which was proposed for a novel energy storage precursor material. The prepared lignin

and CA precursor fibers exhibited good flexibility and thermal stability (Cao et al., 2020). Next, to obtain the biomass-based carbon fibers (CFs), the precursor fibers undergo a short pre-oxidation and carbonization treatment process, which provide uniform fiber diameter, fibrous morphology, good flexibility, high surface areas, and excellent power storage capacity (Cao et al., 2020). For supercapacitor, CFs-5 was prepared with 40% H_3PO_4 content, which obtained the specific capacitance of 346.6 F/g. At the same time, at a power density of 400 W/kg, a high-energy density of 31.5 Wh/kg was delivered by the biomass-based CF supercapacitor. For the preparation of the biomass-based CFs These shows that the introduction of H_3PO_4 reduce the energy consumption of the pre-oxidation treatment process. In the meantime, it will significantly increase the energy storage properties.

To improve the composite mechanical properties, Ghaemi, Tahir, Abdullah, and Kargarzadeh (2017) fabricated natural fiber of cellulose nanofiber (CNF1) and synthetic fiber of carbon nanofiber (CNF2) as reinforcement fillers in polypropylene (PP) polymer. By using the mechanical method, the CNF1 was produced from kenaf bast fibers, while chemical vapor deposition (CVD) technique synthesized the CNF2. While to manufacture the nanocomposites (CNF1/PP and CNF2/PP), the produced fillers were dispersed into polypropylene. It is noted that CNF2/PP composite has a stronger structure than CNF1/PP, while the Young's modulus and tensile stress are higher than CNF1/PP and neat PP (Ghaemi et al., 2017).

9.3 Properties of cellulose-based composite carbon nanofibers

Newly emerging cellulose-based composites carbon nanofibers are smart hybrid materials, which contain cellulose nanoparticles, i.e., nanocrystals and nanofibrils, and carbon nanoparticles, i.e., carbon allotropes (graphene, nanotubes, fullerenes, and nano-diamonds), or other carbon nanostructures (carbon nanofibers, activated carbon, carbon black, carbon quantum dots) (Bacakova et al., 2020). In an aqueous environment, the nanocellulose component and carbon nanoparticles act as dispersing agent and distributes homogeneously, respectively. These composites have many advantageous properties, such as high mechanical flexibility, strength, and stretchability; photodynamic and photothermal activity; high adsorption capacity and nano porous character; tunable thermal, optical transparency and electrical conductivity (Bacakova et al., 2020).

Kuzmenko et al. (2017) studied the sustainable and efficient CNFs and reduced graphene oxide (rGO) composite. In comparison, for supercapacitors with high volumetric, the interpenetrated dense packed of conductive rGO sheets and CNFs makes this structure suitable, which fulfill the demands. Based on previously reported carbon electrodes (Zhang & Zhao, 2009) the properties either too low packing density (Presser et al., 2011) or high in resistance (Zhou et al., 2015). Furthermore, among the 3D graphene nanomaterials, the capability of CNFs and rGO sheets act as excellent conductive bridges, whereas the composite's electrical conductivity is one of the

highest (He & Chen, 2015). For high power applications, this exceptional feature crucially leads to the efficient electron transport (Li, Liu, Jiang, & Thundat, 2016). The orientation of the materials is also vital and another important aspect for the future of energy storage devices (Larcher & Tarascon, 2015). Produced graphene is preferably used only as an additive and not a sustainable carbon material, even though it enhances the valuable properties of electrode composites (Raccichini, Varzi, Passerini, & Scrosati, 2015). Cost-effective biomass-derived nanocarbons is used in a large-scale application and have less harm to the environment than the fossil fuels derived nanocarbons (Titirici et al., 2015). After the Paris Agreement declaration, the world's biggest economies finally unite their efforts which make the agreement relevant for most people to play their role to slow down the detrimental climate changes through reductions of greenhouse gas emissions (UNFCCC, 2015).

9.4 Applications of cellulose-based carbon nanofibers

Cellulose based carbon nanofibers composites show promising properties in biomedical applications, even though it is less frequently used in the biomedical applications compared with other industrial applications. In the biomedical applications, it may include pathogenic bacteria photothermal ablation (Luo et al., 2018), radical scavenging (Awan, Bulger, Berry, & Tam, 2016; Lin et al., 2017), combined chemo-photothermal and photodynamic therapy against cancer (Anirudhan et al., 2019; Herreros-López et al., 2017), drug delivery (Fu et al., 2019; Jia, Yu, Zhang, Dong, & Li, 2016; Luo et al., 2018; Ranjbar & Shahrokhian, 2018), particularly tissue engineering for wound dressings (Buzid, Hayes, Glennon, & Luong, 2019; Jung et al., 2017; Luo et al., 2016; Zheng et al., 2019), and biosensorics (Zhu, Zhou, Liu, & Fu, 2019; Zhu et al., 2019; Zou et al., 2018) (Anirudhan, Deepa, & Binussreejayan, 2018; Fu et al., 2019; Jia, Yu, Zhang, Dong, & Li, 2016; Li, Islam, Ren, Li, & Fan, 2019; Ruiz-Palomero, Benítez-Martínez, Soriano, & Valcárcel, 2017; Santhiago et al., 2017; Shi, Shi Phillips, & Yang, 2013; Xue et al., 2019; Li, Wang, et al., 2016; Ma et al., 2016; Shi et al., 2019; Xu et al., 2018; Yuan et al., 2018). While for the nanocarbons and nanocellulose hybrid materials stimulated the osteogenic differentiation and growth of human bone marrow mesenchymal stem cells (Hibino, Kobayashi, Nagao, & Kawasaki, 2015; Jin et al., 2016; Liu, Yang, et al., 2017; Zhou et al., 2015). For the attachment, particularly under electrical stimulation, it also provided good growth, substrates and differentiation of human neuroblastoma and neural cells (Anirudhan, Sekhar, Shainy, & Thomas, 2019; Chen et al., 2016; Kuzmenko, Karabulut, Pernevik, Enoksson, & Gatenholm, 2018; Bos et al., 2004; Chen & Porter, 1994; Doan et al., 2006; Kalia, 2005; López Manchado et al., 2003; Pan et al., 2008; Sahoo et al., 2005; Sahoo et al., 2018; Sarkhel & Choudhury, 2008; Thygesen et al., 2006). In vivo, from rat dorsal root ganglions, it shows that the enhancement was seen on the stimulated nerve regeneration and outgrowth of neurites in vitro (Sun et al., 2019). The growth also promoted and enhanced angiogenesis, especially on the vascular endothelial cells, and

arteriogenesis in a chick chorioallantoic membrane model (Bonaccorso et al., 2015; Hu et al., 2015; Novoselo, 2004; Novoselov et al., 2012). In dogs, used by surgically applied and disrupted myocardium, it is also noted that it improved cardiac conduction. Moreover, these materials supported the growth mouse subcutaneous fibroblasts, promoted wound healing in vivo in mice, growth in human dermal fibroblasts, and used as antibacterial effect (Ashfaq, Verma, & Khan, 2017; Chakraborty, Ponrasu, Chandel, Dixit, & Muthuvijayan, 2018; Chen, Low, Loi, Merel, & Mohd Cairul Iqbal, 2019; Javanbakht & Namazi, 2018; Mahdavi, Mahmoudi, Anaran, & Simchi, 2016; Ostadhossein et al., 2015; Pedrotty et al., 2019; Wang et al., 2019; Luo et al., 2016; Rasoulzadeh & Namazi, 2017; Shamsipour, Mansouri, & Moradipour, 2019; Wang, Yu, et al., 2019; Wong et al., 2013). Therefore, most of these materials are promising, especially for neural, bone, and vascular tissue engineering, for advanced wound dressings and for creating cardiac patches.

9.5 Conclusions

In conclusion, as for graphene, the cellulose-derived carbon nanofibers is combined with other various nanostructures and nanoparticles which are lithium ion batteries, Fe_3O_4 nanoparticles and TiO_2 films whereas, platinum (Pt) nanoparticles were used for methanol oxidation reaction. $NiCO_2S_4$ and tin oxide (SnO) nanoparticles were used for hydrogen evolution reaction and lithium-sulfur batteries respectively. The carbon nanofibers by using PVA, and GO were carbonization and prepared aerogels for enhanced the specific surface area, hydrophobic properties, and adsorption capacity. These materials are used for environmental protection and oil–water separation. Meanwhile, for biomedical applications, carbon nanofibers show promising results, particularly to those bone tissue engineering.

Acknowledgment

The authors would like to thank and acknowledge Universiti Malaysia Sarawak (UNIMAS) for the support.

References

Anirudhan, T. S., Deepa, J. R., & Binussreejayan. (2018). Electrochemical sensing of cholesterol by molecularly imprinted polymer of silylated graphene oxide and chemically modified nanocellulose polymer. *Materials Science and Engineering C*, *92*, 942–956. https://doi.org/10.1016/j.msec.2018.07.041.

Anirudhan, T. S., Sekhar, V. C., Shainy, F., & Thomas, J. P. (2019). Effect of dual stimuli responsive dextran/nanocellulose polyelectrolyte complexes for chemophotothermal synergistic cancer therapy. *International Journal of Biological Macromolecules*, 776–789. https://doi.org/10.1016/j.ijbiomac.2019.05.218.

Ashfaq, M., Verma, N., & Khan, S. (2017). Highly effective Cu/Zn-carbon micro/nanofiber-polymer nanocomposite-based wound dressing biomaterial against the *P. aeruginosa* multi- and extensively drug-resistant strains. *Materials Science and Engineering*, *77*, 630–641. https://doi.org/10.1016/j.msec.2017.03.187.

Augier, L., Sperone, G., Vaca-Garcia, C., & Borredon, M. E. (2007). Influence of the wood fibre filler on the internal recycling of poly(vinyl chloride)-based composites. *Polymer Degradation and Stability*, *92*(7), 1169–1176. https://doi.org/10.1016/j.polymdegradstab.2007.04.010.

Awan, F., Bulger, E., Berry, R. M., & Tam, K. C. (2016). Enhanced radical scavenging activity of polyhydroxylated C60 functionalized cellulose nanocrystals. *Cellulose*, *23*(6), 3589–3599. https://doi.org/10.1007/s10570-016-1057-0.

Bacakova, L., Pajorova, J., Tomkova, M., Matejka, R., Broz, A., Stepanovska, J., et al. (2020). Applications of nanocellulose/nanocarbon composites: Focus on biotechnology and medicine. *Nanomaterials*, *10*(2). https://doi.org/10.3390/nano10020196.

Bakri, M. K. B., Jayamani, E., Hamdan, S., et al. (2018). Potential of Borneo *Acacia* wood in fully biodegradable bio-composites' commercial production and application. *Polymer Bulletin*, *75*, 5333–5354. https://doi.org/10.1007/s00289-018-2299-9.

Bao, L., & Li, X. (2012). Towards textile energy storage from cotton T-shirts. *Advanced Materials*, *24*(24), 3246–3252. https://doi.org/10.1002/adma.201200246.

Béguin, F., Presser, V., Balducci, A., & Frackowiak, E. (2014). Carbons and electrolytes for advanced supercapacitors. *Advanced Materials*, *26*(14), 2219–2251. https://doi.org/10.1002/adma.201304137.

Bledzki, A. K., & Faruk, O. (2006). Influence of processing temperature on microcellular injection-moulded wood-polypropylene composites. *Macromolecular Materials and Engineering*, *291*(10), 1226–1232. https://doi.org/10.1002/mame.200600210.

Bledzki, A. K., & Gassan, J. (1999). Composites reinforced with cellulose based fibres. *Progress in Polymer Science (Oxford)*, *24*(2), 221–274. https://doi.org/10.1016/S0079-6700(98)00018-5.

Bonaccorso, F., Colombo, L., Yu, G., Stoller, M., Tozzini, V., Ferrari, A. C., et al. (2015). Graphene, related two-dimensional crystals, and hybrid systems for energy conversion and storage. *Science*, *347*(6217). https://doi.org/10.1126/science.1246501.

Bos, H. L., Molenveld, K., Teunissen, W., Van Wingerde, A. M., & Van Delft, D. R. V. (2004). Compressive behaviour of unidirectional flax fibre reinforced composites. *Journal of Materials Science*, *39*(6), 2159–2168. https://doi.org/10.1023/B:JMSC.0000017779.08041.49.

Buzid, A., Hayes, P. E., Glennon, J. D., & Luong, J. H. T. (2019). Captavidin as a regenerable biorecognition element on boron-doped diamond for biotin sensing. *Analytica Chimica Acta*, *1059*, 42–48. https://doi.org/10.1016/j.aca.2019.01.058.

Cao, X., Yin, Z., & Zhang, H. (2014). Three-dimensional graphene materials: Preparation, structures and application in supercapacitors. *Energy and Environmental Science*, *7*(6), 1850–1865. https://doi.org/10.1039/c4ee00050a.

Cao, Q., Zhu, M., Chen, J., Song, Y., Li, Y., & Zhou, J. (2020). Novel lignin-cellulose-based carbon nanofibers as high-performance supercapacitors. *ACS Applied Materials and Interfaces*, *12*(1), 1210–1221. https://doi.org/10.1021/acsami.9b14727.

Celik, K. B., Cengiz, E. C., Sar, T., Dursun, B., Ozturk, O., Akbas, M. Y., et al. (2018). In-situ wrapping of tin oxide nanoparticles by bacterial cellulose derived carbon nanofibers and its application as freestanding interlayer in lithium sulfide based lithium-sulfur batteries.

Journal of Colloid and Interface Science, *530*, 137–145. https://doi.org/10.1016/j.jcis.2018.06.054.

Chakraborty, S., Ponrasu, T., Chandel, S., Dixit, M., & Muthuvijayan, V. (2018). Reduced graphene oxide-loaded nanocomposite scaffolds for enhancing angiogenesis in tissue engineering applications. *Royal Society Open Science*, 172017. https://doi.org/10.1098/rsos.172017.

Chee, W. K., Lim, H. N., Zainal, Z., Harrison, I., Huang, N. M., Andou, Y., et al. (2017). Electrospun nanofiber membranes as ultrathin flexible supercapacitors. *RSC Advances*, *7*(20), 12033–12040. https://doi.org/10.1039/c7ra00406k.

Chen, X. Y., Low, H. R., Loi, X. Y., Merel, L., & Mohd Cairul Iqbal, M. A. (2019). Fabrication and evaluation of bacterial nanocellulose/poly(acrylic acid)/graphene oxide composite hydrogel: Characterizations and biocompatibility studies for wound dressing. *Journal of Biomedical Materials Research—Part B Applied Biomaterials*, *107*(6), 2140–2151. https://doi.org/10.1002/jbm.b.34309.

Chen, H.-. L., & Porter, R. S. (1994). Composite of polyethylene and kenaf, a natural cellulose fiber. *Journal of Applied Polymer Science*, *54*(11), 1781–1783. https://doi.org/10.1002/app.1994.070541121.

Chen, C., Zhang, T., Zhang, Q., Chen, X., Zhu, C., Xu, Y., et al. (2016). Biointerface by cell growth on graphene oxide doped bacterial cellulose/poly(3,4-ethylenedioxythiophene) nanofibers. *ACS Applied Materials and Interfaces*, *8*(16), 10183–10192. https://doi.org/10.1021/acsami.6b01243.

Dikobe, D. G., & Luyt, A. S. (2007). Effect of poly(ethylene-co-glycidyl methacrylate) compatibilizer content on the morphology and physical properties of ethylene vinyl acetate-wood fiber composites. *Journal of Applied Polymer Science*, *104*(5), 3206–3213. https://doi.org/10.1002/app.26080.

Doan, T. T. L., Gao, S. L., & Mäder, E. (2006). Jute/polypropylene composites I. Effect of matrix modification. *Composites Science and Technology*, *66*(7–8), 952–963. https://doi.org/10.1016/j.compscitech.2005.08.009.

Eichhorn, S. J., Dufresne, A., Aranguren, M., Marcovich, N. E., Capadona, J. R., Rowan, S. J., et al. (2010). Review: Current international research into cellulose nanofibres and nanocomposites. *Journal of Materials Science*, *45*(1), 1–33. https://doi.org/10.1007/s10853-009-3874-0.

Fu, W., Dai, Y., Meng, X., Xu, W., Zhou, J., Liu, Z., et al. (2019). Electronic textiles based on aligned electrospun belt-like cellulose acetate nanofibers and graphene sheets: Portable, scalable and eco-friendly strain sensor. *Nanotechnology*, *30*(4). https://doi.org/10.1088/1361-6528/aaed99.

Gao, K., Shao, Z., Li, J., Wang, X., Peng, X., Wang, W., et al. (2013). Cellulose nanofiber-graphene all solid-state flexible supercapacitors. *Journal of Materials Chemistry A*, *1*(1), 63–67. https://doi.org/10.1039/c2ta00386d.

Ghaemi, F., Tahir, P. M., Abdullah, L. C., & Kargarzadeh, H. (2017). Comparative study of cellulose nanofiber and carbon nanofiber effects as reinforcement fillers on mechanical properties of polypropylene composites. *AIP Conference Proceedings*, *1901*. https://doi.org/10.1063/1.5010456. American Institute of Physics Inc.

Ghidiu, M., Lukatskaya, M. R., Zhao, M. Q., Gogotsi, Y., & Barsoum, M. W. (2015). Conductive two-dimensional titanium carbide "clay" with high volumetric capacitance. *Nature*, *516*(7529), 78–81. https://doi.org/10.1038/nature13970.

Gray, D. G. (1974). Polypropylene transcrystallization at the surface of cellulose fibers. *Journal of Polymer Science: Polymer Letters Edition*, 509–515. https://doi.org/10.1002/pol.1974.130120903.

He, S., & Chen, W. (2015). 3D graphene nanomaterials for binder-free supercapacitors: Scientific design for enhanced performance. *Nanoscale*, *7*(16), 6957–6990. https://doi.org/10.1039/c4nr05895j.

Herreros-López, A., Carini, M., Da Ros, T., Carofiglio, T., Marega, C., La Parola, V., et al. (2017). Nanocrystalline cellulose-fullerene: Novel conjugates. *Carbohydrate Polymers*, *164*, 92–101. https://doi.org/10.1016/j.carbpol.2017.01.068.

Hibino, T., Kobayashi, K., Nagao, M., & Kawasaki, S. (2015). High-temperature supercapacitor with a proton-conducting metal pyrophosphate electrolyte. *Scientific Reports*, *5*. https://doi.org/10.1038/srep07903.

Hristov, V., & Vlachopoulos, J. (2007). Influence of coupling agents on melt flow behavior of natural fiber composites. *Macromolecular Materials and Engineering*, *292*(5), 608–619. https://doi.org/10.1002/mame.200600459.

Hu, S., & Hsieh, Y. L. (2017). Lignin derived activated carbon particulates as an electric supercapacitor: Carbonization and activation on porous structures and microstructures. *RSC Advances*, *7*(48), 30459–30468. https://doi.org/10.1039/c7ra00103g.

Hu, C., Song, L., Zhang, Z., Chen, N., Feng, Z., & Qu, L. (2015). Tailored graphene systems for unconventional applications in energy conversion and storage devices. *Energy and Environmental Science*, *8*(1), 31–54. https://doi.org/10.1039/c4ee02594f.

Huang, Y., Liang, J., & Chen, Y. (2012). An overview of the applications of graphene-based materials in supercapacitors. *Small*, *8*(12), 1805–1834. https://doi.org/10.1002/smll.201102635.

Huang, J., Wang, J., Wang, C., Zhang, H., Lu, C., & Wang, J. (2015). Hierarchical porous graphene carbon-based supercapacitors. *Chemistry of Materials*, *27*(6), 2107–2113. https://doi.org/10.1021/cm504618r.

Javanbakht, S., & Namazi, H. (2018). Doxorubicin loaded carboxymethyl cellulose/graphene quantum dot nanocomposite hydrogel films as a potential anticancer drug delivery system. *Materials Science and Engineering C*, *87*, 50–59. https://doi.org/10.1016/j.msec.2018.02.010.

Jia, Y., Yu, H., Zhang, Y., Dong, F., & Li, Z. (2016). Cellulose acetate nanofibers coated layer-by-layer with polyethylenimine and graphene oxide on a quartz crystal microbalance for use as a highly sensitive ammonia sensor. *Colloids and Surfaces B: Biointerfaces*, *148*, 263–269. https://doi.org/10.1016/j.colsurfb.2016.09.007.

Jin, L., Zeng, Z., Kuddannaya, S., Wu, D., Zhang, Y., & Wang, Z. (2016). Biocompatible, free-standing film composed of bacterial cellulose nanofibers-graphene composite. *ACS Applied Materials and Interfaces*, *8*(1), 1011–1018. https://doi.org/10.1021/acsami.5b11241.

Jost, K., Stenger, D., Perez, C. R., McDonough, J. K., Lian, K., Gogotsi, Y., et al. (2013). Knitted and screen printed carbon-fiber supercapacitors for applications in wearable electronics. *Energy and Environmental Science*, *6*(9), 2698–2705. https://doi.org/10.1039/c3ee40515j.

Jung, M., Kim, K., Kim, B., Lee, K. J., Kang, J. W., & Jeon, S. (2017). Vertically stacked nanocellulose tactile sensor. *Nanoscale*, *9*(44), 17212–17219. https://doi.org/10.1039/c7nr03685j.

Kalia, S. (2005). Preparation of flax-g-copolymer reinforced phenol-formaldehyde composites and evaluation of their physical and mechanical properties. *International Journal of Plastics Technology*, *9*, 427–435.

Karmarkar, A., Chauhan, S. S., Modak, J. M., & Chanda, M. (2007). Mechanical properties of wood-fiber reinforced polypropylene composites: Effect of a novel compatibilizer with isocyanate functional group. *Composites Part A: Applied Science and Manufacturing*, *38*(2), 227–233. https:/doi.org/10.1016/j.compositesa.2006.05.005.

Kühne, R. (2010). Electric buses—An energy efficient urban transportation means. *Energy*, *35* (12), 4510–4513. https:/doi.org/10.1016/j.energy.2010.09.055.

Kuzmenko, V., Karabulut, E., Pernevik, E., Enoksson, P., & Gatenholm, P. (2018). Tailor-made conductive inks from cellulose nanofibrils for 3D printing of neural guidelines. *Carbohydrate Polymers*, *189*, 22–30. https:/doi.org/10.1016/j.carbpol.2018.01.097.

Kuzmenko, V., Naboka, O., Gatenholm, P., & Enoksson, P. (2014). Ammonium chloride promoted synthesis of carbon nanofibers from electrospun cellulose acetate. *Carbon*, *67*, 694–703. https:/doi.org/10.1016/j.carbon.2013.10.061.

Kuzmenko, V., Naboka, O., Staaf, H., Haque, M., Göransson, G., Lundgren, P., et al. (2015). Capacitive effects of nitrogen doping on cellulose-derived carbon nanofibers. *Materials Chemistry and Physics*, *160*, 59–65. https:/doi.org/10.1016/j.matchemphys.2015.04.006.

Kuzmenko, V., Naboka, O., Haque, M., Staaf, H., Göransson, G., Gatenholm, P., et al. (2015). Sustainable carbon nanofibers/nanotubes composites from cellulose as electrodes for supercapacitors. *Energy*, *90*, 1490–1496. https:/doi.org/10.1016/j.energy.2015.06.102.

Kuzmenko, V., Wang, N., Haque, M., Naboka, O., Flygare, M., Svensson, K., et al. (2017). Cellulose-derived carbon nanofibers/graphene composite electrodes for powerful compact supercapacitors. *RSC Advances*, *7*(73), 45968–45977. https:/doi.org/10.1039/c7ra07533b.

Lahyani, A., Venet, P., Guermazi, A., & Troudi, A. (2013). Battery/supercapacitors combination in uninterruptible power supply (UPS). *IEEE Transactions on Power Electronics*, *28* (4), 1509–1522. https:/doi.org/10.1109/TPEL.2012.2210736.

Larcher, D., & Tarascon, J. M. (2015). Towards greener and more sustainable batteries for electrical energy storage. *Nature Chemistry*, *7*(1), 19–29. https:/doi.org/10.1038/nchem.2085.

Lei, Y., Wu, Q., Yao, F., & Xu, Y. (2007). Preparation and properties of recycled HDPE/natural fiber composites. *Composites Part A: Applied Science and Manufacturing*, *38*(7), 1664–1674. https:/doi.org/10.1016/j.compositesa.2007.02.001.

Li, Y., Li, Z., & Shen, P. K. (2013). Simultaneous formation of ultrahigh surface area and three-dimensional hierarchical porous graphene-like networks for fast and highly stable supercapacitors. *Advanced Materials*, *25*(17), 2474–2480. https:/doi.org/10.1002/adma.201205332.

Li, S., Wang, M., Luo, Y., & Huang, J. (2016). Bio-inspired hierarchical nanofibrous Fe3O4-TiO2-carbon composite as a high-performance anode material for Lithium-ion batteries. *ACS Applied Materials and Interfaces*, *8*(27), 17343–17351. https:/doi.org/10.1021/acsami.6b05206.

Li, Z., Liu, J., Jiang, K., & Thundat, T. (2016). Carbonized nanocellulose sustainably boosts the performance of activated carbon in ionic liquid supercapacitors. *Nano Energy*, *25*, 161–169. https:/doi.org/10.1016/j.nanoen.2016.04.036.

Li, W., Islam, N., Ren, G., Li, S., & Fan, Z. (2019). AC-filtering supercapacitors based on edge oriented vertical graphene and cross-linked carbon nanofiber. *Materials*, *12*(4). https:/doi.org/10.3390/ma12040604.

Lin, J., Zhong, Z., Li, Q., Tan, Z., Lin, T., Quan, Y., et al. (2017). Facile low-temperature synthesis of cellulose nanocrystals carrying buckminsterfullerene and its radical scavenging property in vitro. *Biomacromolecules*, *18*(12), 4034–4040. https:/doi.org/10.1021/acs.biomac.7b01095.

Liu, Q., Yang, J., Wang, R., Wang, H., & Ji, S. (2017). Manganese dioxide core-shell nanostructure to achieve excellent cycling stability for asymmetric supercapacitor applications. *RSC Advances*, *7*(53), 33635–33641. https:/doi.org/10.1039/c7ra06076a.

Liu, X., Shen, H., Song, S., Chen, W., & Zhang, Z. (2017). Accelerated biomineralization of graphene oxide—Incorporated cellulose acetate nanofibrous scaffolds for mesenchymal stem cell osteogenesis. *Colloids and Surfaces B: Biointerfaces*, *159*, 251–258. https:/doi.org/10.1016/j.colsurfb.2017.07.078.

López Manchado, M. A., Arroyo, M., Biagiotti, J., & Kenny, J. M. (2003). Enhancement of mechanical properties and interfacial adhesion of PP/EPDM/flax fiber composites using maleic anhydride as a compatibilizer. *Journal of Applied Polymer Science*, *90*(8), 2170–2178. https:/doi.org/10.1002/app.12866.

Lu, J. Z., Negulescu, I. I., & Wu, Q. (2005). Maleated wood-fiber/high-density-polyethylene composites: Coupling mechanisms and interfacial characterization. *Composite Interfaces*, *12*(1–2), 125–140. https:/doi.org/10.1163/1568554053542133.

Luo, X., Zhang, H., Cao, Z., Cai, N., Xue, Y., & Yu, F. (2016). A simple route to develop transparent doxorubicin-loaded nanodiamonds/cellulose nanocomposite membranes as potential wound dressings. *Carbohydrate Polymers*, *143*, 231–238. https:/doi.org/10.1016/j.carbpol.2016.01.076.

Luo, J., Deng, W., Yang, F., Wu, Z., Huang, M., & Gu, M. (2018). Gold nanoparticles decorated graphene oxide/nanocellulose paper for NIR laser-induced photothermal ablation of pathogenic bacteria. *Carbohydrate Polymers*, *198*, 206–214. https:/doi.org/10.1016/j.carbpol.2018.06.074.

Ma, L., Liu, R., Niu, H., Xing, L., Liu, L., & Huang, Y. (2016). Flexible and freestanding supercapacitor electrodes based on nitrogen-doped carbon networks/graphene/bacterial cellulose with ultrahigh areal capacitance. *ACS Applied Materials and Interfaces*, *8*(49), 33608–33618. https:/doi.org/10.1021/acsami.6b11034.

Mahdavi, M., Mahmoudi, N., Anaran, F. R., & Simchi, A. (2016). Electrospinning of nanodiamond-modified polysaccharide nanofibers with physico-mechanical properties close to natural skins. *Marine Drugs*, *14*(7). https:/doi.org/10.3390/md14070128.

Miller, J. R., & Simon, P. (2008). Electrochemical capacitors for energy management. *Science*, *321*(5889), 651. https:/doi.org/10.1126/science.1158736.

Nabi, S. D., & Jog, J. P. (1999). Natural fiber polymer composites: A review. *Advances in Polymer Technology*, 351–363. https:/doi.org/10.1002/(SICI)1098-2329(199924)18:4<351::AID-ADV6>3.3.CO;2-O.

Niu, Z., Liu, L., Zhang, L., Zhou, W., Chen, X., & Xie, S. (2015). Programmable nanocarbon-based architectures for flexible supercapacitors. *Advanced Energy Materials*, *5*(23). https:/doi.org/10.1002/aenm.201500677.

Nourbakhsh, A., & Ashori, A. (2008). Fundamental studies on wood-plastic composites: Effects of fiber concentration and mixing temperature on the mechanical properties of poplar/PP composite. *Polymer Composites*, *29*(5), 569–573. https:/doi.org/10.1002/pc.20578.

Novoselov, K. S. (2004). Electric field effect in atomically thin carbon films. *Science*, 666–669. https:/doi.org/10.1126/science.1102896.

Novoselov, K. S., Fal'Ko, V. I., Colombo, L., Gellert, P. R., Schwab, M. G., & Kim, K. (2012). A roadmap for graphene. *Nature*, *490*(7419), 192–200. https://doi.org/10.1038/nature11458.

Ostadhossein, F., Mahmoudi, N., Morales-Cid, G., Tamjid, E., Navas-Martos, F. J., Soriano-Cuadrado, B., et al. (2015). Development of chitosan/bacterial cellulose composite films containing nanodiamonds as a potential flexible platform for wound dressing. *Materials*, *8*(9), 6401–6418. https://doi.org/10.3390/ma8095309.

Pan, P., Zhu, B., Dong, T., Serizawa, S., Iji, M., & Inoue, Y. (2008). Kenaf fiber/poly(ε-caprolactone) biocomposite with enhanced crystallization rate and mechanical properties. *Journal of Applied Polymer Science*, *107*(6), 3512–3519. https://doi.org/10.1002/app.27470.

Patrice, S., & Yury, G. (2008). Materials for electrochemical capacitors. *Nature Materials*, 845–854. https://doi.org/10.1038/nmat2297.

Pavković, D., Hoić, M., Deur, J., & Petrić, J. (2014). Energy storage systems sizing study for a high-altitude wind energy application. *Energy*, *76*, 91–103. https://doi.org/10.1016/j.energy.2014.04.001.

Pedrotty, D. M., Kuzmenko, V., Karabulut, E., Sugrue, A. M., Livia, C., Vaidya, V. R., et al. (2019). Three-dimensional printed biopatches with conductive ink facilitate cardiac conduction when applied to disrupted myocardium. *Circulation Arrhythmia and Electrophysiology*, *12*(3). https://doi.org/10.1161/CIRCEP.118.006920.

Peigney, A., Laurent, C., Flahaut, E., Bacsa, R. R., & Rousset, A. (2001). Specific surface area of carbon nanotubes and bundles of carbon nanotubes. *Carbon*, *39*(4), 507–514. https://doi.org/10.1016/S0008-6223(00)00155-X.

Presser, V., Zhang, L., Niu, J. J., McDonough, J., Perez, C., Fong, H., et al. (2011). Flexible nano-felts of carbide-derived carbon with ultra-high power handling capability. *Advanced Energy Materials*, *1*(3), 423–430. https://doi.org/10.1002/aenm.201100047.

Price, R. L., Ellison, K., Haberstroh, K. M., & Webster, T. J. (2004). Nanometer surface roughness increases select osteoblast adhesion on carbon nanofiber compacts. *Journal of Biomedical Materials Research—Part A*, *70*(1), 129–138. https://doi.org/10.1002/jbm.a.30073.

Quesada Cabrera, R., Meersman, F., McMillan, P. F., & Dmitriev, V. (2011). Nanomechanical and structural properties of native cellulose under compressive stress. *Biomacromolecules*, *12*(6), 2178–2183. https://doi.org/10.1021/bm200253h.

Raccichini, R., Varzi, A., Passerini, S., & Scrosati, B. (2015). The role of graphene for electrochemical energy storage. *Nature Materials*, *14*(3), 271–279. https://doi.org/10.1038/nmat4170.

Rahman, M. R., Hamdan, S., & Bakri, M. K. B. (2021). Polylactic acid activated bamboo carbon nanocomposites. In M. R. Rahman (Ed.), *Bamboo Polymer Nanocomposites. Engineering Materials*. Cham: Springer. https://doi.org/10.1007/978-3-030-68090-9_4.

Ranjbar, S., & Shahrokhian, S. (2018). Design and fabrication of an electrochemical aptasensor using Au nanoparticles/carbon nanoparticles/cellulose nanofibers nanocomposite for rapid and sensitive detection of *Staphylococcus aureus*. *Bioelectrochemistry*, *123*, 70–76. https://doi.org/10.1016/j.bioelechem.2018.04.018.

Rasoulzadeh, M., & Namazi, H. (2017). Carboxymethyl cellulose/graphene oxide bionanocomposite hydrogel beads as anticancer drug carrier agent. *Carbohydrate Polymers*, *168*, 320–326. https://doi.org/10.1016/j.carbpol.2017.03.014.

Ruiz-Palomero, C., Benítez-Martínez, S., Soriano, M. L., & Valcárcel, M. (2017). Fluorescent nanocellulosic hydrogels based on graphene quantum dots for sensing laccase. *Analytica Chimica Acta*, *974*, 93–99. https://doi.org/10.1016/j.aca.2017.04.018.

Sahoo, P. K., Sahu, G. C., Rana, P. K., & Das, A. K. (2005). Preparation, characterization, and biodegradability of jute-based natural fiber composite superabsorbents. *Advances in Polymer Technology*, *24*(3), 208–214. https://doi.org/10.1002/adv.20042.

Sahoo, S. K., Mohanty, S., & Nayak, S. K. (2018). Mechanical, dynamic mechanical, and interfacial properties of sisal fiber-reinforced composite with epoxidized soybean oil-based epoxy matrix. *Polymer Composites*, *39*(6), 2065–2072. https://doi.org/10.1002/pc.24168.

Santhiago, M., Corrêa, C. C., Bernardes, J. S., Pereira, M. P., Oliveira, L. J. M., Strauss, M., et al. (2017). Flexible and foldable fully-printed carbon black conductive nanostructures on paper for high-performance electronic, electrochemical, and wearable devices. *ACS Applied Materials and Interfaces*, *9*(28), 24365–24372. https://doi.org/10.1021/acsami.7b06598.

Sarkhel, G., & Choudhury, A. (2008). Dynamic mechanical and thermal properties of PE-EPDM based jute fiber composites. *Journal of Applied Polymer Science*, *108*(6), 3442–3453. https://doi.org/10.1002/app.28024.

Shamsipour, M., Mansouri, A. M., & Moradipour, P. (2019). Temozolomide conjugated carbon quantum dots embedded in core/shell nanofibers prepared by coaxial electrospinning as an implantable delivery system for cell imaging and sustained drug release. *AAPS PharmSciTech*, *20*(7). https://doi.org/10.1208/s12249-019-1466-0.

Shi, Z., Shi Phillips, G. O., & Yang, G. (2013). Nanocellulose electroconductive composites. *Nanoscale*, *5*(8), 3194–3201. https://doi.org/10.1039/c3nr00408b.

Shi, Q., Liu, D., Wang, Y., Zhao, Y., Yang, X., & Huang, J. (2019). High-performance sodium-ion battery anode via rapid microwave carbonization of natural cellulose nanofibers with graphene initiator. *Small*, *15*(41). https://doi.org/10.1002/smll.201901724.

Sretenovic, A., Müller, U., & Gindl, W. (2006). Mechanism of stress transfer in a single wood fibre-LDPE composite by means of electronic laser speckle interferometry. *Composites Part A: Applied Science and Manufacturing*, *37*(9), 1406–1412. https://doi.org/10.1016/j.compositesa.2005.06.018.

Staaf, L. G. H., Lundgren, P., & Enoksson, P. (2014). Present and future supercapacitor carbon electrode materials for improved energy storage used in intelligent wireless sensor systems. *Nano Energy*, *9*, 128–141. https://doi.org/10.1016/j.nanoen.2014.06.028.

Stankovich, S., Dikin, D. A., Dommett, G. H. B., Kohlhaas, K. M., Zimney, E. J., Stach, E. A., et al. (2006). Graphene-based composite materials. *Nature*, *442*(7100), 282–286. https://doi.org/10.1038/nature04969.

Sun, Y., Quan, Q., Meng, H., Zheng, Y., Peng, J., Hu, Y., et al. (2019). Enhanced neurite outgrowth on a multiblock conductive nerve scaffold with self-powered electrical stimulation. *Advanced Healthcare Materials*, *8*(10). https://doi.org/10.1002/adhm.201900127.

Thygesen, A., Daniel, G., Lilholt, H., & Thomsen, A. B. (2006). Hemp fiber microstructure and use of fungal defibration to obtain fibers for composite materials. *Journal of Natural Fibers*, *2*(4), 19–37. https://doi.org/10.1300/J395v02n04_02.

Titirici, M. M., White, R. J., Brun, N., Budarin, V. L., Su, D. S., Del Monte, F., et al. (2015). Sustainable carbon materials. *Chemical Society Reviews*, *44*(1), 250–290. https://doi.org/10.1039/c4cs00232f.

UNFCCC. (2015). *Adoption of the Paris agreement*. https://unfccc.int/resource/docs/2015/cop21/eng/l09r01.pdf.

Wambua, P., Ivens, J., & Verpoest, I. (2003). Natural fibres: Can they replace glass in fibre reinforced plastics? *Composites Science and Technology*, *63*(9), 1259–1264. https://doi.org/10.1016/S0266-3538(03)00096-4.

Wang, Y., Wu, Y., Huang, Y., Zhang, F., Yang, X., Ma, Y., et al. (2011). Preventing graphene sheets from restacking for high-capacitance performance. *Journal of Physical Chemistry C*, *115*(56), 23192–23197. https://doi.org/10.1021/jp206444e.

Wang, Z., Tammela, P., Zhang, P., Strømme, M., & Nyholm, L. (2014). High areal and volumetric capacity sustainable all-polymer paper-based supercapacitors. *Journal of Materials Chemistry A*, *2*(39), 16761–16769. https://doi.org/10.1039/c4ta03724c.

Wang, X., Yu, K., An, R., Han, L., Zhang, Y., Shi, L., et al. (2019). Self-assembling GO/modified HEC hybrid stabilized Pickering emulsions and template polymerization for biomedical hydrogels. *Carbohydrate Polymers*, *207*, 694–703. https://doi.org/10.1016/j.carbpol.2018.12.034.

Wang, Y., Shi, L., Wu, H., Li, Q., Hu, W., Zhang, Z., et al. (2019). Graphene oxide-IPDI-Ag/ZnO@Hydroxypropyl cellulose nanocomposite films for biological wound-dressing applications. *ACS Omega*, *4*(13), 15373–15381. https://doi.org/10.1021/acsomega.9b01291.

Wong, B. S., Yoong, S. L., Jagusiak, A., Panczyk, T., Ho, H. K., Ang, W. H., et al. (2013). Carbon nanotubes for delivery of small molecule drugs. *Advanced Drug Delivery Reviews*, *65*(15), 1964–2015. https://doi.org/10.1016/j.addr.2013.08.005.

Xu, Z., Zhou, H., Tan, S., Jiang, X., Wu, W., Shi, J., et al. (2018). Ultralight super-hydrophobic carbon aerogels based on cellulose nanofibers/poly(vinyl alcohol)/graphene oxide (CNFs/PVA/GO) for highly effective oil-water separation. *Beilstein Journal of Nanotechnology*, *9*(1), 508–519. https://doi.org/10.3762/bjnano.9.49.

Xu, J., Rong, J., Qiu, F., Zhu, Y., Mao, K., Fang, Y., et al. (2019). Highly dispersive NiCo2S4 nanoparticles anchored on nitrogen-doped carbon nanofibers for efficient hydrogen evolution reaction. *Journal of Colloid and Interface Science*, *555*, 294–303. https://doi.org/10.1016/j.jcis.2019.07.104.

Xue, T., Sheng, Y., Xu, J., Li, Y., Lu, X., Zhu, Y., et al. (2019). In-situ reduction of Ag + on black phosphorene and its NH2-MWCNT nanohybrid with high stability and dispersibility as nanozyme sensor for three ATP metabolites. *Biosensors and Bioelectronics*, *145*. https://doi.org/10.1016/j.bios.2019.111716.

Yuan, L., Xiao, X., Ding, T., Zhong, J., Zhang, X., Shen, Y., et al. (2012). Paper-based supercapacitors for self-powered nanosystems. *Angewandte Chemie—International Edition*, *51*(20), 4934–4938. https://doi.org/10.1002/anie.201109142.

Yuan, F., Huang, Y., Fan, M., Chen, C., Qian, J., Hao, Q., et al. (2018). N-doped carbon nanofibrous network derived from bacterial cellulose for the loading of Pt nanoparticles for methanol oxidation reaction. *Chemistry—a European Journal*, *24*(8), 1844–1852. https://doi.org/10.1002/chem.201704266.

Zhang, J., Cao, Y., Feng, J., & Wu, P. (2012). Graphene-oxide-sheet-induced gelation of cellulose and promoted mechanical properties of composite aerogels. *Journal of Physical Chemistry C*, *116*(14), 8063–8068. https://doi.org/10.1021/jp2109237.

Zhang, L., & Zhao, X. S. (2009). Carbon-based materials as supercapacitor electrodes. *Chemical Society Reviews*, *38*(9), 2520–2531. https://doi.org/10.1039/b813846j.

Zheng, Q., Cai, Z., Ma, Z., & Gong, S. (2015). Cellulose nanofibril/reduced graphene oxide/carbon nanotube hybrid aerogels for highly flexible and all-solid-state supercapacitors.

ACS Applied Materials and Interfaces, *7*(5), 3263–3271. https://doi.org/10.1021/am507999s.

Zheng, C., Yue, Y., Gan, L., Xu, X., Mei, C., & Han, J. (2019). Highly stretchable and self-healing strain sensors based on nanocellulose-supported graphene dispersed in electro-conductive hydrogels. *Nanomaterials*, *9*(7). https://doi.org/10.3390/nano9070937.

Zhou, Q., Ye, X., Wan, Z., & Jia, C. (2015). A three-dimensional flexible supercapacitor with enhanced performance based on lightweight, conductive graphene-cotton fabric electrode. *Journal of Power Sources*, *296*, 186–196. https://doi.org/10.1016/j.jpowsour.2015.07.012.

Zhu, L., Zhou, X., Liu, Y., & Fu, Q. (2019). Highly sensitive, ultrastretchable strain sensors prepared by pumping hybrid fillers of carbon nanotubes/cellulose nanocrystal into electro-spun polyurethane membranes. *ACS Applied Materials and Interfaces*, *11*(13), 12968–12977. https://doi.org/10.1021/acsami.9b00136.

Zhu, P., Liu, Y., Fang, Z., Kuang, Y., Zhang, Y., Peng, C., et al. (2019). Flexible and highly sensitive humidity sensor based on cellulose nanofibers and carbon nanotube composite film. *Langmuir*, *35*(14), 4834–4842. https://doi.org/10.1021/acs.langmuir.8b04259.

Zou, Y., Zhang, Y., Xu, Y., Chen, Y., Huang, S., Lyu, Y., et al. (2018). Portable and label-free detection of blood bilirubin with graphene-isolated-Au-nanocrystals paper strip. *Analytical Chemistry*, *90*(22), 13687–13694. https://doi.org/10.1021/acs.analchem.8b04058.

CHAPTER

Cellulose-reinforced rubber composites

10

Md Rezaur Rahman, Perry Law Nyuk Khui, and Muhammad Khusairy Bin Bakri
Department of Chemical Engineering and Energy Sustainability, Faculty of Engineering, Universiti Malaysia Sarawak (UNIMAS), Kota Samarahan, Sarawak, Malaysia

Chapter outline

10.1 An introduction to cellulose reinforced rubber composites

Cellulose reinforced rubber composites generally consist of the matrix made from rubber and cellulose as reinforcement filler material. Rubbers are known as "elastomers," a class of polymer which is amorphous with "elastic" properties, which are attributed to the notably low Young's modulus and high yield strain (McKeen & McKeen, 2019). Elastomers could be categorized as thermoset elastomers and thermoplastic elastomer; depending on its ambient conditions, where they are relatively malleable. Some common examples of the different types of rubbers include:

Natural rubber
Polyurethane
Styrene-butadiene rubber
Butyl rubber
Nitrile (acrylonitrile butadiene rubber)
Silicone (polysiloxane)

Fundamentals and Recent Advances in Nanocomposites Based on Polymers and Nanocellulose.
https://doi.org/10.1016/B978-0-323-85771-0.00013-0

Neoprene (polychloroprene)
Ethylene propylene diene monomer (EPDM)

Application wise, rubbers are a multi-purpose materials, where it could be used as sealers, coatings, adhesives, and molded elastic or rubberized products. The mechanical, electrical, chemical, and thermal properties of rubbers are attractive, especially in the field of biomedical, engineering and science (McKeen & McKeen, 2019). However, most of these rubbers need to undergo specific treatments and manufacturing processes, in order to cater for different application needs, in which modifies the rubber's properties. Another method of modifying the rubber's properties, includes adding reinforcement materials, i.e., cellulose. Researchers implement cellulose into polymer matrices to modify the fabricated composites properties for different applications needs (Chakrabarty & Teramoto, 2018; Kalia et al., 2011).

Cellulose is a renewable organic polymer extracted majority from natural plant source (Khui, Rahman, & Bakri, 2021). Depending on the extraction processes, cellulose from plant sources commonly yield as (i) crystalline nanocellulose (CNC) and (ii) cellulose nanofibrils (CNF). There are many derivations of the cellulose, depending on the treatment and manufacturing processes (Rahman & Bakri, 2021a, 2021b; Rahman, Hamdan, & Ngaini, 2019). Nevertheless, the resulting cellulose are applicable reinforcement material, acting mostly as filler for the fabricated composite materials (Jonoobi et al., 2015). In comparison to other form of reinforcement materials, CNC and CNF have an unique key features such as high surface area, lightweight, biodegradability, with good mechanical properties (Mariano, El Kissi, & Dufresne, 2014). If cellulose is added into the biodegradable polymer matrix, the biodegradability properties of the composite material at end-of-life state could be improve (Nasir, Hashim, Sulaiman, & Asim, 2017). Due to cellulose being derived from a natural plant source, hence it increases the organic content in the composite material. Considering the performance of the composite material remains similar to other synthetic material polymer reinforced composites. Biodegradability is a significant issue to address due to on-going problems of plastic waste availability globally. The incorporation of cellulose and the applications of cellulose, as reinforcement/biocompatible materials are gaining popular among researchers (Robles, Labidi, Halász, & Csóka, 2017).

The reinforcing rubbers requires materials that are rigid to modify the rubber formulation. The incorporation of fillers into rubbers are optimized to achieve a reinforced rubber nanocomposite with the desired properties, which can cater it for a specific application or performance specifications. General preparation processes of reinforced rubber nanocomposites include (Nunes, 2017; Srivastava & Mishra, 2018);

Solvent blending/casting
Melt intercalation/blending
In situ polymerization
Latex compounding/blending

There are numerous preparation process for fabricating rubber nanocomposites; however, many literatures show that rubber nanocomposites are mostly prepared by latex

blending, solution, and melt blending for convenience of certain production of materials applications (Nunes, 2017; Srivastava & Mishra, 2018; Wu, Ma, Wang, & Zhang, 2004). Additionally, most of the literatures utilizing cellulose as fillers for elastomeric-based nanocomposites involves using natural rubbers as matrices. This trend could be due to the availability of natural rubber, and ease of processing or method.

10.2 Solution blending of cellulose and rubber nanocomposites

Solution blending involves the dispersion of fillers and blending of rubber in the appropriate solvent with proper optimization formulation. The fillers could be dispersed in a separate solvent solution to allow swelling to occur, prior to blending in the dissolution rubber. Depending on the cellulose derivatives, CNC and CNF could be swollen and dissolution by organic solvents. However, both filler and rubber could be processed together in the same solvent type (Nunes, 2014, 2017). Most of the literatures, which uses cellulose as fillers, prepare the polymeric-nanocomposites by incorporating the cellulose into the dissolution matrix (Azeredo, Rosa, & Mattoso, 2017; Jonoobi et al., 2015; Kalia et al., 2011).

Blending processes such as shear mixing, magnetic stirrer, and ultrasonication are typically utilized by researchers for solution blending, especially during the intercalation of filler process and matrix occurs (Rane et al., 2018). The blended solution is casted into a specific mold and the solvent is left to evaporate under controlled conditions under certain pressure or vacuum. Typically, the resulting reinforced rubber nanocomposites from solution blending may resulted in the form of sheets or films (Pramanik, Srivastava, Samantaray, & Bhowmick, 2003). Common types of rubbers that could be prepared by solution blending includes, i.e., natural rubber, styrene-butadiene rubber, and silicone rubber. However, the preparation of solution blending is not environmentally friendly and cost effective due to the excessive amount of solvents used during the processing process (Srivastava & Mishra, 2018). Fig. 10.1 illustrates a general solution blending flowchart for preparing cellulose reinforced rubber nanocomposites.

10.3 Melt blending of cellulose and rubber nanocomposites

Melt blending for rubber nanocomposites are mainly for rubbers that are categorized as thermoplastic elastomers (Bao, Yang, Liu, Xie, & Yang, 2015). The melt blending process involves an external heat source combination with a mechanical process, which melt blends the matrix and filler to form rubber nanocomposites (Lu et al., 2007). There are six classes of thermoplastics elastomer (rubbers) which could be prepared by melt blending includes; (i) polystyrenes, (ii) polyolefins, (iii) polyetherimides, (iv) polyurethanes, (v) polyesters, and (vi) polyamides (Amin & Amin, 2011). The process of melt blending of rubber with filler is an effective way to fabricate rubber nanocomposites for specific commercial applications. The mechanical

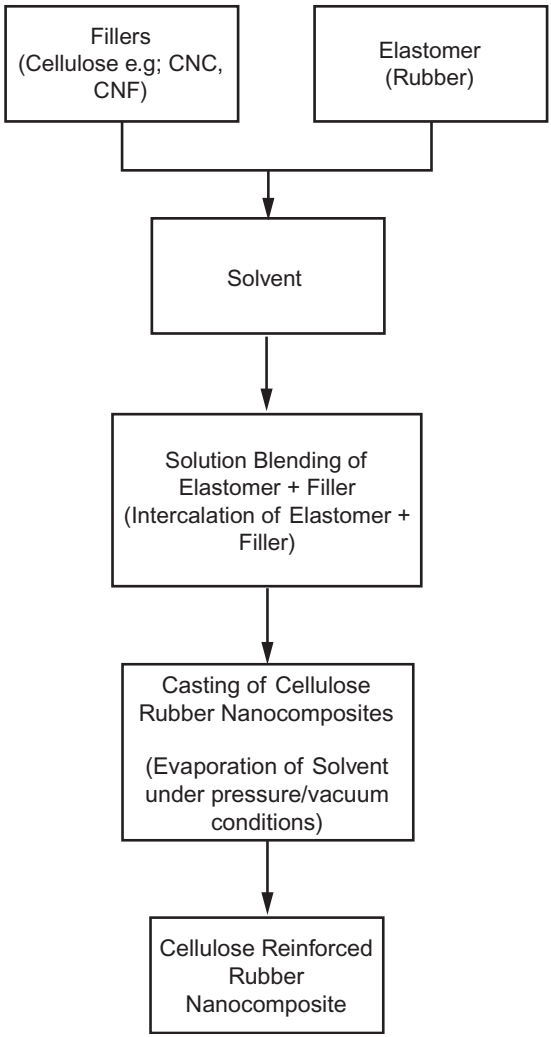

FIG. 10.1

Solution blending process for cellulose reinforced rubber nanocomposites.

processes of the melt blending may affect the homogeneous dispersion of fillers by agglomeration, hence affecting the rubber nanocomposites properties (Norazlina, Firdaus, & Hafizuddin, 2015). However, melt blending is more environmentally friendly, and does not require solvents, in comparison to the solution blending (Srivastava & Mishra, 2018). Fig. 10.2 illustrates a general melt blending flowchart for preparing cellulose reinforced rubber nanocomposites.

The general melt blending process combines both cellulose and rubber into a masterbatch, prior to the heating and mechanical process, whereas this step is also known as dry mixing. Dry mixing may help disperse the cellulose in the matrix

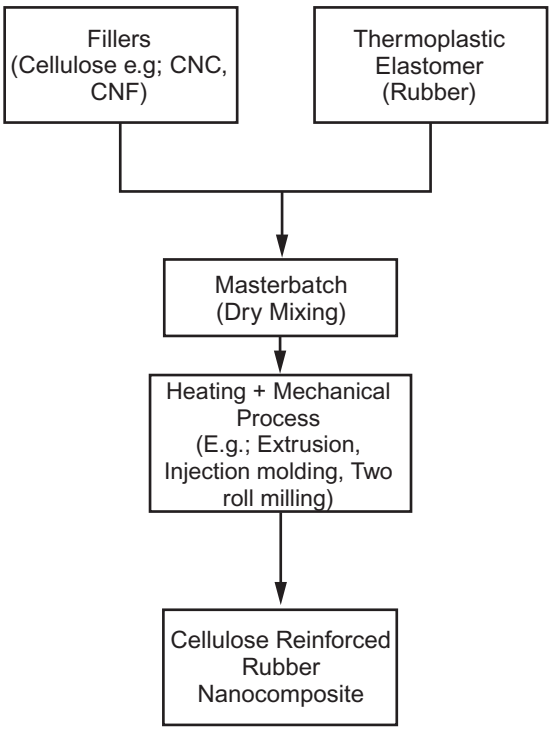

FIG. 10.2

Melt blending process for cellulose reinforced rubber nanocomposites.

better, influencing the melt blending process, and assisting the intercalation between cellulose and rubber (Narimissa, Gupta, Kao, Choi, & Bhattacharya, 2015). However, some manufacturers initially melt the rubber matrix, and introduce the fillers (cellulose) afterwards during the heating and mechanical process (Tarawneh, Ahmad, Yahya, & Rozaidi, 2011). If the heating and mechanical processing is inadequate, agglomeration of fillers (cellulose) might occur, as well as poor matrix, and filler intercalation (Ercan, Durmus, & Kaşgöz, 2017) which will directly affect the final products or materials properties.

10.3.1 Latex blending

Over the years, latex compounding or blending technology has been developed to effectively overcome difficulties in manufacturing. Examples of the difficulties of manufacturing stems mostly from proper dispersion of fillers within the elastomeric matrix and the management of solvents used (Hao et al., 2019).

The developed latex blending technology could be separated into two main categories:

In-situ emulsion polymerization
Latex mixing

As most these rubber products origin is sourced from natural rubber in the form of latex, hence latex mixing has become a more practical choice, compared to in situ emulsion polymerization. However, even with the developments made to latex blending technology, problems of obtaining a stable aqueous dispersion of fillers is still arise and still a difficult task to be overcome. A general latex blending preparation process for cellulose reinforced rubber nanocomposites is shown in Fig. 10.3.

Most of the literatures synthesize reinforced latex based composites from procured latex matrix in a liquid state, and typically the fillers are simply incorporated and mechanical processed as a masterbatch (Hao et al., 2019; Mekonnen, Ah-Leung, Hojabr, & Berry, 2019; Srivastava & Mishra, 2018). The masterbatch mixing could be conducted by a variety of mechanical processes, i.e., ultrasonication, shear blender and homogenizer, which allows exfoliation and intercalation to occur between the latex matrix and cellulose fillers. This allows proper dispersion of cellulose fillers within the liquid latex. The coagulation process utilizes acids such as acetic acid and formic acid to engage the latex to coagulate, hence bonding with the dispersed cellulose fillers (Mekonnen et al., 2019). At this stage, the fabricated

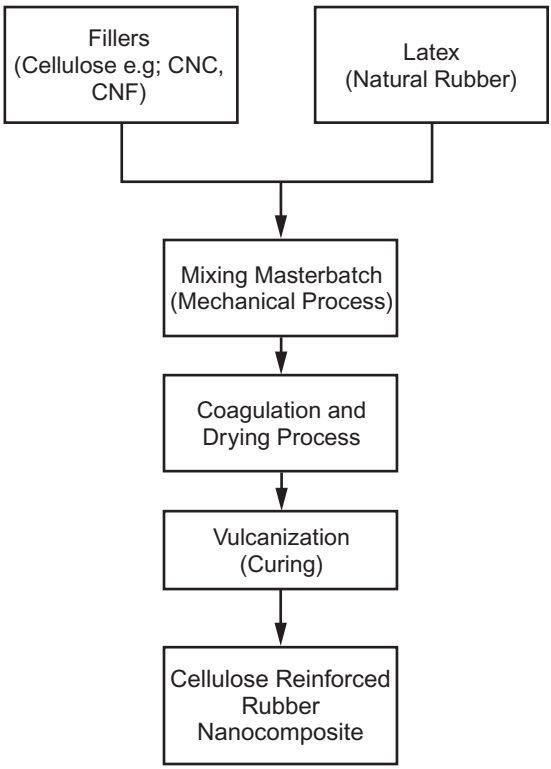

FIG. 10.3

Latex blending process for cellulose reinforced rubber nanocomposites.

cellulose reinforced rubber nanocomposites have a very poor mechanical properties. Therefore, vulcanization is required to further cure the cellulose reinforced rubber nanocomposites to improve it mechanical and other properties (Hao et al., 2019). Vulcanization is the crosslinking process for natural and synthetic rubbers, generally with sulfur and heating processes. Sulfur is considered as the cross-linking agent, and other additives may modify the rubber physical and mechanical properties. Examples of additives added for the vulcanization process includes (Akib & Hashim, 1997; Coran, 2005, 2013; Nunes, 2014, 2017):

Activator
Accelerator
Coagulants
Antioxidants
Color pigments
Surfactants
Softeners
Ant-foaming agents
Anti-tack agents

As sulfur and additives are added, slow cross-linking of rubber starts to occur. The mixture is typically placed in a mold to attain the desired shape. This must be conducted before the heating stage, as it is not possible to shape the rubber after vulcanization. The operating temperature for the heating process is generally between 120 and 200 °C. Literatures shown that, heating during the vulcanization process may result in quicker and complete cross-linking (Akib & Hashim, 1997; Coran, 2005, 2013). In contrast, for the latex blending method, to prevent the development of brittle cellulose rubber nanocomposites, the density in respect to the filler type/content must be optimized (Limousin, Ballard, & Asua, 2019).

10.4 Cellulose reinforced natural rubber nanocomposites

Over the past 10 years, many literatures have shown interest in utilizing cellulose as fillers for numerous polymeric-based materials for developing polymer nanocomposites (Ahsan, Fei, Man, Wei, & Zuowan, 2020; Sharma, Thakur, Bhattacharya, Mandal, & Goswami, 2019). However, the introduction of cellulose as fillers for elastomers are relatively new area of research, whereas the natural rubbers are some of first choice of elastomeric matrices to be utilized for investigating its characteristics (Nunes, 2014; Sienkiewicz, Janik, Borzędowska-Labuda, & Kucińska-Lipka, 2017).

Natural rubber is an elastomer classified as polyisoprene (2-methyl-1,3-butadiene), which is widely recognized to be the oldest known rubber. Before natural rubber is attained, it is first extracted from the origin source, in the form of an aqueous dispersion of rubber particles, which was now known as latex (Blackley, 1997). Commercially produced natural rubbers are from latex extracted from the rubber tree

(*Hevea brasiliensis*). Natural rubber is the based material used to manufacture gaskets, automotive components, adhesives, tires, gloves, coatings, etc. (Samsuri & Abdullahi, 2017; Tarawneh, Ahmad, Yahya, & Rozaidi, 2011). This signifies that natural rubber has an exceptional economic value and social importance, as natural rubber could be found in majority of many products and applications used in current society. The application of natural rubber in its uncured form yield poor mechanical properties and are applicable for limited applications. However, natural rubber could undergo vulcanization, where long chains of rubber molecules are cross-linked, transforming the natural rubber to yield good mechanical properties, improved fatigue resistance, and elasticity with reversible deformability (Hao et al., 2019).

The natural rubbers mechanical properties can be modified by including fillers such as CNC and CNF, the optimization of fillers can be catered accordingly to different applications. Cellulose and their derivatives have great potential as filler for reinforcing polymeric/elastomeric matrices (Limousin et al., 2019; Mekonnen et al., 2019; Nunes, 2017; Sindhu, Prasanth, & Thakur, 2014; Venugopal & Gopalakrishnan, 2018). The appeal of cellulose (CNC and CNF) as filler, are due to factors such as low cost, low density, easy process-ability, renewability, biodegradability, in comparison to synthetic fillers.

Numerous literatures show the reinforcement of natural rubber using CNC and CNF exhibit promising properties (Limousin et al., 2019; Mekonnen et al., 2019; Rosli, Ahmad, Anuar, & Abdullah, 2019; Venugopal & Gopalakrishnan, 2018). CNF extracted from Coconut spathe has a high aspect ratio with Scanning and Transmission Electron Microscopy imagery revealed that CNF diameter to be around 30–60 nm. CNF reinforced natural rubber nanocomposites prepared by latex blending method yield good mechanical properties. The literature showed that the CNF was able to improve the natural rubber tensile strength up to 29% above 34 MPa at 3 parts per hundred rubber (phr) and 52% improvement in tearing strength up to 60 N/mm at 7 phr (Venugopal & Gopalakrishnan, 2018).

Similarly, hydrolyzed cellulose, cellulose nanostructures, and micro fibrillated cellulose (MFC) produced from oil palm empty fruit bunch by mechanical and enzymatic treatments has a positive effect reinforcing natural rubber matrices (Fiorote et al., 2019). The literature shown MFC reinforced natural rubber nanocomposites has both higher modulus of elasticity and tensile strength in comparison to the neat natural rubber control sample, hydrolyzed cellulose and cellulose nanostructures reinforced natural rubber nanocomposite. The added MFC influence the developed reinforced natural rubber nanocomposites to increase in stiffness, resist and elastic deformation. The reinforced natural rubber nanocomposite 5.0 phr has a modulus of elasticity of 12.138 MPa and tensile strength of 1.609 MPa with elongation of 69.6% (Fiorote et al., 2019).

It is widely known that rubber and its reinforced rubbers composites have a great influence in today manufacturing industries in the field of engineering and science. It is utilized in the majority of applications for sound, thermal and electrical insulations. In addition to the applications for insulations, the mechanical and physical properties are important features to be considered for product reliability, durability,

and performance. For reinforced rubber composites, majority of the reinforcement materials utilized are synthetic with the addition of additives. Common reinforced rubber composites which prioritize the physical and mechanical properties includes the incorporation of carbon black as fillers, for the tire and thread manufacturing industries. The basic function of carbon black is to improve mechanical and physical properties of the rubber matrix, increase volume, and strengthen vulcanization of the developed reinforced rubber composite. Carbon black is a synthetic carbon-based material which is related to combustion-based products derived from hydrocarbon. However, there are some carbon black materials that could be derived from pyrolysis processes with an origin source from organic biomass. Factors affecting the aggregate size of carbon black includes the combustion temperature, time, and source material. Majority of the manufacturers for tires and thread compounds which incorporates carbon black, has the intention of strengthen the bonds between compound-forming molecules. The functional groups of carbon black reinforcement fillers enable the strengthening of bonds between molecules, which modifies reinforced rubber composites properties. Surface structure and aggregate size of carbon black influences the ideal filler content utilized in the rubber matrix (Balber, 2002; Li, Zhang, & Chen, 2008).

Some literature attribute smaller grain size of carbon black fillers to have a strengthening effect on rubber matrix physical properties (Farida, Bukit, Ginting, & Bukit, 2019; Habeeb, 2014; Hong, Xiaoxiang, & Jianhong, 2018). Furthermore, in terms of manufacturing processes, carbon black does attribute toward the viscosity and reduces the stickiness of the master batch. The difficulty of incorporating carbon black is the poor intercalation with other constituent materials during mixing.

In the tire and thread manufacturing industry, it is known that natural rubber properties are inadequate for high specification/performance products. In order to further progress with the usage of natural rubber in this industry, modifications through incorporating fillers is required. The increase in hardness, wear and tear resistance, and high breaking stress was attributed to carbon black as fillers (Farida et al., 2019). Over the past 10 years, natural rubber and carbon black composite products are popular for road tyres, and treads products (Hirata, Kondo, & Ozawa, 2014; Jayalakshmy & Mishra, 2019). Similar to most reinforced polymer composites, the resulting improvement of mechanical properties of natural rubber composites is due to better compatibility/interaction between filler and matrix (Lee, Aitomäki, Berglund, Oksman, & Bismarck, 2014; Lu et al., 2007; Mekonnen et al., 2019; Nordli, Chinga-Carrasco, Rokstad, & Pukstad, 2016). The incorporation of carbon black fillers in natural rubber/polypropylene do increase the mechanical tensile strength. However, it also decreases the elongation at break, in which is attributed to the carbon black having lacking in elastic properties (Farida et al., 2019).

Literatures on cellulose as fillers to reinforce the rubber matrix are scarce, some literature do show potential in the tire and thread manufacturing industries, which may replace carbon black and even silica as fillers (Liang, Liu, Wang, & Sun, 2017; Zhou, Fan, Chen, & Zhuang, 2015). Microcrystalline cellulose (MCC)—Zinc oxide (ZnO) hybridized natural rubber composites have a good compatibility and interaction between matrix and filler, which show potential as a green option of tire

thread manufacturing. In comparison to carbon black, cellulose as fillers has the advantage of being high strength, low cost, biodegradable and deriving from a renewable source, which gain attention of researchers and manufacturers utilizing elastomeric matrices (natural rubber). Naturally, cellulose contains both amorphous and crystalline regions; however, the removal of most amorphous regions would yield a stronger and stiffer cellulose. Hence, enabling the cellulose to increase its potential as reinforcing fillers for different application (Bai, Holbery, & Li, 2009). Micro crystalline cellulose (MCC) forms large micro particle sizes between 20 and 90 μm and considered to be highly polar, which deteriorates effectiveness to reinforce nonpolar polymer-matrices. Numerous mechanical treatments could be utilized to decrease the size of MCC particles such as ball milling and shear mixing (Chirayil, Mathew, Hassan, Mozetic, & Thomas, 2014; Phanthong, Guan, Ma, Hao, & Abudula, 2016). Even after mechanical treatments, the polarity of MCC still remains high and agglomeration may occur, which makes it difficult to disperse within the matrix (Abdulkhani, Hosseinzadeh, Ashori, Dadashi, & Takzare, 2014; Liang et al., 2017). To improve the interfacial interactions and compatibility of MCC and rubber matrix, the hydroxyl groups of MCC must be modified through chemical treatments, i.e., esterification, etherification, grafting, and salinization.

These chemical treatments could help improve the compatibility and interfacial bonding between MCC and rubber matrix greatly. However, chemical treatments are not suited for large-scale manufacturer, due to high usage of chemicals, hazardous reaction conditions and high costs. Modification of MCC with (ZnO) on the surface and interspaces of MCC, showed potential as replacement in some portion of the silica in natural rubber nanocomposites. MCC-ZnO hybrid composites displayed better mechanical and physical properties, in comparison to the control samples. Vulcanization of the MCC-ZnO hybrid composite further improved wet-skid and rolling resistance performance. Which is important for applications as tire tread compounds, hence demonstrating MCC-ZnO have the potential as replacement filler (Liang et al., 2017; Zhou et al., 2015).

10.5 Summary

In summary, cellulose have great potential as reinforcement materials, especially for various types of reinforced polymer composites applications in the engineering and science field. The modification of the rubber matrix by adding cellulose enhanced and yield different properties, which is useful depending on its applications. Cellulose rubber composites have great potential as an eco-friendly option as filler for rubber composites in comparison to silica and carbon black filler based rubber composites.

Acknowledgment

The authors would like to acknowledge Universiti Malaysia Sarawak (UNIMAS) for the support.

References

Abdulkhani, A., Hosseinzadeh, J., Ashori, A., Dadashi, S., & Takzare, Z. (2014). Preparation and characterization of modified cellulose nanofibers reinforced polylactic acid nanocomposite. *Polymer Testing*, *35*, 73–79. https://doi.org/10.1016/j.polymertesting.2014.03.002.

Ahsan, Z., Fei, H., Man, J., Wei, W., & Zuowan, Z. (2020). Preparation, properties, and applications of natural cellulosic aerogels: A review. *Energy and Built Environment*, 60–76. https://doi.org/10.1016/j.enbenv.2019.09.002.

Akiba, M., & Hashim, A. S. (1997). Vulcanization and crosslinking in elastomers. *Progress in Polymer Science*, 475–521. https://doi.org/10.1016/s0079-6700(96)00015-9.

Amin, S., & Amin, M. (2011). Thermoplastic elastomeric (TPE) materials and their use in outdoor electrical insulation. *Reviews on Advanced Materials Science*, *29*(1), 15–30. http://www.ipme.ru/e-journals/RAMS/no_12911/02_amin.pdf.

Azeredo, H. M. C., Rosa, M. F., & Mattoso, L. H. C. (2017). Nanocellulose in bio-based food packaging applications. *Industrial Crops and Products*, *97*, 664–671. https://doi.org/10.1016/j.indcrop.2016.03.013.

Bai, W., Holbery, J., & Li, K. (2009). A technique for production of nanocrystalline cellulose with a narrow size distribution. *Cellulose*, *16*(3), 455–465. https://doi.org/10.1007/s10570-009-9277-1.

Balberg, I. (2002). A comprehensive picture of the electrical phenomena in carbon black–polymer composites. *Carbon*, *40*(2), 164–166. https://doi.org/10.1016/S0008-6223(01.

Bao, R. Y., Yang, W., Liu, Z. Y., Xie, B. H., & Yang, M. B. (2015). Polymorphism of a high-molecular-weight racemic poly(l-lactide)/poly(d-lactide) blend: Effect of melt blending with poly(methyl methacrylate). *RSC Advances*, *5*(25), 19058–19066. https://doi.org/10.1039/c5ra00691k.

Blackley, D. C. (1997). *Synthetic latices: Individual types* (pp. 303–390). Springer Science and Business Media LLC. https://doi.org/10.1007/978-94-011-5866-4_3.

Chakrabarty, A., & Teramoto, Y. (2018). Recent advances in nanocellulose composites with polymers: A guide for choosing partners and how to incorporate them. *Polymers*, *10*(5). https://doi.org/10.3390/polym10050517.

Chirayil, C. J., Mathew, L., Hassan, P. A., Mozetic, M., & Thomas, S. (2014). Rheological behaviour of nanocellulose reinforced unsaturated polyester nanocomposites. *International Journal of Biological Macromolecules*, *69*, 274–281. https://doi.org/10.1016/j.ijbiomac.2014.05.055.

Coran, A. Y. (2005). Vulcanization. In *Science and technology of rubber* (pp. 321–366). Elsevier Inc. https://doi.org/10.1016/B978-012464786-2/50010-9.

Coran, A. Y. (2013). Vulcanization. In *The science and technology of rubber* (pp. 337–381). Elsevier Inc. https://doi.org/10.1016/B978-0-12-394584-6.00007-8.

Ercan, N., Durmus, A., & Kaşgöz, A. (2017). Comparing of melt blending and solution mixing methods on the physical properties of thermoplastic polyurethane/organoclay nanocomposite films. *Journal of Thermoplastic Composite Materials*, *30*(7), 950–970. https://doi.org/10.1177/0892705715614068.

Farida, E., Bukit, N., Ginting, E. M., & Bukit, B. F. (2019). The effect of carbon black composition in natural rubber compound. *Case Studies in Thermal Engineering*, *16*. https://doi.org/10.1016/j.csite.2019.100566.

Fiorote, J. A., Freire, A. P., de Sousa Rodrigues, D., Martins, M. A., Andreani, L., & Valadares, L. F. (2019). Preparation of composites from natural rubber and oil palm empty fruit bunch

cellulose: Effect of cellulose morphology on properties. *BioResources*, *14*(2), 3168–3181. https://doi.org/10.15376/biores.14.2.3168-3181.

Habeeb, S. (2014). The influence surface area and structure of particles carbon black on cure characteristics and mechanical properties of natural rubber. *International Journal of Engineering and Technology*, *5*, 149–159.

Hao, Z., Wang, X., Hengyi, L., Zhengtian, X., Guangsu, H., & Jinrong, W. (2019). Fundamental researches on graphene/rubber nanocomposites. *Advanced Industrial and Engineering Polymer Research*, 32–41. https://doi.org/10.1016/j.aiepr.2019.01.001.

Hirata, Y., Kondo, H., & Ozawa, Y. (2014). Natural rubber (NR) for the tyre industry. In *Chemistry, manufacture and applications of natural rubber* (pp. 325–352). Elsevier Inc. https://doi.org/10.1533/9780857096913.2.325.

Hong, H. L., Xiaoxiang, Y., & Jianhong, G. (2018). Study on microstructure effect of carbon black particles in filled rubber composites. *International Journal of Polymer Science*, 1–11. https://doi.org/10.1155/2018/2713291.

Jayalakshmy, M. S., & Mishra, R. K. (2019). Applications of carbon-based nanofiller-incorporated rubber composites in the fields of tire engineering, flexible electronics and EMI shielding. In *Carbon-based nanofillers and their rubber nanocomposites: Fundamentals and applications* (pp. 441–472). Elsevier. https://doi.org/10.1016/B978-0-12-817342-8.00014-7.

Jonoobi, M., Oladi, R., Davoudpour, Y., Oksman, K., Dufresne, A., Hamzeh, Y., et al. (2015). Different preparation methods and properties of nanostructured cellulose from various natural resources and residues: A review. *Cellulose*, *22*(2), 935–969. https://doi.org/10.1007/s10570-015-0551-0.

Kalia, S., Dufresne, A., Cherian, B. M., Kaith, B. S., Avérous, L., Njuguna, J., et al. (2011). Cellulose-based bio- and nanocomposites: A review. *International Journal of Polymer Science*, *2011*. https://doi.org/10.1155/2011/837875.

Khui, PLN, Rahman, MR, & Bakri, MKB. (June 2021). A review on the extraction of cellulose and nanocellulose as a filler through solid waste management. *Journal of Thermoplastic Composite Materials*. https://doi.org/10.1177/08927057211020800.

Lee, K. Y., Aitomäki, Y., Berglund, L. A., Oksman, K., & Bismarck, A. (2014). On the use of nanocellulose as reinforcement in polymer matrix composites. *Composites Science and Technology*, *105*, 15–27. https://doi.org/10.1016/j.compscitech.2014.08.032.

Li, Z. H., Zhang, J., & Chen, S. J. (2008). Effects of carbon blacks with various structures on vulcanization and reinforcement of filled ethylene-propylene-diene rubber. *Express Polymer Letters*, *2*(10), 695–704. https://doi.org/10.3144/expresspolymlett.2008.83.

Liang, Y., Liu, X., Wang, L., & Sun, J. (2017). The fabrication of microcrystalline cellulose-nanoZnO hybrid composites and their application in rubber compounds. *Carbohydrate Polymers*, *169*, 324–331. https://doi.org/10.1016/j.carbpol.2017.04.022.

Limousin, E., Ballard, N., & Asua, J. M. (2019). Synthesis of cellulose nanocrystal armored latex particles for mechanically strong nanocomposite films. *Polymer Chemistry*, *10*(14), 1823–1831. https://doi.org/10.1039/c8py01785a.

Lu, Y. L., Li, Z., Yu, Z. Z., Tian, M., Zhang, L. Q., & Mai, Y. W. (2007). Microstructure and properties of highly filled rubber/clay nanocomposites prepared by melt blending. *Composites Science and Technology*, *67*(14), 2903–2913. https://doi.org/10.1016/j.compscitech.2007.05.018.

Mariano, M., El Kissi, N., & Dufresne, A. (2014). Cellulose nanocrystals and related nanocomposites: Review of some properties and challenges. *Journal of Polymer Science, Part B: Polymer Physics*, *52*(12), 791–806. https://doi.org/10.1002/polb.23490.

McKeen, L. W., & McKeen, L. W. (2019). 10—Elastomers and rubbers. In *Plastics design library* (pp. 279–359). William Andrew Publishing. https://doi.org/10.1016/B978-0-12-816457-0.00010-1.

Mekonnen, T. H., Ah-Leung, T., Hojabr, S., & Berry, R. (2019). Investigation of the co-coagulation of natural rubber latex and cellulose nanocrystals aqueous dispersion. *Colloids and Surfaces A: Physicochemical and Engineering Aspects*, *583*. https://doi.org/10.1016/j.colsurfa.2019.123949.

Narimissa, E., Gupta, R. K., Kao, N., Choi, H. J., & Bhattacharya, S. N. (2015). The comparison between the effects of solvent casting and melt intercalation mixing processes on different characteristics of polylactide-nanographite platelets composites. *Polymer Engineering and Science*, *55*(7), 1560–1570. https://doi.org/10.1002/pen.23996.

Nasir, M., Hashim, R., Sulaiman, O., & Asim, M. (2017). Nanocellulose: Preparation methods and applications. In *Cellulose-reinforced nanofibre composites: Production, properties and applications* (pp. 261–276). Elsevier Inc. https://doi.org/10.1016/B978-0-08-100957-4.00011-5.

Norazlina, H., Firdaus, R. M., & Hafizuddin, W. M. (2015). Enhanced properties from mixing natural rubber with recycled polyvinyl chloride by melt blending. *Journal of Mechanical Engineering and Sciences*, *8*, 1440–1447. https://doi.org/10.15282/jmes.8.2015.18.0140.

Nordli, H. R., Chinga-Carrasco, G., Rokstad, A. M., & Pukstad, B. (2016). Producing ultrapure wood cellulose nanofibrils and evaluating the cytotoxicity using human skin cells. *Carbohydrate Polymers*, *150*, 65–73. https://doi.org/10.1016/j.carbpol.2016.04.094.

Nunes, R. C. R. (2014). Natural rubber (NR) composites using cellulosic fiber reinforcements. In *Chemistry, manufacture and applications of natural rubber* (pp. 284–302). Elsevier Inc. https://doi.org/10.1533/9780857096913.2.284.

Nunes, R. C. R. (2017). Rubber nanocomposites with nanocellulose. In *Progress in rubber nanocomposites* (pp. 463–494). Elsevier Inc. https://doi.org/10.1016/B978-0-08-100409-8.00013-9.

Phanthong, P., Guan, G., Ma, Y., Hao, X., & Abudula, A. (2016). Effect of ball milling on the production of nanocellulose using mild acid hydrolysis method. *Journal of the Taiwan Institute of Chemical Engineers*, *60*, 617–622. https://doi.org/10.1016/j.jtice.2015.11.001.

Pramanik, M., Srivastava, S. K., Samantaray, B. K., & Bhowmick, A. K. (2003). Rubber–clay nanocomposite by solution blending. *Journal of Applied Polymer Science*, *87*(14), 2216–2220. https://doi.org/10.1002/app.11475.

Rahman, M. R., & Bakri, M. K. B. (2021). Bamboo nanocellulose reinforced polylactic acid nanocomposites. In M. R. Rahman (Ed.), *Bamboo Polymer Nanocomposites. Engineering Materials*. Cham: Springer. https://doi.org/10.1007/978-3-030-68090-9_8.

Rahman, M. R., & Bakri, M. K. B. (2021). Bamboo cellulose gel/MMT polymer nanocomposites for high strength materials. In M. R. Rahman (Ed.), *Bamboo Polymer Nanocomposites. Engineering Materials*. Cham: Springer. https://doi.org/10.1007/978-3-030-68090-9_7.

Rahman, M. R., Hamdan, S., Ngaini, Z. B., et al. (2019). Cellulose fiber-reinforced thermosetting composites: impact of cyanoethyl modification on mechanical, thermal and morphological properties. *Polymer Bulletin*, *76*, 4295–4311. https://doi.org/10.1007/s00289-018-2598-1.

Rane, A. V., Kanny, K., Abitha, V. K., Thomas, S., Mohan Bhagyaraj, S., Oluwafemi, O. S., et al. (2018). Chapter 5—Methods for synthesis of nanoparticles and fabrication of nanocomposites. In *Micro and nano technologies* (pp. 121–139). Woodhead Publishing. https://doi.org/10.1016/B978-0-08-101975-7.00005-1.

Robles, E., Labidi, J., Halász, K., & Csóka, L. (2017). Key issues in reinforcement involving nanocellulose. In *Cellulose-reinforced nanofibre composites: Production, properties and applications* (pp. 401–425). Elsevier Inc. https://doi.org/10.1016/B978-0-08-100957-4.00018-8.

Rosli, N. A., Ahmad, I., Anuar, F. H., & Abdullah, I. (2019). Application of polymethylmethacrylate-grafted cellulose as reinforcement for compatibilised polylactic acid/natural rubber blends. *Carbohydrate Polymers*, *213*, 50–58. https://doi.org/10.1016/j.carbpol.2019.02.074.

Samsuri, A. B., & Abdullahi, A. A. (2017). *Reference Module in Materials Science and Materials Engineering*. Elsevier BV. https://doi.org/10.1016/b978-0-12-803581-8.09212-2.

Sharma, A., Thakur, M., Bhattacharya, M., Mandal, T., & Goswami, S. (2019). Commercial application of cellulose nano-composites—A review. *Biotechnology Reports*, *21*. https://doi.org/10.1016/j.btre.2019.e00316.

Sienkiewicz, M., Janik, H., Borzędowska-Labuda, K., & Kucińska-Lipka, J. (2017). Environmentally friendly polymer-rubber composites obtained from waste tyres: A review. *Journal of Cleaner Production*, *147*, 560–571. https://doi.org/10.1016/j.jclepro.2017.01.121.

Sindhu, K. A., Prasanth, R., & Thakur, V. K. (2014). Medical applications of cellulose and its derivatives: Present and future. In *Vol. 9781118871904. Nanocellulose polymer nanocomposites: Fundamentals and applications* (pp. 437–477). Wiley Blackwell. https://doi.org/10.1002/9781118872246.ch16.

Srivastava, S. K., & Mishra, Y. K. (2018). Nanocarbon reinforced rubber nanocomposites: Detailed insights about mechanical, dynamical mechanical properties, payne, and mullin effects. *Nanomaterials*, *8*(11). https://doi.org/10.3390/nano8110945.

Tarawneh, M. A., Ahmad, S. H., Yahya, S. Y., & Rozaidi, R. (2011). Mechanical properties of thermoplastic natural rubber reinforced with multi-walled carbon nanotubes. *Journal of Reinforced Plastics and Composites*, 363–368. https://doi.org/10.1177/0731684410397407.

Venugopal, B., & Gopalakrishnan, J. (2018). Reinforcement of natural rubber using cellulose nanofibres isolated from Coconut spathe. *Materials Today: Proceedings*, *5*(8), 16724–16731. Elsevier Ltd. https://doi.org/10.1016/j.matpr.2018.06.036.

Wu, Y. P., Ma, Y., Wang, Y. Q., & Zhang, L. Q. (2004). Effects of characteristics of rubber, mixing and vulcanization on the structure and properties of rubber/clay nanocomposites by melt blending. *Macromolecular Materials and Engineering*, *289*(10), 890–894. https://doi.org/10.1002/mame.200400085.

Zhou, Y., Fan, M., Chen, L., & Zhuang, J. (2015). Lignocellulosic fibre mediated rubber composites: An overview. *Composites Part B: Engineering*, *76*, 180–191. https://doi.org/10.1016/j.compositesb.2015.02.028.

CHAPTER

Cellulose-derived carbon fibers

11

Elammaran Jayamani[a], **Md Rezaur Rahman**[b], **and Muhammad Khusairy Bin Bakri**[b]

[a]*Faculty of Engineering, Computing and Science, Swinburne University of Technology Sarawak Campus, Kuching, Sarawak, Malaysia,* [b]*Department of Chemical Engineering and Energy Sustainability, Faculty of Engineering, Universiti Malaysia Sarawak (UNIMAS), Kota Samarahan, Sarawak, Malaysia*

Chapter outline

Fundamentals and Recent Advances in Nanocomposites Based on Polymers and Nanocellulose.
https://doi.org/10.1016/B978-0-323-85771-0.00006-3

11.1 Introduction

Most of the fiber produced has a range of 90%–99% carbon content, while the filament diameter ranges from 5 to 15 μm (Souto, Calado, & Pereira, 2018). Due to the manufacturing processes, the cost of carbon fiber composites productions is expensive of both its fibers and composites. Nevertheless, the reasons why the demand of carbon fibers has grown tremendously over the decade is due to its heat resistant, low density, high strength, lightweight, flexible, low thermal expansion, and biologically inert properties of carbon fibers. Since 2009, in 7 years, it has staggeringly increased up to 140% and is expected continuously grow in the future. Polyacrylonitrile (PAN), a conventional precursors pitch is used to manufacture carbon fibers with an expensive cost. The price of PAN with the total cost to manufacture carbon fibers, may take up to 51% (Souto et al., 2018).

To meet the standard requirement, many researches were carried out by government and industry, with considerations emphasized on the weight reduction technologies. For example, in the automotive manufacturing industry, especially for production of new cars, the Energy Policy and Conservation Act of 1975 and the Clean Air Act of 1970 must be obligated (Warren, Shaffer, Paulauskas, & Abdullah, 2002). Therefore, a limitation for fuel consumption to be economical is stetted, mandatory targeting production of emission, and obligate on the use of carbon fiber composites, which are highly sought (Warren et al., 2002).

While maintaining the cost, comfort, safety, performance, and recyclability of the automotive requirement, all these changes made in the designs were able to reach its standards (Koronis & Silva, 2018). While having low density, which are favorable for manufacturers, carbon fiber composites compose of a great amount of physical strength. It can be utilized to lower the vehicle mass by replacing the heavy materials used, which in return improve the fuel economy, reduce exhaust emissions, and provide superior dynamics of the vehicle (Koronis & Silva, 2018).

Extra precautions must be taken, as it involved in the combination of application and material, whereas an involvement in weight reduction is considered, especially pairing carbon fiber composite with metals, i.e., the carbon fiber body structure of a vehicle replacement with steel, magnesium, aluminum, or zinc alloy components. Referring to the periodic table, the aluminum, magnesium, and zinc are nearer to the alkaline end, while the carbon is nearer to the acidic end (Matlin, Mehta, Hopf, & Krief, 2019). Corrosion would occur, whereas the metals will act as the

sacrificial metal, if electrolyte such as sodium chloride is in contact with the metals and carbon (Popoola, Grema, Latinwo, Gutti, & Balogun, 2013). Surface treatment or the presence of the insulating component could avoid corrosion to happened (Popoola et al., 2013). To join them together, adhesive method is the easiest way to use, as it created a barrier, which could keep moisture and air out. Surface treatment could be considered, such as phosphating an anodization process to minimize interface contact (Popoola et al., 2013).

11.2 Physical properties of carbon fiber materials

Generally, in the automotive industry, carbon fiber composites used are in the form of a yarn woven from carbon filaments impregnated with epoxy resin. Due to the volume fraction of fiber to resin, the lay of filaments, and the characteristics of the resin utilized, the physical properties may vary (Evans, 2006). These specifications in the properties directly affects the carbon fiber modulus of elasticity. The elasticity modulus may range from 3 to 2000 GPa. This is wide comparable to those carbon steel, which only has around 200 GPa.

Carbon content makes it a conductive material, especially in carbon fibers. As the application of this material is focused on carrying electric current, it can be useful such as in a supercapacitor (Evans, 2006). Alternatively, the carbon fiber composites are used to make the complete structural monocoques of production cars or the body panel areas, which can also be an issue for designers of automotive electrical distribution systems (EDS). The reason behind this is due to the electrical properties of carbon fibers, which are very different from the electrical properties of copper, aluminum, or steel.

11.3 Electrical properties of carbon fiber materials

As mentioned before, the carbon fiber material electrical properties are affected by its physical construction, such as the lay direction, thickness, and fiber density. A direct conductive path is present as metallic contact is connected horizontally/parallel to the direction of carbon/resin matrix. With an addition of efficient electrical, the contact of cross section can be obtained with the conductivity equivalent to steel with 1×10^{-3} (Evans, 2006). As electrical charges do not have to cross over through each carbon fiber bundles, this electrical contact direction is less complex.

The conductive path is more complex, as the metallic contact is connected to the direction of carbon/resin matrix vertically/perpendicular, it must pass through each of the fiber bundle. This makes the conductivity even smaller than the previous orientation, as it only achieves 1×10^{-3}. If the bundle of carbon fibers is in bulk, then the presence of surface resistance can be decreased (Evans, 2006).

Carbon fiber materials consist of high impedance, which makes its weak in electromagnetic compatibility (EMC) performance. Before weaving process or molding

process, it can be intensified through fibers metallization, but then again, this will be quite expensive process. Due to its high impedance, instead of utilizing the conventional metal body as a part of the electrical circuit for the carbon fiber material used to make a vehicle's body, the electrical connection was connected through electric cables.

Combustion may occur in the presence of oxygen if a short-circuit were to occur between the carbon fiber body as the initiating energy source, where the carbon itself is one of the materials that can easily be caught on fire. The carbon fiber material impedance resulted in limitation of current flow, which makes it harder to blow a conventional fuse. The temperature may rise due to the power dissipated in the body structure, which may also correlate and lead to combustion to occur (Evans, 2006).

11.4 Advantages of carbon fiber materials

The weight and the components can be reduced and decreased by 60%, if the small body structure of a four-passenger vehicle is made from carbon fiber composite instead of steel. Additionally, the static and dynamic bend stiffness of the body structure is decreased by 30% and increase by 60%, respectively, making it susceptible to withstand bending, which make it stiffer than a steel body structure. Significantly, the dynamic torsional stiffness is increased by 75% (Evans, 2006). Being lighter makes it a very good alternative to all those gains performance materials than its steel equivalent.

Carbon fiber anisotropic physical characteristics are favorable for enhancing crash performance. According to the specific vehicle structure, as a precursor, the modification to the structure of the weave carbon fiber can be done as the carbon filaments are extremely strong in tension but are weak in compression (Evans, 2006). By adjusting the carbon fiber lay direction, designers may able to increase the safety of the vehicle, just instead of needing to add more parts, as they exhibit isotropic characteristics, especially when working with steel and aluminum sheet (Evans, 2006).

11.5 Disadvantages of conventional carbon fiber feedstock

Around one ton, at least 30% of the weight of an average vehicle must be replaced by carbon fiber composite. In order to replace all their ferrous metal for an annual production of 15 million cars and light trucks, 4 million tons of carbon fiber will need to be produced (Leitten, Griffith, Compere, & Shaffe, 2002). Merely less than 1% of the weight needed for current production capacity, whereas the cost of the metals it replaced is barely equate with. A drawback on the use of carbon fiber composite was due to the high volume and cost competitive nature of the automotive industry. Furthermore, this material is expensive to manufacture, which is due to the complex manufacturing process and its limited amount of feedstock used for carbon fiber

composite production. To meet the goal of reduction in manufacturing cost, while making it environmentally friendly and in order to incorporate carbon fiber composite into automotive production, carbon fiber composite manufacturer must be altered in the production process.

11.6 Solution for meeting the increasing demand of carbon fiber composite

Changing the precursor material to environmentally friendly raw material would lower the cost of carbon fiber used to produce the product, which can be acquired in high volume. Government and private sectors extensive researches show that cellulose based material can replace conventional carbon fiber, such as regenerated cellulosic, Kraft lignin and lignin blend fibers (Leitten et al., 2002). Essentially, the organic polymers bound together by long strings of carbon atoms. In early decades, which is around 1960s and 1970s, these materials were already being used, due to poor quality and public interests, it was not completely commercialized (Warren et al., 2002).

As it depends on the material and processing conditions precursor, the cellulose-derived carbon fibers may have fluctuating mechanical properties. After carbonization of 2000°C and above, the cellulose-derived carbon fibers tensile strength may range between 0.5 and 1.5 GPa, while the Young's moduli maximum at 100 GPa (Spörl et al., 2017). Theoretically, cellulose carbonization can yield up to 44.4 wt% of carbon, but during pyrolysis degradation reactions leads to maximum 90% of mass loss. Carbonization aid usage greatly reduces defects caused by degradation reactions.

For high performance carbon fiber application, viscose and Lyocell, a man-made regenerated cellulose fiber can be used. Rayon fibers are a type of viscose, which have continuous filaments (Spörl et al., 2017). Most often burned for process heat and power, the Kraft lignin, as it is the by-product, can be acquired from paper making process (Warren et al., 2002). As the raw material is widely available renewable as a resource, lignin precursors based are superb for lowering manufacturing cost, which can be obtained from an affordable price range. Instead of using a melt-spun production method, this type of precursor material eliminates the need for dissolution of the principal precursor into solvent during production.

Lignin-based carbon fibers have a lot of advantages over conventional precursors, such as: (i) Independent of fossil fuels, (ii) Minimal environment toxicity, (iii) reduction of 30%–40% of finished carbon fiber production cost, (iv) emits around 22% less CO_2-equivalent greenhouse gas emission, (v) Less energy consumption (MJ/fiber kg), and (vi) High carbon yield (>60%).

However, lignin is still not adopted by many companies widely, as specific conditions are needed, as the mechanical properties of the fiber is restricted, especially when using neat lignin. The drawback is crucial in extrusion procedure, due to lack of knowledge in the optimum range of molecular weight distribution. To ensure

efficiency on the use of this material, further researches in lignin utilization as carbon fiber precursors is needed.

11.7 Lignin

In nature, one of the most abundant organic macromolecules are lignin and chitin. To be the carbon fiber composite precursors, lignin makes a better choice, as it has around 60% carbon content (Souto et al., 2018). In the pulp and paper industry, around 50–60 million tons of lignin are produced, unfortunately 98% of it are used to generate energy in combustion. The lignin underutilization loses a huge amount of potential profit, whereas if used in carbon fiber manufacturing, it would be valued US$ 800,000/fiber ton.

Namely, *p*-hydroxyphenyl (H), guaiacyl (G), and syringyl (S) is three randomly subunits formed by lignin structure. Due to the high concentration of guaiacyl, softwoods are called guaiacyl lignin, while due to their heterogeneous structure, hard woods and grass are called syringyl lignin. The thermal mobility and mechanical properties of carbon fibers lignin-based distinguishes, due to the ratio of syringyl and guaiacyl. Due to cleavage in different sites of the molecular chain, a variety of molecular weight with different extraction process of lignin from the vegetal can be produced. It is hard to generalize the physiochemical properties of lignin, as many other factors such as pressure, contaminants, thermal history, and cross linking may influence it.

11.8 Yield from carbon fiber feedstocks

By its yield, the carbon fiber feasibility and production cost of can be evaluated, which can be calculated by dividing the weight of carbon fiber over the weight of raw feedstock. To produce a relatively high amount of carbon fiber, high yield is more favorable, as it shows that low amount of feedstock needed, which in turn not needing large facilities (Leitten et al., 2002). It is also preferred, due to its low emissions. For polyolefins, the family of polyethylene and polypropylene thermoplastics, one of the ways to increase the yield sulfonation is through concentrated acids, as it replaces the carbonization and graphitization processes that produces low yield. The expected around 0.45–0.55 lignin is carbon yield, which is comparable around 0.33–0.50 to the carbon yield from PAN (Leitten et al., 2002).

11.9 Processing

Generally, no matter what type of precursors that has been chosen for the production, there are five steps in carbon fiber processing. The steps include extrusion/spinning, oxidation/thermo-stabilization, carbonization and graphitization, surface treatment

and sizing. To turn the raw material into fiber strands is the first step, which through washed and stretched. Secondly, to stabilize the bonds, thermo-stabilization or oxidation is carried out. To form tightly bonded carbon crystals, carbonization and graphitization are the steps that heat the stabilized fibers. While to improve bonding properties of the carbonized fibers with polymeric matrix, surface treatment is then carried out after carbonization and graphitization. Finally, the carbonized fibers are coated and wound onto bobbins.

11.9.1 Extrusion/spinning

The acceptable range for melt-spinning precursor formulations, consist of 80%–85% lignin and 15%–20% PET (Warren et al., 2002). With proper temperatures and times, stabilization and graphitization were possible. As the precursor, Souto et al. (Souto et al., 2018) was able to use 100% of lignin. The first step is to turn the lignin into lignin green fiber. Extrusion and spinning of lignin affect the precursor fiber morphology, tenacity, and diameter. For extrusion of lignin, melt-spinning is used, this simplifies the steps to only fusing raw material without any other resources, as it does not require toxic solvents or coagulation baths used to melt PAN. However, in order to have proper or improved fluidity of melt-spinning lignin, operational and structure parameters must be fulfilled with better mechanical properties, as lignin must be purified and fractionated for melt-spinning.

The structural parameters to be met are the decomposition temperature (T_d), and glass transition temperature (T_g), which is through condensation of carbonyl, phenolic, aliphatic hydroxyls, and aryl-ether bonds (β-O-4′). In melt spinning step, condensation of structures should be avoided, as it makes it difficult to be carried out. While syringyl do not, guaiacyl and *p*-hydroxyphenyl C_5-position may causes condensation of structure. Therefore, as mentioned before, instead of softwood lignin chars, it is a guaiacyl lignin that melt. Condensation hinders molecular rotation as a result of β-5′ and 5-5′ linkages formation (Souto et al., 2018). The rising temperature may cause crosslinking of some functional groups that end up hindering the molecular rotation.

Technically in lignin, carbonyl can be found concentrated with phenolic or cinnamic acids in herbaceous. It is favorable as the carbonyl chains restrict C-C linkage on aliphatic chain and in turn increases plasticity and thermal mobility. However, condensation of structures will occur in herbaceous, as it has higher guaiacyl and *p*-hydroxyphenyl ratio and this will decrease thermal mobility.

As it decreases thermal mobility, aliphatic hydroxyl should be eliminated as a result of the intermolecular hydrogen bonds formation. As it forms intramolecular hydrogen bonds, this can be countered by phenolic hydroxyls, which can stop intermolecular hydrogen bonds from forming, resulting in increased thermal mobility. As it increases thermal mobility due to its ether linkage which forms linear structure, higher concentration of β-O-4′ are also favorable.

Due to discontinuous extrusion, T_d must be as high as possible to prevent voids and defects to the fibers produced. By preventing impurities, T_d can be increased, especially the phenolic acids and aliphatic hydroxyls in the mixture. On the other

hand, the fusibility of lignin and thermal mobility can be increased, if T_g is low as possible. Respectively, by avoiding aliphatic hydroxyl and condensation, it can be lowered, as it produces intermolecular bonds and decreases free volume.

On the other hand, for lignin to undergo melt-spin, the operational parameters will be the perfect condition set by Oak Ridge National Laboratory (ORNL). The condition includes minimum 99% purity level, maximum of 500 ppm of particulate matter with a minimum diameter of 1 μm, maximum of 1000 ppm of ash content, maximum of 5% volatile content at 250°C, and maximum of 500 ppm of carbohydrate residual (Souto et al., 2018). When there is presence of impurities, the extrusion will be limited, such as volatiles, proteins, particulates, carbohydrates, ashes, water, and polydispersity.

Multiple researches were done, and many ways has been identified, especially to remove each of the listed impurities. To reduce carbohydrate content, membranes or polysaccharide enzymes can be used. While to prevent the extruder form clogging up by particulates, sand, diatom, and cellulosic fibers can be removed through filtration. Hot aqueous acid is used to remove amino acids (protein) and ashes. During melt-spinning, water and volatiles promote voids. At high temperatures, the removal of these two impurities are to be done, after ash removal through vacuum treatment. As high index impedes melting but provides enough viscosity, a roper polydispersity index is harder to be identified, while low index makes it hard to spin lignin into fibers due to low viscosity (Souto et al., 2018).

Other than melt-spinning, several extrusions were also applicable such as wet spinning, dry spinning, electrospinning, and melt-blown. Soluble lignin is required for electrospinning, wet and dry spinning but electrospinning produces nanofibers instead of carbon fibers.

11.9.2 Oxidation/thermo-stabilization

The oxidation or thermo-stabilization is the second step to manufacture carbon fiber. However, due to its long processing time with high energy consumption makes it the most expensive step. Gradually, in this step, the temperature is increased to remove thermoplastic characteristic of lignin, which is to avoid softening of the fiber before the next step. To form crosslinking between structures, oxidized groups are presented to increase the T_g. Quick heating may result the fibers to melt, which is not favorable. In order to stabilize the green lignin fibers, for optimum yield, the temperature range for oxidation to occur is between 260°C and 290°C, with an average heating rate from $0.2°C\,min^{-1}$ to $1°C\,min^{-1}$. Turbostratic structure begins to form below 260°C. Aromatic structure begins to form alongside with pyrolysis, as the temperature rises. Due to pyrolysis at temperature above 290°C, turbostratic structure overweighs the ordered structures, thus carbonization will begin at this point.

Thermo-stabilization step can be carried out easily as softwood have higher amount of crosslinked structures and oxygen than the latter, even though when compared to hardwood, softwood is harder to melt. Overall, lignin-based carbon fibers are still easier to oxidized than PAN-based carbon fibers, as oxygen diffusion is

easier due to the less dense structure of lignin, which makes a faster rate oxygen penetration (Souto et al., 2018). In the oxidation step, this probably means that time reduction and lower temperature is possible.

11.9.3 Carbonization and graphitization

According to the carbonization and graphitization steps, the mechanical, thermal, and electrical properties of carbon fibers can be determined. In an inert atmosphere, depending on the precursors used, these processes are done with different temperature range. Matsumura et al. (Matsumura, Kinumoto, Matsuoka, Tsumura, & Toyoda, 2015) deduce the optimal point at 2500°C, which carbonization and graphitization temperature reached. On the other hand, carbonization temperature of lignin ranges between 500°C and 1000°C with average heating rate from 1°C min^{-1} to 5°C min^{-1} and graphitization temperature is around 1200°C (Souto et al., 2018).

To prevent unnecessary wastage of inert gas, once carbonization starts, the heating rate is increased from the oxidation step. However, if it is too fast, defects will occur in the fiber structure, as it should be within a specific rate mentioned (Souto et al., 2018). To improve the carbonization of rayon, Sporl et al. (Spörl et al., 2017) utilized the application of carbonization aids fibers, which increase the rayon-derived carbon fibers yield and its mechanical properties. The carbonization aids are ammonium dihydrogen phosphate (ADHP) and ammonium tosylate (ATS).

Continuous and discontinuous are the two types of carbonization were tested. As discontinuous carbonization is carried out, carbonization of the rayon fiber without any carbonization aids results in poor mechanical properties. So, pure rayon fiber continuous carbonization is impossible to carry out. Carbonization of the rayon fiber stabilized in ADHP (RC/ADHP) and ATS (RC/ATS) showed better properties than pure rayon fiber with RC/ATS having the best results. Maximum tensile force and tension resistance are higher in RC/ATS, while optimum dwell time before filament breakage was only half of RC/ADHP, which was determined to be 12 min only with a maximum carbonization temperature of 1400°C.

For dehydration reaction in cellulose, these carbonization aids act as catalysts, making it less likely to have degradation reactions. The main components are H_3PO_4 decomposed from ADHP and *p*-toluene sulfonic acid decomposed from ATS. Respectively, with optimum concentration at 1.0 wt% of P or S of ADHP and ATS, the result is an increase of 20% and 21% in residual mass at 1400°C. With ATS than ADHP, the temperature of dehydration of cellulose was able to be lowered more.

Moreover, due to increased emission of moisture during the dehydration reaction, stable fibers were able to form at low temperature, which caused by the carbonization aids. This means that carbon-containing volatiles and tar have been mostly reduced which in turn increase carbonization yield, reduce filament fusion and contamination in the furnace. Increased carbon yield results in improvement of elongation at break of 2.5%–3% instead of 1%–2% from PAN-based carbon fibers.

11.9.4 Surface treatment

The surface of carbonized fibers needs to be treated after the carbonization and graphitization process, because it cannot bond properly with polymeric matrix to form quality composite materials. It makes the product distinctive, as this step is very important to fiber performance. Henceforth, to improve the mechanical and chemical bonding properties, slight oxidation is needed.

In various fashions, gas, liquid, or electrolytic coating oxidation can be carried out. As the gas source for this oxidation, air, ozone, or carbon dioxide can be used, while the fibers can be immersed into liquid, such as sodium hypochlorite or nitric acid to oxidize the surface (Souto et al., 2018). In a bath filled with different electrically conductive materials, fibers can also be coated electrolytically. Most of these materials were not listed, as it is considered as a trade secret. Nevertheless, this process must be conducted in a controlled environment, so that surface defects, which cause fiber failure, can be avoided, such as pits.

11.9.5 Sizing

The fibers are ready for winding and weaving onto bobbins or tows after the surface treatment. However, before that, a thin resin layer of coating is applied onto the fibers to protect physical characteristics from damages. In order to have high quality carbon fiber composites, the coating must be compatible with the adhesive used. In the industry, epoxy, polyester, nylon, and urethane are example of coating used.

11.10 Microwave-assisted plasma processing

To enhance conventional processing methods, this technique can be used, with microwave energy generated plasmas to shorten the process of furnacing, by replacing thermal pyrolysis, during carbonization and graphitization (Warren et al., 2002). This technique resulted in indistinguishable properties, when compared with a conventional processing method without microwave-assisted plasma processing. Furthermore, it brings several advantages such as faster processing, which leads to lower hazardous gaseous emissions from conventional PAN graphitization and lower overall furnacing cost.

11.11 Pulp mill black liquor gasification

Gasification is a process, where combustion is replaced with pumping-controlled amount of oxygen and/or steam into a chamber, to react with the contained material at high temperatures, which producing carbon monoxide, hydrogen, and carbon dioxide. The materials in the chamber may be lignin and/or other recycle process chemicals. In pulp and paper, applying this method to lignin, will produce a fuel gas stream and reduced-cost electric power, that can be used to provide energy to

the furnacing process (Leitten et al., 2002). From the raw materials, this method boosts the amount of lignin recovered and dried, which become the stabilized and oxidized fiber feedstock for carbon fiber production. This method can go up to 950–1000°C, which is highly efficient, as through the temperature produced by the furnace.

11.12 Applications

While needed due to performance, as the usage are small scale, commercial application of composites such as carbon fiber can be traced all the way back to the past of aerospace, marine and construction industries (Warren et al., 2002). Traditionally, for the purpose of the use of this material, mainly in aerospace, carbon fiber composites such as those use in airplanes and missiles show a positive outcome. To reduce weight while providing equal or better rigidity of the material it replaced, carbon fiber composite can also be found in consumer products such as golf club shafts, fishing rods and shoes.

On the other hand, in the past and with its current technology, the automotive industry was not as invested, due to the lack of commercial pull and high-volume production, which being the disadvantages for the usage of carbon-fiber composites. In addition, the steep current cost, also one of its disadvantages, when compared with potential alternatives. Therefore, to reduce vehicle weight and increase performance, carbon fiber composites are mostly found on high-end automobile or auto racing, which are utilized such to increase its rigidity and reduce lap time. Koenigsegg, Bugatti, McLaren, Ferrari, and Lamborghini are current pioneers in automotive industry, who use carbon fiber composite. It is to an extent, where the monocoque is made of this composite. Some manufacturers include panels made from carbon fiber composite, just for esthetic purposes, but will increase the cost of the vehicle steeply.

11.12.1 2006 Corvette Z06 fender

General Motor decided to further the use of this technology on the replacement model for the C5, following the success on the use of carbon fiber reinforced composites (CFRC) for the hood of the 2004 C5 Commemorative Edition Z06 Corvette, which is the C6 Z06 model. Additionally, when compared with the conventional fenders made from Sheet Molded Compound (SMC) and Reaction Injection Molding (RRIM), in order to reach a weight reduction of 6 kg, this time, carbon fiber is used to manufacture the fenders of C6 Z06 (Remy, Voss, Blackwell, & Natale, 2005). To acquire substantial mass reduction, this switch of material can be done without affecting the overall vehicle performance, such as the stiffness and thermal stability. The quality of the finished product such as the gap, flushness, and visual appearance are also on par as the RRIM fender.

To replace conventional materials such as chopped fiberglass preform, SMC, and low-density polyester resin, carbon fiber's high strength and stiffness-to-mass ratio are great advantage. As it only provides aerodynamic shape and acts as sealing of internal parts and compartments from the environment, the fenders have been selected because they have a minor contribution to structural dynamics. As it is located on the front of the vehicle, fenders are also a great selection; better vehicle weight ratio between the front and rear can be achieved.

RRIM fender was used to analyses the minimum panel thickness to act as the baseline criteria which is 0.8 mm. While strictly following the 0.8 mm baseline-thickness, an individual layers of unidirectional carbon fiber were used to manufacture the fenders. Additional of two layers of carbon fiber were used at return flanges of the fenders, so that the localized thickness will reach 1.2 mm. This is to ensure these areas will be able to withstand cracking, part handling damage, and other rigorous assembly process. Changing the ply orientations will also result in a more rigid structure than RRIM fender, other than adding two layers of carbon fiber. Additional plies are added to areas that are utilizing common fasteners with the base car fenders to increase the thickness up to 3.0 mm. By adding more carbon fiber plies to locally stiffen the fender, the areas that are susceptible to higher loading are also strengthened. Significantly, the stiffness of the whole structure is increased, with these additional layers. However, the mass of the fender is affected insignificantly. The mass of a carbon fiber fender is less than half of its weight when compared with RRIM fender.

11.12.2 Advanced protective helmet for formula one

To produce an advance helmet, which aim to improve protection within the Formula One crash environment, has led the Transport Research Laboratory (LRA) commissioned by the Federation Internationale de l' Automobile (FIA) to serve better than the existing homologated motorsport helmets, worn by Formula One drivers at the time, in the hopes of reducing the frequency of life threatening injury, specifically on the driver's head (Mellor, 2004).

While having same geometry, size, and mass or less than the existing protective helmet, the advanced protective helmet must meet and exceed every specific requirement of the Formula One environment. This could be achieved by building the entire protective helmet, using a 3 mm thick solid laminate, consisting of a maximum of 13 plies of woven T1000 Carbon Fiber. Impact tests are conducted in accordance with Snell SA 2000, a standard for protective headgear use in automotive sports. The helmet liner consists combination of different expanded bead polystyrene and open cell, viscoelastic foam with a thickness of 35 mm. The new helmet which became the FIA Standard has improved in all criteria which includes crush protection, linear impact, penetration, shell hardness, chin guard, oblique impact, and mass. The mass of the assembled helmet is 1.2 kg, which is 15% lighter than the Snell SA 2000 typical mass of protective headgear. Respectively, the linear impact resistance and penetration resistance were increased by 150 J to 225 J, and 3 kg at 3 m to 4 kg at 3 m. In order

to establish the final performance are successfully made into a new FIA standard for automotive sports called FIA Standard 8860-2004, all the tests done in accordance with the new protocol.

11.12.3 Supercapacitors

Due to their superb characteristics, electrospun porous carbon fibers (ECNFs) are being used as electrode materials for supercapacitors, which includes ultrafine diameter, tune pore structure, high electrical conductivity, standing nature and high surface area. To fabricate porous ultrafine carbon fibers by electrospinning, most of the carbon precursors pitch such as polyacrylonitrile (PAN), polyvinyl alcohol, phenolic resin, and polyvinylpyrrolidone are being used (Ma et al., 2018). Due to the depletion crisis of fossil fuels, as these materials are all derived from fossil fuels, which makes it unsustainable.

To produce a nano-porous ultrafine carbon fiber, Ma et al. (Ma et al., 2018) experimented with cellulose acetate (CA), which replaces part of PAN for utilization of supercapacitor electrode by using $ZnCl_2$ as an activation agent through one-step activation of electrospinning both the materials mentioned before. To aid sustainability, adjust porous structure, and improve specific surface area in fossil resources, CA is added.

To prepare N-doped porous carbon materials for the same purpose, CA Co-carbonization and urea is also possible (Cheng et al., 2019). The source of CA can be derived from waste cigarette, while urea is the source of nitrogen, which acts as an activation agent for this one-step method. Cigarette butt filter tip is made from nonbiodegradable CA, so it makes sense to use it as a precursor, as this can help reduce waste by reusing it, in making cellulose-based carbon fiber composite. To create a proper nitrogen atmosphere for doping porous carbon materials that contains mesopores and micropores, urea has high nitrogen content, which makes it a great solution.

impurities from cigarette smoke such as Cd, As and Cr were not present due to low concentrations, when tested with an inductively coupled plasma analysis (ICP) (Lee, Kim, Song, Park, & Yi, 2014). For fast electrolyte ion transfer, the mesopores characteristic found in CA are important for providing pathways. On the other hand, micropores characteristic increases the surface area, which in turn enhance the electrical double-layer capacitance (EDLC). The highest specific capacitance measured is in the range of 152.0–153.8 $F g^{-1}$ at 1 $A g^{-1}$ which is higher than conventional activated carbon, measuring at 125.0 $F g^{-1}$ (Cheng et al., 2019).

11.12.4 Thermal link

In the field of earth observation and astrophysics research, highly accurate and sensitive detectors are important. The heat sinks connected to the detectors must be linked together with a thermal link that can transport heat efficiently and also flexible

enough to be able to bend into any direction due to different alignments of heat sinks and detectors to avoid any stress on the highly sensitive mounting of the detectors.

Hauser and Dolce (Hauser & Dolce, 1996) compared a few materials with different shapes used to design this advanced flexible thermal link, which are braided solid conductor made from carbon fiber thermal link, metallic foils, and spring-shaped axial grooved heat pipe. Over the other two material/design, carbon fiber thermal link is chosen not just because it is an innovative technology, but there are several other perspectives that can be focused on.

The lightweight property of carbon fiber made it a preferable choice, as it has more than half of the weight of metallic foils made from aluminum or copper. This property is crucial, when weight saving is needed. It also showcases an advantage of not giving excess stress on the mounting of the detectors, which could be present, if it was too heavy, especially during launch where gravity forces will act on it. Furthermore, carbon fiber based flexible thermal link is superior than the other two design/material when application at higher temperature around 150–300 K. At this range, it has high specific thermal conductivities of up to 2000 W/mK. The small fiber diameter of the individual fibers used in the thermal link allows certain flexibility to be possible, even though carbon fiber has high elastic modulus. Significantly, at high temperature, the stiffness of a carbon fiber link is proven to be higher than braided metallic foil and heat pipe.

11.12.5 Compressed natural gas (CNG) storage tanks

For conventional fuels such as gasoline and diesel fuel, CNG is an alternative. The CNG storage tank must be able to withstand high pressure and hold the ability to be lightweight. There are four types of storage tank and the most used is Type 4, due to its properties. It is the lightest design, which consist of plastic liner and carbon fiber composite. While the carbon fiber composite fully overwrapped the structure as it carries the entire pressure loading, the plastic liner is used to prevent gas permeation (Starbuck and Cataquiz, 2000). Sometimes reinforcement might be added which are glass fiber or a combination of carbon fiber and glass fiber bind together with an epoxy resin.

Carbon fiber composite's unique properties make it favorable especially when weight reduction is important and sacrificing the pressure load resistance is not an option. But, CNG is still inferior to conventional fuels primarily, due to the expensive cost to manufacture the storage tank and limited durability of the current design.

11.12.6 Gas diffusion layer (GDLL) for proton exchange membrane fuel cell (PEMFC)

To generate power through electrochemical conversion of hydrogen-containing fuels mainly in transportation and portable power generation, PEMFC is an alternative power source. a part of the membrane electrode assembly (MEA) is the GDL. To act as an electrode, it is placed on both side of the fuel cell membrane, which allow

the flow of reactants across the catalyst layered membrane, as well as providing moisture control. As the high-power densities produced are constantly changing in load, GDL provides stability to PEMFC (Starbuck & Cataquiz, 2000). However, when there is water deficiency Ionic conductivity of PEMFC in the catalyst, layered membrane will be reduced. On the contrary, for electrochemical reactions excess water in the system reduces catalytic sites.

GDL is made up of carbon fibers in the form of carbon paper or woven carbon fabrics, which have flexibility, high porosity, electronic conductivity, and are stable in acidic environment. To produce carbonized bamboo fiber sheet (CBFS), Matsumura et al. (Matsumura et al., 2015) incorporated Phyllostachys (bamboo). Respectively after the defibration procedure, an estimated content of 10.4 wt%, 17.9 wt% and 72 wt% in bamboo contents are lignin, hemicellulose, and cellulose. Due to the high content of cellulose, CBFS is also classified as a hard carbon material.

At different incremental temperature, carbonization of bamboo shows that the fiber diameter and weight loss rate was affected directly. The in-plane and consolidation electric conductivities of CBFS were measured and compared with carbon paper. To get the optimum electric conductivity, the peak temperature of carbonization is around 2500°C. However, the results were disappointing, as the in-plane conductivity of CBFS was 110 $S\,cm^{-1}$ lower than carbon paper and the electric conductivity of CBFS, which is 10 times lower than the electric conductivity of carbon paper. A PEMFC operation tests with the carbonized CBFS as the GDL produces lower open-circuit voltage than a carbon paper GDL (Matsumura et al., 2015). The maximum power was ca. 140 mW cm^{-2} at 0.45 V, which is 30 mW cm^{-2} lower than a PEMFC that uses carbon paper at 0.55 V.

11.13 Microstructure carbon fiber mats

11.13.1 Microstructure of a mixture of PAN & CA with different ratio

Fig. 11.1 shows the scanning electron microscope (SEM) images of carbon fiber morphology, with different mass ratio of PAN to CA = 10:0, 9:1, 8:2 and 7:3. It can be seen that for the pure PAN carbon fiber, along all the fibers, it has a high degree of tortuosity. When more CA is added into the mixture of carbon precursors, the twisting of fibers is shown to be decreasing, and the fibers in turn is becoming straighter. In improving thermal stability and structural stability, this shows that CA is beneficial.

Before the formation of carbon during carbonization process, the nature of CA having thermoplastic properties was assumed to make it liquify and deform. But the results from Fig. 11.1 proof that this is not the case. CA aided the fibrous structure instead of damaging the carbon skeleton contrast to the belief. Ma et al. (Ma et al., 2018) deduced that the oxidative cross-linking of PAN during preoxidation process was aided by the high oxygen content of CA. All the fibers indicate the absence of phase separation as shown in Fig. 11.1, whereas there are no visible holes and

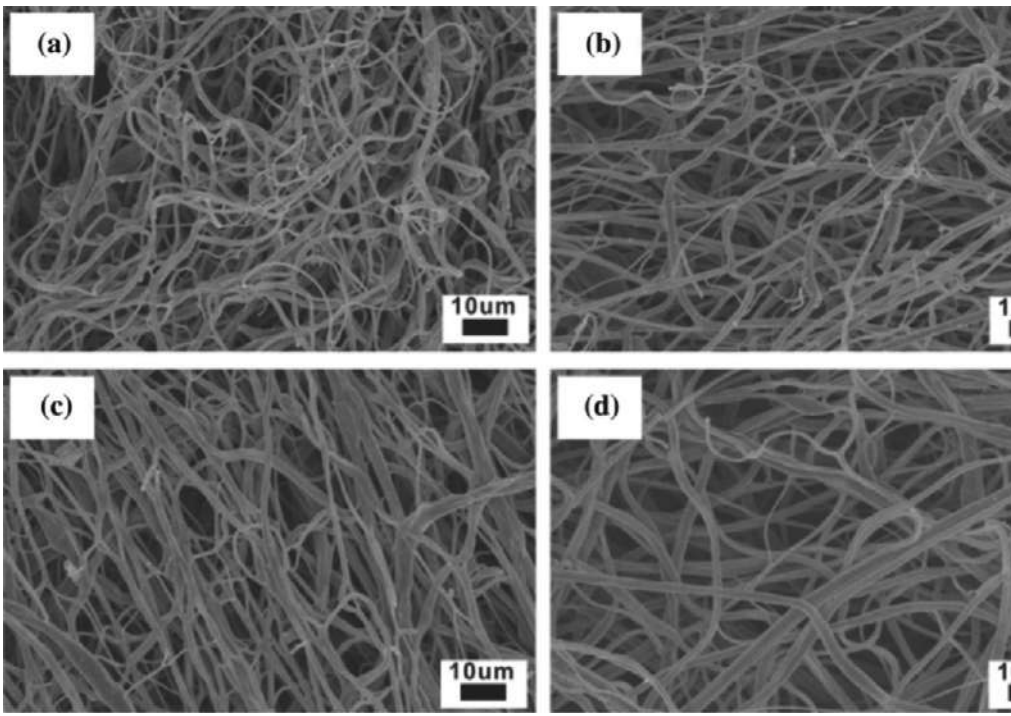

FIG. 11.1

SEM images of carbon fibers. (A) PANCA-10-0; (B) PANCA-9-1; (C) PANCA-8-2; (D) PANCA-7-3 (Ma et al., 2018).

maintained a smooth surface. Due to the achievement of a molecular-level dispersion, the phase separation procedure has been eliminated, which caused by electrospinning process that brings instantaneous solvent removal for the compatible pair of PAN and CA.

11.13.2 Microstructure of cellulose-based carbon fiber

High and specific surface area of electrodes, of supercapacitor, are ideal properties, which increase the capacitance. At 750°C (C-750), the directly carbonized CA shows no presence of pores, while using urea as activating agent, pores formation has occurred for all the as-prepared N-doped CA (CN-750, CN-600 and CN-900). Similarly, in the samples CN-750, CN-600 and CN-900, fibers are visible, while in sample C-750, it is no longer visible. This shows that from the cigarette butts, the nitrogen activating agent can preserve the fiber structures. When comparing the pore size of each sample, it is also obvious that CN-750 has the largest pore size. This shows that among the three different temperature adopted in the research, the carbonization temperature will affect the pore size, and that 750°C is the most suitable temperature to produce an electrode, which has high porosity.

11.14 Summary

The purpose of the use of this material to reduce weight while providing equal or better rigidity of the material it replaced. Carbon fiber composite can also be found at consumer products such as golf club shafts, fishing rods and shoes. On the other hand, in the past and with its current technology, the automotive industry was not as invested, due to the lack of commercial pull and high-volume production, which being the disadvantages for the usage of carbon-fiber composites. Therefore, to reduce vehicle weight and increase performance, carbon fiber composites are mostly found on high-end automobile or auto racing, which are utilized such to increase its rigidity and reduce lap time. Koenigsegg, Bugatti, McLaren, Ferrari, and Lamborghini are current pioneers in automotive industry, who use carbon fiber composite.

Acknowledgment

The authors would like to acknowledge Swinburne University of Technology Sarawak Campus and Universiti Malaysia Sarawak (UNIMAS) for the support.

References

Cheng, Y., Zhang, Q., Fang, C., Huang, Z., Chen, J., Wu, L., et al. (2019). Synthesis of N-doped porous carbon materials derived from waste cellulose acetate fiber via urea

activation and its potential application in supercapacitors. *Journal of the Electrochemical Society*, *166*, A1231–A1238.

Evans, H. (2006). Electrical distribution systems for carbon fibre bodied vehicles. In *SAE technical papers* SAE International. https://doi.org/10.4271/2006-01-1664.

Hauser, A., & Dolce, S. (1996). Design concepts for flexible thermal links. In *SAE technical papers* SAE International. https://doi.org/10.4271/961459.

Koronis, G., & Silva, A. (2018). Green composites for automotive applications. In *Green composites for automotive applications* (pp. 1–332). Elsevier. https://doi.org/10.1016/C2016-0-04188-8.

Lee, M., Kim, G., Song, H., Park, S., & Yi, J. (2014). Preparation of energy storage material derived from a used cigarette filter for a supercapacitor electrode. *Nanotechnology*, *25*(34), 1–8. https://doi.org/10.1088/0957-4484/25/34/345601.

Leitten, C., Griffith, W., Compere, A., & Shaffer, J. T. (2002). High-volume, low-cost precursors for carbon fiber production. *SAE Transactions*, *111*, 727–734.

Ma, C., Chen, J., Fan, Q., Guo, J., Liu, W., Cao, E., et al. (2018). Preparation and one-step activation of nanoporous ultrafine carbon fibers derived from polyacrylonitrile/cellulose blend for used as supercapacitor electrode. *Journal of Materials Science*, *53*(6), 4527–4539. https://doi.org/10.1007/s10853-017-1887-7.

Matlin, S. A., Mehta, G., Hopf, H., & Krief, A. (2019). The periodic table of the chemical elements and sustainable development. *European Journal of Inorganic Chemistry*, *2019* (39–40), 4170–4173. https://doi.org/10.1002/ejic.201801409.

Matsumura, T., Kinumoto, T., Matsuoka, M., Tsumura, T., & Toyoda, M. (2015). Preparation of carbonaceous fiber sheets derived from bamboo and application to gas diffusion layer of proton exchange membrane fuel cells. *ECS Transactions*, *64*(45), 19–27. Electrochemical Society Inc. https://doi.org/10.1149/06445.0019ecst.

Mellor, A. (2004). Advanced protective helmet for formula one. In *SAE Technical Papers* SAE International. https://doi.org/10.4271/2004-01-3514.

Popoola, L. T., Grema, A. S., Latinwo, G. K., Gutti, B., & Balogun, A. S. (2013). Corrosion problems during oil and gas production and its mitigation. *International Journal of Industrial Chemistry*, *4*(1). https://doi.org/10.1186/2228-5547-4-35.

Remy, J., Voss, M., Blackwell, D., & Natale, D. (2005). 2006 Corvette Z06 carbon fiber fender- engineering, design, and material selection considerations. *SAE Transactions*, *114*, 131–136.

Souto, F., Calado, V., & Pereira, N., Jr. (2018). Lignin-based carbon fiber: A current overview. *Materials Research Express*, *5*(7), 1–54. https://doi.org/10.1088/2053-1591/aaba00.

Spörl, J. M., Beyer, R., Abels, F., Cwik, T., Müller, A., Hermanutz, F., et al. (2017). Cellulose-derived carbon fibers with improved carbon yield and mechanical properties. *Macromolecular Materials and Engineering*, *302*(10). https://doi.org/10.1002/mame.201700195.

Starbuck, J., & Cataquiz, L. B. (2000). Evaluation of large tow-size carbon fiber for reducing the cost of CNG storage tanks. *SAE Transactions*, *109*, 793–798.

Warren, C., Shaffer, J., Paulauskas, F., & Abdullah, M. G. (2002). Low cost carbon fiber for the next generation of vehicles: Novel technologies. *SAE Transactions*, *111*, 719–726.

CHAPTER

Cellulose-based foaming materials

12

Faisal Islam Chowdhury[a], **Md Rezaur Rahman**[b], **and Jahidul Islam**[a]

[a]*Nanotechnology and Renewable Energy Research Laboratory (NRERL), Department of Chemistry, University of Chittagong, Chittagong, Bangladesh,* [b]*Department of Chemical Engineering and Energy Sustainability, Faculty of Engineering, Universiti Malaysia Sarawak (UNIMAS), Kota Samarahan, Sarawak, Malaysia*

Chapter outline

12.1 Introduction

Foam is made of two phases: gas bubble and a liquid or solid. The gas bubble phase is dispersed in a continuous liquid or a solid phase (Karim & Wai, 1999). Foams are lightweight, high specific strength, high absorbing impact load and outstanding thermal and sound insulation properties. It is the major petrochemical industrial product that is neither easy recyclable nor biodegradable (Lackner, 2015).

The waste of these fossil oil-based foams is normally treated by either combustion or landfill deposition, which pollutes the environment and endangers human health by contaminating air, water, and soil. It is necessary to replace petroleum-based products with environmental friendly biodegradable materials, i.e., bio-based alternatives (Nechyporchuk, Belgacem, & Bras, 2016).

Cellular solids such as cork, sponge, coral, wood, and pumice stone are quite diffusive. Cellular structure can be found in many foods such yeast fermented bread,

Fundamentals and Recent Advances in Nanocomposites Based on Polymers and Nanocellulose.
https://doi.org/10.1016/B978-0-323-85771-0.00002-6

meringue made of egg's white with sugar (Demitri et al., 2014; Nussinovitch, Gershon, & Peleg, 1998) etc. As plant cellulose is abundant in nature, low cost, renewable and bio-degradable, the cellulose-based foam has huge prospects in diversified application (Lavoine & Bergström, 2017) specially in absorption of pollutants from the air and water.

Many authors reported the preparation of zeolitic imidazole-based metal–organic framework combined with cellulose (ZIF-8/cellulose) composite materials and applied in PM2.5 (diameter of particulate matters $\leq$2.5 μm) removal and nitrogen adsorption (Duan et al., 2018; Ma et al., 2018, 2019; Qian et al., 2018; Su et al., 2018). Some reports suggested that metal–organic frameworks on to cellulose (MOF/cellulose) exhibited excellent metal ions adsorption removal performance. Some examples of such materials are (i) MOF-5/cellulose paper-based materials having good gas adsorption abilities (Yang, Zhang, Song, & Yang, 2017), (ii) UiO-66 and UiO-66-NH_2 based cellulose aerogels exhibiting great adsorption ability for heavy metal ions such as Pb^{2+} and Cu^{2+} in water (Lei et al., 2019) and (iii) ZIF-8, UiO-66 and MIL-100 loaded porous nanocellulose aerogel with good removal ability of rhodamine B, Cr (VI) and benzotriazole (Zhu, Yang, Cranston, & Zhu, 2016). The UiO-66 (UiO) stands for Universiteteti (Oslo), regarded as a typical MOF built of $[Zr_6O_4(OH)_4]$ octahedron clusters and 1,4-benzene dicarboxylic acid (BDC) ligands (Cavka et al., 2008), which has attracted a lot of attention due to its chemical and physical features (Chavan et al., 2010; Garibay & Cohen, 2010; Kandiah et al., 2010; Valenzano et al., 2011).

Though the cellulose-based foams are superior in comparison to their petroleum-based analogs, they are suffering from some drawbacks due to their larger pore size compared originated from their longer length (1–3 mm) and width (10–40 μm) than those of petroleum based materials (Kalia, Avérous, Njuguna, Dufresne, & Cherian, 2011). This lowers the structural homogeneity results the limited applicability of the cellulose-based foam materials (Mosiewicki & Aranguren, 2013).

12.2 Cellulose-based polyurethane foams

Polymeric composites with cellulose fibers have shown improved adsorption properties. Physical and chemical modification of the fiber surface can enhance the adhesion between the fiber and the polymer matrix (Bledzki & Gassan, 1999; Brasileiro, Colodette, & Piló-Veloso, 2001; John & Anandjiwala, 2008) resulting increased adsorption efficiency of the cellulose. Exposing the hydroxyl groups (-OH) of cellulose through chemical modification can increase the reactivity of the fiber surface (Bledzki & Gassan, 1999). In maceration process, hydrogen peroxide oxidizes acetic acid to form peracetic acid, which is highly selective in acidic medium to oxidize the aromatic rings of lignin (Brasileiro et al., 2001). Isocyanates groups can chemically modify the fibers increasing their compatibility with the matrix that significantly increase the performance of composites and nanocomposites (Dufresne & Belgacem, 2013; Fornasieri et al., 2011; Rowell, 2006).

Reaction of polyfunctional alcohols (polyol polyether or polyol polyester) and polyisocyanate form urethane linkages yielding polyurethanes (PUs). The PUs

can be prepared by various methods such as solvent-free and in organic solvents. A solvent-free method is the process to produce flexible and rigid foams. The one-shot process is the most extensively applied process, where co-reactants are direct mixed and a blowing agent, catalysts and other additives are simultaneously added. The additives such as fillers stabilizers, cross-linking agents and chain extenders extensively affect the properties of foam (Rivera-Armenta, Heinze, & Mendoza-Martínez, 2004). PU materials are widely used in furniture industry, building construction, transportation and shoe industry, agricultural industry, and medical application. As they are not biodegradable, they can seriously contaminate the environment. One of the potential solutions of this problem is to combine PUs with natural materials to alter them in to biodegradable composite materials.

The PUs are notable polymeric materials having versatile properties and ability in forming chemical bondswith hydroxyl groups of cellulosic fibers (Dilik, Erdinler, Hazir, Koç, & Hiziroglu, 2015; Liu, Martin, Moon, & Youngblood, 2015; Wu, Henriksson, Liu, & Berglund, 2007). For PUs foam preparation, other natural materials such as saccharides, cashew nut shell liquid, soybean oil and soy flour have been also used (Bhunia, Jana, Basak, Lenka, & Nando, 1998; Chang, Xue, & Hsieh, 2001a, 2001b; Guo, Javni, & Petrovic, 2000).

There are a range of cellulose derivatives with different properties like solubility and thermal behavior. Rivera-Armenta et al. studied some PUs composite foams prepared with various derivative of cellulose such as carboxymethyl cellulose (CMC), cellulose sulfate (CS), cellulose acetate (CA) and trimethylsilyl cellulose (TMSC) (Rivera-Armenta et al., 2004). The degree of substitution (DS) and chemical structures are shown in Table 12.1. All the derivatives have free –OH group based on their degree of substitution (DS) which can react to form PU foams. In the micrographs of the foams, different shape for each derivative was observed as shown in Fig. 12.1. Dynamic mechanical analysis (DMA) measurements showed the increased storage modulus with increasing cellulose derivative content. Cellulose sulfate-based foam exhibited the highest storage modulus.

Mohammadi and coworkers synthesized microcrystalline cellulose and polyurethane based elastomeric nanocomposites having strongly improved modulus, high tensile strength, and high strain-to-failure properties (Mohammadi, Daemi, & Barikani, 2014). They observed reinforcement of micromechanical stiffness in nanofibrils structure in the rubbery polymeric composite matrix. In addition, polyurethane molecules interact physically and chemically with cellulose nanofibril surfaces resulting entropic effects. Polyurethane foams prepared with thiacalixarene instead of glycerol as the crosslinking agent showed better adsorption of malachite green dye (Wang et al., 2014). Alternatively, the industrial wood residues are used to synthesize polyurethane composites foams, which are used for industrial wastewater treatment as well as add financial value to the industries (Bala, Lalung, & Ismail, 2015; O'Connell, Birkinshaw, & O'Dwyer, 2008).

Góes et al. studied three types of polyurethane foams (i) without cellulose (PU), (ii) with unmodified cellulose (PU/CEL), and (iii-a) with chemically modified cellulose 1:1 (PU/CEL 1:1) and (iii-b) with chemically modified cellulose 3:1 (PU/CEL3:1) (Góes et al., 2016). In the maceration process, the peracetic acid

Table 12.1 Specification of the cellulose derivatives used in foam formulations (Heinze, Erler, Nehls, & Klemm, 1994; Klemm, Heublein, Fink, & Bohn, 2005; Rivera-Armenta et al., 2004; Schulz, Burchard, & Dönges, 1998).

Type	DS[a]	Abbreviation	Structure	References
Cellulose acetate	2.4	CA1[b]	Cell–O–CO-CH_3	Schulz et al. (1998)
Cellulose acetate	1.7	CA2		
Carboxymethyl cellulose	1.3	CMC1	Cell–O–CH_2COONa	Heinze et al. (1994)
Carboxymethyl cellulose	0.8	CMC2[b]		
Cellulose sulfate	1.5	CS1	Cell-O–SO_3Na	Klemm, Philpp, Heinze, Heinze, and Wagenknecht (1998)
Cellulose sulfate	1.0	CS2		
Trimethylsilyl cellulose	2.9	TMSC1	Cell–O–Si–$(CH_3)^3$	
Trimethylsilyl cellulose	2.1	TMSC2		

[a]DS = degree of substitution calculated by ^1H NMR after perpropionylation (CA), HPLC after chain degradation (CMC), elemental analysis (CS) and (TMSC).
[b]Commercial samples. Cell = $(-CH_2-COOH)_n$.

removes substances such as greases, waxes, part of the hemicellulose and lignin from the wood fiber surface remaining just the cellulose with exposed hydroxyl groups that may serve as reaction sites for 4,4′-diphenylmethane di-isocyanate (MDI). The chemical structure can be shown for the chemical modification of cellulose with 4,4′-diphenylmethane di-isocyanate (MDI) in Fig. 12.1 (Góes et al., 2016).

Fig. 12.2 shows the scanning electron microscopic (SEM) images of, cellulose, chemically modified cellulose at molar ratio of OH/NCO 1:1 and chemically modified cellulose at molar ratio of OH/NCO 3:1 and Fig. 12.3 displays the SEM images of polyurethane without cellulose, polyurethane with unmodified cellulose, polyurethane with chemically modified cellulose at molar ratio of OH/NCO 1:1, polyurethane with chemically modified cellulose at molar ratio of OH/NCO 3:1 and camera images of Polyurethane foam synthesized with cellulose modified with MDI at molar ratio of OH/NCO 1:1. The SEM micrographs of the polyurethane-cellulose foams show irregular size and shape of pores of foam cells. The open cells are observed and no skin is formed. Foam cells form intercommunicated inner region and "voids" is formed in the cell wall, as shown in Fig. 12.4.

The authors observed that the addition of cellulose (with or without modification) in to the polyurethane increases the sorption capacity of the Procion Red HE-7B and Procion Yellow HE-4R dyes but and does not affect the sorption capacity of the

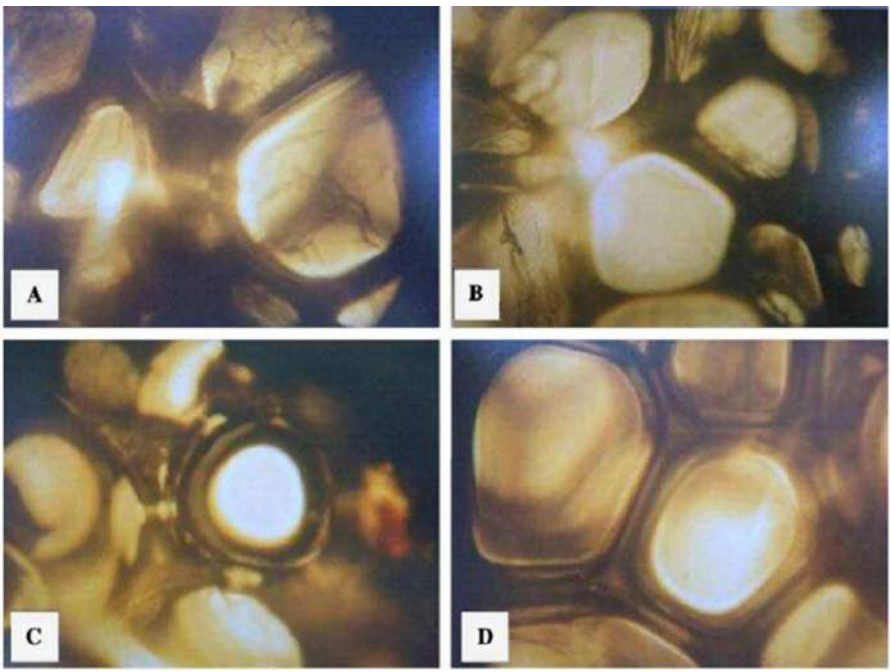

FIG. 12.1

Light micrograph of PU foams containing different cellulose derivatives: (A) cellulose acetate, (B) carboxymethyl cellulose, (C) cellulose sulfate, (D) trimethylsilyl cellulose (Góes et al., 2016).

Methylene Blue dye. It was suggested that the sorption process was governed by chemisorption and surface adsorption and intraparticle diffusion took place simultaneously (Góes et al., 2016).

12.3 Nanocomposites

In the field of nanocomposites, the most common biopolymer cellulose, (Klemm et al., 2005) has got attention as an interesting source of nano-reinforcements forming cellulose nanofibers (CNF) or cellulose nanocrystals (CNCs) which have excellent properties such as low density, high modulus and tensile strength, biodegradability, renewability, and availability (Fortunati et al., 2013). Also, nano-reinforcements can enhance the mechanical properties of the matrix even at low levels of filler content, (Mittal, 2009) which results lower environmental influence. Due to such outstanding mechanical properties and environmental friendliness, CMCs have been extensively used with polyurethane to prepare

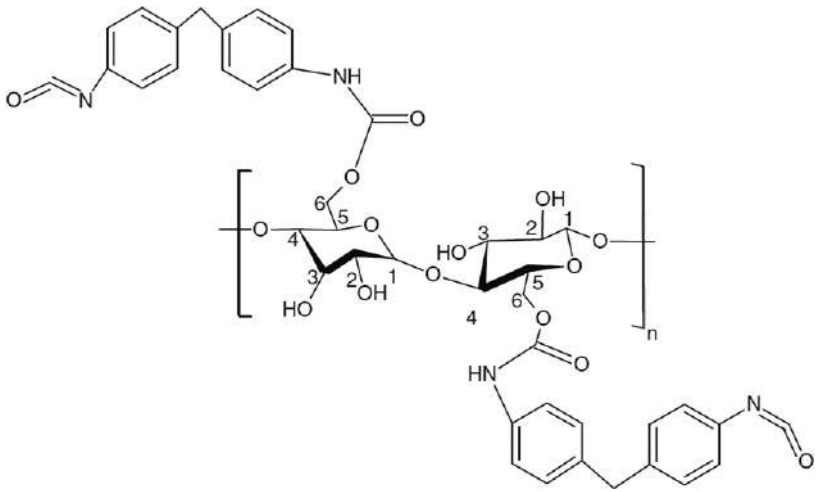

FIG. 12.2

The chemical structure proposed for the chemically modified cellulose with 4,4′-diphenylmethane diisocyanate (MDI) (Góes et al., 2016).

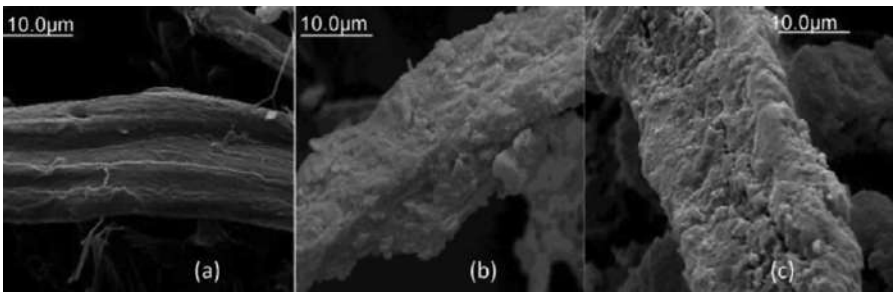

FIG. 12.3

Scanning microscopy (SEM) of (A) cellulose, (B) chemically modified cellulose at molar ratio of OH/NCO 1:1 and (C) chemically modified cellulose at molar ratio of OH/NCO 3:1 (Góes et al., 2016).

cellulose-polyurethane nanocomposites. There are some common methods to synthesize polyurethane nanocomposites such as: solvent casting (De Oliveira Patricio et al., 2013; Rueda et al., 2013), melt blending (Ramôa et al., 2013; Valentini, Piana, Pionteck, Lamastra, & Nanni, 2015) and in situ polymerization (Rueda et al., 2013; Saralegi, Gonzalez, Valea, Eceiza, & Corcuera, 2014). To prepare polyurethane foams, that have crosslinked structure, the in situ polymerization technique is applied with the addition of no reinforcement to the polyurethane precursors in starting of the polymerization. For enhancement of mechanical properties of the nanocomposites, closer interaction between the matrix and the

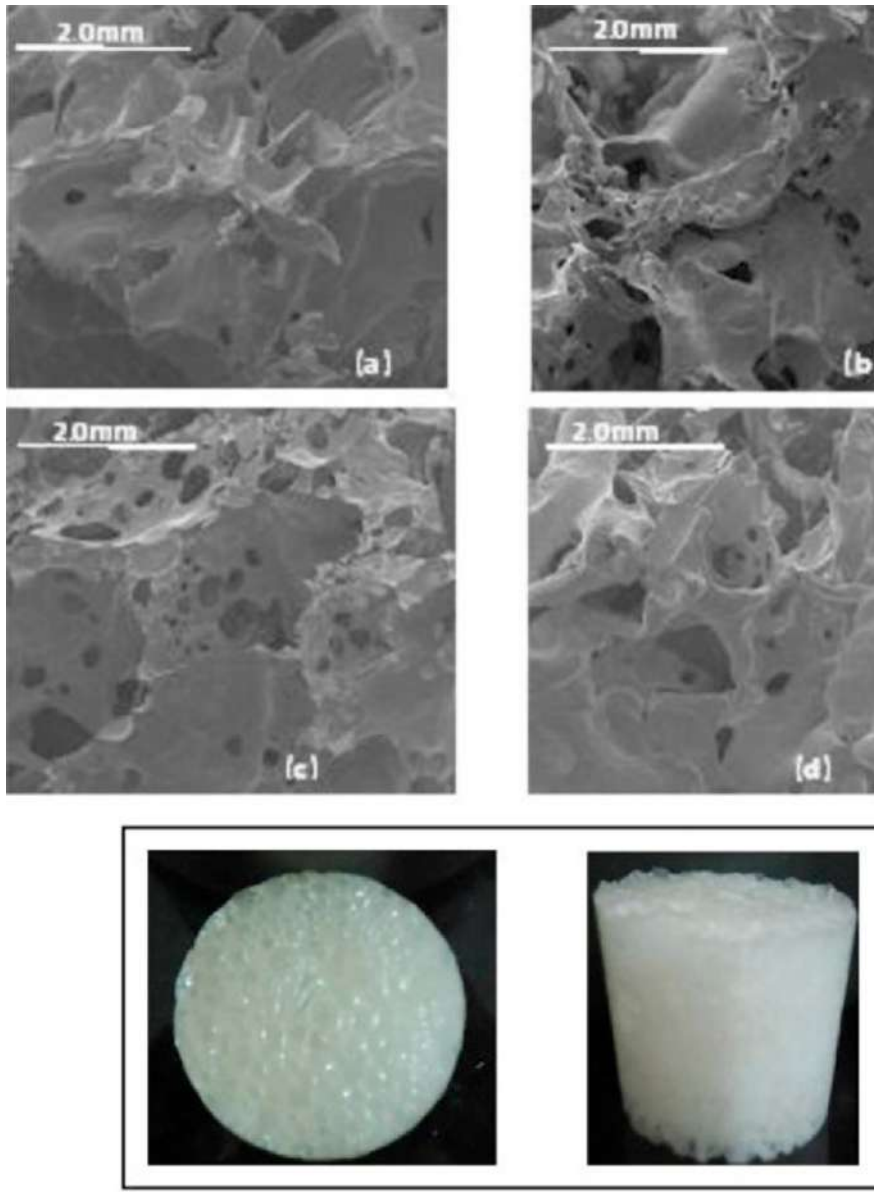

FIG. 12.4

Scanning microscopy (SEM) of polyurethane without cellulose (A), polyurethane with unmodified cellulose (B). Polyureth
molar ratio of OH/NCO 1:1 (C) and polyurethane with chemically modified cellulose at molar ratio of OH/NCO 3:1 (D) (uppe
foam synthesized with cellulose modified with MDI at molar ratio of OH/NCO 1:1 (down) (Góes et al., 2016).

nano-reinforcement, which is the result of good dispersion of nano-entities, is necessary but nano-reinforcements incorporation is one of the main challenges. Practically, nano-entities are incorporated to the polyol component in solid state to prepare concerned flexible polyurethane foam/CNC nanocomposites. Mosiewicki and Aranguren (2013) used mechanical stirring to mix commercial micro/nano cellulose and the polyol.

The aqueous suspension is stable as the sulfate groups at the CNC surface reintroduced by sulfuric acid hydrolysis can create electrostatic repulsion between particles. Nevertheless, the agglomerates could be formed by drying CNCs depending on the drying technique and their redispersibility even in limited water because of formation of strong hydrogen bonding present in the cellulose backbone. Alternatively, polar organic solvents are used for redispersion and subsequently they are removed. However, in this way, the redispersion cannot be occurred completely.

Isolated CNCs by acid hydrolysis of microcrystalline cellulose (MCC).The CNCs was directly incorporated in a renewably sourced polyol mixture to obtain aqueous CNCs dispersion. Foams formed in a one shot method in open molds after removing water from polyol-CNCs mixture. The effect of different CNC percentages on the morphology, microstructure and final properties of the foam nanocomposites were analyzed by Fourier-transform infrared (FTIR) spectroscopy, scanning electron microscopy (SEM), dynamical mechanic analysis (DMA), compressive mechanical tests, resilience test, AFM and infrared near-field microscopy (IR s-SNOM) and nano-spectroscopy (nano-FTIR).

Figs. 12.5 and 12.6 show SEM images of CNC/PU foams both in perpendicular and parallel directions to cell growth together with cell size distribution in longitudinal and transversal directions. The CNCs incorporation influenced the foam morphology by increasing cell size which may be due to their effect in the mechanisms involving the cellular structure formation. Particularly, the increase in cell dimensions could be thought that CNCs acted as particulate surfactants in spite of nucleating agents. In addition, the incorporation of polyol can also affect the formation of cellular structure due to its higher reactivity as it has primary hydroxyl groups and higher hydroxyl number. The foam density is dependent on cell size, cell density and wall and/or strut thickness.

12.4 Cellulose-phenolic foams

The utilization of phenolic foams for insulation applications has developed over the most recent couple of decades, as they are more beneficial than the other commercially available polymeric foams. Phenolic foams are thermally stable in a broad range of temperature and exhibit excellent fire-resistance properties such as low flammability, no dripping combustion, and low smoke density (Klempner & Frisch, 1991. In contrast, these polymeric foams show relatively low mechanical performance and high brittleness. For improving the mechanical performance of polymeric materials, some modifiers such as inert fillers and synthetic fibers are doped (Shen, Lavoie, & Nutt, 2003).

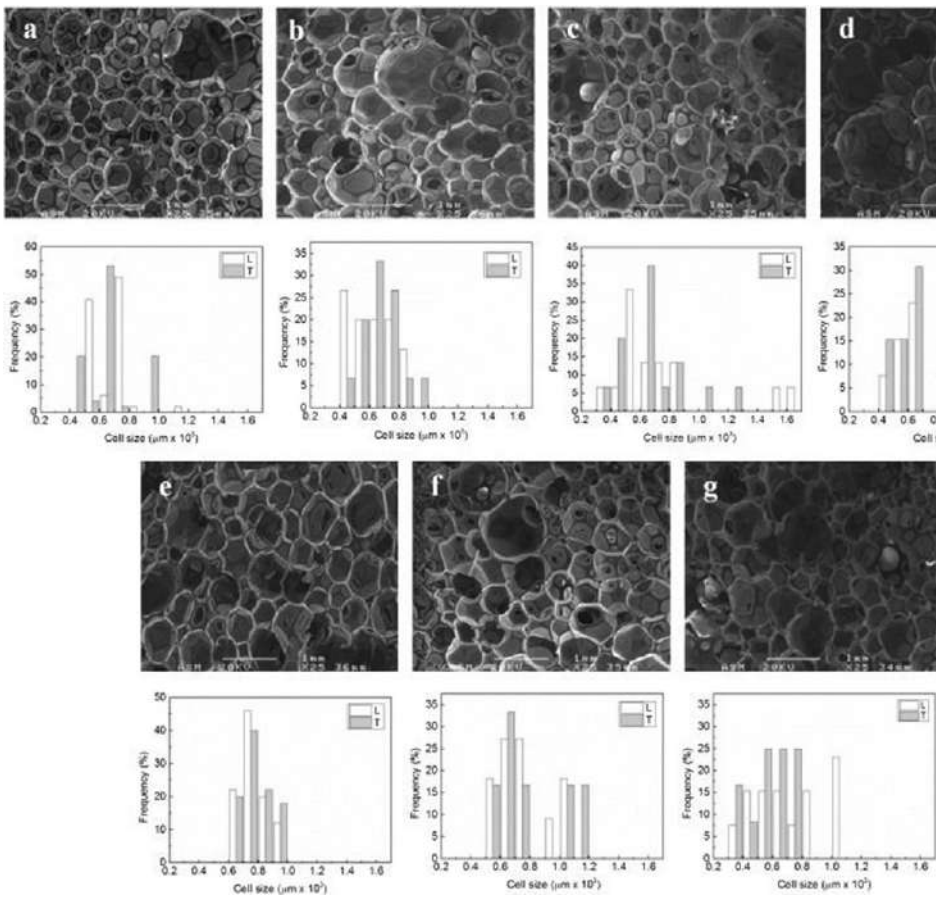

FIG. 12.5

SEM images (X25) and the corresponding cell size distribution in the longitudinal (L) and transversal (T) direction
(C) PF100-0.75, (D) PF100-1.5, (E) PF80, (F) PF80-0.75 and (G) PF80-1.5 in the perpendicular direction to fo

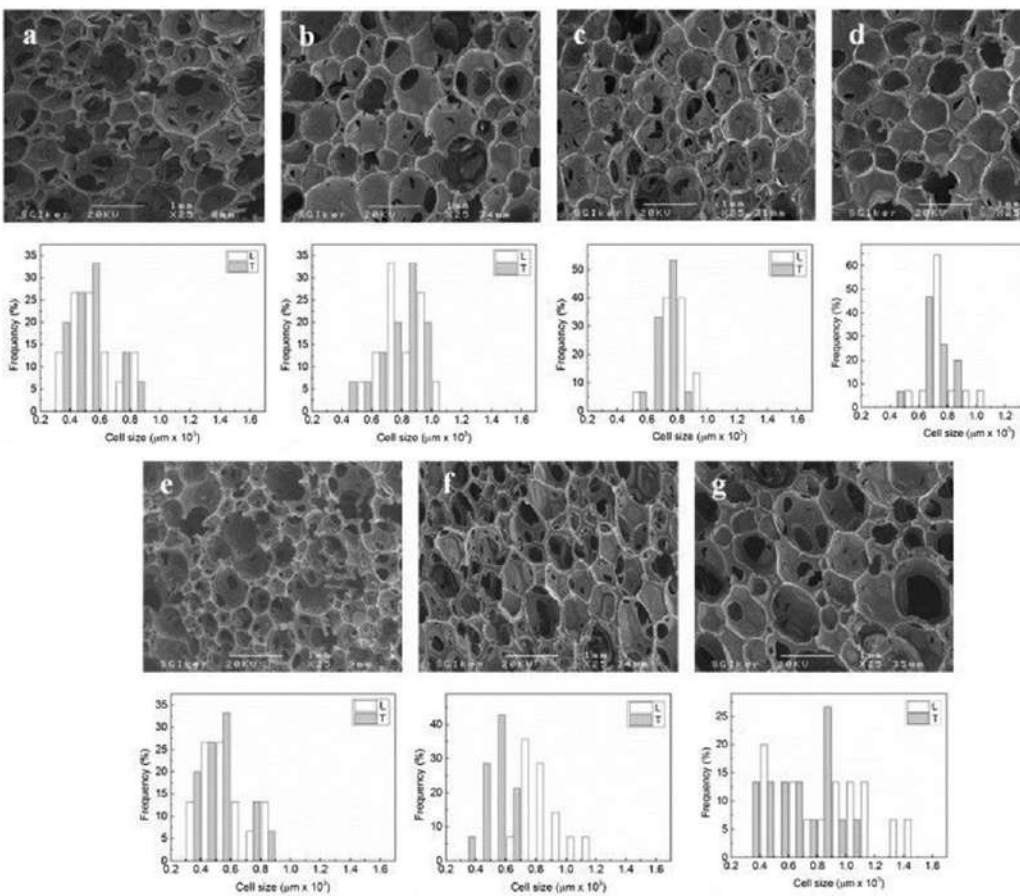

FIG. 12.6

SEM images (X25) and the corresponding cell size distribution in the longitudinal (L) and transversal (T) directions of (A) P
(C) PF100-0.75, (D)PF100-1.5, (E) PF80, (F) PF80-0.75 and (G) PF80-1.5 in the parallel direction to foam growth.

Natural resource based reinforcement agents such as jute, sisal, hemp, kenaf and wood fiber were incorporated into the polymeric materials for developing mechanical performance (Jawaid & Khalil, 2011). Saz-Orozco and coworkers incorporated wood flour and lignin nanoparticle into phenolic foam for enhancing the compressive mechanical properties (Del Saz-Orozco, Alonso, Oliet, Domínguez, & Rodriguez, 2014; Del Saz-Orozco, Oliet, Alonso, Rojo, & Rodríguez, 2012). However, incorporation of cellulose fiber into phenolic polymer matrix is new compared to other phenolic natural fiber composite foaming materials.

Rojo, Oliet, Virginia Alonso, Del Saz-Orozco, and Rodriguez (2014) used regenerated cellulose fiber to reinforce a polymeric phenolic matrix. According to their report, the best cellulose fiber-reinforced phenolic matrix composites with most excellent most properties was observed by treating the fibers with 1.5% of 3-(2-aminoethylamino) propyltrimethoxysilane (AAPS) for 100 min. The AAPS silane was proved as an efficient coupling agent between the viscose cellulosic fibers and the phenolic matrix resulted the enhanced mechanical properties in tension and flexion. It also improved the fiber–matrix compatibility by forming cohesive interfaces between both materials and developed the better dispersion of the viscose cellulosic fibers into the phenolic matrix.

Silva, Takahashi, Chaussy, Belgacem, and Silva (2010) studied rigid polyurethane foams (RPFs) composites with different concentrations of cellulose fiber in the presence of water and pentane as blowing agents. These fibers were collected as an industrial residue of bleached cellulose pulp production (Silva et al., 2008). This industrial waste exhibited a high proportion of cellulose with conserved fibrillar morphology and low contents of lignin and inorganic residue. They observed the behavior of the modified phenolic matrix evaluated by the measured values of strength, elongation, modulus, and strain energy density. The values of tensile and flexural responses for the different combinations of curing temperature and time of the phenolic matrix are shown in Table 12.2. Tensile strength of the foaming matrix decreases at curing temperatures above 87.5 °C and/or times over 3.5 h because of the formation of bubbles in the foaming material (Zhang, Shang, Zhang, Wang, & Hourston, 1995). The flexural strength of the cured matrix can be varied in the range 11.7–13.7 MPa and also increases with the curing temperature for any time studied. At a particular temperature, flexural strength rises with the curing time to a constant value and even it can be decreased. The predicted and experimental values of mechanical properties for the cured phenolic matrix are compared in Table 12.3.

If the curing temperatures and times are low, the material gains more plasticity with constant stiffness (Hawkins, O'Toole, & Jackovich, 2005). The properties of the material changes from brittle to ductile with the increasing of its elongation until it undergoes break down. This also can reduce its strength. Furthermore, compressive strength decreased due to the presence of defects in the foaming materials caused by changing morphology and the presence of more irregular cells. Generally, the morphological properties such as the shape of the cells and the density of RPFs have strong influence on their thermal and mechanical properties (Hawkins et al.,

Table 12.2 Experimental conditions and results obtained in tensile (T) and flexural (F) tests for the phe
(Silva et al., 2010).

			σ (MPa)		ε (%)		*E*(MPa)	
Run	***T*(°C)**	***t*(h)**	**T**	**F**	**T**	**F**	**T**	**F**
1	50	1	7.31	11.78	5.57	5.86	232.83	212.17
2	70	2.5	8.54	12.82	4.21	4.41	290.90	246.56
3	90	1	8.22	12.03	3.81	3.84	294.86	273.62
4	70	0.4	7.17	11.58	4.53	5.69	240.36	221.34
5	70	2.5	8.40	1254	4.28	4.60	300.94	249.29
6	50	4	7.82	11.28	5.12	5.10	241.17	211.32
7	70	2.5	8.41	12.70	4.39	4.74	289.29	236.91
8	70	4.6	8.15	1274	3.77	4.66	286.75	278.31
9	41.7	2.5	7.24	11.72	5.44	5.81	231.30	211.23
10	90	4	7.88	13.57	2.91	3.76	309.05	320.85
11	98.3	2.5	8.16	13.84	2.85	3.62	332.13	317.85

Table 12.3 Comparison between predicted and experimental values of mechanical properties for
under optimal conditions (Silva et al., 2010).

	Tension			Fl	
Response	**Predicted**	**Experimental**	**Dried**[a]	**Predicted**	**Experim**
σ (MPa)	8.51	8.50	13.28 [156%]	12.90	12.82
ε (%)	3.97	3.91	1.86 [48%]	4.49	4.93
E(MPa)	297.29	282.14	835 [296%]	265.38	262.06
SED ($J \times 10^{-5}/m^3$)	1.99×10^5	1.87×10^5	1.32×10^5 [71%]	1.89×10^5	1.79×10

[a]*Mechanical properties of the phenolic matrix after drying. Values in parentheses represent the mechanical properties of dried undried material (100%).*

2005; Tabor, Lepovitz, Potts, Latham, & Latham, 1997). Foams is formed with isotropic cells having similar mechanical resistances in the horizontal and vertical directions. In contrary, anisotropic cells exhibit higher mechanical resistance in the direction of growth.

SEM images for RPF0 (rigid polyurethane foams without cellulose fiber) and the composite foams (with 0%, 1%, 3%, 4%, 8%, 12%, and 16% *w*/w cellulose fiber having sample ID of RPF0, RPF1, RPF2, RPF3, RPF4, RPF8, RPF12 and RPF16, respectively) are presented in Fig. 12.7. The average diameters of the RPF cellular foaming materials are shown in Table 12.4.

Small anisotropic features of the foam matrix were observed in the SEM image (Fig. 12.7A). These properties could be validated by the average vertical and horizontal diameters of the material with the values of around 464, 126 and 394 μm, respectively. The addition of the cellulose fibers into the composite foams did not alter the anisotropic characteristic of the foam. However, the cells grew to be more irregular and defective features in comparison with the unfilled matrix foam cells as illustrated in Fig. 12.7B–G. About 30% in the average diameters reduction of the cells was found in the structure of the composite foams with the addition of the fibers in the range 1–12% w/w (samples RPF1–RPF12) (Table 12.4). The foam composite sample RPF16 (Fig. 12.7G) had a smaller cell diameter with a close to 50% reduction in the average diameter compared to the matrix foam.

Del Saz-Orozco, Alonso, Oliet, Domínguez, and Rodriguez (2015) reported the compressive mechanical properties, thermal stability and morphology of phenolic foams reinforced with cellulose fiber. The highest compressive mechanical properties was observed by incorporating 2 wt% of the reinforcement. This foam (2 wt% cellulose fiber-reinforced) had 21% and 18% increased compressive modulus and strength, respectively, compared to the unreinforced material. The incorporation of the cellulose fibers to the phenolic foam decreased the thermal stability of the material by a little amount. Electron microscopy (SEM) morphology images of the reinforced foams indicated a strong bonding between the fibers and phenolic matrix. The addition of the cellulose fibers into the foam resulted in a decreased cell size and increased cell density of the material.

Fig. 12.8 represents the SEM images of the edges and walls of the 4 and 8 wt% cellulose fiber-reinforced phenolic foams (CRPFs). The cellulose fibers are observed at the edges of the cells foam. It is also observed that a good fiber-matrix bonding has been occurred, as both the cellulose fibers and phenolic matrix are hydrophilic (Azwa, Yousif, Manalo, & Karunasena, 2013). A good fiber/matrix bonding in the composite foam material results in better mechanical performance (Jawaid & Khalil, 2011; Soykeabkaew, Supaphol, & Rujiravanit, 2004), which is quite conceivable with the compressive mechanical properties (Fig. 12.7) of the materials.

The effect of the cellulose fibers on the morphology of the phenolic foam was studied by SEM images for PF and CRPFs (2, 4, 6 and 8 wt% of cellulose fibers) at a low magnification (×50) which are presented in Fig. 12.9 along with their respective cell diameter distributions. The mean cell diameter and cell density of the cellulose fiber foams are tabulated in Table 12.5.

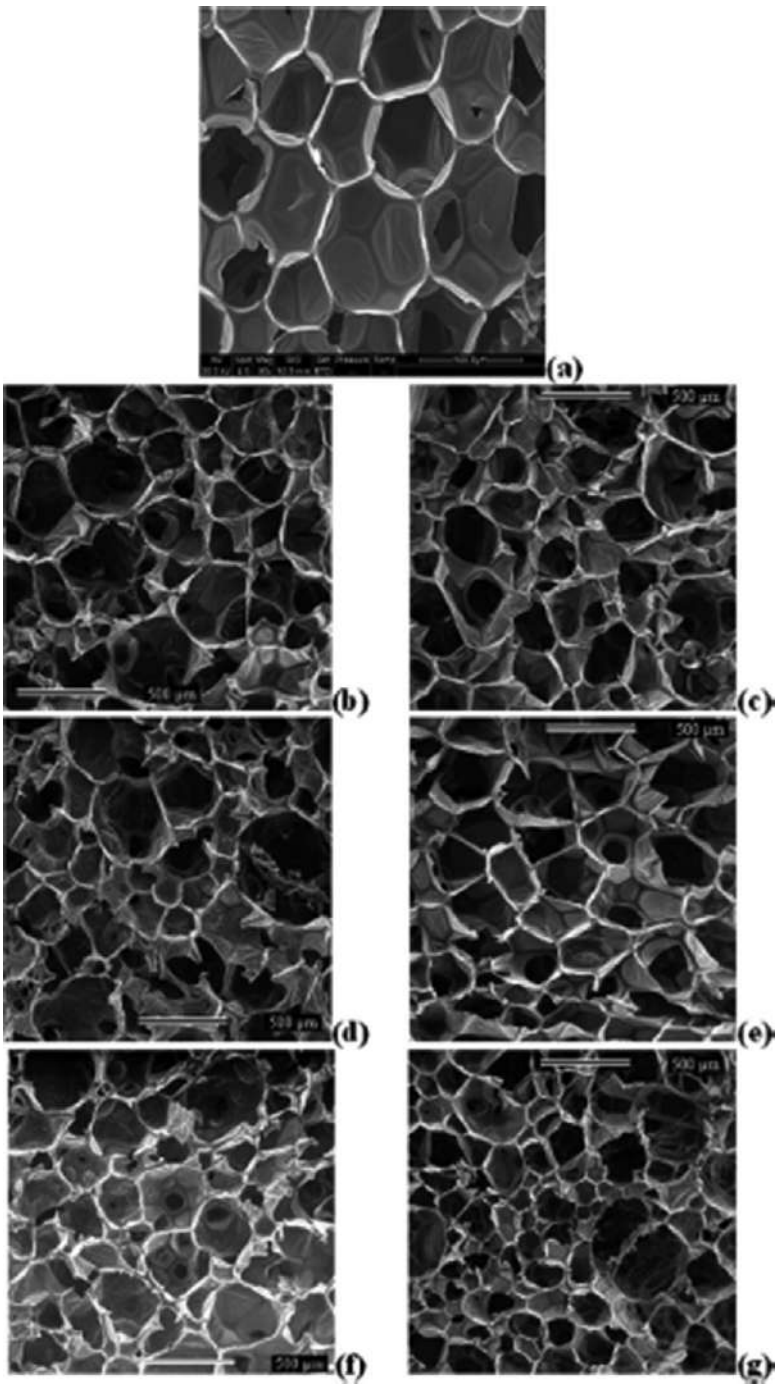

FIG. 12.7

SEM micrographs for the (A) matrix foam RF0 and the composite foams, (B) RPF1, (C) RPF3, (D) RPF4, (E) RPF8, (F) RPF12, and (G) RPF16 (the scale bar is 500 μm) (Silva et al., 2010).

Table 12.4 Average density and cell average diameter in the vertical direction for the unfilled matrix foam and the composite foams (Silva et al., 2010).

Sample	Average density (kg/m^3)	Cell average diameter (μm)
RPF0	29 ± 2	464 ± 126
RPF1	29 ± 2	348 ± 110
RPF3	27 ± 3	327 ± 89
RPF4	28 ± 2	342 ± 108
RPF8	32 ± 2	307 ± 96
RPF12	33 ± 2	368 ± 101
RPF16	37 ± 2	228 ± 81

With the increase of percentage of cellulose fibers into the phenolic foam, the cell size of the foam material decreases. For instance, mean cell diameter of the 2 wt% CRPF was 0.069 mm, while for 8 wt% CRPF was 0.053 mm. The viscosity of the foam matrix increases with limiting cells growing by the incorporation of the cellulose fibers (Ribeiro Da Silva et al., 2013). Desai, Basbagill, Nutt, and Alonso (2010) also observed same trend. Also, the mean cell diameter of a phenolic foam decreased with the addition of glass and aramid fibers into the foam material. Similarly, Del Saz-Orozco et al. (2015) reported the similar trend for lignin nanoparticle- and wood floor-reinforced phenolic foams (Del Saz-Orozco et al., 2014, 2012).

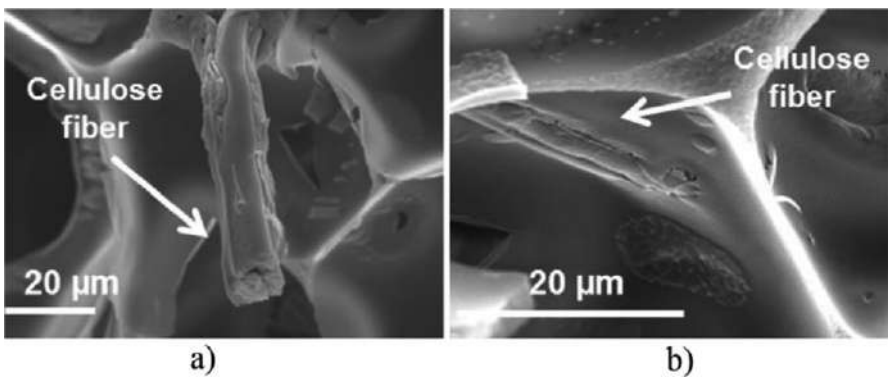

FIG. 12.8

SEM images for cellulose fiber-reinforced phenolic foams (A) 4 wt% CRPF and (B) 8 wt% CRPF (Del Saz-Orozco et al., 2015).

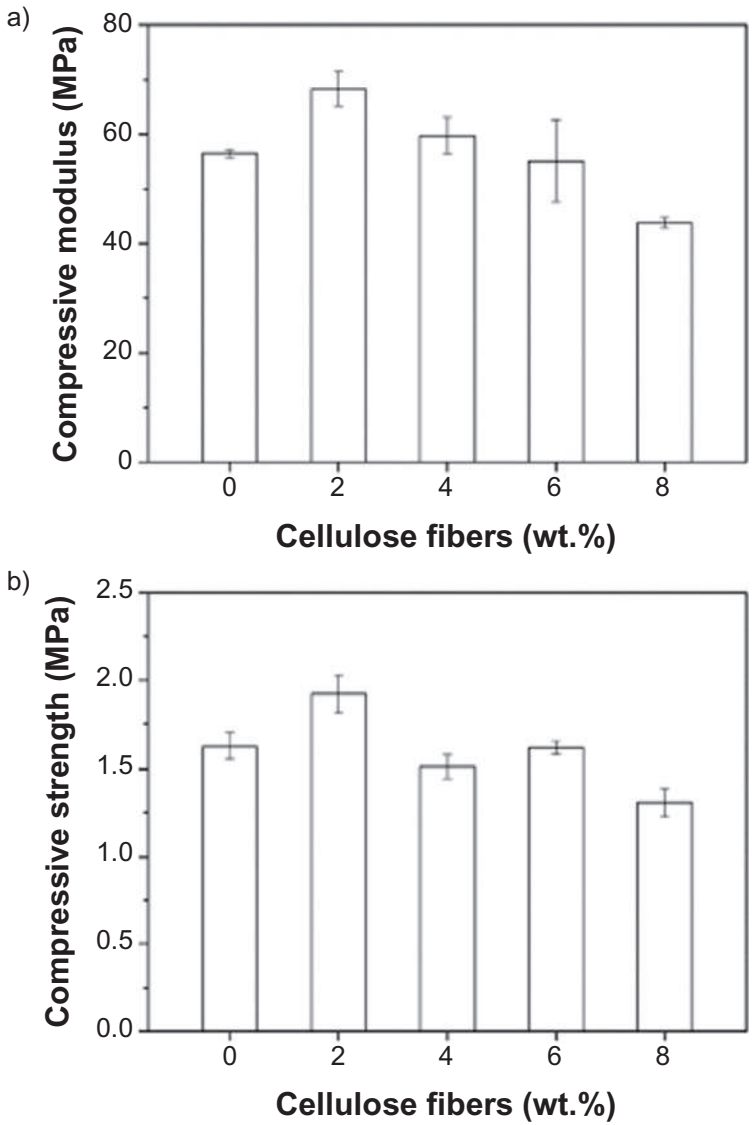

FIG. 12.9

Compressive mechanical properties for PF and CRPFs with 2, 4, 6 and 8 wt% of cellulose fibers: (A) Modulus (MPa) and (B) Strength (MPa) (Del Saz-Orozco et al., 2015).

Alternatively, the cell density of the foam material increased with the increasing cellulose fiber percentage into the phenolic foam. The density of the cell of 2 and 8 wt% CRPF were 2.71×10^6 cells/cm^3 and 5.63×10^6 cells/cm^3, respectively. This increasing trend was occurred because of formation of bubble with increased

Table 12.5 Mean cell diameter (D), cell density (NF) and cell wall density for the PF and CRPFs formulated at several cellulose fiber weight fractions.

Cellulose fibers (wt%)	D (mm)	N_F (10^6 cells/cm^3)	Cell wall density (kg/m^3)
0	0.079	2.46	438
2	0.069	2.71	300
4	0.064	3.30	292
6	0.061	3.48	273
8	0.053	5.63	285

rate by adding the cellulose fibers into the foam matrix. The cell with smaller diameter generally causes higher cell density of the foams (Gautham, 1991).

12.5 Cellulose in starch foams

In particular, starch foams are considered as environmentally friendly alternatives of the traditional petroleum based foaming materials. Starch is a weak, brittle and water sensitive carbohydrate based natural polymer which is used to prepare starch foams. Considerable efforts such as extrusion, hot-mold baking/compression, microwave heating, freeze-drying/solvent exchange, and supercritical fluid extrusion have been put forth to produce starch based foams with different cellular structures and properties. To increase microstructure, mechanical and thermal properties, moldability, water resistance, lightness, and other properties of starch-based foams enormous efforts, e.g., chemical modification of starches, blending with various biodegradable polymers, incorporation of natural fibers, and the addition of nanofillers, have been given by many researchers worldwide. Plasticizers (usually water and glycerol) are generally incorporated into starch to develop the flexibility of the foam product. Also, the plasticizer lower melting temperature of a plasticized starch below its decomposition temperature results considerable improvement in processability of starch as a thermoplastic (Neus Angles & Dufresne, 2000; Svagan, Azizi Samir, & Berglund, 2007). Some additives such as $CaCO_3$, talc, and salts (e.g., NaCl and $CaCl_2$) can also be added to lower the foam processing time, in addition to raising aesthetic performance and improved foam cell structure resulting better mechanical strength of the foam (Zhang et al., 1995; Zhou, Song, & Parker, 2006, 2007). Moreover, the starches have been chemically modified such as: poly(lactic acid) (PLA), poly(ε-caprolactone) (PCL), poly(hydroxyester ether) (PHEE), poly(vinyl al*co*hol) (PVA), chitosan, poly(hydroxybutyrate-co-valerate) (PHBV), poly(butylenes-succinate) (PBSA), poly(ester amide) (PEA) butanediol-terephthalate-adipate terpolymer (PBAT), cellulose acetate (CA) and blended with starches for the enhancement of water resistance and strength of the foams (Duanmu, Gamsted, & Rosling, 2007; Guan & Hanna, 2004; Kaisangsri, Kerdchoechuen, & Laohakunjit,

2012; Preechawong, Peesan, Supaphol, & Rujiravanit, 2005; Pushpadass, Babu, Weber, & Hanna, 2008; Shey, Imam, Glenn, & Orts, 2006; Shogren, Lawton, & Tiefenbacher, 2002; Willett & Shogren, 2002; Zhang & Sun, 2007). Addition of reinforcing agents into a starch matrix has been shown to be an effective way to develop high-performance starch-based composite foaming materials. There are many natural lignocellulosic fibers such as jute, flax, aspen, corn, soft wood, eucalypt cellulose, kraft pulp, sugarcane bagasse, cotton linter, hemp, α-cellulose, and wheat bran as well as some nanofillers such as clays and nanocelluloses that can be introduced to reinforce starch foams (Aguilar-Palazuelos, Zazueta-Morales, Jiménez-Arévalo, & Martínez-Bustos, 2007; Bénézet, Stanojlovic-Davidovic, Bergeret, Ferry, & Crespy, 2012; Bergeret & Benezet, 2011; Carr, Parra, Ponce, Lugão, & Buchler, 2006; Debiagi, Mali, Grossmann, & Yamashita, 2011; Duanmu et al., 2007; Guan & Hanna, 2004, 2006; Kaisangsri et al., 2012; Lawton, Shogren, & Tiefenbacher, 2004; Soykeabkaew et al., 2004; Svagan et al., 2007).

There are wide varieties of sources especially most green plants that produce the natural polymer, starch which is renewable, low cost, and inherently biodegradable or can be completely converted to carbon dioxide, water, mineral and biomass by microorganisms, with no negative environmental impact or ecotoxicity (Neus Angles & Dufresne, 2000; Wrolstad, 2012). It exists in small, dense, discrete packages known as granules, which are insoluble in cold water (BeMiller & Whistler, 2009). Starch granules gather at high concentrations in cereal grains (e.g., wheat, rice, maize, barley, rye, oats, millet, sorghum) and in vegetative structures such as tubers (potatoes) and roots (cassava and taro). These granules have various shapes and sizes (spheres, ellipsoids, polygons, platelets, irregular tubules) with dimensions generally ranging from 2 to $>100\,\mu m$, depending on their source plants as represented in Fig. 12.10 (Pérez, Baldwin, & Gallant, 2009).

Amylose and amylopectin are two major starch polymers available in nature. Amylose is an essential linear polymer with α-1-4 linked glucopyranosyl units having two smaller polymers (around the order of 10^4 to 10^5 of molecular weight and a degree of polymerization (DP) of 250–1000 D-glucose units) (BeMiller & Whistler, 2009). Amylopectin is an exceedingly branched molecular structure with $(1\rightarrow4)$-linked α-D-glucopyranosyl units in chains joined by $(1\rightarrow6)$ linkages. Amylopectin is one of the largest molecules produced naturally with molecular weight in the order of 10^6 to 10^8 (DP$\approx$5000 to 50,000 D-glucose units). There are 20%–30% amylose and 70%–80% amylopectin in normal starches, such as normal maize, rice, wheat, and potato, contain (BeMiller & Whistler, 2009). The molecular orientation of amylose and amylopectin inside a starch granule is very interesting. The starch granule has both amorphous and crystalline portions assembled in the grain in an onion like structure. Crystallinity of starch mainly comes from amylopectin chains with the formation of a double helical crystalline structure. Amylose constitutes the amorphous structure and part of the amylose is present as a helical complex with the lipids. In addition, Amylose places adjacent to, or intertwined with amylopectin so that the integrity of the granule can be maintained (BeMiller & Whistler, 2009; Izquierdo-Roca et al., 2008; Madrigal, Sandoval, & Müller, 2011).

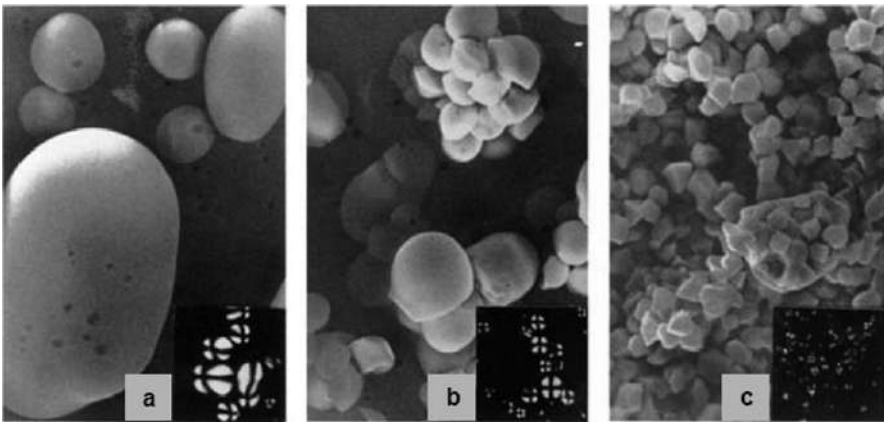

FIG. 12.10

Starch granules observed by scanning electron microscopy: (A) potato; (B) cassava; and (C) rice starches. The corresponding granules under polarized light are shown in insets [33].

The thermal characteristics of starches is much more complicated than conventional thermoplastics as the diverse physicochemical properties are observed when they are heated, for example, gelatinization, glass transition, melting, crystallization, crystal structure alteration, volume expansion, degradation of molecular structure, and motion of water. The water-starch content ratio is the governing factor for all these thermal behaviors (Liu, Yu, Xie, & Chen, 2006; Maaruf, Che Man, Asbi, Junainah, & Kennedy, 2001; Yu & Christie, 2001; Dilik et al., 2015; Liu et al., 2015; Wu et al., 2007).

The polymer mobility greatly depends on the glass transition at low water content in. At adequately lower temperatures, starches become glassy state results stopping large-scale molecular motions. At a higher temperature called glass transition temperature (Tg), molecules start to move which allows segmental mobility of the starch. At the temperature upper the Tg, a brittle, glassy-like solid (crystalline) converted into a more soft, flexible rubbery state (amorphous). Practically, in this state starch has more amorphous portions than crystalline portions. Additionally, absorption of increasing amount of moisture from the atmosphere by the amorphous regions, water molecules affect the starch as plasticizer to drop the T_g (Biliaderis, 2009; Madrigal et al., 2011).

As only starch made extrudates are brittle, they cannot be used alone for foam preparation (Mitrus & Moscicki, 2014). The extrudate properties can be improved by incorporating natural fiber additive. Cellulose is one of the major components that is available in the nature. All natural fibers have hydrophilic characteristics (Mohanty, Misra, & Drzal, 2005) For the preparation of starch foam, amount and nature of the fiber should be considered. An excessive amounts of fiber may lose the structural integrity of starch foam by breaking the air cells in the extrudates which can reduce the expansion ratio (Wang et al., 2014). Alternatively, lower amount of fiber cellulose addition into extrudates can exhibit nucleating characteristics causing

cell expansion results higher cells production (Bénézet et al., 2012; Ganjyal & Hanna, 2004). Some reports have concluded that higher percentage of fiber (more than 15%) can diminish extrudates' expansion quality (Altan, McCarthy, & Maskan, 2008; Kaisangsri et al., 2016; Wang et al., 2017). According to the study of Kumar, Sarkar, and Sharma (2010), carrot fiber could affect the expansion of the rice flour extrudate. They observed that 11.75% carrot fiber could cause the maximum expansion of rice flour extrudates. Altan et al. (2008) incorporated tomato pomace into barley flour in a co-rotating twin screw extruder and observed that the mixtures of 2% and 10% tomato pomace had superior performance in appearance, taste, texture, color and in general satisfactoriness than the control samples.

Also, the size of the fiber particle significantly influences the various product parameters. In general, the smaller particle size of fiber result in extrudate with superior expansion ratio (Kallu, Kowalski, & Ganjyal, 2017). Alam et al. (2014) observed that fine rye bran (28 μm) particle produced more expanded, crispy, and soft characteristics than the coarse sized particle (440 μm). Wang et al. (2017) reported that smallest particle size of 5% cherry pomace (<125 μm) addition produced extrudates with the highest expansion ratio among all treatments. In the starch polymer matrix, fibers are used as a filler material. If the particles size of fiber is smaller, they can easily disperse and fill pores of the walls of the expanded starch matrix with maintaining structural continuity (Kallu et al., 2017; Wang et al., 2017). Conversely, if the fiber size is larger, they could fill up the starch matrix evenly with a higher structural disruption tendency of the starch matrix during expansion leading to decrease in the expansion (Wang et al., 2017).

Kaisangsri, Kowalski, Kerdchoechuen, Laohakunjit, and Ganjyal (2019) studied the influence of cellulose on the physical properties of cassava starch foams. Cellulose fibers with 2 different particle sizes (C1: 32 μm and C2: 32–200 μm) were added at 0, 5, and 10% with three different moisture contents (15%, 17.5% and 20%) into cassava starch using a twin-screw extruder. The barrel temperature was optimized at 50, 100, 140 and 140 °C for all the experiments and the speed of extruder screw was varied (150, 200, and 250 rpm). The cassava starch foam properties significantly depend on cellulose fiber content and feed moisture content of the mixture. The expansion ratio increases with the addition of 5% C1 and C2 in comparison with the control (without the inclusion of any cellulose fiber) condition. The highest expansion ratio was obtained in the cassava starch foam having 5% cellulose fiber, and at 15% mixture moisture content with screw speed of 250 rpm. Alternatively, the expansion ratio reduced with up to 10% of increased cellulose fiber. According to scanning electron microscope images (Fig. 12.11), 5% cellulose fiber reinforced cellular structure of cassava starch foam was similar for the control. The water absorption index of cassava starch foams did not vary considerably, while water solubility index of cassava starch foam with C2 deferred extensively.

Fig. 12.11 shows the cross-sectional SEM images of cassava starch foam at 15%, 17.5%, and 20% feed moisture content and 0%, 5%, and 10% of cellulose fiber (C1 and C2) at the screw speed of 250 rpm. The cross-sectional SEM images of cassava starch foam with 5% C1 and C2 content at 15% moisture content of blend with

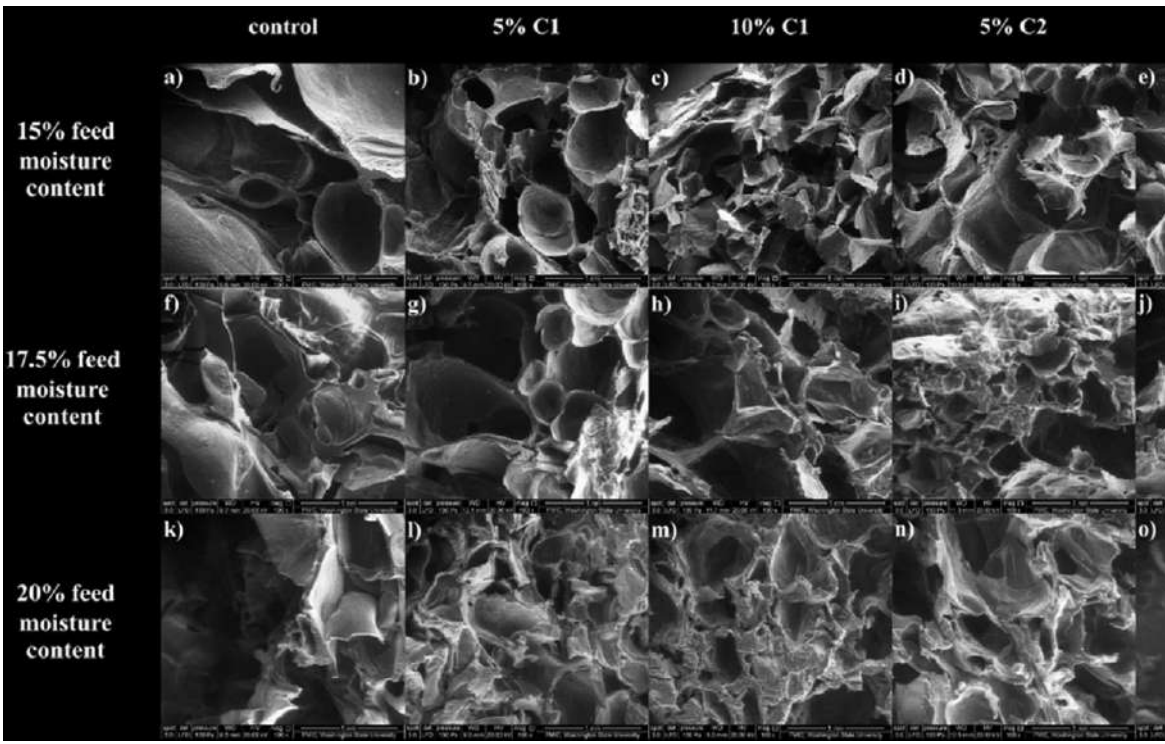

FIG. 12.11

SEM of cross-sections of cassava starch extrudates at 15% feed moisture content (A) control (0% cellulose), (B) 5% C1, (C
(E) 10% C2, 17.5% feed moisture content (F) control (0% cellulose), (G) 5% C1, (H) 10% C1, (I) 5% C2, (J) 10% C2, a
content (K) control (0% cellulose), (L) 5% C1, (M) 10% C1, (N) 5% C2, (O) 10% C2 (Kaisangsri et al., 2019).

250 rpm screw speed depicted that the cellular structure was similar to the control (without cellulose) (Fig. 12.11A–E). It is also evident that if the contents of C1 and C2 were increased to 10%, the cell walls distorted and the cell sizes reduced (Fig. 12.11C and E). This was ascribed to the fact that the higher fiber level had more probable for accumulation. This might create non-uniform distribution of fiber in the starch foam matrix that reduced the cell size. At 17.5% feed moisture content, cell size of cassava starch extrudates with 5% C2 (Fig. 12.11I) declining compared to control (Fig. 12.11F) and the foam with 5% C1 (Fig. 12.11G). This is justifiable as the smaller size fibers are more compatible with starch matrix without creating discontinuity of the foam structure (Bénézet et al., 2012; Wang et al., 2017). If the moisture content of blend raised, the cell walls diminished as shown in all the images of the cassava starch foam with a moisture content of 20%. It can be undoubtedly observed that the cell structures were not fully developed which suggested that the starch polymers did not degrade to the same level as that of the foam with 15% moisture content. This can conclude that the excess water in the mixture cannot initially evaporate which results the inhibition of the expansion by condensation (Kaisangsri et al., 2016).

Guan and Hanna studied starch acetate as a base material having a high degree of substitution (DS) of 2.0 to be extruded with α-cellulose, corncobs, talc, and ethanol at 160 °C keeping screw speed of 225 rpm (Guan & Hanna, 2004, 2006). In addition, cellulosic materials reduce the cost of foam materials, as starch acetate has higher cost. The EI, density, and compressive strength of the starch acetate/corncob and starch acetate/cellulose foams do not show significant differences. Both starch acetate foams with corncob and cellulose have good hydrophobic characteristics.

Guan and Hanna (2006) studied starch acetates with 1.68 and 2.30 degrees of substitution (DS) extruded with 10–30 wt% cellulose and 20 wt% ethanol using a twin screw extruder. A central composite response surface design was used to study the effects of starch DS, cellulose content, barrel temperature and screw speed on specific mechanical energy requirement (SME), the radial EI and compressibility of the extruded foams. In this case, higher DS starch blend showed increased SME. This was happened as larger functional groups (acetyl) attached to the pyranosyl rings restricted the movement of starch chains. Hence, greater viscosity as well as the higher EI of the foams with the higher DS starch was observed. Alternatively, EI declined with higher cellulose content resulted increased density. The higher dense foams are convenient for a better protection (absorbing impact forces) for the goods to transport as packaging materials. Also, 40 wt% microfibrillated cellulose (MFC can surely improve the compressibility and water resistance of the amylopectin foam (Soykeabkaew, Thanomsilp, & Suwantong, 2015). It is to be noted that if cellulose content increased, EI decreased, hence, density increased. The cell structure of this foam is presented in Fig. 12.12.

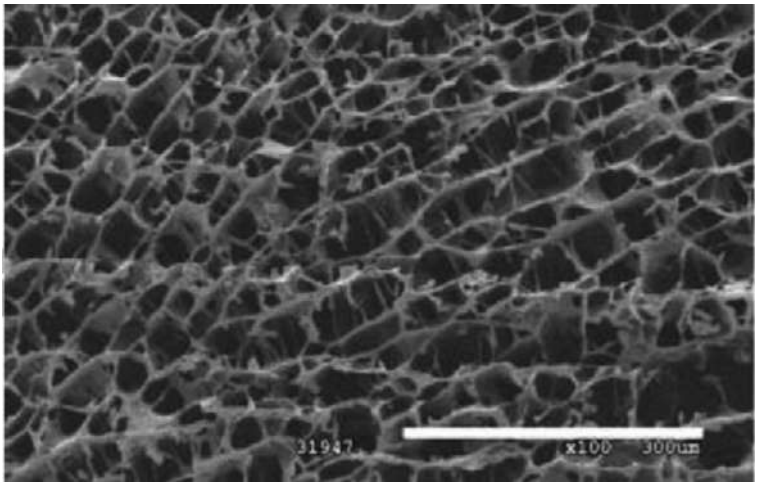

FIG. 12.12

Amylopectin foam with 40 wt% microfibrillated cellulose (MFC) (Soykeabkaew et al., 2015).

12.6 Cellulose as a reinforcing agent

The presently rapidly growing sector, bio-economy explores the demand of using more renewable feedstocks. In foam production industries, soybean oil which consists mainly triglycerides has become suitable. Lee and coworkers (Lee, Wong, Blaker, Hodgkinson, & Bismarck, 2011) used the mechanical frothing for preparing a gas–liquid foam from soybean-derived renewable monomers blended with bacterial cellulose (BC) nanofibrils dispersed in the monomer phase. Mechanically frothed gas-AESO-BC foam was polymerized by microwave heating with lauroyl peroxide as a thermal initiator. The produced bio-based macroporous polymer with a porosity of 60% has higher stability in the presence of bacterial nanofibrils. The Bacterial cellulose worked as a reinforcement agent for enhancing the mechanical properties. The incorporation of cellulose fibers in foam processing was essential to develop the three-dimensional polymer foams. Cellulose fibers can be used as an excellent foam stabilizer as it prevents the liquid draining from the film region of the gas-oil interfaces while concurrently behaving as a reinforcing agent in the polymer foam. The cellulose fibers reinforced foams have porosity of approximately 56%, and thermal behavior is unaffected (Kumari, Rath, Sri Hari Kumar, & Tiwari, 2015).

Fig. 12.13B–D depict the cellulose fibers effect that enhance the cellsize possibly because of the higher number of nucleating sites added by the cellulose fiber surfaces (Bergeret & Benezet, 2011).Simultaneously, the cellulose fiber-reinforced foams contained uniform pore structure, which is due to the distribution of cellulose fiber into the polymer matrix and the interactions between fiber and matrix.

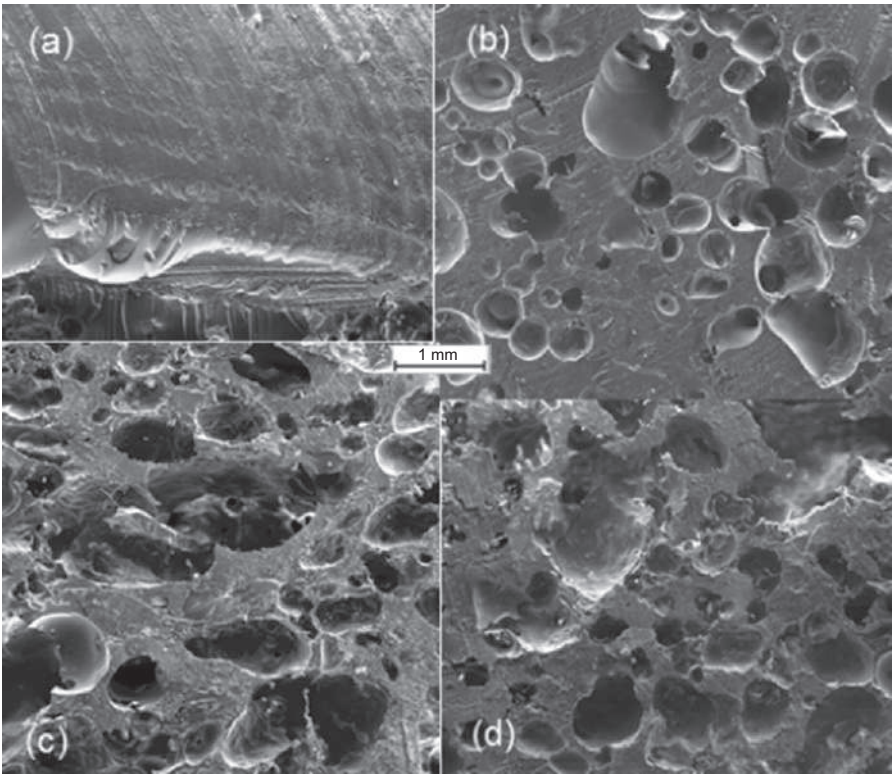

FIG. 12.13

The SEM images of foams consisting of pristine AESO material (A); as well as AESO foam reinforced with 2.0% cellulose fibers (B); 3.0% cellulose fibers (C); and 4.0% cellulose fibers (D) (Obradovic, Voutilainen, Virtanen, Lassila, & Fardim, 2017).

Due to local fiber-matrix bonding, holes are induced in which the gas loss protects the ability of cell growing in foam causing the non-uniform cell size distribution (Fig. 12.14). The increased cellulose fiber loading creates more viscous monomer phase causing the gas bubbles expansion in the monomer phase. The bubbles can create the random orientation of the pores in the foam. Porosity is the important parameter in which polymer foams' physical properties are dependent. Grain volume, bulk volume, grain density, and bulk density, along with the calculated porosity of cellulose-reinforced AESO foams, are represented in Table 12.6.

It can be observed that the cellulose fibers incorporation increased the porosity from 4.5% to 57.0%. Cellulose fibers stabilized the gas-soybean oil interface during thermal polymerization raising the total porosity of the foams. In mixing process, air bubbles are introduced into the bio-based soybean oil resin, which results the highly porous nature cellulose-reinforced $AESO_3$ foam. In addition, $AESO_3$ foam had the largest cell size compared to $AESO_2$ and $AESO_4$ foams as depicted in Fig. 12.14C.

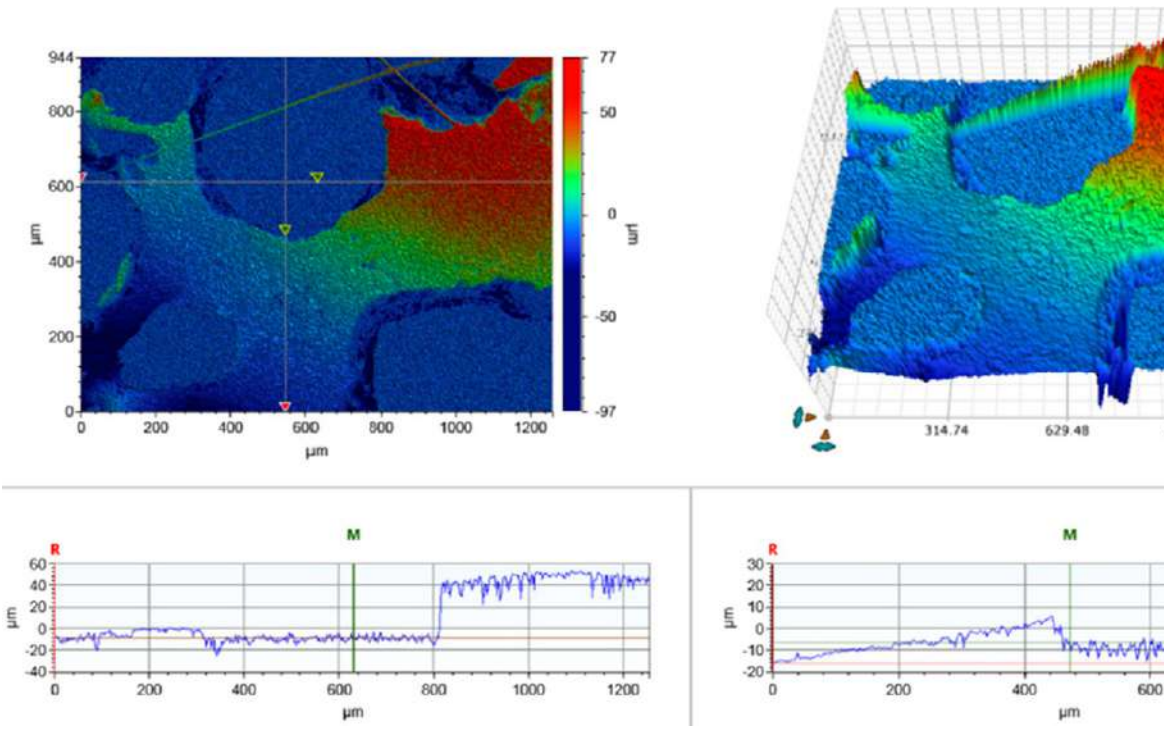

FIG. 12.14

The 3D images of AESO foam reinforced with 2% cellulose fibers (Obradovic et al., 2017).

Table 12.6 The porosity, volumes, and density of the pristine AESO and cellulose-reinforced AESO foams (Obradovic et al., 2017).

Samples	Porosity ε (%)	Grain volume V_G, (cm^3)	Bulk volume V_B, (cm^3)	Bulk density (g/cm^3)
AESO	4.5 ± 4.4	1.58 ± 0.05	1.65 ± 0.06	1.48 ± 0.04
AESO 2	57.0 ± 1.8	1.92 ± 0.05	4.45 ± 0.15	0.538 ± 0.004
AESO 3	58.3 ± 1.5	2.16 ± 0.05	5.17 ± 0.15	0.474 ± 0.003
AESO 4	54.2 ± 1.8	2.08 ± 0.05	4.55 ± 0.15	0.538 ± 0.004

As liquid foams are intrinsically unstable, phase separation in the foam based on the liquid bio-materials are occurred which results the larger pore size in $AESO_3$ (Lau, Wong, Lee, & Bismarck, 2014).

Adusumali et al. (2006) studied a big number of regenerated cellulose fibers by using single-fiber tensile tests and performed comparison with glass fibers and natural flax fibers. It was observed that the regenerated cellulose fiber composites were less strong in comparison to glass fiber reinforced composites, work to fracture performance is quite good. As there is a similar chemical composition in both regenerated cellulose fibers and natural fibers, they have compatibility problems with thermoplastics requiring coupling agents (Trejo-O'Reilly et al., 2000). Furthermore, due to the light-weight, durable, inexpensive, and potentially recyclable parts, cellulosic fiber reinforced composites have prospective application of is the automotive industry (Suddell & Evans, 2003). Compare to conventional glass and mineral filler, natural fibers are strong, lightweight, low-cost, environmentally friendly with comparable stiffness enhancement and better sound damping.

12.7 Conclusion

The emerging environmental awareness in the present world has created opportunity to develop environmentally friendly as well as sustainable materials from renewable resources. A widely abundant naturally occurred low cost biopolymer starch has become lucrative for producing biodegradable foam, which can alternate the petroleum-based non-degradable traditional foaming materials. There are a range of cellulose derivatives with different properties like solubility and thermal behavior. PUs composite foams were prepared with various derivatives of cellulose such as carboxymethyl cellulose (CMC), cellulose sulfate (CS), cellulose acetate (CA) and trimethylsilyl cellulose (TMSC). The addition of cellulose in to the polyurethane increases the sorption capacity, which was governed by chemisorption and surface adsorption and intraparticle diffusion took place simultaneously. Further, cellulose has got attention as an interesting source of nano-reinforcements forming cellulose nanofibers (CNF) or cellulose nanocrystals (CNCs) which have excellent properties

such as low density, high modulus and tensile strength, biodegradability, renewability, and availability. The CNCs incorporation influenced the foam morphology by increasing cell size, which may be due to their effect in the mechanisms involving the cellular structure formation. Also, nanoreinforcements can enhance mechanical properties of the matrix even at low levels of filler content, which results lower environmental influence leading to extensively usability of cellulose-polyurethane nanocomposites.

Cellulose-phenolic polymer matrix is new compared to other phenolic natural fiber composite foaming materials. In a study, the best cellulose fiber-reinforced phenolic matrix composites with most excellent properties was observed by treating the fibers with 1.5% of 3-(2-aminoethylamino) propyltrimethoxysilane (AAPS) for 100 min resulted the enhanced mechanical properties in tension and flexion. It also improved the fiber–matrix compatibility by forming cohesive interfaces between both materials and developed the better dispersion of the viscose cellulosic fibers into the phenolic matrix.

To increase microstructure, mechanical and thermal properties, moldability, water resistance, lightness, and other properties of starch-based foams enormous efforts, e.g., chemical modification of starches, blending with various biodegradable polymers, incorporation of natural fibers, and addition of nanofillers, have been given by many researchers worldwide.

Further, the Bacterial cellulose can be used as a reinforcement agent for enhancing the mechanical properties of the foam, which develops the three-dimensional network in the matrix. Cellulose fibers can also be used as an excellent foam stabilizer as it prevents the liquid draining from the film region of the gas-oil interfaces while concurrently behaving as a reinforcing agent in the polymer foam.

There are extensive literatures on cellulose-based foaming materials, which have covered in this chapter. Still more research works are necessary to develop cellulose-based foams with outstanding properties, completely green and sustainable, economically profitable.

Acknowledgment

The authors would like to thank and acknowledge Universiti Malaysia Sarawak (UNIMAS) and Department of Chemistry, University of Chittagong for the support.

References

Adusumali, R. B., Reifferscheid, M., Weber, H., Roeder, T., Sixta, H., & Gindl, W. (2006). Mechanical properties of regenerated cellulose fibres for composites. *Macromolecular Symposia*, *244*, 119–125. https://doi.org/10.1002/masy.200651211.

Aguilar-Palazuelos, E., Zazueta-Morales, J. D. J., Jiménez-Arévalo, O. A., & Martínez-Bustos, F. (2007). Mechanical and structural properties of expanded extrudates produced

from blends of native starches and natural fibers of henequen and coconut. *Starch/Staerke*, *59*(11), 533–542. https://doi.org/10.1002/star.200700608.

Alam, S. A., Järvinen, J., Kirjoranta, S., Jouppila, K., Poutanen, K., & Sozer, N. (2014). Influence of particle size reduction on structural and mechanical properties of extruded rye bran. *Food and Bioprocess Technology*, *7*(7), 2121–2133. https://doi.org/10.1007/s11947-013-1225-2.

Altan, A., McCarthy, K. L., & Maskan, M. (2008). Twin-screw extrusion of barley-grape pomace blends: Extrudate characteristics and determination of optimum processing conditions. *Journal of Food Engineering*, *89*(1), 24–32. https://doi.org/10.1016/j.jfoodeng.2008.03.025.

Azwa, Z. N., Yousif, B. F., Manalo, A. C., & Karunasena, W. (2013). A review on the degradability of polymeric composites based on natural fibres. *Materials and Design*, *47*, 424–442. https://doi.org/10.1016/j.matdes.2012.11.025.

Bala, J. D., Lalung, J., & Ismail, N. (2015). Studies on the reduction of organic load from palm oil mill effluent (POME) by bacterial strains. *International Journal of Recycling of Organic Waste in Agriculture*, *4*(1). https://doi.org/10.1007/s40093-014-0079-6.

BeMiller, J. N., & Whistler, R. L. (2009). *Starch: Chemistry and technology*. Academic Press.

Bénézet, J. C., Stanojlovic-Davidovic, A., Bergeret, A., Ferry, L., & Crespy, A. (2012). Mechanical and physical properties of expanded starch, reinforced by natural fibres. *Industrial Crops and Products*, *37*(1), 435–440. https://doi.org/10.1016/j.indcrop.2011.07.001.

Bergeret, A., & Benezet, J. C. (2011). Natural fibre-reinforced biofoams. *International Journal of Polymer Science*, *2011*. https://doi.org/10.1155/2011/569871.

Bhunia, H. P., Jana, R. N., Basak, A., Lenka, S., & Nando, G. B. (1998). Synthesis of polyurethane from cashew nut shell liquid (CNSL), a renewable resource. *Journal of Polymer Science, Part A: Polymer Chemistry*, *36*(3), 391–400. https://doi.org/10.1002/(SICI)1099-0518(199802)36:3<391::AID-POLA3>3.0.CO;2-V.

Biliaderis, C. G. (2009). Structural transitions and related physical properties of starch. In *Starch* (pp. 293–372). Elsevier Inc. https://doi.org/10.1016/B978-0-12-746275-2.00008-2.

Bledzki, A. K., & Gassan, J. (1999). Composites reinforced with cellulose based fibres. *Progress in Polymer Science*, 221–274. https://doi.org/10.1016/s0079-6700(98)00018-5.

Brasileiro, L. B., Colodette, J. L., & Piló-Veloso, D. (2001). A utilização de perácidos na deslignificação e no branqueamento de polpas celulósicas. *Quimica Nova*, *24*(6), 819–829. https://doi.org/10.1590/s0100-40422001000600020.

Carr, L. G., Parra, D. F., Ponce, P., Lugão, A. B., & Buchler, P. M. (2006). Influence of fibers on the mechanical properties of cassava starch foams. *Journal of Polymers and the Environment*, *14*(2), 179–183. https://doi.org/10.1007/s10924-006-0008-5.

Cavka, J. H., Jakobsen, S., Olsbye, U., Guillou, N., Lamberti, C., Bordiga, S., et al. (2008). A new zirconium inorganic building brick forming metal organic frameworks with exceptional stability. *Journal of the American Chemical Society*, *130*(42), 13850–13851. https://doi.org/10.1021/ja8057953.

Chang, L. C., Xue, Y., & Hsieh, F. H. (2001a). Comparative study of physical properties of water-blown rigid polyurethane foams extended with commercial soy flours. *Journal of Applied Polymer Science*, *80*(1), 10–19. https://doi.org/10.1002/1097-4628(20010404)80:1<10::AID-APP1068>3.0.CO;2-Y.

Chang, L. C., Xue, Y., & Hsieh, F. H. (2001b). Dynamic-mechanical study of water-blown rigid polyurethane foams with and without soy flour. *Journal of Applied Polymer Science*, *81*(8), 2027–2035. https://doi.org/10.1002/app.1635.

Chavan, S., Vitillo, J. G., Uddin, M. J., Bonino, F., Lamberti, C., Groppo, E., et al. (2010). Functionalization of UiO-66 metal-organic framework and highly cross-linked polystyrene with Cr(CO)3: In situ formation, stability, and photoreactivity. *Chemistry of Materials*, *22*(16), 4602–4611. https://doi.org/10.1021/cm1005899.

De Oliveira Patricio, P. S., Pereira, I. M., Da Silva, N. C. F., Ayres, E., Pereira, F. V., & Oréfice, R. L. (2013). Tailoring the morphology and properties of waterborne polyurethanes by the procedure of cellulose nanocrystal incorporation. *European Polymer Journal*, *49*(12), 3761–3769. https://doi.org/10.1016/j.eurpolymj.2013.08.006.

Debiagi, F., Mali, S., Grossmann, M. V. E., & Yamashita, F. (2011). Biodegradable foams based on starch, polyvinyl alcohol, chitosan and sugarcane fibers obtained by extrusion. *Brazilian Archives of Biology and Technology*, *54*(5), 1043–1052. https://doi.org/10.1590/S1516-89132011000500023.

Del Saz-Orozco, B., Alonso, M. V., Oliet, M., Domínguez, J. C., & Rodriguez, F. (2014). Effects of formulation variables on density, compressive mechanical properties and morphology of wood flour-reinforced phenolic foams. *Composites Part B: Engineering*, *56*, 546–552. https://doi.org/10.1016/j.compositesb.2013.08.078.

Del Saz-Orozco, B., Alonso, M. V., Oliet, M., Domínguez, J. C., & Rodriguez, F. (2015). Mechanical, thermal and morphological characterization of cellulose fiber-reinforced phenolic foams. *Composites Part B: Engineering*, *75*, 367–372. https://doi.org/10.1016/j.compositesb.2015.01.049.

Del Saz-Orozco, B., Oliet, M., Alonso, M. V., Rojo, E., & Rodríguez, F. (2012). Formulation optimization of unreinforced and lignin nanoparticle-reinforced phenolic foams using an analysis of variance approach. *Composites Science and Technology*, *72*(6), 667–674. https://doi.org/10.1016/j.compscitech.2012.01.013.

Demitri, C., Giuri, A., Raucci, M. G., Giugliano, D., Madaghiele, M., Sannino, A., et al. (2014). Preparation and characterization of cellulose-based foams via microwave curing. *Interface Focus*, *4*(1). https://doi.org/10.1098/rsfs.2013.0053.

Desai, A. A., Basbagill, J., Nutt, S. R., & Alonso, M. V. (2010). Diffusivity and climatic simulation of hybrid foams. *Journal of Cellular Plastics*, *46*(5), 461–478. https://doi.org/10.1177/0021955X10373641.

Dilik, T., Erdinler, S., Hazir, E., Koç, H., & Hiziroglu, S. (2015). Adhesion strength of wood based composites coated with cellulosic and polyurethane paints. *Advances in Materials Science and Engineering*, 2015. https://doi.org/10.1155/2015/745675.

Duan, C., Meng, J., Wang, X., Meng, X., Sun, X., Xu, Y., et al. (2018). Synthesis of novel cellulose- based antibacterial composites of ag nanoparticles@ metal-organic frameworks@ carboxymethylated fibers. *Carbohydrate Polymers*, *193*, 82–88. https://doi.org/10.1016/j.carbpol.2018.03.089.

Duanmu, J., Gamsted, E. K., & Rosling, A. (2007). Synthesis and preparation of crosslinked allylglycidyl ether-modified starch-wood fibre composites. *Starch/Staerke*, *59*(11), 523–532. https://doi.org/10.1002/star.200700629.

Dufresne, A., & Belgacem, M. N. (2013). Cellulose-reinforced composites: From micro-to nanoscale. *Polimeros*, *23*(3), 277–286. https://doi.org/10.4322/polimeros.2010.01.001.

Fornasieri, M., Alves, J. W., Muniz, E. C., Ruvolo-Filho, A., Otaguro, H., Rubira, A. F., et al. (2011). Synthesis and characterization of polyurethane composites of wood waste and polyols from chemically recycled pet. *Composites Part A: Applied Science and Manufacturing*, *42*(2), 189–195. https://doi.org/10.1016/j.compositesa.2010.11.004.

Fortunati, E., Puglia, D., Monti, M., Santulli, C., Maniruzzaman, M., & Kenny, J. M. (2013). Cellulose nanocrystals extracted from okra fibers in PVA nanocomposites. *Journal of Applied Polymer Science*, *128*(5), 3220–3230. https://doi.org/10.1002/app.38524.

Ganjyal, G. M., & Hanna, M. A. (2004). Effects of extruder die nozzle dimensions on expansion and micrographic characterization during extrusion of acetylated starch. *Starch/Staerke*, *56*(3–4), 108–117. https://doi.org/10.1002/star.200300200.

Garibay, S. J., & Cohen, S. M. (2010). Isoreticular synthesis and modification of frameworks with the UiO-66 topology. *Chemical Communications*, *46*(41), 7700–7702. https://doi.org/10.1039/c0cc02990d.

Gautham, R. (1991). *Handbook of polymeric foams and foam technology* (pp. 5–15).

Góes, M. M., Keller, M., Masiero Oliveira, V., Villalobos, L. D. G., Moraes, J. C. G., & Carvalho, G. M. (2016). Polyurethane foams synthesized from cellulose-based wastes: Kinetics studies of dye adsorption. *Industrial Crops and Products*, *85*, 149–158. https://doi.org/10.1016/j.indcrop.2016.02.051.

Guan, J., & Hanna, M. A. (2004). Functional properties of extruded foam composites of starch acetate and corn cob fiber. *Industrial Crops and Products*, *19*(3), 255–269. https://doi.org/10.1016/j.indcrop.2003.10.007.

Guan, J., & Hanna, M. A. (2006). Selected morphological and functional properties of extruded acetylated starch-cellulose foams. *Bioresource Technology*, *97*(14), 1716–1726. https://doi.org/10.1016/j.biortech.2004.09.017.

Guo, A., Javni, I., & Petrovic, Z. (2000). Rigid polyurethane foams based on soybean oil. *Journal of Applied Polymer Science*, *77*(2), 467–473. https://doi.org/10.1002/(SICI)1097-4628(20000711)77:2<467::AID-APP25>3.0.CO;2-F.

Hawkins, M. C., O'Toole, B., & Jackovich, D. (2005). Cell morphology and mechanical properties of rigid polyurethane foam. *Journal of Cellular Plastics*, *41*(3), 267–285. https://doi.org/10.1177/0021955X05053525.

Heinze, T., Erler, U., Nehls, I., & Klemm, D. (1994). Determination of the substituent pattern of heterogeneously and homogeneously synthesized carboxymethyl cellulose by using high-performance liquid chromatography. *Die Angewandte Makromolekulare Chemie*, *215*(1), 93–106. https://doi.org/10.1002/apmc.1994.052150108.

Izquierdo-Roca, V., Pérez-Rodríguez, A., Morante, J. R., Álvarez-García, J., Calvo-Barrio, L., Bermudez, V., et al. (2008). Analysis of S-rich CuIn (S, Se)2 layers for photovoltaic applications: Influence of the sulfurization temperature on the crystalline properties of electrodeposited and sulfurized CuInSe2 precursors. *Journal of Applied Physics*, *103*(12). https://doi.org/10.1063/1.2939833.

Jawaid, M., & Khalil, H. P. S. A. (2011). Cellulosic/synthetic fibre reinforced polymer hybrid composites: A review. *Carbohydrate Polymers*, 1–18. https://doi.org/10.1016/j.carbpol.2011.04.043.

John, M. J., & Anandjiwala, R. D. (2008). Recent developments in chemical modification and characterization of natural fiber-reinforced composites. *Polymer Composites*, *29*(2), 187–207. https://doi.org/10.1002/pc.20461.

Kaisangsri, N., Kerdchoechuen, O., & Laohakunjit, N. (2012). Biodegradable foam tray from cassava starch blended with natural fiber and chitosan. *Industrial Crops and Products*, *37*(1), 542–546. https://doi.org/10.1016/j.indcrop.2011.07.034.

Kaisangsri, N., Kowalski, R. J., Kerdchoechuen, O., Laohakunjit, N., & Ganjyal, G. M. (2019). Cellulose fiber enhances the physical characteristics of extruded biodegradable cassava starch foams. *Industrial Crops and Products*, 142. https://doi.org/10.1016/j.indcrop.2019.111810.

Kaisangsri, N., Kowalski, R. J., Wijesekara, I., Kerdchoechuen, O., Laohakunjit, N., & Ganjyal, G. M. (2016). Carrot pomace enhances the expansion and nutritional quality of corn starch extrudates. *LWT - Food Science and Technology*, *68*, 391–399. https://doi.org/10.1016/j.lwt.2015.12.016.

Kalia, S., Avérous, L., Njuguna, J., Dufresne, A., & Cherian, B. M. (2011). Natural fibers, bio- and nanocomposites. *International Journal of Polymer Science*, *2021*, 1–2. https://doi.org/10.1155/2011/735932.

Kallu, S., Kowalski, R. J., & Ganjyal, G. M. (2017). Impacts of cellulose fiber particle size and starch type on expansion during extrusion processing. *Journal of Food Science*, *82*(7), 1647–1656. https://doi.org/10.1111/1750-3841.13756.

Kandiah, M., Nilsen, M. H., Usseglio, S., Jakobsen, S., Olsbye, U., Tilset, M., et al. (2010). Synthesis and stability of tagged UiO-66 Zr-MOFs. *Chemistry of Materials*, *22*(24), 6632–6640. https://doi.org/10.1021/cm102601v.

Karim, A. A., & Wai, C. C. (1999). Characteristics of foam prepared from starfruit (Averrhoa carambola L.) puree by using methyl cellulose. *Food Hydrocolloids*, *13*(3), 203–210. https://doi.org/10.1016/S0268-005X(98)00086-1.

Klemm, D., Heublein, B., Fink, H. P., & Bohn, A. (2005). Cellulose: Fascinating biopolymer and sustainable raw material. *Angewandte Chemie, International Edition*, *44*(22), 3358–3393. https://doi.org/10.1002/anie.200460587.

Klemm, D., Philpp, B., Heinze, T., Heinze, U., & Wagenknecht, W. (1998). *Comprehensive cellulose chemistry. Volume 1: Fundamentals and analytical methods*. Wiley-VCH Verlag GmbH.

Klempner, D., & Frisch, K. C. (1991). *Handbook of polymeric foams and foam technology. Vol. 404*. Wiley.

Kumar, N., Sarkar, B. C., & Sharma, H. K. (2010). Development and characterization of extruded product using carrot pomace and rice flour. *International Journal of Food Engineering*, *6*(3). https://doi.org/10.2202/1556-3758.1824.

Kumari, S., Rath, P., Sri Hari Kumar, A., & Tiwari, T. N. (2015). Extraction and characterization of chitin and chitosan from fishery waste by chemical method. *Environmental Technology and Innovation*, *3*, 77–85. https://doi.org/10.1016/j.eti.2015.01.002.

Lackner, M. (2015). *Bioplastics Kirk-Othmer encyclopedia of chemical technology*. Wiley.

Lau, T. H. M., Wong, L. L. C., Lee, K. Y., & Bismarck, A. (2014). Tailored for simplicity: Creating high porosity, high performance bio-based macroporous polymers from foam templates. *Green Chemistry*, *16*(4), 1931–1940. https://doi.org/10.1039/c3gc41807c.

Lavoine, N., & Bergström, L. (2017). Nanocellulose-based foams and aerogels: Processing, properties, and applications. *Journal of Materials Chemistry A*, *5*(31), 16105–16117. https://doi.org/10.1039/c7ta02807e.

Lawton, J. W., Shogren, R. L., & Tiefenbacher, K. F. (2004). Aspen fiber addition improves the mechanical properties of baked cornstarch foams. *Industrial Crops and Products*, *19*(1), 41–48. https://doi.org/10.1016/S0926-6690(03)00079-7.

Lee, K. Y., Wong, L. L. C., Blaker, J. J., Hodgkinson, J. M., & Bismarck, A. (2011). Bio-based macroporous polymer nanocomposites made by mechanical frothing of acrylated epoxidised soybean oil. *Green Chemistry*, *13*(11), 3117–3123. https://doi.org/10.1039/c1gc15655a.

Lei, C., Gao, J., Ren, W., Xie, Y., Abdalkarim, S. Y. H., Wang, S., Ni, Q., & Yao, J. (2019). Fabrication of metal-organic frameworks@ cellulose aerogels composite materials for removal of heavy metal ions in water. *Carbohydrate Polymers*, *205*, 35–41.

Liu, H., Yu, L., Xie, F., & Chen, L. (2006). Gelatinization of cornstarch with different amylose/amylopectin content. *Carbohydrate Polymers*, *65*(3), 357–363. https://doi.org/10.1016/j.carbpol.2006.01.026.

Liu, J. C., Martin, D. J., Moon, R. J., & Youngblood, J. P. (2015). Enhanced thermal stability of biomedical thermoplastic polyurethane with the addition of cellulose nanocrystals. *Journal of Applied Polymer Science*, *132*(22). https://doi.org/10.1002/app.41970.

Ma, S., Zhang, M., Nie, J., Yang, B., Song, S., & Lu, P. (2018). Multifunctional cellulose-based air filters with high loadings of metal–organic frameworks prepared by in situ growth method for gas adsorption and antibacterial applications. *Cellulose*, *25*(10), 5999–6010. https://doi.org/10.1007/s10570-018-1982-1.

Ma, S., Zhang, M., Yang, B., Song, S., Nie, J., & Lu, P. (2019). Preparation of cellulosic air filters with controllable pore structures via organic solvent-based freeze casting: The key role of fiber dispersion and pore size. *BioResources*, *13*(3), 5894–5908. https://doi.org/10.15376/biores.13.3.5894-5908.

Maaruf, A. G., Che Man, Y. B., Asbi, B. A., Junainah, A. H., & Kennedy, J. F. (2001). Effect of water content on the gelatinisation temperature of sago starch. *Carbohydrate Polymers*, *46*(4), 331–337. https://doi.org/10.1016/S0144-8617(00)00335-0.

Madrigal, L., Sandoval, A. J., & Müller, A. J. (2011). Effects of corn oil on glass transition temperatures of cassava starch. *Carbohydrate Polymers*, *85*(4), 875–884. https://doi.org/10.1016/j.carbpol.2011.04.013.

Mitrus, M., & Moscicki, L. (2014). Extrusion-cooking of starch protective loose-fill foams. *Chemical Engineering Research and Design*, *92*(4), 778–783. https://doi.org/10.1016/j.cherd.2013.10.027.

Mittal, V. (2009). *Optimization of polymer nanocomposite properties*. Wiley.

Mohammadi, A., Daemi, H., & Barikani, M. (2014). Fast removal of malachite green dye using novel superparamagnetic sodium alginate-coated Fe3O4 nanoparticles. *International Journal of Biological Macromolecules*, *69*, 447–455. https://doi.org/10.1016/j.ijbiomac.2014.05.042.

Mohanty, A. K., Misra, M., & Drzal, L. T. (2005). *Natural fibers, biopolymers, and biocomposites*. CRC Press.

Mosiewicki, M. A., & Aranguren, M. I. (2013). A short review on novel biocomposites based on plant oil precursors. *European Polymer Journal*, *49*(6), 1243–1256. https://doi.org/10.1016/j.eurpolymj.2013.02.034.

Nechyporchuk, O., Belgacem, M. N., & Bras, J. (2016). Production of cellulose nanofibrils: A review of recent advances. *Industrial Crops and Products*, *93*, 2–25. https://doi.org/10.1016/j.indcrop.2016.02.016.

Neus Angles, M., & Dufresne, A. (2000). Plasticized starch/tuniein whiskers nanocomposites. 1. Structural analysis. *Macromolecules*, *33*(22), 8344–8353. https://doi.org/10.1021/ma0008701.

Nussinovitch, A., Gershon, Z., & Peleg, L. (1998). Characteristics of enzymatically produced agar-starch sponges. *Food Hydrocolloids*, *12*(1), 105–110. https://doi.org/10.1016/S0268-005X(98)00047-2.

O'Connell, D. W., Birkinshaw, C., & O'Dwyer, T. F. (2008). Heavy metal adsorbents prepared from the modification of cellulose: A review. *Bioresource Technology*, *99*(15), 6709–6724. https://doi.org/10.1016/j.biortech.2008.01.036.

Obradovic, J., Voutilainen, M., Virtanen, P., Lassila, L., & Fardim, P. (2017). Cellulose fibre-reinforced biofoam for structural applications. *Materials*, *10*(6). https://doi.org/10.3390/ma10060619.

Pérez, S., Baldwin, P. M., & Gallant, D. J. (2009). Structural features of starch granules I. In *Starch* (pp. 149–192). Elsevier Inc. https://doi.org/10.1016/B978-0-12-746275-2.00005-7.

Preechawong, D., Peesan, M., Supaphol, P., & Rujiravanit, R. (2005). Preparation and characterization of starch/poly(l-lactic acid) hybrid foams. *Carbohydrate Polymers*, *59*(3), 329–337. https://doi.org/10.1016/j.carbpol.2004.10.003.

Pushpadass, H. A., Babu, G. S., Weber, R. W., & Hanna, M. A. (2008). Extrusion of starch-based loose-fill packaging foams#: Effects of temperature, moisture and talc on physical properties. *Packaging Technology and Science*, *21*(3), 171–183. https://doi.org/10.1002/pts.809.

Qian, L., Lei, D., Duan, X., Zhang, S., Song, W., Hou, C., et al. (2018). Design and preparation of metal-organic framework papers with enhanced mechanical properties and good antibacterial capacity. *Carbohydrate Polymers*, *192*, 44–51. https://doi.org/10.1016/j.carbpol.2018.03.049.

Ramôa, S. D., Barra, G. M., Oliveira, R. V., De Oliveira, M. G., Cossa, M., & Soares, B. G. (2013). Electrical, rheological and electromagnetic interference shielding properties of thermoplastic polyurethane/carbon nanotube composites. *Polymer International*, *62*(10), 1477–1484. https://doi.org/10.1002/pi.4446.

Ribeiro Da Silva, V., Mosiewicki, M. A., Yoshida, M. I., Coelho Da Silva, M., Stefani, P. M., & Marcovich, N. E. (2013). Polyurethane foams based on modified tung oil and reinforced with rice husk ash II: Mechanical characterization. *Polymer Testing*, *32*(4), 665–672. https://doi.org/10.1016/j.polymertesting.2013.03.010.

Rivera-Armenta, J. L., Heinze, T., & Mendoza-Martínez, A. M. (2004). New polyurethane foams modified with cellulose derivatives. *European Polymer Journal*, *40*(12), 2803–2812. https://doi.org/10.1016/j.eurpolymj.2004.07.015.

Rojo, E., Oliet, M., Virginia Alonso, M., Del Saz-Orozco, B., & Rodriguez, F. (2014). Mechanical and interfacial properties of phenolic composites reinforced with treated cellulose fibers. *Polymer Engineering and Science*, *54*(10), 2228–2238. https://doi.org/10.1002/pen.23772.

Rowell, R. M. (2006). Chemical modification of wood: A short review. *Wood Material Science & Engineering*, *1*(1), 29–33. https://doi.org/10.1080/17480270600670923.

Rueda, L., Saralegi, A., Fernández-d'Arlas, B., Zhou, Q., Alonso-Varona, A., Berglund, L. A., et al. (2013). In situ polymerization and characterization of elastomeric polyurethane-cellulose nanocrystal nanocomposites. Cell response evaluation. *Cellulose*, *20*(4), 1819–1828. https://doi.org/10.1007/s10570-013-9960-0.

Saralegi, A., Gonzalez, M. L., Valea, A., Eceiza, A., & Corcuera, M. A. (2014). The role of cellulose nanocrystals in the improvement of the shape-memory properties of castor oil-based segmented thermoplastic polyurethanes. *Composites Science and Technology*, *92*, 27–33. https://doi.org/10.1016/j.compscitech.2013.12.001.

Schulz, L., Burchard, W., & Dönges, R. (1998). Cellulose derivatives: Modification, characterization and nanostructures. In *ACS, symposium series*.

Shen, H., Lavoie, A. J., & Nutt, S. R. (2003). Enhanced peel resistance of fiber reinforced phenolic foams. *Composites Part A: Applied Science and Manufacturing*, *34*(10), 941–948. https://doi.org/10.1016/S1359-835X(03)00210-0.

Shey, J., Imam, S. H., Glenn, G. M., & Orts, W. J. (2006). Properties of baked starch foam with natural rubber latex. *Industrial Crops and Products*, *24*(1), 34–40. https://doi.org/10.1016/j.indcrop.2005.12.001.

Shogren, R. L., Lawton, J. W., & Tiefenbacher, K. F. (2002). Baked starch foams: Starch modifications and additives improve process parameters, structure and properties. *Industrial Crops and Products*, *16*(1), 69–79. https://doi.org/10.1016/S0926-6690(02)00010-9.

Silva, M. C., Lopes, O. R., Colodette, J. L., Porto, A. O., Rieumont, J., Chaussy, D., et al. (2008). Characterization of three non-product materials from a bleached eucalyptus Kraft pulp mill, in view of valorising them as a source of cellulose fibres. *Industrial Crops and Products*, *27*(3), 288–295. https://doi.org/10.1016/j.indcrop.2007.11.005.

Silva, M. C., Takahashi, J. A., Chaussy, D., Belgacem, M. N., & Silva, G. G. (2010). Composites of rigid polyurethane foam and cellulose fiber residue. *Journal of Applied Polymer Science*, *117*(6), 3665–3672. https://doi.org/10.1002/app.32281.

Soykeabkaew, N., Supaphol, P., & Rujiravanit, R. (2004). Preparation and characterization of jute-and flax-reinforced starch-based composite foams. *Carbohydrate Polymers*, *58*(1), 53–63. https://doi.org/10.1016/j.carbpol.2004.06.037.

Soykeabkaew, N., Thanomsilp, C., & Suwantong, O. (2015). A review: Starch-based composite foams. *Composites Part A: Applied Science and Manufacturing*, *78*, 246–263. https://doi.org/10.1016/j.compositesa.2015.08.014.

Su, Z., Zhang, M., Lu, Z., Song, S., Zhao, Y., & Hao, Y. (2018). Functionalization of cellulose fiber by in situ growth of zeolitic imidazolate framework-8 (ZIF-8) nanocrystals for preparing a cellulose-based air filter with gas adsorption ability. *Cellulose*, *25*(3), 1997–2008. https://doi.org/10.1007/s10570-018-1696-4.

Suddell, B. C., & Evans, W. J. (2003). The increasing use and application of natural fiber composite materials within the automotive industry. In *Seventh composite conference on woodfiber–plastic composites* (pp. 7–14).

Svagan, A. J., Azizi Samir, M. A. S., & Berglund, L. A. (2007). Biomimetic polysaccharide nanocomposites of high cellulose content and high toughness. *Biomacromolecules*, *8*(8), 2556–2563. https://doi.org/10.1021/bm0703160.

Tabor, R., Lepovitz, J., Potts, W., Latham, D., & Latham, L. (1997). The effect of polyol functionality on water blown rigid foams. *Journal of Cellular Plastics*, *33*(4), 372–399.

Trejo-O'Reilly, J. A., Cavaillé, J. Y., Paillet, M., Gandini, A., Herrera-Franco, P., & Cauich, J. (2000). Interfacial properties of regenerated cellulose fiber/polystyrene composite materials. Effect of the coupling agent's structure on the micromechanical behavior. *Polymer Composites*, *21*(1), 65–71. https://doi.org/10.1002/pc.10165.

Valentini, M., Piana, F., Pionteck, J., Lamastra, F. R., & Nanni, F. (2015). Electromagnetic properties and performance of exfoliated graphite (EG)—Thermoplastic polyurethane (TPU) nanocomposites at microwaves. *Composites Science and Technology*, *114*, 26–33. https://doi.org/10.1016/j.compscitech.2015.03.006.

Valenzano, L., Civalleri, B., Chavan, S., Bordiga, S., Nilsen, M. H., Jakobsen, S., et al. (2011). Disclosing the complex structure of UiO-66 metal organic framework: A synergic combination of experiment and theory. *Chemistry of Materials*, *23*(7), 1700–1718. https://doi.org/10.1021/cm1022882.

Wang, S., Kowalski, R. J., Kang, Y., Kiszonas, A. M., Zhu, M. J., & Ganjyal, G. M. (2017). Impacts of the particle sizes and levels of inclusions of cherry pomace on the physical and structural properties of direct expanded corn starch. *Food and Bioprocess Technology*, *10*(2), 394–406. https://doi.org/10.1007/s11947-016-1824-9.

Wang, H., Yuan, X., Zeng, G., Leng, L., Peng, X., Liao, K., et al. (2014). Removal of malachite green dye from wastewater by different organic acid-modified natural adsorbent: Kinetics, equilibriums, mechanisms, practical application, and disposal of dye-loaded adsorbent. *Environmental Science and Pollution Research*, *21*(19), 11552–11564. https://doi.org/10.1007/s11356-014-3025-2.

Willett, J. L., & Shogren, R. L. (2002). Processing and properties of extruded starch/polymer foams. *Polymer*, *43*(22), 5935–5947. https://doi.org/10.1016/S0032-3861(02)00497-4.

Wrolstad, R. E. (2012). *Food carbohydrate chemistry. Vol. 48*. Wiley.

Wu, Q., Henriksson, M., Liu, X., & Berglund, L. A. (2007). A high strength nanocomposite based on microcrystalline cellulose and polyurethane. *Biomacromolecules*, *8*(12), 3687–3692. https://doi.org/10.1021/bm701061t.

Yang, Q., Zhang, M., Song, S., & Yang, B. (2017). Surface modification of PCC filled cellulose paper by MOF-5 (Zn3(BDC)2) metal–organic frameworks for use as soft gas adsorption composite materials. *Cellulose*, *24*(7), 3051–3060. https://doi.org/10.1007/s10570-017-1331-9.

Yu, L., & Christie, G. (2001). Measurement of starch thermal transitions using differential scanning calorimetry. *Carbohydrate Polymers*, 179–184. https://doi.org/10.1016/s0144-8617(00)00301-5.

Zhang, Y., Shang, S., Zhang, X., Wang, D., & Hourston, D. J. (1995). Influence of structure of hydroxyl-terminated maleopimaric acid ester on thermal stability of rigid polyurethane foams. *Journal of Applied Polymer Science*, *58*(10), 1803–1809. https://doi.org/10.1002/app.1995.070581019.

Zhang, J. F., & Sun, X. (2007). Biodegradable foams of foly(lactic acid)/starch. I. Extrusion condition and cellular size distribution. *Journal of Applied Polymer Science*, *106*(2), 857–862. https://doi.org/10.1002/app.26715.

Zhou, J., Song, J., & Parker, R. (2006). Structure and properties of starch-based foams prepared by microwave heating from extruded pellets. *Carbohydrate Polymers*, *63*(4), 466–475. https://doi.org/10.1016/j.carbpol.2005.09.019.

Zhou, J., Song, J., & Parker, R. (2007). Microwave-assisted moulding using expandable extruded pellets from wheat flours and starch. *Carbohydrate Polymers*, *69*(3), 445–454. https://doi.org/10.1016/j.carbpol.2007.01.001.

Zhu, H., Yang, X., Cranston, E. D., & Zhu, S. (2016). Flexible and porous nanocellulose aerogels with high loadings of metal–organic-framework particles for separations applications. *Advanced Materials*, *28*(35), 7652–7657. https://doi.org/10.1002/adma.201601351.

CHAPTER

13 Utilization of nanocellulose as reinforcement in biodegradable biomaterials

Perry Law Nyuk Khui[a], Md Rezaur Rahman[a], Muhammad Khusairy Bin Bakri[a], Sinin Hamdan[a], Khairuddin Sanaullah[a], and Faisal Islam Chowdhury[b]

[a]*Department of Chemical Engineering and Energy Sustainability, Faculty of Engineering, Universiti Malaysia Sarawak (UNIMAS), Kota Samarahan, Sarawak, Malaysia,* [b]*Nanotechnology and Renewable Energy Research Laboratory (NRERL), Department of Chemistry, University of Chittagong, Chittagong, Bangladesh*

Chapter outline

13.1 Introduction

In recent times, there is an increase of interest regarding the use of biomass as a source of renewable energy and composite material (Law et al., 2020; Nyuk Khui, Rahman, Ahmad et al., 2021; Nyuk Khui, Rahman, Kuok et al., 2021).

Fundamentals and Recent Advances in Nanocomposites Based on Polymers and Nanocellulose.
https://doi.org/10.1016/B978-0-323-85771-0.00014-2

Cellulose, a natural polymer, has highly diverse applications in numerous industries (Khui, Rahman, & Bakri, 2021; Dufresne, 2017). Cellulose is the principal cell's wall component of vascular plants, which is the most abundant biological compound and carbohydrate polymer on Earth. Other than vascular plants, cellulose is also present as the principal cell wall material in all vegetables and fruits consumed by humans. Cellulose is a linear polysaccharide, consisting of monomeric units of anhydrous-D-glucose units with a β-(1→4)-linkage (Mohan, Pittman, & Steele, 2006; Pasangulapati et al., 2012; Pérez, Muñoz-Dorado, De La Rubia, & Martínez, 2002). It was reported that the cellulose microfibrils were embedded in the matrix that contained both hemicellulose and lignin (Pasangulapati et al., 2012; Pérez et al., 2002). The formation of polycrystalline, and fibrous bundles occur through molecules representing over extended regions, in which the molecular chains within crystalline regions are held together by the hydrogen bonds (BeMiller & BeMiller, 2019).

According to some studies, plants (Robert, Ashlie, John, John, & Jeff, 2011), algae's (Klemm, Heublein, Fink, & Bohn, 2005), tunics (Sacui et al., 2014) and bacterial organism (Araújo et al., 2018; de Lima Fontes et al., 2018; Ferreira et al., 2018; Pacheco et al., 2017) are some viable extraction sources of cellulose. Lignocellulosic biomass or dry agricultural waste contains about 85–90% cellulose, hemicellulose, and lignin, while the remaining percentages constitute of organic extracts and inorganic minerals (Pasangulapati et al., 2012). Cellulose is insoluble in water, except in some special solvents that can disrupt its intermolecular hydrogen bonds. However, there are other derivatives of cellulose, which are water soluble, hence they are classified as hydrocolloids (BeMiller & BeMiller, 2019). Due to the rapid growth of biocomposites, extraction, and application of cellulose composite reinforcement of biomass will also rise in demand (Dungani et al., 2017). After extraction, cellulose fibrils can further be process into nanosized particles, which are applicable in many applications due to their low density, optical transparency, high mechanical properties, large surface area (high aspect ratio), flexibility, specific barrier properties, low thermal expansion, biodegradability, and environmentally friendly (Dungani et al., 2017; Liu, Chen, Yue, Chen, & Wu, 2011; Mariano, El Kissi, & Dufresne, 2014; Robert et al., 2011).

Nanocellulose can considered to be a good reinforcement material as a composite due to the large surface area, with high aspect ratio resulting from interconnected network structures through hydrogen bonding (Dungani et al., 2017). Hence, it brings benefits in many different applications and industries, such as transparent films (Zhu, Fang, Preston, Li, & Hu, 2014), strength enhancers in paper manufacturing (Tang, He, Mosseler, & Ni, 2014), polymer composite reinforcements (Miao & Hamad, 2013), emulsions and oxygen barrier films for plastics packaging (Chen, Li, et al., 2015; Chen, Xu, Liu, & Zeng, 2015; Lin & Dufresne, 2014; Metreveli et al., 2014). Nanocelluloses is classified by the cellulose nanosize dimensions, which is less than or equal to 100 nm (Mondal, 2017). Through various extraction methods, some examples of the nanocelluloses derivatives are cellulose nanofibrils (CNFs), cellulose nanocrystals (CNCs) and bacterial nanocellulose (BNC) (Charreau,

Foresti, & Vázquez, 2013; David, Kevin, John, & Helen, 2014; Jorfi & Foster, 2015; Lee, Aitomäki, Berglund, Oksman, & Bismarck, 2014; Lin & Dufresne, 2014).

Nanocellulose can be extracted from various lignocellulosic sources with the application of mechanical and chemical extraction methods (Chen, Li, et al., 2015; Chen, Wu, Huang, Huang, & Ai, 2014; Lin & Dufresne, 2014; Metreveli et al., 2014). The structure of cellulose consists of amorphous and crystalline regions. It is relatively easy to break the amorphous regions of cellulose with mechanical and chemical processes. However, it is relatively difficult to break the crystalline regions of cellulose due to the presence of strong hydrogen bonds. The extraction of nanocellulose from the lignocellulosic biomass includes two major parts, which is the pretreatment of lignocellulosic biomass and the removal of amorphous regions by using appropriate extraction methods such as acid hydrolysis, etc. (Kim et al., 2015).

Pretreatments such as alkaline/acidic treatment and bleaching are typically applied during the extraction process, prior to the removal of the amorphous regions. The key objectives of the pretreatment processes of lignocellulosic biomass source materials that involve the complete or partial removal of matrix materials such as hemicellulose, lignin, pectin, and wax, hence revealing the cellulose (Shankaran, Mohan Bhagyaraj, Oluwafemi, Kalarikkal, & Thomas, 2018; Wang, Tavakoli, & Tang, 2019; Wang et al., 2019). Pretreatment using the application of the alkaline chemical depolymerization on the native cellulose structure, which defibrillates the external cellulose microfibrils, thus, resulting in the short length crystallites. Bleaching treatment on the other hand, removes the cementing material from the fibers (Abraham et al., 2011). Dimensions, quality, and yield of the nanocellulose depend on the source of the lignocellulosic biomass, considering the method of extraction is maintained throughout the numerous samples used during extraction processes. Hence, if a different morphology is desired, the extraction/treatment process will be selected and applied as according to the desired conditions (Shankaran et al., 2018; Wang, Tavakoli, & Tang, 2019; Wang, Yao, et al., 2019). Table 13.1 shows the nanocellulose derivatives, and synthesis reagents used to produce the nanocellulose, while Table 13.2 shows the mechanical properties of numerous biodegradable polymer matrix for composite materials.

13.2 Nanocellulose types and properties

13.2.1 Esters and ethers cellulose derivates

Numerous derivatives of cellulose were formed such as ethers, esters, and microbial/bacterial cellulose. However, several additional derivatives were developed to further utilization due to the cellulose insoluble and infusible characteristics. Hydroxyl groups (–OH) of cellulose could be partially or fully reacted with numerous/various reagents to generate derivatives with advantageous properties. Table 13.1 shows the example of cellulose ester and ether derivatives.

Table 13.1 Example of synthesis of cellulose esters and ethers derivatives (Abdul Khalil et al., 2017).

Ester bases	Cellulose ester	Reagent	Ether bases	Cellulose ether
Organic esters	Cellulose acetate	Acetic acid and acetic anhydride	**Alkyl**	Methylcellulose
	Cellulose triacetate	Acetic acid and acetic anhydride		Ethyl cellulose
	Cellulose propionate	Propanoic acid		Ethyl methyl cellulose
	Cellulose acetate propionate	Acetic acid and propanoic acid		Hydroxyethyl cellulose
	Cellulose acetate butyrate	Acetic acid and butyric acid	**Hydroxyalkyl**	Hydroxypropyl cellulose (HPC)
	Cellulose Xanthate	Xanthic acid		Hydroxyethyl methyl cellulose
Inorganic esters	Nitrocellulose (cellulose nitrate)	Nitric acid or another powerful nitrating agent		Hydroxypropyl methyl cellulose (HPMC)
	Cellulose sulfate	Sulfuric acid or another powerful sulfuring agent		Ethyl hydroxyethyl cellulose
	Cellulose phosphate	Phosphoric or another powerful phosphoring agent	**Carboxyalkyl**	Carboxymethyl cellulose (CMC)

Table 13.2 Examples of biodegradable polymer matrix mechanical properties for composites (Alizadeh-Osgouei, Li, & Wen, 2019; Wnek & Bowlin, 2008; Ghasemi, Behrooz, Ghasemi, Yassar, & Long, 2018).

Biodegradable polymer matrix	Tensile modulus (GPa)	Tensile strength (MPa)	References
Polylactic acid (PLA)	1.1 ± 0.66	22.4 ± 0.7483	Ghasemi et al. (2018)
Poly-L-lactic acid (PLLA)	2.7–4.14	15.5–150	Alizadeh-Osgouei et al. (2019)
Polylactic-coglycolic acid (PLGA)	2.0–4.0	6.0–8.0	Wnek and Bowlin (2008)
Polyglycolic acid (PGA)	6.0–7.0	60–99.7	Alizadeh-Osgouei et al. (2019)

13.2.2 Esterification of cellulose ester

The esterification of cellulose involves the use of inorganic acids, organic acids, and anhydrides under different reaction conditions. The classification and methods to synthesize cellulose esters, depend on the reactions involving acids, anhydrides, and acid chlorides. Esterified derivatives of cellulose could be prepared through numerous homogeneous and heterogeneous methods (Tajeddin, 2014; Tosh, 2014). One of the most known process of manufacturing cellulose acetate at commercial scale involves esterification of either dissolving pulp or dissolving cellulose utilizing acid anhydrides in the presence of a mineral acid catalyst. The manufacturing process can be further categorized through pretreatment of cellulose, acetylation, hydrolysis, and purification. Acetic acid could be used either as a single constituent or in combination either with the partial or total esterification through evaporation. The esterification reaction will occur by adding anhydride to the activated dissolving cellulose and the complete dissolving of activated cellulose indicates the end of the esterification reaction. However, distilled water can be added to the mixture to curtail the esterification reaction, thus, removing combined sulfates from the byproducts (Tosh, 2014). Cellulose ester is filtered and washed with more distilled water to remove all the incumbent acids. Esterification of cellulose, degrades the cellulose, hence highly pure esterified celluloses are difficult to be obtained. In 1984, a U.S. Patent for the preparation of cellulose ester was issued by (Kuo & Leonard, 1983). Some of the studies reported the performance and utilization of cellulose esters as coatings, controlled release of drugs (drug delivery system), biodegradable plastics, composites and laminates, optical films, and membranes (Azeredo, Rosa, & Mattoso, 2017; Sharma, Thakur, Bhattacharya, Mandal, & Goswami, 2019; Tajeddin, 2014).

The production of high-quality cellulose esters is dependent on such materials include highly purified lint cotton with cellulose content of over 99%, wood pulp containing between 90% and 97% cellulose (Tosh, 2014). The cellulose fiber-cellulose ester interface has good adhesion characteristics; as cellulose derivatives

have the potential to provide reinforcement in composites. However, there are limited studies, which have emphasized the utilization of cellulose esters as matrices for biocomposites. Cellulose esters could be blended into composites with other synthetic and natural materials, which were utilized as matrix binders, whereby cellulose esters could be manipulated via injection molding, extruded, blow and rotationally molded into numerous components, thermoformed sheets, and films (Amaral et al., 2019). Table 13.1 shows some examples of cellulose ester derivatives. Esters can be categorized by organic esters and inorganic ester.

13.2.3 Etherification of cellulose ether

Etherification involves the process of altering a substance, such as an alcohol to ether, that is formed by treating alkaline cellulose with various reagents. Esterification includes treatment of acidic cellulose with reagents, whereas, the etherification involves ionization of hydroxyl, i.e., C-OH → C-O, which is the principal method control the reaction between cellulose and an etherifying agent as stated in U.S. Patent 2492524 (Darling, 1945). Most ethers are water soluble and are utilized as thickeners in foods, cosmetics, pharmaceuticals, and paint manufacturer. The critical properties of ethers include solubility, water-binding capacity, nontoxicity, and chemical stability, which are determined by the degree of substitution (DS). DS determines properties of ethers based on the average number of –OHs substituted upon on anhydrous glucose units. Table 13.1 shows some examples of ether cellulose derivatives. One of the most important etherified cellulose is carboxymethyl cellulose (CMC). CMC is a water-soluble cellulose derivative, with several applications in the food, cosmetics, pharmaceutical and other commercialized industries. CMC DS is around 0.4–1.4, whereas if the DS is larger than 0.6–0.8 the cellulose may attain good water solubility.

A study (Asl, Mousavi, & Labbafi, 2017) reported that the synthesis of CMC is possible with the use of cellulose powder from sugarcane bagasse, sodium hydroxide (NaOH) and isopropanol solvent, reaction shows good ability to etherify cellulose (Asl et al., 2017). The mixture was stirred in the beaker and was kept still for 30 min at ambient temperature. Sodium mono chloroacetate was then added and mechanically stirred for 90 min and after that the mixture was covered and kept at 55°C for about 180 min. Within this timeframe, the chemical reaction proceeded, and the mixture was divided into two layers. The upper layer was disposed, and the sedimentary layer was suspended with 70% methanol and was finally neutralized with glacial acetic acid. The mixture was filtered and washed five times with 70% ethanol to remove undesirable salts. The resulting CMC was washed again with absolute methanol and filtered and was dried in an oven at 55°C (Asl et al., 2017).

CMC is widely used as an additive in numerous industries, due to CMC advantageous properties, especially solubility in water, immiscibility in oil and organic solvency, henceforth acts as a multifunctioning agent. In addition, it could also function as a stabilizer, binder and suspension agent in food and pharmaceutical

industries. The analysis of CMC production process has been explored by researchers and manufacturers to improve processing efficiency to achieve specific properties required for manufacturing. There are also certain studies reported on the optimization of CMC production from etherification cellulose (Tajeddin, 2014; Ye, Xu, Wu, & Chen, 2018). On the other hand, the effects of methylcellulose coating on the storage life postharvest for chilies was evaluated. Hence, as a result, it showed that the coating may increase overall acceptability and increase the quality and shelf life (Chaple, Vishwasrao, & Ananthanarayan, 2017). The conducted study also shows that the cellulose composite coating may benefit the food and biomedical industry, regarding packaging and shelf life of products (Chaple et al., 2017).

13.2.4 Extraction of bacterial cellulose

Torres, Arroyo, and Troncoso (2019) stated that plant fiber origin cellulose composed of lignin, hemicelluloses, pectin and only 40%–70% cellulose. On the other hand, bacterial cellulose (BC) is composed of pure cellulose fibers, displaying high purity without utilizing numerous treatments for synthesis or extraction of the cellulose fibers. BC has unique characteristics, which has been extensively studied and characterized (Du, Zhao, Peng, Zhou, & Han, 2018; Römling & Galperin, 2015; Shankaran et al., 2018; Wang, Yao, et al., 2019). In comparison to cellulose from a lignocellulosic plant origin, BC has different properties characterized by its high purity, strength, moldability and increased water holding characteristics. As BC is a product in nature, currently numerous methods that are being investigated to improve BC growth from cultures in laboratories for large-scale processes. In a laboratory scale, synthesis procedures could be controlled and tailored to obtain specific desirable BC properties.

There are a range of studies being conducted on the application of BC, where attempts were made to improve the applicability of BC to progress into new areas and characterization (Petersen & Gatenholm, 2011; Tajeddin, 2014; Ullah, Wahid, Santos, & Khan, 2016). Studies reported the potential of the applications of BC as a new resource for some of the products. It was reported regarding the use of agricultural by products as feedstock and the advantages for the growth and production of BC, in relation to the low cost of the raw material (Abdelraof, Hasanin, & El-Saied, 2019; Soemphol, Hongsachart, & Tanamool, 2018). The lignocellulosic feedstocks were pretreated at a high temperature and pressure, which gave rise to inhibitory compounds as a result of the breakdown of polysaccharides and lignin (Chen, Hong, Yang, & Han, 2013; Tajeddin, 2014).

Among the most effective bacteria for the laboratory synthesis of BC are *Gluconacetobacter xylinum*, *Gluconacetobacter hansenii*, and *Gluconacetobacter pasteurianus* (Torres et al., 2019). An example of the cultivation of BC by *Acetobacter xylinum* was achieved by Yan et al. (2017) using naturally fermented coconut-water. Fermented coconut-water in combination of sucrose, agar-agar, disodium phosphate (Na_2HPO_4), ammonium sulfate ($(NH_4)_2SO_4$) and magnesium

sulfate ($MgSO_4$) was mixed thoroughly to form a uniform medium for bacterial growth (Yan et al., 2017). The cultivation of *Acetobacter xylinum* was conducted at 30°C for 12 days. The resulting BC gelatinous membranes were removed from the cultures and was washed with deionized water. BC nanocellulose was prepared by sulfuric acid hydrolysis of BC aqueous suspension, where the full method of synthesis was in accordance to the study conducted by Yan et al. (2017). Based on the weight of BC, the yield of BC nanocellulose was 61.6% (Yan et al., 2017). Table 13.2 showed the mechanical properties of composites materials with polymer matrix.

13.3 Extraction processses

Some examples of the extraction process and synthesis reagents of cellulose derivatives are compiled in Table 13.3, some of the cellulose derivatives, which were synthesized from the extracted cellulose based on lignocellulosic sources.

13.4 Biomaterials for biomedical application

Biomedical engineering is a multidisciplinary field which combines concepts and principles of medicine, biology, and engineering for healthcare purposes (Garza-Ulloa, 2018). The development of biomedical devices or products are based upon the interaction or reaction with human muscles, bones, nervous system, organs, joints, and limbs (Garza-Ulloa, 2018). Composite products have been recently researched and developed, for a variety of biomedical applications, such as orthopedics, dentistry, tissue engineering, antimicrobial properties, wound dressings, drug delivery, cancer therapy, stem cell therapy, biosensors, etc. (Hasnain, Ahmad, Minhaj, Ara, & Nayak, 2018).

Numerous biomedical applications such as treatments for orthopedic and bone-related disorders are topics of interest in the field of biomedical engineering. Due to the importance, application and effects toward human life, the area of research and development has generated attention, and would be expected to remain active in years to come (Kakar, Jayamani, Bakri, & Rahman, 2018). Bone-related disorders are one of the main clinical health issues for the elderly that are gaining worldwide attention. To repair and properly treat damaged hard tissues, several types of biomaterials and devices have been widely applied to remedy the damaged parts of the skeletal systems (Alizadeh-Osgouei et al., 2019). Biomaterials could be divided into two categories, inorganic (e.g., metals and ceramics) and organic (e.g., polymers). A biomaterial manufactured from a single material may not be able to satisfy all the requirements for a given implant application. Therefore, by the combination of two or more materials, biocomposites with different structures and properties for specific applications are attainable as desired (Alizadeh-Osgouei et al., 2019).

Table 13.3 Examples of the extraction and synthesis of cellulose and their ester and ether deri
Resagian, Yuwono, & Hasanudin, 2017; Abdel-Halim, 2014; Abdel-Halim, Alanazi, & Al-Deyab
Candido, Godoy, & Gonçalves, 2017; Carneiro, Lopes, de Andrade, Nisgoski, & de Muniz, 2019; C
2013; Huang et al., 2011; Kumar, Negi, Bhardwaj, & Choudhary, 2012; Nabili, Fattoum, Broch
2017; Shui et al., 2017; Sim et al., 2016).

Derivative	Source	Cellulose extraction method	Cellulose derivative synt
Cellulose acetate (cellulose diacetate)	Sugarcane bagasse	Acid treatment (H_2SO_4), alkaline treatment (NaOH), chelating (EDTA), and bleaching (H_2O_2, $MgSO_4$)	Cellulose acetate was synth from the extracted sugarcan cellulose using water (H_2O) acetic acid (CH_3COOH), su (H_2SO_4), and acetic anhydr ($C_4H_6O_3$)
Cellulose triacetate	Date seeds (*Phoenix dactylifera* L.)	Soxhlet extractor (H_2O, $(C_2H_5)_2O$), alkaline treatment (NaOH), and bleaching (acidified sodium chlorite, KOH, H_3BO_3)	Cellulose triacetate was syn from the extracted date see using water (H_2O) acetic ac (CH_3COOH), acetic anhydr ($C_4H_6O_3$) and sulfuric acid
Cellulose acetate propionate	Sugarcane bagasse	Acid treatment (HNO_3), alkaline treatment (NaOH), and bleaching (H_2O_2)	Cellulose acetate propionat synthesized from sugarcan using an ionic solution mixt methylimidazole and allyl cl (AmimCl), propionic anhydr ($C_6H_{10}O_3$), acetic anhydride and water (H_2O)
Cellulose acetate butyrate	Sugarcane bagasse	Acid treatment (HNO_3), alkaline treatment (NaOH), and bleaching (H_2O_2)	Cellulose acetate butyrate synthesized from sugarcan cellulose using an ionic solu mixture of 1-methylimidazo chloride (AmimCl), butyric

Table 13.3 Examples of the extraction and synthesis of cellulose and their ester and ether derivatives Resagian, Yuwono, & Hasanudin, 2017; Abdel-Halim, 2014; Abdel-Halim, Alanazi, & Al-Deyab, 2015 Candido, Godoy, & Gonçalves, 2017; Carneiro, Lopes, de Andrade, Nisgoski, & de Muniz, 2019; Chen, Zh 2013; Huang et al., 2011; Kumar, Negi, Bhardwaj, & Choudhary, 2012; Nabili, Fattoum, Brochier-Sal 2017; Shui et al., 2017; Sim et al., 2016). *Cont'd*

Derivative	Source	Cellulose extraction method	Cellulose derivative synthesis
			anhydride($C_8H_{14}O_3$), acetic anhydri ($C_4H_6O_3$), and water (H_2O)
Cellulose xanthate	Sugarcane bagasse	Purification process includes acid treatment (HNO_3), and alkaline treatment (NaOH)	Cellulose xanthate was synthesized from purified sugarcane bagasse using sodium hydroxide (NaOH), carbon disulfide (CS_2) and water (H_2
Nitrocellulose (cellulose nitrate)	Kraft pulps of *Pinus* sp. and *Eucalyptus* sp. bleached	Mechanical processing (defibrillator mill)	Cellulose nitrate was synthesized fr defibrillated cellulose from kraft pul using a nitration process with wate (H_2O), sulfuric acid (H_2SO_4) and nit acid (HNO_3)
Sodium cellulose sulfate	Native cotton 87%–90% cellulose content	–	Sodium cellulose sulfate was synthesized from a native cotton as cellulose material, using a heterogeneous reaction with sulfuri acid (H_2SO_4), ethanol (C_2H_5OH), Anhydrous sodium sulfate (Na_2SO_4 sodium hydroxide (NaOH) and deionized water (H_2O)
Cellulose phosphate	Rice husk	Alkaline treatment (NaOH), bleaching (NaClO) and acid treatment (HNO_3)	Cellulose phosphate was synthesiz from rice husk cellulose using orthophosphoric acid (H_3PO_4) and urea (CH_4N_2O)
Methylcellulose	Sugarcane bagasse	Soxhlet extractor (C_6H_6, CH_3OH), alkaline treatment (NaOH), and bleaching (acidified sodium chlorite, KOH)	Methylcellulose was synthesized fr purified sugarcane bagasse cellulos using sodium hydroxide (NaOH), acetone (C_3H_6O), dimethyl sulfate ($C_2H_6O_4S$), acetic acid (CH_3COOH

Hydroxyethyl cellulose	Sugarcane bagasse	Alkaline treatment (NaOH, nonionic wetting agent), and delignification/ bleaching ($NaClO_2$, $C_6H_{12}N_4$ and nonionic wetting agent)	Hydroxyethyl cellulose was synthesized from extracted bagasse cellulose using So hydroxide (NaOH), liquid et oxide (C_2H_4O), cold isoprop (C_3H_8O), acetic acid (CH_3C acetone (C_3H_6O)
Hydroxypropyl cellulose (HPC)	Olive tree branch waste powder	–	Hydroxypropyl cellulose wa synthesized from olive tree waste powder involving alk and etherification using soc hydroxide (NaOH), isoprop (C_3H_8O), propylene oxide (acetic acid (CH_3COOH), an acetone solution (C_3H_6O)
Hydroxypropyl carboxymethyl cellulose (HPCMC)	Olive tree branch hydroxypropyl cellulose (HPC)	Alkalization and etherification using sodium hydroxide (NaOH), isopropyl alcohol (C_3H_8O), propylene oxide (C_3H_6O), acetic acid (CH_3COOH), and aqueous acetone solution (C_3H_6O)	Hydroxypropyl carboxymet cellulose was synthesized v method involving the use o alcohol (C_3H_8O), aqueous s hydroxide solution (NaOH), monochloroacetic acid (C_2 sodium carbonate (Na_2CO_3 acetic acid (CH_3COOH), an methanol solution (CH_3OH)
Sodium carboxymethyl cellulose (CMC)	Cornstalk	Fractionation solvent mixture (CH_3COOH, CH_2O_2, H_2O), ($C_4H_8O_2$), and bleaching (sodium chlorite, CH_3COOH)	Sodium carboxymethyl cell synthesized from crude co cellulose involving alkalizati etherification using sodium (NaOH), chloroacetic acid (hydrochloric acid (HCl), eth (C_2H_5OH) and water (H_2O)

13.4.1 Bacterial nanocellulose

In biomedical applications, biomaterials are typically selected by their cellular reaction. The biomaterial interactions are mainly related to the material surface properties, wettability, topography, chemistry, surface charge, hydrophobic and hydrophilic nature, biocompatibility, and mechanical properties (Picheth et al., 2017). Bacterial nanocellulose (BNC) could be an ideal biomaterial for biomedical applications due to its unique characteristics such as high porosity, excellent wet mechanical properties, noncytotoxicity, and biocompatibility (Lin & Dufresne, 2014; Picheth et al., 2017; Ullah et al., 2016). BNC characteristics combined with several surfaces and macromolecular properties, which are critical for bone tissue engineering, drug delivery system, dental grafting, wound dressing, etc. (Picheth et al., 2017).

There are numerous BNC based biomaterials, which were FDA approved as tissue surgical sheets or reinforcing matrices (Petersen & Gatenholm, 2011; Picheth et al., 2017). The application of these BNC biomaterials had a lack of skin irritation and the slower coagulation rates than the other biomaterials (Ullah et al., 2016). Some examples of the BNC products are *Biofill* as a temporary skin substitute, *Gengiflex* as either dental implants or grafting material, and *Xcell* for wound dressings (Picheth et al., 2017). BNC exhibits various advantages over other nanocellulose extracted from different sources that might require other processes such as mechanical, acid, alkali, and pollutant treatments (Petersen & Gatenholm, 2011; Picheth et al., 2017). The extraction of BNC requires a simple aerobic cultivation of the bacterium *Gluconacetobacter xylinus* in a glucose enriched medium (Petersen & Gatenholm, 2011). According to Picheth et al. (2017), future perspectives of the application of BNC as biomaterial for biomedical applications, will be supported by the extraction processes, lack of contaminants and the ability to modify the biomaterial properties during synthesis, for instance, crystallinity index, aspect ratio and morphology (Petersen & Gatenholm, 2011).

13.4.2 Cellulosic hydrogels

According to many studies, 2,2,6,6-tetramethylpiperidine-1-oxyl (TEMPO) oxidized nanocellulose biofilms exhibited good cell adhesion and proliferation as a potential biomaterial (Cheng, Park, & Hyun, 2014; Mondal, 2017; Park, Lee, & Hyun, 2015). According to Cheng et al. (2014), TEMPO oxidized bacterial nanocellulose could be fabricated into hydrogel with elastin likes polypeptide (ELP). In relation to the biomedical field, hybrid hydrogel has useful properties such as noncytotoxicity and capability to encapsulate cells (Cheng et al., 2014; Mondal, 2017; Park et al., 2015). Ahrem et al. (2014) reported synthesis of bacterial nanocellulose in a mode of static cultivation, which displayed high crystallinity, and formation of flat shaped hydrogels on the surface of the culture medium. The laser perforation process can make the BNC hydrogel to support cell growth for cartilage reconstruction/implants for the joint (Ahrem et al., 2014).

According to Ahrem et al. (2014), the structure and shaping of BNC during biosynthesis allows a structural imitation of host body tissue. It was reported by Ahrem et al. (2014) that the irregular alignment of the BNC nanofibers exhibited structures comparable to those of collagen matrices. In comparison to smooth surfaces without the laser structuring, the 3D biomimetic network structure of BNC enables adhesion and prevent dedifferentiation of connective tissue cells such as chondrocytes. Alternative to BNC hydrogels, Chinga-Carrasco and Syverud (2014) reported that pretreated wood pulp source nanocellulose cellulosic hydrogel had the potential for wound-healing applications due to the capacity of the biomaterial to keep a moist environment and functionalize as a drug delivery system (Chinga-Carrasco & Syverud, 2014).

13.5 Nanocellulose biocomposites

13.5.1 Biodegradable polymers as matrix material

A wide scope of polymers has been researched as stand-alone products and composite matrix material for several applications, i.e., bone-tissue engineering and drug delivery systems (Ozdil & Aydin, 2014). Biodegradable polymeric materials may be categorized into natural and synthetic polymers. Naturally derived polymers such as collagen and gelatin have issue with instability and immunogenicity (Khan & Khan, 2013). Synthetic polymers such as polylactic-*co*-glycolic acid (PLGA) and polylactic acid (PLA) offer good applies for medical purposes (Guo & Ma, 2014). According to Alizadeh-Osgouei et al. (2019) these synthetic biodegradable polymers could be applicable for wound management, orthopedic devices, dentistry applications, cardiovascular applications, drug delivery, and tissue engineering. PLA, PLGA, poly-L-lactic acid (PLLA), and polymethyl methacrylate (PMMA) are the most recognized polymers applicable for biomedical purposes, predominantly due to their valuable properties (Dilayda, Hatice, Hulya, & Ozan, 2018; Eppley, 2005; Guo & Ma, 2014). The PLA can be considered as a good alternative material for numerous biomedical applications, due to the biocompatibility with the human tissue, ease of manufacturing, hydrophobic nature, and biodegradability properties (Dilayda et al., 2018; Eppley, 2005; Guo & Ma, 2014). Extracted from renewable resources such as potato and cassava starch, the PLA was categorized as a biodegradable thermoplastic polymer and considered as a well-researched polymer in the materials science community.

Alizadeh-Osgouei et al. (2019) synthesized PLA having much improved mechanical properties, and proposed PLA implants to fix the damaged parts without the need for additional surgery or supports. The degradation of PLA in the human body, however, could cause inflammatory reactions, thus some reinforced materials such as cellulose and ceramics were incorporated into the PLA matrix as composites to improve biocompatibility and other properties (Alizadeh-Osgouei et al., 2019). The medical applications of the polymers depend on the damage area of the soft and hard tissue

within the human body (Guo & Ma, 2014; Martina & Hutmacher, 2007; Ozdil & Aydin, 2014; Ozdil, Wimpenny, Aydin, & Yang, 2017). For instance, soft tissue can be categorized as skin, muscle, tendons, and ligaments, whereas hard tissues can be categorized as bone, teeth and cartilage (Guo & Ma, 2014).

PLGA is among the biodegradable synthetic polymers that shows great potential to be used for biomedical purposes owing to its safety, mechanical properties, great cell adhesion, and controllable degradation rate (Eppley, 2005). According to Alizadeh-Osgouei et al. (2019), some PLGA implants were found a great rate of acceleration regarding bone healing and growth (Alizadeh-Osgouei et al., 2019; Martina & Hutmacher, 2007; Ozdil & Aydin, 2014). PLGA could be identified as a random ring-opening copolymerization of PLA and polyglycolic acid (PGA) (Alizadeh-Osgouei et al., 2019; Göktürk & Erdal, 2017). The degradation rate of PLGA were found to be controlled according to the varied percentage of PLA and PGA, therefore, PLGA was most favored than the PGA and PLA regarding biomedical applications such as sutures and drug delivery systems (Alizadeh-Osgouei et al., 2019; Chereddy, Vandermeulen, & Préat, 2016).

13.5.2 Nanocellulose as reinforcement material

Nanocellulose as reinforcement fillers has issues regarding compatibility with the nonpolar polymer matrix (Abdulkhani, Hosseinzadeh, Ashori, Dadashi, & Takzare, 2014; Mondal, 2017). Cellulose nanocrystals (CNCs) hydroxyl groups limit their dispersion in the hydrophobic polymer matrix. To overcome poor dispersion of CNC in the polylactic acid (PLA), Lee et al. (Gwon et al., 2016) modified CNC with addition of the toluene diisocyanate (TDI) into it, which resulted into an improved CNC having higher interfacial interaction between the nanofillers and polymer matrix and the modified CNC exhibited good dispersion in the PLA matrix during solvent casting (Gwon et al., 2016). Sullivan, Moon, and Kalaitzidou (2015) found that the incorporation of CNC into PLA with an increased CNC content, increases crystallinity, and storage modulus of the PLA-CNC nanocomposite, hence indicating the CNC could act as a nucleating agent (Sullivan et al., 2015).

The nanocomposites were fabricated through melt compounding and melt fiber spinning followed by compression molding (Sullivan et al., 2015). Hervy, Evangelisti, Lettieri, and Lee (2015) studied the environmental impact of bacterial nanocellulose (BNC) and nanofibrillated cellulose (NFC)-reinforced epoxy composites, using life cycle assessment (LCA). In comparison to the neat PLA the specific tensile moduli of the nanocellulose composites were higher [88]. According to Hervy et al. (2015), the life cycle scenario analysis showed the cradle-to-grave GWP and ADF of BNC- and NFC-reinforced epoxy composites could be lower than pure PLA when the composites contained more than 60% vol. nanocellulose (Hervy et al., 2015). This indicates that nanocellulose composites with higher nanocellulose content is desirable for developing composites with better environmentally friendly characteristics.

According to certain studies, nanocellulose could be used to graft onto natural fibers to modify and improve the mechanical and interfacial properties by filling the cavities and improving the bonding with interfibrils of the natural fibers (Dai & Fan, 2013; Wei & McDonald, 2016). According to Arboleda et al. (2013), soya protein-based aerogel has limited applications due to its brittleness. However, the mechanical properties of the aerogel could be improved by incorporating nanocellulose reinforcement filler. The product of the nanocellulose composite aerogel, showed improvements in mechanical properties, and displayed a high surface area with low density, which enabled the aerogel nanocellulose composite to have potential in applications such as packaging, thermal and sound insulation, etc. (Arboleda et al., 2013).

Studies (Auad et al., 2012) indicated that shape memory polymer composites have numerous advantages such as low cost, light weight, and ease in storage, than other shape memory materials such as ceramic, metal, alloy, etc. Shape memory polymer composites bear potential application in the biomedical field, and biomimetic devices. Polymer such as segmented polyurethane displays shape memory properties and has low stiffness than the other shape memory ceramic and metal alloys. Mechanical properties of shape memory polyurethane were improved by modifying the material with reinforced nanocellulose fillers (Auad et al., 2012; Pilate, Toncheva, Dubois, & Raquez, 2016). Regarding the fabrication of nanocellulose composites, a study (Mabrouk, Salon, Magnin, Belgacem, & Boufi, 2014; Pilate, Toncheva, Dubois, & Raquez, 2016) suggested reinforcement of nanocellulose efficiently within the polymer matrix by in situ polymerization. According to Mabrouk, Salon, Magnin, Belgacem, and Boufi (2014), nanocellulose crystal polymer composite was prepared by incorporating nanocellulose crystal by mini emulsion polymerization of acrylic monomers and methacryloxypropyl trimethoxysilane (MPMS), acting as a coupling agent.

Chirayil, Mathew, Hassan, Mozetic, and Thomas (2014) reported that the properties of nanocomposites would depend on the dispersion of the nanocellulose filler, interfacial adhesion, and the interactions between polymer matrix and nanocellulose reinforcement fillers (Chirayil et al., 2014). The tensile and impact test conducted by Chirayil et al. (2014) showed that the optimal filler weightage was at 0.5% and the decreased strength was contributed by the overlapping of the nanocellulose within the unsaturated polyester matrix (Chirayil et al., 2014). Another study by Cho and Park (2011) also demonstrated similar findings as Chirayil et al. (2014), where the mechanical properties of the nanocellulose polyvinyl alcohol composite has improved with the incorporation of the reinforcement nanocellulose fillers. The tensile strength of the composite increased until an optimal filler weightage of 5%, then decreased thereafter (Cho & Park, 2011). Nanocellulose composite has potential applications to improve quality, and safety regarding packaging of products (e.g., food industry and medicines) (Rahman & Bakri, 2021). Due to their nontoxic, mechanical and barrier properties, nanocellulose composite could become a good carrier of bioactive substances, hence improve the safety and storage life of the packaged products by allowing a controlled and sustained release of antimicrobials or

bioactive agents (Bakri, Rahman, Khui, Jayamani, & Khan, 2021; Rahman & Bakri, 2021; Rahman, Khui, & Bakri, 2021; Khan & Khan, 2013). Bioactive agents such as organic acids, essential oils, and plant extracts, bacteriocins could improve their quality and safety, about the storage by preventing the growth of microorganisms (Khan, Huq, Khan, Riedl, & Lacroix, 2014).

13.6 Summary

In summary of this review, nanocellulose and biodegradable polymers are known for their usage in numerous applications as a stand-alone biomaterial product. There are various derivatives of both nanocellulose and biodegradable polymers with different characteristics and properties. Most of the studies reported that the combination of nanocellulose as fillers in a biodegradable polymer matrix have useful properties, which have been implemented effectively in packaging, biomedical applications, food industry etc. Regarding nanocellulose as a reinforcement material for biodegradable polymer-based composites, mechanical and chemical stability are important properties that need assessment in relation with the composite structure over a long period, especially for biomedical applications. Several studies reported the difficulty of proper dispersion of the nanocellulose fillers, and there were numerous techniques implemented by the researchers to develop the composite. Potentially the development of nanocellulose biodegradable polymer composite products depends on the mechanical and chemical properties, reliability, and repeatable production techniques for commercialization purposes.

Acknowledgment

The authors are grateful for the support of Universiti Malaysia Sarawak (UNIMAS) with financial grant F02/CDRG/1826/2019.

References

Abdel-Halim, E. S. (2014). Chemical modification of cellulose extracted from sugarcane bagasse: Preparation of hydroxyethyl cellulose. *Arabian Journal of Chemistry*, *7*(3), 362–371. https://doi.org/10.1016/j.arabjc.2013.05.006.

Abdel-Halim, E. S., Alanazi, H. H., & Al-Deyab, S. S. (2015). Utilization of olive tree branch cellulose in synthesis of hydroxypropyl carboxymethyl cellulose. *Carbohydrate Polymers*, *127*, 124–134. https://doi.org/10.1016/j.carbpol.2015.03.037.

Abdelraof, M., Hasanin, M. S., & El-Saied, H. (2019). Ecofriendly green conversion of potato peel wastes to high productivity bacterial cellulose. *Carbohydrate Polymers*, *211*, 75–83. https://doi.org/10.1016/j.carbpol.2019.01.095.

Abdul Khalil, H. P. S., Tye, Y. Y., Leh, C. P., Saurabh, C. K., Ariffin, F., Mohammad Fizree, H., et al. (2017). Cellulose reinforced biodegradable polymer composite film for

packaging applications. In *Bionanocomposites for packaging applications* (pp. 49–69). Springer International Publishing. https://doi.org/10.1007/978-3-319-67319-6_3.

Abdulkhani, A., Hosseinzadeh, J., Ashori, A., Dadashi, S., & Takzare, Z. (2014). Preparation and characterization of modified cellulose nanofibers reinforced polylactic acid nanocomposite. *Polymer Testing*, *35*, 73–79. https://doi.org/10.1016/j.polymertesting.2014.03.002.

Abraham, E., Deepa, B., Pothan, L. A., Jacob, M., Thomas, S., Cvelbar, U., et al. (2011). Extraction of nanocellulose fibrils from lignocellulosic fibres: A novel approach. *Carbohydrate Polymers*, *86*(4), 1468–1475. https://doi.org/10.1016/j.carbpol.2011.06.034.

Ahrem, H., Pretzel, D., Endres, M., Conrad, D., Courseau, J., Müller, H., et al. (2014). Laser-structured bacterial nanocellulose hydrogels support ingrowth and differentiation of chondrocytes and show potential as cartilage implants. *Acta Biomaterialia*, *10*(3), 1341–1353. https://doi.org/10.1016/j.actbio.2013.12.004.

Alizadeh-Osgouei, M., Li, Y., & Wen, C. (2019). A comprehensive review of biodegradable synthetic polymer-ceramic composites and their manufacture for biomedical applications. *Bioactive Materials*, *4*(1), 22–36. https://doi.org/10.1016/j.bioactmat.2018.11.003.

Amaral, H. R., Cipriano, D. F., Santos, M. S., Schettino, M. A., Ferreti, J. V. T., Meirelles, C. S., et al. (2019). Production of high-purity cellulose, cellulose acetate and cellulose-silica composite from babassu coconut shells. *Carbohydrate Polymers*, *210*, 127–134. https://doi.org/10.1016/j.carbpol.2019.01.061.

Araújo, I. M. S., Silva, R. R., Pacheco, G., Lustri, W. R., Tercjak, A., Gutierrez, J., et al. (2018). Hydrothermal synthesis of bacterial cellulose–copper oxide nanocomposites and evaluation of their antimicrobial activity. *Carbohydrate Polymers*, *179*, 341–349. https://doi.org/10.1016/j.carbpol.2017.09.081.

Arboleda, J. C., Hughes, M., Lucia, L. A., Laine, J., Ekman, K., & Rojas, O. J. (2013). Soy protein–nanocellulose composite aerogels. *Cellulose*, *20*(5), 2417–2426. https://doi.org/10.1007/s10570-013-9993-4.

Asl, S. A., Mousavi, M., & Labbafi, M. (2017). Synthesis and characterization of carboxymethyl cellulose from sugarcane bagasse. *Journal of Food Processing & Technology*, *8*(8), 1–6. https://doi.org/10.4172/2157-7110.10006.

Auad, M. L., Richardson, T., Hicks, M., Mosiewicki, M. A., Aranguren, M. I., & Marcovich, N. E. (2012). Shape memory segmented polyurethanes: Dependence of behavior on nanocellulose addition and testing conditions. *Polymer International*, *61*(2), 321–327. https://doi.org/10.1002/pi.3193.

Azeredo, H. M. C., Rosa, M. F., & Mattoso, L. H. C. (2017). Nanocellulose in bio-based food packaging applications. *Industrial Crops and Products*, *97*, 664–671. https://doi.org/10.1016/j.indcrop.2016.03.013.

Bae, D. H., Choi, H. J., Choi, K., Nam, J. D., Islam, M. S., & Kao, N. (2017). Fabrication of phosphate microcrystalline rice husk based cellulose particles and their electrorheological response. *Carbohydrate Polymers*, *165*, 247–254. https://doi.org/10.1016/j.carbpol.2017.02.037.

Bakri, M. K. B., Rahman, M. R., Khui, P. L. N., Jayamani, E., & Khan, A. (2021). Use of sustainable polymers to make green composites. In Rahman (Ed.), *Advances in Sustainable Polymer Composites* (pp. 109–129). Woodhead Publishing. https://doi.org/10.1016/B978-0-12-820338-5.00005-9.

BeMiller, J. N., & BeMiller, J. N. (2019). *8—Cellulose and cellulose-based hydrocolloids* (pp. 223–240). AACC International Press. https://doi.org/10.1016/B978-0-12-812069-9.00008-X.

Candido, R. G., Godoy, G. G., & Gonçalves, A. (2017). Characterization and application of cellulose acetate synthesized from sugarcane bagasse. *Carbohydrate Polymers*, *167*, 280–289. https://doi.org/10.1016/j.carbpol.2017.03.057.

Carneiro, M. E., Lopes, M. S., de Andrade, A. L. F. B., Nisgoski, S., & de Muniz, G. I. B. (2019). Characterization of cellulose and cellulose nitrate nanofilms. *Floresta*, *49*(2). https://revistas.ufpr.br/floresta/article/view/56909/37969.

Chaple, S., Vishwasrao, C., & Ananthanarayan, L. (2017). Edible composite coating of methyl cellulose for post-harvest extension of shelf-life of finger hot Indian pepper (Pusa jwala). *Journal of Food Processing and Preservation*, *41*(2). https://doi.org/10.1111/jfpp.12807.

Charreau, H., Foresti, M. L., & Vázquez, A. (2013). Nanocellulose patents trends: A comprehensive review on patents on cellulose nanocrystals, microfibrillated and bacterial cellulose. *Recent Patents on Nanotechnology*, *7*(1), 56–80. https://doi.org/10.2174/187221013804484854.

Chen, L., Hong, F., Yang, X.x., & Han, S.f. (2013). Biotransformation of wheat straw to bacterial cellulose and its mechanism. *Bioresource Technology*, *135*, 464–468. https://doi.org/10.1016/j.biortech.2012.10.029.

Chen, W., Li, Q., Cao, J., Liu, Y., Li, J., Zhang, J., et al. (2015). Revealing the structures of cellulose nanofiber bundles obtained by mechanical nanofibrillation via TEM observation. *Carbohydrate Polymers*, *117*, 950–956. https://doi.org/10.1016/j.carbpol.2014.10.024.

Chen, Y., Wu, Q., Huang, B., Huang, M., & Ai, X. (2014). Isolation and characteristics of cellulose and nanocellulose from lotus leaf stalk agro-wastes. *BioResources*, *10*(1). https://ojs.cnr.ncsu.edu/index.php/BioRes/article/view/BioRes_10_1_684_Chen_Isolation_Cellulose_Lotus_Leaf.

Chen, Y., Xu, W., Liu, W., & Zeng, G. (2015). Responsiveness, swelling, and mechanical properties of PNIPA nanocomposite hydrogels reinforced by nanocellulose. *Journal of Materials Research*, *30*(11), 1797–1807. https://doi.org/10.1557/jmr.2015.94.

Chen, G., Zhang, B., Zhao, J., & Chen, H. (2013). Improved process for the production of cellulose sulfate using sulfuric acid/ethanol solution. *Carbohydrate Polymers*, *95*(1), 332–337. https://doi.org/10.1016/j.carbpol.2013.03.003.

Cheng, J., Park, M., & Hyun, J. (2014). Thermoresponsive hybrid hydrogel of oxidized nanocellulose using a polypeptide crosslinker. *Cellulose*, *21*(3), 1699–1708. https://doi.org/10.1007/s10570-014-0208-4.

Chereddy, K. K., Vandermeulen, G., & Préat, V. (2016). PLGA based drug delivery systems: Promising carriers for wound healing activity. *Wound Repair and Regeneration*, *24*(2), 223–236. https://doi.org/10.1111/wrr.12404.

Chinga-Carrasco, G., & Syverud, K. (2014). Pretreatment-dependent surface chemistry of wood nanocellulose for pH-sensitive hydrogels. *Journal of Biomaterials Applications*, *29*(3), 423–432. https://doi.org/10.1177/0885328214531511.

Chirayil, C. J., Mathew, L., Hassan, P. A., Mozetic, M., & Thomas, S. (2014). Rheological behaviour of nanocellulose reinforced unsaturated polyester nanocomposites. *International Journal of Biological Macromolecules*, *69*, 274–281. https://doi.org/10.1016/j.ijbiomac.2014.05.055.

Cho, M. J., & Park, B. D. (2011). Tensile and thermal properties of nanocellulose-reinforced poly(vinyl alcohol) nanocomposites. *Journal of Industrial and Engineering Chemistry*, *17*(1), 36–40. https://doi.org/10.1016/j.jiec.2010.10.006.

Dai, D., & Fan, M. (2013). Green modification of natural fibres with nanocellulose. *RSC Advances*, *3*(14), 4659–4665. https://doi.org/10.1039/c3ra22196b.

Darling, R. (1945). *Manufacture of cellulose ethers*. US Patent 2492524 A.

David, P., Kevin, L., John, J., & Helen, B. (2014). A review of nanocellulose as a novel vehicle for drug delivery. *Nordic Pulp & Paper Research Journal*, 105–118. https://doi.org/10.3183/npprj-2014-29-01-p105-118.

de Lima Fontes, M., Meneguin, A. B., Tercjak, A., Gutierrez, J., Cury, B. S. F., dos Santos, A. M., et al. (2018). Effect of in situ modification of bacterial cellulose with carboxymethylcellulose on its nano/microstructure and methotrexate release properties. *Carbohydrate Polymers*, *179*, 126–134. https://doi.org/10.1016/j.carbpol.2017.09.061.

Dilayda, K., Hatice, A. K. T., Hulya, O., & Ozan, T. (2018). Electrospun polylactic acid based nanofibers for biomedical applications. *Material Science Research India*, 224–240. https://doi.org/10.13005/msri/150304.

Du, R., Zhao, F., Peng, Q., Zhou, Z., & Han, Y. (2018). Production and characterization of bacterial cellulose produced by Gluconacetobacter xylinus isolated from Chinese persimmon vinegar. *Carbohydrate Polymers*, *194*, 200–207. https://doi.org/10.1016/j.carbpol.2018.04.041.

Dufresne, A. (2017). Cellulose nanomaterial reinforced polymer nanocomposites. *Current Opinion in Colloid and Interface Science*, *29*, 1–8. https://doi.org/10.1016/j.cocis.2017.01.004.

Dungani, R., Abdul Khalil, H. P. S., Aprilia, N. A. S., Sumardi, I., Aditiawati, P., Darwis, A., et al. (2017). Bionanomaterial from agricultural waste and its application. In *Cellulose-reinforced nanofibre composites: production, properties and applications* (pp. 45–88). Elsevier Inc. https://doi.org/10.1016/B978-0-08-100957-4.00003-6.

Eppley, B. L. (2005). Biomechanical testing of alloplastic PMMA cranioplasty materials. *The Journal of Craniofacial Surgery*, *16*(1), 140–143. https://doi.org/10.1097/00001665-200501000-00028.

Ferreira, F. V., Dufresne, A., Pinheiro, I. F., Souza, D. H. S., Gouveia, R. F., Mei, L. H. I., et al. (2018). How do cellulose nanocrystals affect the overall properties of biodegradable polymer nanocomposites: A comprehensive review. *European Polymer Journal*, *108*, 274–285. https://doi.org/10.1016/j.eurpolymj.2018.08.045.

Garza-Ulloa, J. (2018). Introduction to biomechatronics/biomedical engineering. In Garza-Ulloa (Ed.), *Applied Biomechatronics using Mathematical Models* (pp. 1–51). Academic Press.

Ghasemi, S., Behrooz, R., Ghasemi, I., Yassar, R. S., & Long, F. (2018). Development of nanocellulose-reinforced PLA nanocomposite by using maleated PLA (PLA-g-MA). *Journal of Thermoplastic Composite Materials*, *31*(8), 1090–1101. https://doi.org/10.1177/0892705717734600.

Göktürk, E., & Erdal, H. (2017). Biomedical applications of polyglycolic acid (PGA). *Sakarya University Journal of Science*, *21*(6), 1237–1244. https://doi.org/10.16984/saufenbilder.283156.

Guo, B., & Ma, P. X. (2014). Synthetic biodegradable functional polymers for tissue engineering: A brief review. *SCIENCE CHINA Chemistry*, *57*(4), 490–500. https://doi.org/10.1007/s11426-014-5086-y.

Gwon, J.-G., Cho, H.-J., Chun, S.-J., Lee, S., Wu, Q., & Lee, S.-Y. (2016). Physiochemical, optical and mechanical properties of poly(lactic acid) nanocomposites filled with toluene diisocyanate grafted cellulose nanocrystals. *RSC Advances*, *6*(12), 9438–9445. https://doi.org/10.1039/C5RA26337A.

Hasnain, M. S., Ahmad, S. A., Minhaj, M. A., Ara, T. J., & Nayak, A. K. (2018). Nanocomposite materials for prosthetic devices. In *Applications of nanocomposite materials in orthopedics* (pp. 127–144). Elsevier. https://doi.org/10.1016/B978-0-12-813740-6.00007-7.

Hervy, M., Evangelisti, S., Lettieri, P., & Lee, K. Y. (2015). Life cycle assessment of nanocellulose-reinforced advanced fibre composites. *Composites Science and Technology*, *118*, 154–162. https://doi.org/10.1016/j.compscitech.2015.08.024.

Huang, K., Wang, B., Cao, Y., Li, H., Wang, J., Lin, W., et al. (2011). Homogeneous preparation of cellulose acetate propionate (CAP) and cellulose acetate butyrate (CAB) from sugarcane bagasse cellulose in ionic liquid. *Journal of Agricultural and Food Chemistry*, *59*(10), 5376–5381. https://doi.org/10.1021/jf104881f.

Iryani, D. A., Risthy, N. M., Resagian, D. A., Yuwono, S. D., & Hasanudin, U. (2017). Preparation and evaluation adsorption capacity of cellulose xanthate of sugarcane bagasse for removal heavy metal ion from aqueous solutions. In *IOP conference series: Earth and environmental science* (p. 012039). https://doi.org/10.1088/1755-1315/65/1/012039.

Jorfi, M., & Foster, E. J. (2015). Recent advances in nanocellulose for biomedical applications. *Journal of Applied Polymer Science*, *132*(14). https://doi.org/10.1002/app.41719.

Kakar, A., Jayamani, E., Bakri, M. K. B., & Rahman, M. R. (2018). Biomedical and packaging application of silica and various clay dispersed nanocomposites. In M. R. Rahman (Ed.), *Silica and Clay Dispersed Polymer Nanocomposites* (pp. 109–136). Woodhead Publishing. https://doi.org/10.1016/B978-0-08-102129-3.00008-7.

Khan, A., Huq, T., Khan, R. A., Riedl, B., & Lacroix, M. (2014). Nanocellulose-based composites and bioactive agents for food packaging. *Critical Reviews in Food Science and Nutrition*, *54*(2), 163–174. https://doi.org/10.1080/10408398.2011.578765.

Khan, R., & Khan, M. H. (2013). Use of collagen as a biomaterial: An update. *Journal of Indian Society of Periodontology*, *17*(4), 539–542. https://doi.org/10.4103/0972-124X.118333.

Khui, PLN, Rahman, MR, & Bakri, MKB. (2021). A review on the extraction of cellulose and nanocellulose as a filler through solid waste management. *Journal of Thermoplastic Composite Materials*. https://doi.org/10.1177/08927057211020800.

Kim, J. H., Shim, B. S., Kim, H. S., Lee, Y. J., Min, S. K., Jang, D., et al. (2015). Review of nanocellulose for sustainable future materials. *International Journal of Precision Engineering and Manufacturing - Green Technology*, *2*(2), 197–213. https://doi.org/10.1007/s40684-015-0024-9.

Klemm, D., Heublein, B., Fink, H. P., & Bohn, A. (2005). Cellulose: Fascinating biopolymer and sustainable raw material. *Angewandte Chemie, International Edition*, *44*(22), 3358–3393. https://doi.org/10.1002/anie.200460587.

Kumar, A., Negi, Y. S., Bhardwaj, N. K., & Choudhary, V. (2012). Synthesis and characterization of methylcellulose/PVA based porous composite. *Carbohydrate Polymers*, *88*(4), 1364–1372. https://doi.org/10.1016/j.carbpol.2012.02.019.

Kuo, C.-M., & Leonard, A. P. (1983). *Process for esterification of cellulose using as the catalyst the combination of sulfuric acid.* US Patent.

Law, P., Rahman, M., Hamdan, S., Jayamani, E., Bakri, M., & Sanaullah, K. (2020). Synthesis and characterization of micro-nano carbon filler from Jatropha seeds. BioResources, 15(2), 3237–3251. Retrieved from https://ojs.cnr.ncsu.edu/index.php/BioRes/article/view/BioRes_15_2_3237_Law_Synthesis_Characterization_Micro_Nano_Carbon.

Lee, K. Y., Aitomäki, Y., Berglund, L. A., Oksman, K., & Bismarck, A. (2014). On the use of nanocellulose as reinforcement in polymer matrix composites. *Composites Science and Technology*, *105*, 15–27. https://doi.org/10.1016/j.compscitech.2014.08.032.

Lin, N., & Dufresne, A. (2014). Nanocellulose in biomedicine: Current status and future prospect. *European Polymer Journal*, *59*, 302–325. https://doi.org/10.1016/j.eurpolymj.2014.07.025.

Liu, D., Chen, X., Yue, Y., Chen, M., & Wu, Q. (2011). Structure and rheology of nanocrystalline cellulose. *Carbohydrate Polymers*, *84*(1), 316–322. https://doi.org/10.1016/j.carbpol.2010.11.039.

Mabrouk, A. B., Salon, M. C. B., Magnin, A., Belgacem, M. N., & Boufi, S. (2014). Cellulose-based nanocomposites prepared via mini-emulsion polymerization: Understanding the chemistry of the nanocellulose/matrix interface. *Colloids and Surfaces A: Physicochemical and Engineering Aspects*, *448*(1), 1–8. https://doi.org/10.1016/j.colsurfa.2014.01.077.

Mariano, M., El Kissi, N., & Dufresne, A. (2014). Cellulose nanocrystals and related nanocomposites: Review of some properties and challenges. *Journal of Polymer Science, Part B: Polymer Physics*, *52*(12), 791–806. https://doi.org/10.1002/polb.23490.

Martina, M., & Hutmacher, D. W. (2007). Biodegradable polymers applied in tissue engineering research: A review. *Polymer International*, *56*(2), 145–157. https://doi.org/10.1002/pi.2108.

Metreveli, G., Wågberg, L., Emmoth, E., Belák, S., Strømme, M., & Mihranyan, A. (2014). A size-exclusion nanocellulose filter paper for virus removal. *Advanced Healthcare Materials*, *3*(10), 1546–1550. https://doi.org/10.1002/adhm.201300641.

Miao, C., & Hamad, W. Y. (2013). Cellulose reinforced polymer composites and nanocomposites: A critical review. *Cellulose*, *20*(5), 2221–2262. https://doi.org/10.1007/s10570-013-0007-3.

Mohan, D., Pittman, C. U., & Steele, P. H. (2006). Pyrolysis of wood/biomass for bio-oil: A critical review. *Energy & Fuels*, *20*(3), 848–889. https://doi.org/10.1021/ef0502397.

Mondal, S. (2017). Preparation, properties and applications of nanocellulosic materials. *Carbohydrate Polymers*, *163*, 301–316. https://doi.org/10.1016/j.carbpol.2016.12.050.

Nabili, A., Fattoum, A., Brochier-Salon, M. C., Bras, J., & Elaloui, E. (2017). Synthesis of cellulose triacetate-I from microfibrillated date seeds cellulose (Phoenix dactylifera L.). *Iranian Polymer Journal (English Edition)*, *26*(2), 137–147. https://doi.org/10.1007/s13726-017-0505-5.

Nyuk Khui, P., Rahman, M., Ahmed, A., King Kuok, K., Bakri, M., Tazeddinova, D., Kazhmukanbetkyzy, Z., & Baibatyrov Torebek, B. (2021). Morphological and thermal properties of composites prepared with poly(lactic acid), poly(ethylene-alt-maleic anhydride), and biochar from microwave-pyrolyzed Jatropha seeds. *BioResources* 16(2), 3171–3185. Retrieved from https://ojs.cnr.ncsu.edu/index.php/BioRes/article/view/BioRes_16_2_3171_Nyuk_Khui_Morphological_Thermal_Properties_Composites.

Nyuk Khui, P., Rahman, M., Kuok, K., Bin Bakri, M., Adamu, M., Tazeddinova, D., Kazhmukanbetkyzy, Z., & Torebek, B. (2021). Small-size Jatropha seed biochar extracted from microwave pyrolysis: Optimization of its biocomposites mechanical properties by mixture design. *BioResources* 16(3), 4716–4730. Retrieved from https://ojs.cnr.ncsu.edu/index.php/BioRes/article/view/BioRes_16_3_4716_Nyuk_Khui_Jatropha_Seed_Biochar_Microwave.

Ozdil, D., & Aydin, H. M. (2014). Polymers for medical and tissue engineering applications. *Journal of Chemical Technology and Biotechnology*, *89*(12), 1793–1810. https://doi.org/10.1002/jctb.4505.

Ozdil, D., Wimpenny, I., Aydin, H. M., & Yang, Y. (2017). Biocompatibility of biodegradable medical polymers. In *Science and principles of biodegradable and bioresorbable medical polymers: Materials and properties* (pp. 379–414). Elsevier Inc. https://doi.org/10.1016/B978-0-08-100372-5.00013-1.

Pacheco, G., Nogueira, C. R., Meneguin, A. B., Trovatti, E., Silva, M. C. C., Machado, R. T. A., et al. (2017). Development and characterization of bacterial cellulose produced by cashew tree residues as alternative carbon source. *Industrial Crops and Products*, *107*, 13–19. https://doi.org/10.1016/j.indcrop.2017.05.026.

Park, M., Lee, D., & Hyun, J. (2015). Nanocellulose-alginate hydrogel for cell encapsulation. *Carbohydrate Polymers*, *116*, 223–228. https://doi.org/10.1016/j.carbpol.2014.07.059.

Pasangulapati, V., Ramachandriya, K. D., Kumar, A., Wilkins, M. R., Jones, C. L., & Huhnke, R. L. (2012). Effects of cellulose, hemicellulose and lignin on thermochemical conversion characteristics of the selected biomass. *Bioresource Technology*, *114*, 663–669. https://doi.org/10.1016/j.biortech.2012.03.036.

Pérez, J., Muñoz-Dorado, J., De La Rubia, T., & Martínez, J. (2002). Biodegradation and biological treatments of cellulose, hemicellulose and lignin: An overview. *International Microbiology*, *5*(2), 53–63. https://doi.org/10.1007/s10123-002-0062-3.

Petersen, N., & Gatenholm, P. (2011). Bacterial cellulose-based materials and medical devices: Current state and perspectives. *Applied Microbiology and Biotechnology*, *91*(5), 1277–1286. https://doi.org/10.1007/s00253-011-3432-y.

Picheth, G. F., Pirich, C. L., Sierakowski, M. R., Woehl, M. A., Sakakibara, C. N., de Souza, C. F., et al. (2017). Bacterial cellulose in biomedical applications: A review. *International Journal of Biological Macromolecules*, *104*, 97–106. https://doi.org/10.1016/j.ijbiomac.2017.05.171.

Pilate, F., Toncheva, A., Dubois, P., & Raquez, J. M. (2016). Shape-memory polymers for multiple applications in the materials world. *European Polymer Journal*, *80*, 268–294. https://doi.org/10.1016/j.eurpolymj.2016.05.004.

Rahman, M. R., & Bakri, M. K. B. (2021). Bamboo cellulose Gel/MMT polymer nanocomposites for high strength materials. In M. R. Rahman (Ed.), *Bamboo Polymer Nanocomposites. Engineering Materials*. Cham: Springer. https://doi.org/10.1007/978-3-030-68090-9_7.

Rahman, M. R., & Bakri, M. K. B. (2021). Educational and awareness of bamboo nanocomposites towards sustainable environment. In M. R. Rahman (Ed.), *Bamboo Polymer Nanocomposites. Engineering Materials*. Cham: Springer. https://doi.org/10.1007/978-3-030-68090-9_10.

Rahman, M. R., Khui, P. L. N., & Bakri, M. K. B. (2021). Bamboo nanocomposites future development and applications. In M. R. Rahman (Ed.), *Bamboo Polymer Nanocomposites. Engineering Materials*. Cham: Springer. https://doi.org/10.1007/978-3-030-68090-9_9.

Robert, J. M., Ashlie, M., John, N., John, S., & Jeff, Y. (2011). Cellulose nanomaterials review: Structure, properties and nanocomposites. *Chemical Society Reviews*, *3941*. https://doi.org/10.1039/c0cs00108b.

Römling, U., & Galperin, M. Y. (2015). Bacterial cellulose biosynthesis: Diversity of operons, subunits, products, and functions. *Trends in Microbiology*, *23*(9), 545–557. https://doi.org/10.1016/j.tim.2015.05.005.

Sacui, I. A., Nieuwendaal, R. C., Burnett, D. J., Stranick, S. J., Jorfi, M., Weder, C., et al. (2014). Comparison of the properties of cellulose nanocrystals and cellulose nanofibrils isolated from bacteria, tunicate, and wood processed using acid, enzymatic, mechanical, and oxidative methods. In *Vol. 6. ACS applied materials and interfaces* (pp. 6127–6138). American Chemical Society. https://doi.org/10.1021/am500359f. Issue 9.

Shankaran, D. R., Mohan Bhagyaraj, S., Oluwafemi, O. S., Kalarikkal, N., & Thomas, S. (2018). Chapter 14—Cellulose nanocrystals for health care applications. In *Micro*

and nano technologies (pp. 415–459). Woodhead Publishing. https://doi.org/10.1016/B978-0-08-101971-9.00015-6.

Sharma, A., Thakur, M., Bhattacharya, M., Mandal, T., & Goswami, S. (2019). Commercial application of cellulose nano-composites—A review. *Biotechnology Reports*, *21*. https://doi.org/10.1016/j.btre.2019.e00316.

Shui, T., Feng, S., Chen, G., Li, A., Yuan, Z., Shui, H., et al. (2017). Synthesis of sodium carboxymethyl cellulose using bleached crude cellulose fractionated from cornstalk. *Biomass and Bioenergy*, *105*, 51–58. https://doi.org/10.1016/j.biombioe.2017.06.016.

Sim, B., Bae, D. H., Choi, H. J., Choi, K., Islam, M. S., & Kao, N. (2016). Fabrication and stimuli response of rice husk-based microcrystalline cellulose particle suspension under electric fields. *Cellulose*, *23*(1), 185–197. https://doi.org/10.1007/s10570-015-0836-3.

Soemphol, W., Hongsachart, P., & Tanamool, V. (2018). Production and characterization of bacterial cellulose produced from agricultural by-product by Gluconacetobacter strains. In *Vol. 5. Materials today: Proceedings* (pp. 11159–11168). Elsevier Ltd. https://doi.org/10.1016/j.matpr.2018.01.036. Issue 5.

Sullivan, E. M., Moon, R. J., & Kalaitzidou, K. (2015). Processing and characterization of cellulose nanocrystals/polylactic acid nanocomposite films. *Materials*, *8*(12), 8106–8116. https://doi.org/10.3390/ma8125447.

Tajeddin, B. (2014). Cellulose-based polymers for packaging applications. In *Lignocellulosic polymer composites: Processing, characterization, and properties* (pp. 477–498). Wiley Blackwell. https://doi.org/10.1002/9781118773949.ch21. Vol. 9781118773574.

Tang, Y., He, Z., Mosseler, J. A., & Ni, Y. (2014). Production of highly electro-conductive cellulosic paper via surface coating of carbon nanotube/graphene oxide nanocomposites using nanocrystalline cellulose as a binder. *Cellulose*, *21*(6), 4569–4581. https://doi.org/10.1007/s10570-014-0418-9.

Torres, F. G., Arroyo, J. J., & Troncoso, O. P. (2019). Bacterial cellulose nanocomposites: An all-nano type of material. *Materials Science and Engineering C*, *98*, 1277–1293. https://doi.org/10.1016/j.msec.2019.01.064.

Tosh, B. (2014). Synthesis and sustainable applications of cellulose Esters and ethers: A review. *International Journal of Energy, Sustainability and Environmental Engineering*, *1*(2), 56–78.

Ullah, H., Wahid, F., Santos, H. A., & Khan, T. (2016). Advances in biomedical and pharmaceutical applications of functional bacterial cellulose-based nanocomposites. *Carbohydrate Polymers*, *150*, 330–352. https://doi.org/10.1016/j.carbpol.2016.05.029.

Wang, J., Tavakoli, J., & Tang, Y. (2019). Bacterial cellulose production, properties and applications with different culture methods—A review. *Carbohydrate Polymers*, *219*, 63–76. https://doi.org/10.1016/j.carbpol.2019.05.008.

Wang, Z., Yao, Z., Zhou, J., He, M., Jiang, Q., Li, S., et al. (2019). Isolation and characterization of cellulose nanocrystals from pueraria root residue. *International Journal of Biological Macromolecules*, *129*, 1081–1089. https://doi.org/10.1016/j.ijbiomac.2018.07.055.

Wei, L., & McDonald, A. G. (2016). A review on grafting of biofibers for biocomposites. *Materials*, *9*(4). https://doi.org/10.3390/ma9040303.

Wnek, G., & Bowlin, G. (Eds.). (2008). *Encyclopedia of Biomaterials and Biomedical Engineering* (2nd ed.). CRC Press. https://doi.org/10.1201/9780429154065.

Yan, H., Chen, X., Song, H., Li, J., Feng, Y., Shi, Z., et al. (2017). Synthesis of bacterial cellulose and bacterial cellulose nanocrystals for their applications in the stabilization of olive oil pickering emulsion. *Food Hydrocolloids*, *72*, 127–135. https://doi.org/10.1016/j.foodhyd.2017.05.044.

Ye, H., Xu, S., Wu, S., & Chen, W. (2018). Optimization of sodium carboxymethyl cellulose preparation from bagasse by response surface methodology. In *Vol. 381. IOP conference series: Materials science and engineering* Institute of Physics Publishing. https://doi.org/10.1088/1757-899X/381/1/012043. Issue 1.

Zhu, H., Fang, Z., Preston, C., Li, Y., & Hu, L. (2014). Transparent paper: Fabrications, properties, and device applications. *Energy and Environmental Science*, *7*(1), 269–287. https://doi.org/10.1039/c3ee43024c.

CHAPTER

Applications of cellulose materials and their composites

14

Muhammad Khusairy Bin Bakri and Md Rezaur Rahman

Department of Chemical Engineering and Energy Sustainability, Faculty of Engineering, Universiti Malaysia Sarawak (UNIMAS), Kota Samarahan, Sarawak, Malaysia

Chapter outline

14.1 Introduction

A fundamental constituent of cellulose is located on its natural fiber wall, which is around 40–50% of dry wood mass. Cellulose is a long molecular chain linked sugar, which provides the wood with its prominent and remarkable strength in the plant structure. In many paper and textile industries, cellulose has become the main basis of block building in all the fibers. An example of purely form of cellulose is cotton and kapok. In laboratory analysis, an ash-less filter paper used is one of the sources of 100% pure cellulose (Orelma, Filpponen, Johansson, Laine, & Rojas, 2011). Cellulose is a natural polymer, which consists and made up from a small long chain molecule. Most of these cellulose application in the form of polymer making is extracted from wood pulp and cotton. Whereas, the main principle of it may be used as paperboard and paper production, while it would be converted into many derivative

Fundamentals and Recent Advances in Nanocomposites Based on Polymers and Nanocellulose.
https://doi.org/10.1016/B978-0-323-85771-0.00010-5

products like rayon, cellophane, etc. In the meantime, many researchers are still exploring the used of cellulose, either as a form of new energy, like converting it into biofuels or biodiesel, while extracting it from crops, i.e., cellulosic ethanol. Many of these researches at present are still going on and prolong, while other are still focusing on the alternative source of fuel (Nishiyama, Langan, & Chanzy, 2002).

14.2 Processing of cellulose matrix composites

Compared it with the traditional synthetic counterparts, the interest in natural cellulosic fibers arises due to its high awareness of economical production, ecofriendly advantages, and higher specific strength/stiffness (El-Saied, El-Diwany, Basta, Atwa, & El-Ghwas, 2008; Shalwan & Yousif, 2013; Singha & Thakur, 2010). Furthermore, these composites procurements and process is far more healthier and friendly, and it provides better working conditions for many large scale industrial applications (Singha & Thakur, 2008a, 2008b). Even though natural fibers provided numerous advantages over its synthetic counterparts, natural fibers have also many disadvantages (Singha & Thakur, 2009a, 2009b, 2009c). In industrial applications, the disadvantages or weaknesses of these natural fibers may include of being water/moisture absorption sensitive, less thermal stability, and its polar and hydrophilic nature (Akil et al., 2011; Bogoeva-Gaceva et al., 2007; Eichhorn et al., 2010; George, Sreekala, & Thomas, 2001). Moreover, overall, based on the properties and its comparison, the natural cellulosic fibers have the advantages of outweighed the disadvantages, when compared with each other and some other synthetic fibers (Singha & Kumar, 2009).

Depending on the applications, the shortcomings of most remedial measures for natural fiber are in the form of chemical treatments and modification (Singha et al., 2009; Thakur, Singha, & Thakur, 2012). For polymer composite applications, to modify the surface of natural cellulosic fibers, many different chemical surface modification techniques have been used and recently reviewed, in which, many of all these reviews, mostly has been discussed in detail, especially on the effect of different surface modification techniques (Azwa, Yousif, Manalo, & Karunasena, 2013; Bledzki & Gassan, 1999; Bogoeva-Gaceva et al., 2007; Eichhorn et al., 2010; George et al., 2001; Mukherjee & Kao, 2011). In 2012, gomuti fiber reinforced thermoset composites have been reviewed with the emphasis on the use of gomuti fibers in different thermoset polymer matrices (Ticoalu, Aravinthan, & Cardona, 2013). Gomuti fiber is obtained from *Arenga pinnata* trees, which also called as sugar-palm, *ijuk*, *serat aren*, *gomutu*, and black fiber (Ticoalu et al., 2013). Based on Ticoalu et al. (2013), it is also observed that gomuti fiber is comparable than other natural fibers. Gomuti fiber is almost similar to coir fiber in its mechanical and physical properties. Therefore, the composites with gomuti fiber may exhibit properties almost similar to coir fiber composites, i.e., lower density, high strength, and modulus, but higher elongation.

In the preparation of natural fibers reinforced composites based on cellulose, both thermoset and thermoplastics polymer matrices may offer the following advantages

(Singha & Thakur, 2008b): (i) Easy processing of natural fibers reinforced composites, as the initial resin system liquid and powder form, which the fibers can be easily mixed with the resin, (ii) For the preparation of these composite systems, simple low cost or self-made system can be used, (iii) Thermoset required less temperature for its composites preparation while compared to the thermoplastic composites, (iv) The pressure composites systems requirement is very low, (v) Depending on the polymer resin viscosity, the natural fibers can be easily wet, and (vi) with the advancement of polymer matrix based composites, fibers with higher loading could easily achieve in both thermoset and thermoplastic.

These thermoset and thermoplastic polymer matrix composites also suffer from few shortcomings, instead of the advantages, such as high curing time and nonrecycling, depending on its resin type (Grigore, 2017; Taofik, 2020; Singha & Thakur, 2009b). Thanks to its outstanding mechanical properties, frequently, thermoset polymer composites are used in numerous numbers of applications, instead of its disadvantages (Singha & Thakur, 2009b, 2009c; Thakur & Thakur, 2014). Therefore, the following important commercialization would be discussed, especially on some of the synthetic thermoset and thermoplastic polymer matrix-based composites from cellulose.

14.3 Engineered parts from cellulose matrix composites

14.3.1 Structural

In structural materials, functional materials such as cellulose-based, can be used as reinforcement. Cellulose is known for its high strength, while having its natural hierarchical and porous structural material. As sustainable reinforcing materials for polymers, carboxyl methyl celluloses (CNCs) have great potential, but there are several obstacles needed to be overcome before commercialize it. To produce CNCs-polymer nanocomposites, there are many greatest challenges needed to be overcome, such as high levels of water absorption, low thermal stabilities, poor miscibility with nonpolar polymers, and irreversible aggregation of the dried CNCs (Fox et al., 2016). Therefore, the manufacture of CNCs nanocomposites as reinforcing agents from biomass had great potential once the obstacles have been overcome.

Moubarik, Grimi, and Boussetta (2013) studies the cellulose fibers extracted from Moroccan sugar cane bagasse and found that the isolated cellulose fiber from Moroccan sugar cane bagasse can be done by using three distinctive treatment, especially for the applications as a reinforcing agent in low density polyethylene. The first stage of the treatment is that the bagasse was subjected to a hot water at the temperature of 70 °C to eliminate hemicellulose. Then, at the second stage, an alkaline aqueous solution of 15% sodium hydroxide (NaOH) is used at temperature of 98°C to eliminate lignin, and finally to the third stage is bleaching stage (Moubarik et al., 2013). As a result, a good interface adhesion between cellulose fibers and matrix was found to improve the mechanical properties of the composites at 25 wt% fiber loading, whereas a gain of 72% in Young's modulus and 85% in flexural modulus was noted (Moubarik et al., 2013).

14.3.2 Nanocomposites

In nanocomposites, CNCs can also be extracted from corncob as reinforcing agent (Silvério, Flauzino Neto, Dantas, & Pasquini, 2013). With only 9 wt% of CNCs, the CNCs/polyvinyl alcohol (PVA) composites showed an improved tensile strength by 140.2%. Based on the crystallinity index, it was found that the tensile properties have a greater influence on the strength, with consideration of its aspect ratio. Not only that, CNCs can also be extracted from plant cell wall successfully as the techniques used in its application had improved efficiently by time, whereas the reinforcing agent can be used as polymers (Ng et al., 2015). As a reinforcing agent, CNCs were modified with silane coupling agent KH-550 (3-Aminopropyltriethoxysilane), while the nanocomposites were prepared by its solution casting method of biopolyester poly(3-hydroxybuty-rate-*co*-4-hydroxybutyrate) (P(3,4)HB)/silane treated cellulose nanowhiskers (STCNW) (Zhang, Zhang, Hang, Min, & Zhang, 2016). The STCNCs enhanced hydrophobicity and facilitated the crystallization of P(3,4)HB, which greatly improved the tensile strength and elastic modulus of P(3,4)HB composites (Zhang et al., 2016). As a lightweight composite, either in the application for transportation, infrastructure, and renewable energy, the miscibility of dried CNCs was enhanced with a nonpolar polymer (epoxy and polystyrene) (Fox et al., 2016).

14.3.3 Water engineering

In water, for engineering applications, by using two different free-radical redox initiators including Fenton's reagent ($Fe_2 + H_2O_2$) and ceric ammonium nitrate, CNCs could also be modified with polymethyl methacrylate (PMMA) grafts (Spinella et al., 2016). In its glassy and rubbery state, PMMA modified CNCs nanocomposites possessed high storage moduli, due to CNCs enhanced dispersion. Moreover, via surface grafting of (2-dodecen-1-yl) succinic anhydride in dimethyl formamide, CNCs can also be modified (Miao & Hamad, 2016). In the nanocomposite, such significant increase in tensile strength and modulus from the resulting materials is due to the good dispersion-ability (dispersibility) in organic solvents with a wide range of polarity. In paper making as reinforcing agent, various forms of cellulose could be applied, such as microfiber composites (MFC) (Adel et al., 2016), natural fiber (NFC) (Balea, Merayo, De La Fuente, Negro, & Blanco, 2017; Huang, Zhao, Kuga, Wu, & Huang, 2016), cellulose nanocrystals (CNC) (Sun, Hou, Liu, & Ni, 2015), and bacterial cellulose (BC) (Santos et al., 2016a, 2016b).

14.3.4 Paper making

For paper making, MFC was prepared as reinforcement with sodium hydroxide-sodium sulfite, respectively, by the mechanical treatment from bagasse, rice straw, and cotton stalk (Adel et al., 2016). By adding different percentages of MFC from bleached rice straw and bagasse pulps, composite sheet papers can also be prepared. As compared with 20 wt% soft wood pulp, the MFC with low

percentage of 5 wt% may also enhance the mechanical and optical properties. To improve the interface between the MFC and hydrophobic matrix, the functioned MFC was produced by the ball milling method (Adel et al., 2016). Succinic anhydride modified NFC due to carboxyl groups on the surface showed the enhanced hydrophilicity and gave a zeta potential of −38.7 mV. The modified dodecyl succinic anhydride NFC had better compatibility with polyethylene and excellent dispersibility in o-xylene. Overall enhanced of the NFC polyethylene composites mechanical properties is also presented. For the paper additives applications, NFC was produced from corn and rape stalk pulps by bleaching, refining, and TEMPO-mediated oxidation (Balea et al., 2017). Higher tensile index values are achieved in the chitosan and NFC combination in recycled paper.

For the applications of paper wet strength additive, Sun et al. used CNCs sodium periodate oxidation and investigated the yield loss of the oxide content of aldehyde groups on CNCs and its reaction conditions' effects. To improve the bonding degree between the cellulosic fibers the oxidized CNCs were functioning as a nanosized additive. Santos et al. (2016a, 2016b) also focused on model papers with the used of BC sheets lining papers as reinforcing material from *Gluconacetobacter sucrofermentans*. The quality of the deteriorated paper with BC is improved without altering the structure information, which is alternatively a promising material for the restoration of paper (Santos et al., 2016a). For sustainable barrier applications, multilayer PLA/MFC biocomposites were fabricated (Meriçer et al., 2016), whereas at 50% RH, in dry conditions, oxygen permeability showed a remarkable barrier effect, which was much lower than most of the conventional oil-based and novel bio-based barrier solutions. For automotive instrument panel applications, biodegradable bark cloth reinforced green epoxy composites were developed (Rwawiire, Tomkova, Militky, Jabbar, & Kale, 2015). The epoxy composites static properties showed a tensile strength and flexural strength of 33 and 207 MPa, respectively. Treatment on the fabric with alkali on the fabric reinforced biocomposites would positively influence the mechanical properties.

14.4 Further applications

In further application, cellulose can also be used as energy storage materials, which include supercapacitors and lithium ion battery. For the potential applications in supercapacitors, the three-dimensional porous structures of reduced graphene oxide (RGO)/cellulose composites were fabricated and assisted by using a ball milling and chemical to reduce the graphene oxide (GO) (Ouyang et al., 2013). Due to the RGO continuous network, its high specific surface area, and fast charge propagation in the composites, 3D porous structures of RGO/cellulose composites showed an electrical conductivity of 15.28 $\Sigma\ m^{-1}$, whereas for supercapacitor applications, the conductive CNCs with high cycling stability were obtained (Wu et al., 2014). The core-shell polypyrrole on poly(*N*-vinylpyrrolidone) was coated with CNCs. A well-defined core-shell structure with well-preserved one-dimensional fibril geometry could

significantly improve the electrochemical performance of possessed the composites. For lithium ion battery applications, as reinforcement in a polymer matrix, four cellulose nanofibril reinforced composite electrolytes were manufactured using NFC nanopaper (Willgert, Leijonmarck, Lindbergh, Malmström, & Johansson, 2014). The composites modified by an equimolar solution of propionyl chloride and acryloyl chloride, had an elastic modulus more than 100 MPa above 100°C, and anion conductivity of around 5×10^{-5} Σcm^{-1} at 25°C. For structural batteries, Snyder, Carter, and Wetzel (2007) set up the criteria with elastic modulus more than 150 MPa and anion conductivity more than 1×10^{-5} Σcm^{-1}. Based on BC/lignin composites, mesoporous, flexible, catalyst free, and highly graphitized carbon aerogels with core-shell structure were synthesized (Xu et al., 2015). These carbon aerogels materials have potential in many applications including catalyst supports, sensors, oil/water separation, and energy storage of supercapacitors and batteries. By utilizing the toughening effect of the BC nanofiber network, large reversible deformations in carbon aerogels were attainable. These materials also created large mesopore concentration, and the blackberry-like structure of facilitated ion transportation and adsorption led to their high capacitance. For green polymer electrolyte application, carboxymethyl cellulose (CMC) and carboxymethyl kappa-carrageenan (CMCK) were produced (Rudhziah, Rani, Ahmad, Mohamed, & Kaddami, 2015). With the addition of CMC, the enhanced CMKC mechanical properties were obtained, whereas the blend with weight percentage (wt%) ratio of 60:40 yielded conductivity of 3.25×10^{-4} Σcm^{-1}, which is the most conductive film. Table 14.1 shows the summary of functions material based on cellulose.

For many such applications many materials have been successfully tested, i.e., materials made from bacterial cellulose (BC) (Bodin et al., 2007; Czaja, Young, Kawecki, & Brown, 2007), and other cellulosic materials (Hong et al., 2006; Müller et al., 2006; Wan et al., 2007). The good mechanical properties of the cellulose composites, especially if it involves with all cellulose composites, maybe allow to be used in an application as substitution of bone or cartilage material (Bodin et al., 2007). Another application may involve in the so-called smart materials, which create a cellophane (Je & Kim, 2004) and regenerated cellulose (Yun, Chen, Nayak, & Kim, 2008), which are used as electro-active paper. For a broad variety of applications, those materials can be used as electrical displays, sensors, and micro-robots (Kim, Yun, & Lee, 2008). The improved cellulose composite mechanical properties may provide an alternative to the mere cellulose paper. So far, the cellulose composite produced in laboratory scale by experiments and little is known on their processability when apply through mass manufacturing methods. Blow molding seems to be one applicable method, whereas all those composites had a film or sheet like structure, especially when it is successfully applied for NMMO-solutions (Weigel, Fink, Frigge, & Schwarz, 2001). The cellulose composite depended much on several other aspects, irrespectively toward the manufacturing method and the production costs. A major role, such as the quality of the cellulose source would play huge in the calculation. Highly purified cellulose or other necessary pretreatments, i.e., excessive drying of the raw materials would increase the costs of the composite, while the use of

Table 14.1 Summary of functionalized materials based on cellulose (Li et al., 2018; Guimarães e 2013; Liu, Song, Anderson, Chang, & Hua, 2012; *Review of progress in quantitative nondestru* Shahzad, 2012; Singha & Thakur, 2008a).

Form of cellulose	Other materials used	Method of preparation	Mechanics of compound	Advantages of th product
MFC	Starch, glycerol	Solvent casting	Mechanical defibrillation and physical blend	Low water vapor permeability and h tensile strength
MFC	Calcium peroxide, catalase	LbL assembly	Physically supported by cellulose	Modulation of the releases of hydrog peroxide (H_2O_2) or oxygen (O_2)
NFC	Laccase (Lac)/ polyaniline/CMC	Complicated processes including electrospinning	In situ polymerization of aniline	Detection limit of 0.374 M
NFC	Kymene	Mechanical defibrillation and spray-freeze-drying	Physical molding and chemical cross-linking	Highly lightweight ($0.0018\,g cm^{-3}$)
NFC	Titania	Three solution reactions	Solution and regeneration, cross-linking	Long-term drug release
NFC and BC	CS	Solvent casting	Ammonium persulfate oxidation, nanoscale reinforcement	High mechanical a biological properti

Table 14.1 Summary of functionalized materials based on cellulose (Li et al., 2018; Guimarães et al., 20
2013; Liu, Song, Anderson, Chang, & Hua, 2012; *Review of progress in quantitative nondestructive ev*
Shahzad, 2012; Singha & Thakur, 2008a). *Cont'd*

Form of cellulose	Other materials used	Method of preparation	Mechanics of compound	Advantages of the product
BC	Gelatin	Immersion	Double-network structures	Hydrophilic property with high mechanical strength
CNC	Xylans	Spin-assisted electrostatic layer-by-layer self-assembly	Structural color	Detection of xylanase activity
CNC	Fibrin	Solution reaction	Molecular reaction	Reinforcement
CNC	CS	Solution reaction	Polymer grafting	Mechanical strength and hydrophilic property
CNC	Poly(propylene imine), FA and others	Five chemical reactions' process	Dendrimer-grafted CNC	High drug load and more sustainable drug release functionality
CNC	2-Ureido-4 [1*H*]-pyrimidone, acrylamide, gelatin methacrylate	Four chemical reactions	Grafted polymer onto CNC and emulsion polymerization	Excellent solid stabilizers, elastic microporous composite hydrogels
CNC	Poly(vinyl acetate)	Five chemical reactions and final solvent cast process	Graft polymer onto CNC by SI-RAFT/MADIX polymerization	High transparency and improved mechanical properties

CNC	Silk fibroin, CS	LbL assembly	Hierarchical lamellar structure	Excellent mechani properties and biological compatibility
CNC	Alginate	Solvent casting	Ca^{2+} cross-linked	High porosity and tensile strength
CMC	Sodium benzoate, glutaraldehyde	Solvent molding process and evaporation method	Photo-cross-linking and chemical cross-linking	High surface hydrophobicity, wa barrier, and mechanical properties
Ethyl cellulose	Poly(e-caprolactone), rhodamine B, and folate acid	Three chemical reactions' process	Functional molecules bonded on comb copolymer	Fluorescent and targeting functiona
Cellulose solution	Phosphor, epichlorohydrin	Physically blended in aqueous solutions	Physically supported by cellulose	Safety, hydrophilic biocompatibility, biodegradability an being inexpensive
Cellulose solution	Polyaniline	Solvent casting and interfacial polymerization	Physically supported by cellulose	Micronanostructur
Electrospun CA nanofibers	Isothiocyanate, folate acid, and poly(amidoamine)	Complicated chemical and physical process	Multifunctional dendrimer-modified electrospun CA nanofibers	Targeted cancel c capture
CA membrane	Amino-propyl-triethoxysilane, sericin, glutaraldehyde	Two steps of surface chemistry	Covalent immobilization onto CA	Safety, hydrophilic biocompatibility, biodegradability an being inexpensive

Table 14.1 Summary of functionalized materials based on cellulose (Li et al., 2018; Guimarães et al., 20
2013; Liu, Song, Anderson, Chang, & Hua, 2012; *Review of progress in quantitative nondestructive ev*
Shahzad, 2012; Singha & Thakur, 2008a). *Cont'd*

Form of cellulose	Other materials used	Method of preparation	Mechanics of compound	Advantages of the product
Chromatography paper	Lipid	Deposit, evaporate, incubate and extract	Macromolecular self-assembly	Microporous media
Methyl cellulose, HEC, and HPMC	Steroid diosgenin	Solution reaction	Covalently linked on cellulose and self-assembling in water	Controlled release of agrochemicals
MCC	ScF_2	Microwave assisted reaction	Physically supported by cellulose	Enhancing the strength of the papers

low-cost raw materials, i.e., as waste products of, for example, the wood or textile industry would reduce the expenses (Bakri, Jayamani, & Hamdan, 2018; Rahman, Khui, & Bakri, 2021; Rahman, Taib, Bakri, & Taib, 2021). A further aspect that must be considered whether cellulose composites could be main reliable "greener" alternative to existing materials. When the processing involves highly hazardous materials, the example of the viscose process shows that using biological raw materials and biodegradation of the product count little (Sweetnam, Taylor, & Elwood, 1987). The cellulose composites ecofriendliness strongly depends on the involved materials and processing methods, whereas the corresponding energy would also need to be accounted. It would be necessary to audits the environmental effects on the composites, as soon their production is ready for industrial fabrication, either if it is "green" or not. In addition, the degradation studies on those composites may provide important information as well.

14.5 Summary and future trends

Despite the promising properties of cellulose composites, to find suitable industrial applications, there many researches needed to be done in order to required and understand the fundamentals of these materials. In long-term application, additional processing is required for the cellulose hydrophilicity to avoid swelling and degradation. During processing, a significant amount of swelling on the cellulosic hydrophilicity raw materials could cause the cellulose composites, which after drying, a resulting in a certain amount of shrinkage. The swelling and shrinkage correlated with the types and amounts of cellulose used and applied during the processing steps. So far, this topic has not been addressed by many researchers, especially on how to as predict and control shrinkage, which is essential for industrial scale composites production. Furthermore, up to now, other different solvent effects on the resulting cellulose composites, especially on its mechanical properties, i.e., single cellulosic fibers have not been investigated in detail. This is necessary to judge the effectiveness of the solvent, which allowed the high classification due to different processing methods, involved costs and resulting material properties.

Assuming the recycling process to be cheap, the materials can be recovered and recycled, whereas the costs of the solvent could be minimized. On the other hand, in case of a nonrecyclable and possibly hazardous solvent, the costs of its disposal must be considered. Another important factor is the amount of dissolvable cellulose and resulting necessary amount of solvent. Different solvents would only work with cellulose, where the sources of it is low in degree of polymerization and crystallinity, whereas others might be the ideal choice for high-class raw materials. Furthermore, more research is necessary to know how the different solvent systems interact with the other components, i.e., such as hemicelluloses and lignin. Financially, attractive cellulose sources like natural fibers and wood in contrast to highly purified cellulosic materials such as microcrystalline cellulose or filter paper. In addition, both cellulosic matrix and reinforcement interfacial properties has not been analyzed with

the typical tests developed for glass- or carbon fiber-reinforced composites, i.e., as pull-out or single-fiber fragmentation tests. A specific analysis of the interfacial properties of cellulose composites is necessary to verify the proposed positive effect of a mono component composite and verify a possible connection to the improved tensile strength. Understanding the formation, structure and quality of the interface would be essential to produce predictable composite materials. So far, the structure of those composites is limited to a simple two-dimensional geometry. Compositions that are more complex would allow competition with other fiber-reinforced polymers. For biomedical applications, as well as structural applications, it could also be possible to be used in cellulose composite.

Acknowledgment

The authors would like to acknowledge Universiti Malaysia Sarawak (UNIMAS) for the support.

References

Adel, A. M., El-Gendy, A. A., Diab, M. A., Abou-Zeid, R. E., El-Zawawy, W. K., & Dufresne, A. (2016). Microfibrillated cellulose from agricultural residues. Part I: Papermaking application. *Industrial Crops and Products*, *93*, 161–174. https://doi.org/10.1016/j.indcrop.2016.04.043.

Akhlaghi, S. P., Berry, R. C., & Tam, K. C. (2013). Surface modification of cellulose nanocrystal with chitosan oligosaccharide for drug delivery applications. *Cellulose*, *20*(4), 1747–1764. https://doi.org/10.1007/s10570-013-9954-y.

Akil, H. M., Omar, M. F., Mazuki, A. A. M., Safiee, S., Ishak, Z. A. M., & Abu Bakar, A. (2011). Kenaf fiber reinforced composites: A review. *Materials and Design*, *32*(8–9), 4107–4121. https://doi.org/10.1016/j.matdes.2011.04.008.

Azwa, Z. N., Yousif, B. F., Manalo, A. C., & Karunasena, W. (2013). A review on the degradability of polymeric composites based on natural fibres. *Materials and Design*, *47*, 424–442. https://doi.org/10.1016/j.matdes.2012.11.025.

Bakri, M. K. B., Jayamani, E., Hamdan, S., et al. (2018). Potential of Borneo *Acacia* wood in fully biodegradable bio-composites' commercial production and application. *Polymer Bulletin*, *75*, 5333–5354. https://doi.org/10.1007/s00289-018-2299-9.

Balea, A., Merayo, N., De La Fuente, E., Negro, C., & Blanco, Á. (2017). Assessing the influence of refining, bleaching and TEMPO-mediated oxidation on the production of more sustainable cellulose nanofibers and their application as paper additives. *Industrial Crops and Products*, *97*, 374–387. https://doi.org/10.1016/j.indcrop.2016.12.050.

Bledzki, A. K., & Gassan, J. (1999). Composites reinforced with cellulose based fibres. *Progress in Polymer Science*, 221–274. https://doi.org/10.1016/s0079-6700(98)00018-5.

Bodin, A., Bäckdahl, H., Fink, H., Gustafsson, L., Risberg, B., & Gatenholm, P. (2007). Influence of cultivation conditions on mechanical and morphological properties of bacterial cellulose tubes. *Biotechnology and Bioengineering*, *97*(2), 425–434. https://doi.org/10.1002/bit.21314.

Bogoeva-Gaceva, G., Avella, M., Malinconico, M., Buzarovska, A., Grozdanov, A., Gentile, G., et al. (2007). Natural fiber eco-composites. *Polymer Composites*, *28*(1), 98–107. https://doi.org/10.1002/pc.20270.

Boujemaoui, A., Mazières, S., Malmström, E., Destarac, M., & Carlmark, A. (2016). SI-RAFT/MADIX polymerization of vinyl acetate on cellulose nanocrystals for nanocomposite applications. *Polymer*, *99*, 240–249. https://doi.org/10.1016/j.polymer.2016.07.013.

Brown, E. E., Hu, D., Abu Lail, N., & Zhang, X. (2013). Potential of nanocrystalline cellulose-fibrin nanocomposites for artificial vascular graft applications. *Biomacromolecules*, *14*(4), 1063–1071. https://doi.org/10.1021/bm3019467.

Cai, H., Sharma, S., Liu, W., Mu, W., Liu, W., Zhang, X., et al. (2014). Aerogel microspheres from natural cellulose nanofibrils and their application as cell culture scaffold. *Biomacromolecules*, *15*(7), 2540–2547. https://doi.org/10.1021/bm5003976.

Chang, S. T., Chen, L. C., Lin, S. B., & Chen, H. H. (2012). Nano-biomaterials application: Morphology and physical properties of bacterial cellulose/gelatin composites via crosslinking. *Food Hydrocolloids*, *27*(1), 137–144. https://doi.org/10.1016/j.foodhyd.2011.08.004.

Chang, C. W., & Wang, M. J. (2013). Preparation of microfibrillated cellulose composites for sustained release of H2O2 or O2 for biomedical applications. *ACS Sustainable Chemistry & Engineering*, *1*(9), 1129–1134. https://doi.org/10.1021/sc400054v.

Cheng, F., Liu, C., Wei, X., Yan, T., Li, H., He, J., et al. (2017). Preparation and characterization of 2,2,6,6-tetramethylpiperidine-1-oxyl (TEMPO)-oxidized cellulose nanocrystal/alginate biodegradable composite dressing for hemostasis applications. *ACS Sustainable Chemistry & Engineering*, *5*(5), 3819–3828. https://doi.org/10.1021/acssuschemeng.6b02849.

Czaja, W. K., Young, D. J., Kawecki, M., & Brown, R. M. (2007). The future prospects of microbial cellulose in biomedical applications. *Biomacromolecules*, *8*(1), 1–12. https://doi.org/10.1021/bm060620d.

Dammak, A., Moreau, C., Beury, N., Schwikal, K., Winter, H. T., Bonnin, E., et al. (2013). Elaboration of multilayered thin films based on cellulose nanocrystals and cationic xylans: Application to xylanase activity detection. *Holzforschung*, *67*(5), 579–586. https://doi.org/10.1515/hf-2012-0176.

Deng, F., Dong, Y. Y., Liu, S., Wang, B., Ma, M. G., & Du, X. (2016). Revealing the influences of cellulose on cellulose/SrF2 nanocomposites synthesized by microwave-assisted method. *Industrial Crops and Products*, *85*, 258–265. https://doi.org/10.1016/j.indcrop.2016.03.018.

Eichhorn, S. J., Dufresne, A., Aranguren, M., Marcovich, N. E., Capadona, J. R., Rowan, S. J., et al. (2010). Review: Current international research into cellulose nanofibres and nanocomposites. *Journal of Materials Science*, *45*(1), 1–33. https://doi.org/10.1007/s10853-009-3874-0.

El-Saied, H., El-Diwany, A. I., Basta, A. H., Atwa, N. A., & El-Ghwas, D. E. (2008). Production and characterization of economical bacterial cellulose. *BioResources*, *3*(4), 1196–1217. http://www.ncsu.edu/bioresources/BioRes_03/BioRes_03_4_1196_ElSaied_EBAE_Prod_Char_Econ_Bacterial_Cellulose.pdf.

Fox, D. M., Rodriguez, R. S., Devilbiss, M. N., Woodcock, J., Davis, C. S., Sinko, R., et al. (2016). Simultaneously tailoring surface energies and thermal stabilities of cellulose nanocrystals using ion exchange: Effects on polymer composite properties for transportation, infrastructure, and renewable energy applications. *ACS Applied Materials and Interfaces*, *8*(40), 27270–27281. https://doi.org/10.1021/acsami.6b06083.

Fu, J., Pang, Z., Yang, J., Huang, F., Cai, Y., & Wei, Q. (2015). Fabrication of polyaniline/carboxymethyl cellulose/cellulose nanofibrous mats and their biosensing application. *Applied Surface Science*, *349*, 35–42. https://doi.org/10.1016/j.apsusc.2015.04.215.

Galkina, O. L., Ivanov, V. K., Agafonov, A. V., Seisenbaeva, G. A., & Kessler, V. G. (2015). Cellulose nanofiber-titania nanocomposites as potential drug delivery systems for dermal applications. *Journal of Materials Chemistry B*, *3*(8), 1688–1698. https://doi.org/10.1039/c4tb01823k.

George, J., Sreekala, M. S., & Thomas, S. (2001). A review on interface modification and characterization of natural fiber reinforced plastic composites. *Polymer Engineering and Science*, *41*(9), 1471–1485. https://doi.org/10.1002/pen.10846.

Golshan, M., Salami-Kalajahi, M., Roghani-Mamaqani, H., & Mohammadi, M. (2017). Poly(propylene imine) dendrimer-grafted nanocrystalline cellulose: Doxorubicin loading and release behavior. *Polymer*, *117*, 287–294. https://doi.org/10.1016/j.polymer.2017.04.047.

Grigore, M. E. (2017). Methods of recycling, properties and applications of recycled thermoplastic polymers. *Recycling*, *2*(4). https://doi.org/10.3390/recycling2040024.

Guimarães, I. C., dos Reis, K. C., Menezes, E. G. T., Rodrigues, A. C., da Silva, T. F., de Oliveira, I. R. N., et al. (2016). Cellulose microfibrillated suspension of carrots obtained by mechanical defibrillation and their application in edible starch films. *Industrial Crops and Products*, *89*, 285–294. https://doi.org/10.1016/j.indcrop.2016.05.024.

He, J. X., Tan, W. L., Han, Q. M., Cui, S. Z., Shao, W., & Sang, F. (2016). Fabrication of silk fibroin/cellulose whiskers–chitosan composite porous scaffolds by layer-by-layer assembly for application in bone tissue engineering. *Journal of Materials Science*, *51*(9), 4399–4410. https://doi.org/10.1007/s10853-016-9752-7.

Hong, L., Wang, Y. L., Jia, S. R., Huang, Y., Gao, C., & Wan, Y. Z. (2006). Hydroxyapatite/bacterial cellulose composites synthesized via a biomimetic route. *Materials Letters*, *60*(13–14), 1710–1713. https://doi.org/10.1016/j.matlet.2005.12.004.

Huang, P., Zhao, Y., Kuga, S., Wu, M., & Huang, Y. (2016). A versatile method for producing functionalized cellulose nanofibers and their application. *Nanoscale*, *8*(6), 3753–3759. https://doi.org/10.1039/c5nr08179c.

Je, C. H., & Kim, K. J. (2004). Cellophane as a biodegradable electroactive polymer actuator. *Sensors and Actuators, A: Physical*, *112*(1), 107–115. https://doi.org/10.1016/j.sna.2003.11.005.

Jian, C., Gong, C., Wang, S., Wang, S., Xie, X., Wei, Y., et al. (2014). Multifunctional comb copolymer ethyl cellulose-g-poly(ε-caprolactone)- rhodamine B/folate: Synthesis, characterization and targeted bonding application. *European Polymer Journal*, *55*(1), 235–244. https://doi.org/10.1016/j.eurpolymj.2014.04.003.

Kim, J., Yun, S., & Lee, S. K. (2008). Cellulose smart material: Possibility and challenges. *Journal of Intelligent Material Systems and Structures*, *19*(3), 417–422. https://doi.org/10.1177/1045389X07083140.

Kresse, K. M., Xu, M., Pazzi, J., García-Ojeda, M., & Subramaniam, A. B. (2016). Novel application of cellulose paper as a platform for the macromolecular self-assembly of biomimetic giant liposomes. *ACS Applied Materials and Interfaces*, *8*(47), 32102–32107. https://doi.org/10.1021/acsami.6b11960.

La Rosa, A. D., Cozzo, G., Latteri, A., Recca, A., Björklund, A., Parrinello, E., et al. (2013). Life cycle assessment of a novel hybrid glass-hemp/thermoset composite. *Journal of Cleaner Production*, *44*, 69–76. https://doi.org/10.1016/j.jclepro.2012.11.038.

Li, Y. Y., Wang, B., Ma, M. G., & Wang, B. (2018). Review of recent development on preparation, properties, and applications of cellulose-based functional materials. *International Journal of Polymer Science*, *2018*. https://doi.org/10.1155/2018/8973643.

Liu, S., Jin, M., Chen, Y., Gao, H., Shi, X., Cheng, W., et al. (2017). High internal phase emulsions stabilised by supramolecular cellulose nanocrystals and their application as cell-adhesive macroporous hydrogel monoliths. *Journal of Materials Chemistry B*, *5*(14), 2671–2678. https://doi.org/10.1039/c7tb00145b.

Liu, D., Song, J., Anderson, D. P., Chang, P. R., & Hua, Y. (2012). Bamboo fiber and its reinforced composites: Structure and properties. *Cellulose*, *19*(5), 1449–1480. https://doi.org/10.1007/s10570-012-9741-1.

Meriçer, Ç., Minelli, M., Angelis, M. G. D., Giacinti Baschetti, M., Stancampiano, A., Laurita, R., et al. (2016). Atmospheric plasma assisted PLA/microfibrillated cellulose (MFC) multilayer biocomposite for sustainable barrier application. *Industrial Crops and Products*, *93*, 235–243. https://doi.org/10.1016/j.indcrop.2016.03.020.

Miao, C., & Hamad, W. Y. (2016). Alkenylation of cellulose nanocrystals (CNC) and their applications. *Polymer*, *101*, 338–346. https://doi.org/10.1016/j.polymer.2016.08.099.

Moubarik, A., Grimi, N., & Boussetta, N. (2013). Structural and thermal characterization of Moroccan sugar cane bagasse cellulose fibers and their applications as a reinforcing agent in low density polyethylene. *Composites Part B: Engineering*, *52*, 233–238. https://doi.org/10.1016/j.compositesb.2013.04.040.

Mukherjee, T., & Kao, N. (2011). PLA based biopolymer reinforced with natural fibre: A review. *Journal of Polymers and the Environment*, *19*(3), 714–725. https://doi.org/10.1007/s10924-011-0320-6.

Müller, F. A., Müller, L., Hofmann, I., Greil, P., Wenzel, M. M., & Staudenmaier, R. (2006). Cellulose-based scaffold materials for cartilage tissue engineering. *Biomaterials*, *27*(21), 3955–3963. https://doi.org/10.1016/j.biomaterials.2006.02.031.

Ng, H. M., Sin, L. T., Tee, T. T., Bee, S. T., Hui, D., Low, C. Y., et al. (2015). Extraction of cellulose nanocrystals from plant sources for application as reinforcing agent in polymers. *Composites Part B: Engineering*, *75*, 176–200. https://doi.org/10.1016/j.compositesb.2015.01.008.

Nishiyama, Y., Langan, P., & Chanzy, H. (2002). Crystal structure and hydrogen-bonding system in cellulose Iβ from synchrotron X-ray and neutron fiber diffraction. *Journal of the American Chemical Society*, *124*(31), 9074–9082. https://doi.org/10.1021/ja0257319.

Orelma, H., Filpponen, I., Johansson, L. S., Laine, J., & Rojas, O. J. (2011). Modification of cellulose films by adsorption of cmc and chitosan for controlled attachment of biomolecules. *Biomacromolecules*, *12*(12), 4311–4318. https://doi.org/10.1021/bm201236a.

Ouyang, W., Sun, J., Memon, J., Wang, C., Geng, J., & Huang, Y. (2013). Scalable preparation of three-dimensional porous structures of reduced graphene oxide/cellulose composites and their application in supercapacitors. *Carbon*, *62*, 501–509. https://doi.org/10.1016/j.carbon.2013.06.049.

Pérez Quiñones, J., Cela Mardare, C., Walter Hassel, A., & Brüggemann, O. (2017). Self-assembled cellulose particles for agrochemical applications. *European Polymer Journal*, *93*, 706–716. https://doi.org/10.1016/j.eurpolymj.2017.02.023.

Rahman, M. R., Khui, P. L. N., & Bakri, M. K. B. (2021). Bamboo nanocomposites future development and applications. In M. R. Rahman (Ed.), *Bamboo Polymer Nanocomposites*. *Engineering Materials*. Cham: Springer. https://doi.org/10.1007/978-3-030-68090-9_9.

Rahman, M. R., Taib, N. A. A. B., Bakri, M. K. B., & Taib, S. N. L. (2021). Importance of sustainable polymers for modern society and development. In M. R. Rahman (Ed.), *Advances in Sustainable Polymer Composites* (pp. 1–35). Woodhead Publishing. https://doi.org/10.1016/B978-0-12-820338-5.00001-1.

Review of progress in quantitative nondestructive evaluation: Vol. 6 (pp. 1257–1265). (1987).

Rudhziah, S., Rani, M. S. A., Ahmad, A., Mohamed, N. S., & Kaddami, H. (2015). Potential of blend of kappa-carrageenan and cellulose derivatives for green polymer electrolyte application. *Industrial Crops and Products*, *72*, 133–141. https://doi.org/10.1016/j.indcrop.2014.12.051.

Rwawiire, S., Tomkova, B., Militky, J., Jabbar, A., & Kale, B. M. (2015). Development of a biocomposite based on green epoxy polymer and natural cellulose fabric (bark cloth) for automotive instrument panel applications. *Composites Part B: Engineering*, *81*, 149–157. https://doi.org/10.1016/j.compositesb.2015.06.021.

Santos, S. M., Carbajo, J. M., Gómez, N., Quintana, E., Ladero, M., Sánchez, A., et al. (2016a). Use of bacterial cellulose in degraded paper restoration. Part I: Application on model papers. *Journal of Materials Science*, *51*(3), 1541–1552. https://doi.org/10.1007/s10853-015-9476-0.

Santos, S. M., Carbajo, J. M., Gómez, N., Quintana, E., Ladero, M., Sánchez, A., et al. (2016b). Use of bacterial cellulose in degraded paper restoration. Part II: Application on real samples. *Journal of Materials Science*, *51*(3), 1553–1561. https://doi.org/10.1007/s10853-015-9477-z.

Shahbazi, M., Ahmadi, S. J., Seif, A., & Rajabzadeh, G. (2016). Carboxymethyl cellulose film modification through surface photo-crosslinking and chemical crosslinking for food packaging applications. *Food Hydrocolloids*, *61*, 378–389. https://doi.org/10.1016/j.foodhyd.2016.04.021.

Shahzad, A. (2012). Hemp fiber and its composites—A review. *Journal of Composite Materials*, *46*(8), 973–986. https://doi.org/10.1177/0021998311413623.

Shalwan, A., & Yousif, B. F. (2013). In state of art: Mechanical and tribological behaviour of polymeric composites based on natural fibres. *Materials and Design*, *48*, 14–24. https://doi.org/10.1016/j.matdes.2012.07.014.

Silvério, H. A., Flauzino Neto, W. P., Dantas, N. O., & Pasquini, D. (2013). Extraction and characterization of cellulose nanocrystals from corncob for application as reinforcing agent in nanocomposites. *Industrial Crops and Products*, *44*, 427–436. https://doi.org/10.1016/j.indcrop.2012.10.014.

Singha, A., & Kumar, T. V. (2009). Physical, chemical and mechanical properties of *Hibiscus sabdariffa* fiber/polymer composite. *International Journal of Polymeric Materials*, 217–228. https://doi.org/10.1080/00914030802639999.

Singha, A. S., & Thakur, V. K. (2008a). Saccaharum cilliare fiber reinforced polymer composites. *E-Journal of Chemistry*, *5*(4), 782–791. https://doi.org/10.1155/2008/941627.

Singha, A. S., & Thakur, V. K. (2008b). Synthesis and characterization of pine needles reinforced RF matrix based biocomposites. *E-Journal of Chemistry*, *5*(1), 1055–1062. https://doi.org/10.1155/2008/395827.

Singha, A. S., & Thakur, V. K. (2009a). Chemical resistance, mechanical and physical properties of biofibers-based polymer composites. *Polymer - Plastics Technology and Engineering*, *48*(7), 736–744. https://doi.org/10.1080/03602550902824622.

Singha, A. S., & Thakur, V. K. (2009b). Fabrication and characterization of H. sabdariffa fiber-reinforced green polymer composites. *Polymer - Plastics Technology and Engineering*, *48*(4), 482–487. https://doi.org/10.1080/03602550902725498.

Singha, A. S., & Thakur, V. K. (2009c). Mechanical, morphological and thermal properties of pine needle-reinforced polymer composites. *International Journal of Polymeric Materials and Polymeric Biomaterials*, *58*(1), 21–31. https://doi.org/10.1080/00914030802461857.

Singha, A. S., & Thakur, V. K. (2010). Mechanical, morphological, and thermal characterization of compression-molded polymer biocomposites. *International Journal of Polymer Analysis and Characterization*, *15*(2), 87–97. https://doi.org/10.1080/10236660903474506.

Singha, A. S., Thakur, V. K., Mehta, I. K., Shama, A., Khanna, A. J., Rana, R. K., et al. (2009). Surface-modified Hibiscus sabdariffa fibers: Physicochemical, thermal, and morphological properties evaluation. *International Journal of Polymer Analysis and Characterization*, *14*(8), 695–711. https://doi.org/10.1080/10236660903325518.

Snyder, J. F., Carter, R. H., & Wetzel, E. D. (2007). Electrochemical and mechanical behavior in mechanically robust solid polymer electrolytes for use in multifunctional structural batteries. *Chemistry of Materials*, *19*(15), 3793–3801. https://doi.org/10.1021/cm070213o.

Spinella, S., Samuel, C., Raquez, J. M., McCallum, S. A., Gross, R., & Dubois, P. (2016). Green and efficient synthesis of dispersible cellulose nanocrystals in biobased polyesters for engineering applications. *ACS Sustainable Chemistry & Engineering*, *4*(5), 2517–2527. https://doi.org/10.1021/acssuschemeng.5b01611.

Sun, B., Hou, Q., Liu, Z., & Ni, Y. (2015). Sodium periodate oxidation of cellulose nanocrystal and its application as a paper wet strength additive. *Cellulose*, *22*(2), 1135–1146. https://doi.org/10.1007/s10570-015-0575-5.

Sweetnam, P. M., Taylor, S. W. C., & Elwood, P. C. (1987). Exposure to carbon disulphide and ischaemic heart disease in a viscose rayon factory. *British Journal of Industrial Medicine*, *44*(4), 220–227. https://doi.org/10.1136/oem.44.4.220.

Taofik, O. A. (2020). *Thermoplastic recycling: Properties, modifications, and applications*. IntechOpen. https://doi.org/10.5772/intechopen.81614.

Thakur, V. K., Singha, A. S., & Thakur, M. K. (2012). In-air graft copolymerization of ethyl acrylate onto natural cellulosic polymers. *International Journal of Polymer Analysis and Characterization*, *17*(1), 48–60. https://doi.org/10.1080/1023666X.2012.638470.

Thakur, V. K., & Thakur, M. K. (2014). Processing and characterization of natural cellulose fibers/thermoset polymer composites. *Carbohydrate Polymers*, *109*, 102–117. https://doi.org/10.1016/j.carbpol.2014.03.039.

Ticoalu, A., Aravinthan, T., & Cardona, F. (2013). A review on the characteristics of gomuti fibre and its composites with thermoset resins. *Journal of Reinforced Plastics and Composites*, *32*(2), 124–136. https://doi.org/10.1177/0731684412463109.

Vecbiskena, L., & Rozenberga, L. (2017). Nanocelluloses obtained by ammonium persulfate (APS) oxidation of bleached Kraft pulp (BKP) and bacterial cellulose (BC) and their application in biocomposite films together with chitosan. *Holzforschung*, *71*(7–8), 659–666. https://doi.org/10.1515/hf-2016-0187.

Voicu, S. I., Condruz, R. M., Mitran, V., Cimpean, A., Miculescu, F., Andronescu, C., et al. (2016). Sericin covalent immobilization onto cellulose acetate membrane for biomedical applications. *ACS Sustainable Chemistry & Engineering*, *4*(3), 1765–1774. https://doi.org/10.1021/acssuschemeng.5b01756.

Wan, Y. Z., Huang, Y., Yuan, C. D., Raman, S., Zhu, Y., Jiang, H. J., et al. (2007). Biomimetic synthesis of hydroxyapatite/bacterial cellulose nanocomposites for biomedical applications. *Materials Science and Engineering C*, *27*(4), 855–864. https://doi.org/10.1016/j.msec.2006.10.002.

Wang, Z., Fan, X., He, M., Chen, Z., Wang, Y., Ye, Q., et al. (2014). Construction of cellulose-phosphor hybrid hydrogels and their application for bioimaging. *Journal of Materials Chemistry B*, *2*(43), 7559–7566. https://doi.org/10.1039/c4tb01240b.

Weigel, P., Fink, H., Frigge, K., & Schwarz, W. (2001). *Process of manufacturing orientated cellulose films*. European Patent EP0766709A1.

Willgert, M., Leijonmarck, S., Lindbergh, G., Malmström, E., & Johansson, M. (2014). Cellulose nanofibril reinforced composite electrolytes for lithium ion battery applications. *Journal of Materials Chemistry A*, *2*(33), 13556–13564. https://doi.org/10.1039/c4ta01139b.

Wu, X., Tang, J., Duan, Y., Yu, A., Berry, R. M., & Tam, K. C. (2014). Conductive cellulose nanocrystals with high cycling stability for supercapacitor applications. *Journal of Materials Chemistry A*, *2*(45), 19268–19274. https://doi.org/10.1039/c4ta04929b.

Xu, D., Fan, L., Gao, L., Xiong, Y., Wang, Y., Ye, Q., et al. (2016). Micro-nanostructured polyaniline assembled in cellulose matrix via interfacial polymerization for applications in nerve regeneration. *ACS Applied Materials and Interfaces*, *8*(27), 17090–17097. https://doi.org/10.1021/acsami.6b03555.

Xu, X., Zhou, J., Nagaraju, D. H., Jiang, L., Marinov, V. R., Lubineau, G., et al. (2015). Flexible, highly graphitized carbon aerogels based on bacterial cellulose/lignin: Catalyst-free synthesis and its application in energy storage devices. *Advanced Functional Materials*, *25*(21), 3193–3202. https://doi.org/10.1002/adfm.201500538.

Yun, S., Chen, Y., Nayak, J. N., & Kim, J. (2008). Effect of solvent mixture on properties and performance of electro-active paper made with regenerated cellulose. *Sensors and Actuators, B: Chemical*, *129*(2), 652–658. https://doi.org/10.1016/j.snb.2007.09.049.

Zhang, R., Zhang, R., Hang, L., Min, L., & Zhang, L. (2016). Bio-polyester P(3, 4) HB-based nanocomposites reinforced by cellulose nanowhiskers. *Journal of Forestry Engineering*, *1*(13), 85–90. https://doi.org/10.13360/j.issn.2096-1359.2016.03.016.

Zhao, Y., Zhu, X., Liu, H., Luo, Y., Wang, S., Shen, M., et al. (2014). Dendrimer-functionalized electrospun cellulose acetate nanofibers for targeted cancer cell capture applications. *Journal of Materials Chemistry B*, *2*(42), 7384–7393. https://doi.org/10.1039/c4tb01278j.

Index

Note: Page numbers followed by *f* indicate figures and *t* indicate tables.

D

E

F

G

N

O

P

R

S

T

FUNDAMENTALS AND RECENT ADVANCES IN NANOCOMPOSITES BASED ON POLYMERS AND NANOCELLULOSE

Edited by Md Rezaur Rahman

An innovative guide to the fundamentals, latest developments, and advanced applications of cellulose-based nanocomposites.

Fundamentals and Recent Advances in Nanocomposites Based on Polymers and Nanocellulose brings together the latest research in cellulose-based nanocomposites, covering fundamentals, processing, properties, performance, applications, and the state of the art.

The book begins by explaining the fundamentals of cellulose and cellulose-based nanocomposites, including sources, extraction, types, classification, linkages, model structure, model compounds, and characterization techniques. The second part of the book covers the incorporation of cellulose fillers to improve the properties or characteristics of nanocomposites, organized by composite category, including in aerogels, thermoplastic composites, thermoset composites, bioplastic composites, carbon nanofibers, rubber composites, carbon fibers, and foaming materials. Throughout these chapters, there is an emphasis on the latest innovations and application potential. Finally, applications are explored in more detail, notably focusing on the utilization of nanocellulose in biodegradable composites for biomedical applications, along with other important industrial application areas.

This book is of great interest to researchers, scientists, and advanced students working with bio-based materials, and across polymer science, nanomaterials, composite materials, plastics engineering, chemical engineering, materials science and engineering, as well as R&D professionals, engineers, and industrialists involved in the development of bio-based materials for advanced applications or material commercialization.

Key Features

- Presents the fundamentals of cellulose-based nanocomposites, including sources, extraction, types, classification, linkages, structure, compounds, and characterization.
- Discusses and analyzes the most suitable fabrication methods and processing techniques for cellulose as a reinforcement in a range of composites.
- Opens the door to a range of cutting-edge applications and considers key aspects such as cost, life cycle, and biodegradability.

About the Editor

Md Rezaur Rahman is currently working as a Senior Lecturer (Assistant Professor) at the Department of Chemical Engineering and Energy Sustainability, Faculty of Engineering, Universiti Malaysia Sarawak (UNIMAS), Malaysia. He received his PhD from the Universiti Malaysia Sarawak, Malaysia. He has more than 12 years of experience in teaching, research, and working with industry. Dr. Rahman's research includes the areas of conducting polymers, silica/clay-dispersed elastomeric polymer nanocomposites, hybrid filler-loaded polymer composites, advanced materials: graphene/nanoclay/fire retardant, nanocellulose (cellulose nanocrystals and nanofibrillar), cellulose-reinforced/cellulose-filled polymer composites, chemical modification and treatment of lignocellulosic fibers, nanocomposites and nanocellulose fibers, and polymer blends. He has published 5 books, 45 book chapters, and more than 100 international journal papers, while overseeing numerous PhD and postgraduate students, as well as acting as a reviewer for several high-impact ISI journals.

Polymer Science

ISBN 978-0-323-85771-0

9 780323 857710

ELSEVIER elsevier.com/books-and-journals